DOCTOR OF PHILOSOPHY

Kinetics of the wood-acetic anhydride reaction

Dunningham, Elizabeth A.

Award date:
2003

Awarding institution:
Bangor University

Kinetics of the wood - acetic anhydride reaction

A thesis submitted for the degree of Doctor of Philosophy in Wood Science
of the University of Wales Bangor

by

Elizabeth A. Dunningham

April 2003

School of Agricultural and Forest Sciences,
University of Wales Bangor,
Gwynedd, United Kingdom

ABSTRACT

The aim of this study was to examine the wood-acetic anhydride reaction by studying the reaction with wood substrates such as wood blocks, ground wood and fibre. Isolated wood polymers such as cellulose, holocellulose, hemicelluloses and lignin, were also examined. One lignin model compound was investigated in order to examine the relative rates of reaction of the different hydroxyl groups. The principal focus of the work was, however, on the acetylation reaction and kinetics of wood blocks.

The reaction between acetic anhydride and solid wood blocks under uncatalysed conditions was found to be diffusion controlled, rather than activation controlled. The rate-determining diffusion was found to be that of the reagent moving through the wood cell wall. Diffusion was also significant in influencing the rate of reaction in the ground wood sample (0.250 – 0.425 mm). It was not possible to form a model for the reaction of solid wood based on its chemical composition. However, it was possible to mathematically model the wood block (and ground wood) reaction based on reaction time and temperature. A relatively low activation energy (Ea) was obtained for radiata pine wood blocks (34 kJ/mol). The equivalent value for ground wood was higher at around 53-62 kJ/mol. The reaction level was lower for the ground wood compared to the wood blocks. It was not possible to obtain reliable kinetic data for the cellulose or holocellulose reactions.

Three ground wood samples were partially delignified to examine the effect of a decreasing lignin content (*in situ*). However, this approach was not very successful. This may be due to the increasing acid soluble lignin content with decreasing lignin content, due to the chlorite delignification process used, or perhaps the removal of lignin created more micropores which aided diffusion.

The reaction of a commercial alkali lignin (AL) from mixed softwoods gave surprisingly similar results to the milled wood lignin (MWL) isolated from radiata pine. Although the lignin reaction (29% of the MWL reaction) was similar in shape to that of the wood block reaction profile, the isolated lignin reaction was not enough to explain or model the wood reaction. This may have been because of the diffusion control of the latter and the reaction over longer reaction times of the hemicelluloses.

The β-O-4 lignin model compound studied showed that the relative rates of acetylation of the hydroxyl groups were: the phenolic hydroxyl reacted more rapidly than the primary hydroxyl, and both reacted a great deal faster than the secondary hydroxyl. The results were similar to those found for four milled wood lignin (MWL) acetylation products : the phenolic and the primary hydroxyl reacted at a similar rate, and that both reacted more rapidly than the secondary hydroxyl.

Overall, this study demonstrated the importance of the wood ultra-structure in determining the rate of reaction of acetylation in wood and wood-based substrates. The isolated wood components were therefore found to be of less importance due to the diffusion control of the reaction

TABLE OF CONTENTS

LIST OF FIGURES

LIST OF TABLES

ACKNOWLEDGEMENTS

Firstly, I would like to acknowledge the wonderful help and support of my supervisors: at the University of Wales, Bangor (UWB), Prof. Bart Banks (now retired), for the guidance through the practical phase of my work and the many valuable discussions; then more recently, Dr Callum Hill, for reading and commenting on my various chapter drafts; at Forest Research (FR), Rotorua, Dr Mervyn Uprichard, for his very helpful comments on the content and structure of my thesis. A number of others (Murray Close, Prof. John Ralph, Dr Ian Suckling) also commented on my thesis, and their input is gratefully acknowledged.

I would also like to extend my thanks to and appreciation of the staff at the UWB and associated BioComposites Centre who helped me set up numerous experiments and were always willing to help obtain elusive equipment. Many colleagues at FR also assisted me in various ways when I returned for my planned final year in Rotorua of practical and writing, and my thanks go to them as well.

Specifically, I would like to acknowledge:

- the assistance of the Analytical Laboratory, FR (later Veritech) for Klason lignin, acid soluble lignin and monosaccharide analyses, as well as some ash content determinations;
- the prompt CHNS analyses of various samples by the Campbell Micro-analytical Laboratory at University of Otago, Dunedin;
- the solid state ^{13}C NMR spectra of various holocellulose and cellulose samples arranged by Dr Noel Owen (Brigham Young University) at a facility in the USA (Cynthia Ridenour, Otsuka Electronics, Colarado);
- the donation of an organosolv bagasse lignin sample from Dr A.J. Varma (National Chemical Laboratory, Pune, India);
- the valuable assistance of (the now Dr) Kate Wingate in completing the synthesis and the reaction of the model compound once I had fallen ill;

- the help received from Dr Roderick Ball (statistician, FR) with the statistical analysis of the variability of the wood reaction and formulating the mathematical equation which describes the wood block reaction.

For funding, I am exceedingly grateful to Forest Research, and in particular, the support and encouragement of Dr Russell Burton. I have been amazed at the continued support and encouragement throughout the years of my illness when I was able to do so little for so long. I would like to thank the SAFS, UWB for its support in the completion of my thesis, and, in particular, Roger Cooper (Head of School), for his enthusiastic warmth and making all the arrangements run smoothly. I also wish to acknowledge the support of a travel grant from the British Council, which assisted me to travel to Wales to undertake these studies.

On a personal note, I wish to thank my family and friends for their support, encouragement and prayers, through what has turned out to be a nine year saga. Falling chronically ill two years and nine months into my studies made the tasks of completing my practical work and writing my thesis so much more complicated and difficult. In particular, I wish to thank my parents, Shirley and Edwin Close, for their loving support and endless encouragement, and my close friend, Elizabeth Pilaar (and her children), for helping keep me sane in the hard times.

Finally, I would like to dedicate this thesis to my husband, Andrew, without whom I would not have even begun this PhD journey, let alone completed it. I am indeed blessed to have him as my husband, and cannot say enough to thank him for his care, love, humour and encouragement over the years. Thank you, Andrew, for believing in me.

LIST OF ABBREVIATIONS

A	Pre-exponential constant in Arrhenius equation
AL	Alkali lignin
ASL	Acid soluble lignin
Ara	Arabinose (monosaccharide)
bpt	Boiling point
BL	Bagasse lignin
C9 unit	A nine-carbon unit, which is the basis of lignin structure
CEL	Cellulolytic enzyme lignin
CV%	Co-efficient of variance
D_2O	Deuterated water
DHP	Dehydro polymers
DMF	Dimethyl formamide
DMSO	Dimethyl sulphoxide
DP	Degree of polymerisation
DRIFT	Diffuse reflectance infrared Fourier transform spectroscopy
DS	Degree of substitution
DW	Distilled water
DWB	Delignified ground wood sample B, lignin content of 18.87%
DWC	Delignified ground wood sample C, lignin content of 15.50%
DWD	Delignified ground wood sample D, lignin content of 10.69%
Ea	Activation energy (kJ/mol)
EDXA	Energy-dispersive X-ray analysis
FTIR	Fourier transform infrared spectroscopy
FR	Forest Research (Rotorua, NZ)
G/GS/GSH	Referring to guaiacyl phenyl propane (G), syringyl phenyl propane (S) and *p*-hydroxyphenyl propane (H) units
Gal	Galactose (monosaccharide)
GC	Gas chromatography
Glu	Glucose (monosaccharide)
GM	Glucomannan
Grd	Ground (wood usually)
GW	Ground wood
k_o	Initial rate constant
k	Rate constant
KBr	Potassium bromide powder (used to make pellets in FTIR)
KL	Klason lignin (acid insoluble)
L	litres
Man	Mannose (monosaccharide)
MC	Model compound of lignin
MDF	Medium density fibreboard
ML	Middle lamella
MMNO	N-methylmorpholine N-oxide monohydrate
M_n	Molecular weight (number average)
M_w	Molecular weight (weight average)
MWL	Milled wood lignin
NMR	Nuclear magnetic resonance spectroscopy
NS	Not significant (for probability (P) values)

NZ FRI	New Zealand Forest Research Institute Ltd
OD	Oven-dried
Ph	Phenolic
R	Gas constant, 8.314 $J.K^{-1}.mol^{-1}$
RSCL	Released suspension-culture lignin
RT	Room temperature
SS	Sum of the squares
std err	Standard error (in Ea usually)
SW	Secondary wall of wood cell
TA	Total acetate
TAPPI	Technical Association of the Pulp and Paper Industry
UWB	University of Wales Bangor
VI	Vacuum impregnation
WPG	Weight percent gain (on oven-dried basis)
WPG_s	Solid WPG (excluding substrate dissolved in reaction solution)
WPG_{tot}	Total WPG (solid + soluble)
Xyl	Xylose (monosaccharide)

CHAPTER 1: INTRODUCTION

1.1. General introduction

This study focused on the reaction of wood and wood-based substrates with one chemical reagent: acetic anhydride. In terms of chemical reactions, wood is a highly complex material, with many contributing chemical entities. The study is concerned with the chemical reactions of wood in the solid state with a liquid reagent. This makes an explanation of the reaction kinetics complex.

This chapter is divided into four parts: the first two cover the structure and chemistry of wood; the third briefly reviews chemical modification treatments of wood and discusses the mechanism of the acetylation reaction; and the fourth part presents and discusses some concepts of chemical kinetics and their application to wood reactions. In this way, the main topics that are relevant to this study are introduced. Then the scope of this work is covered, chapter by chapter.

1.2. Wood structure

Wood is a complex three-dimensional matrix of various bio-polymers and low molecular weight organic compounds, and the exact chemical and physical composition vary from tree to tree and species to species. Tree species are broadly divided into two main groups: hardwoods (angiosperms) and softwoods (gymnosperms). One species of softwood, radiata pine (*Pinus radiata*), was used in this study. This choice was made because of the importance of this species in New Zealand forestry; radiata pine comprises about 90% of New Zealand´s plantation species (NZ FOA, 1995). Therefore, only softwoods will be considered in this discussion of wood structure.

The complex structure of softwoods is illustrated in Figure 1.1, where an engineered model (Harrington, 1996) is shown from the living tree, to sawn timber, through to the different levels of wood structure, down to the molecular level.

Figure 1.1. Wood structure from the tree to the molecular level (Harrington, 1996; used with permission)

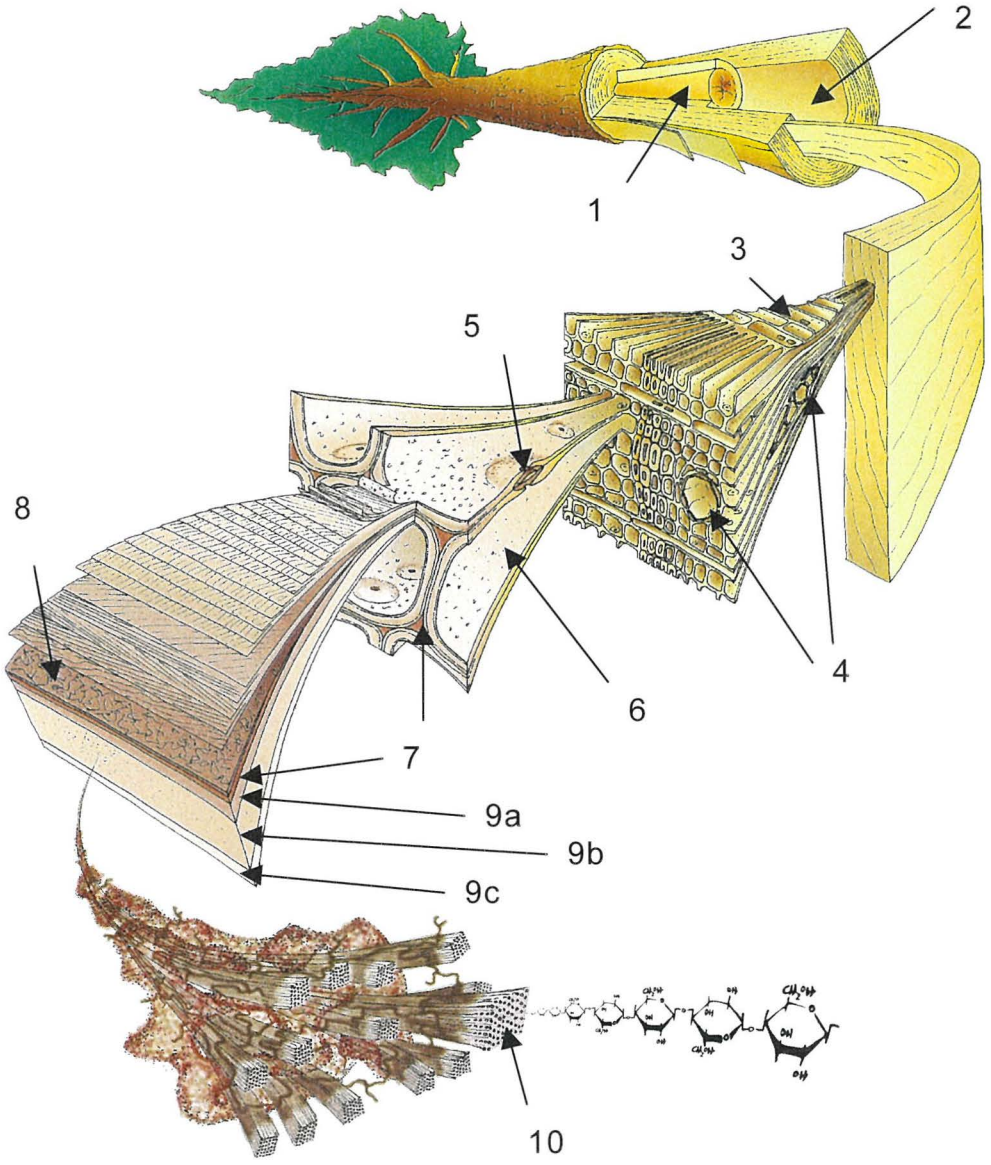

Key: 1 = heartwood, 2 = sapwood, 3 = rays, 4 = resin canals, 5 = bordered pits, 6 = tracheid, 7 = middle lamella, 8 = primary wall, 9a,b,c = secondary wall, S1, S2, S3 respectively, 10 = microfibrils

The heartwood (1) is the inner zone of the tree that contains no living cells, and contains a higher proportion of extractives than the sapwood (2). It also contains less water than the sapwood. The wood (or xylem) is arranged around the core concentrically in annual rings. It has ray cells (3) which run from the bark to the pith (radially). Resin canals (4) are tunnels through the tissue, which are surrounded by short parenchyma cells that secrete resin into the resin canals in the living tree. Pits (5) connect the cell lumens of the tracheid cells (6). Tracheids are long tube-like cells, making up 90-95% of softwood cells, and are held together by the middle lamella (7), which contains 60-70% lignin (Fengel and Wegener, 1989). The primary wall (8) and the secondary wall (9a,b,c) make up the cell wall: these are composed of microfibril bundles (10), which are made of cellulose chains and are embedded in a lignin and hemicellulose matrix.

1.2.1. Macroscopic structure of wood

Several physical features of wood structure are easily visible to the naked eye, for example, growth rings, with their zones of earlywood and latewood, and the tissue known as pith (Figure 1.2). The pith is the darker core of the tree and consists of the tissue formed in the first year of growth. Annual growth rings arise in response to seasonal changes in climate. In conditions where rapid growth occurs, cells with a thin wall and large diameters are produced (earlywood). Later in the season, when growth conditions are not as favourable, the cells have thicker walls with smaller diameters (latewood). The cambium is a very thin layer (between the xylem (wood) and inner bark) where the growth of the living tree takes place (cell division), and the phloem is a zone of inner bark, which contains living cells. The outer bark does not contain living cells and it's purpose is to protect the woody cells from mechanical damage and climatic variations (Sjöström, 1981).

Wood is an anisotropic material. Many properties vary in the different principal directions (Figure 1.2). These features influence many wood properties, such as permeability, treatability, dimensional stability, and the warping and checking of wood during drying.

Figure 1.2. Basic wood structure (Sjöström, 1981)

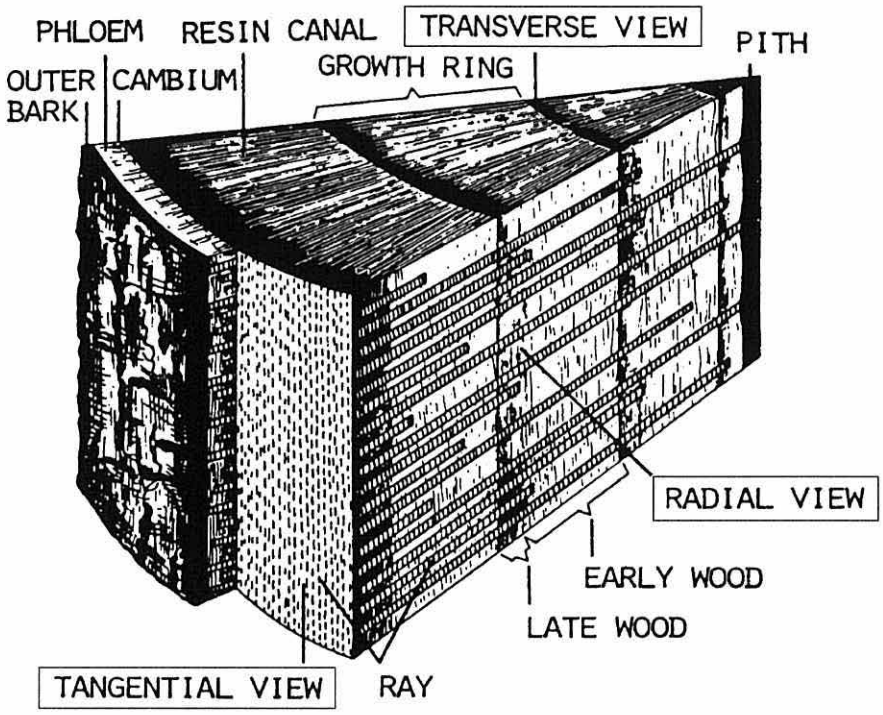

1.2.2. Microscopic structure of wood

Wood cells are joined together by the middle lamella (ML), which contains a high concentration of lignin. However, the middle lamella is but a small percentage of wood and it contains only about 20-25% of the total lignin in wood (Sjöström, 1981). Cell walls are composed of several layers: the secondary cell wall (S1, S2, sometimes S3) and the primary cell wall (P), with a warty layer (W) on the inside of the cell lumen (Figure 1.3). The microfibrils that make up these layers are found to be at a different angle to the axis of the cell in the different layers (Sjöström, 1981). This contributes to the strength of the cell structure and ultimately the tree itself. The microfibrils are composed of a cellulose core, which is highly crystalline, surrounded by hemicelluloses and joined together by lignin. There are a number of theories of how intermixed these main wood components are, and what form the cellulose core takes. However, these matters are outside the scope of this study. Fengel and Wegener (1989) give a good review of the topic.

Figure 1.3. Structure of wood cells
(Sjöström, 1981; originally from Côté, 1967)

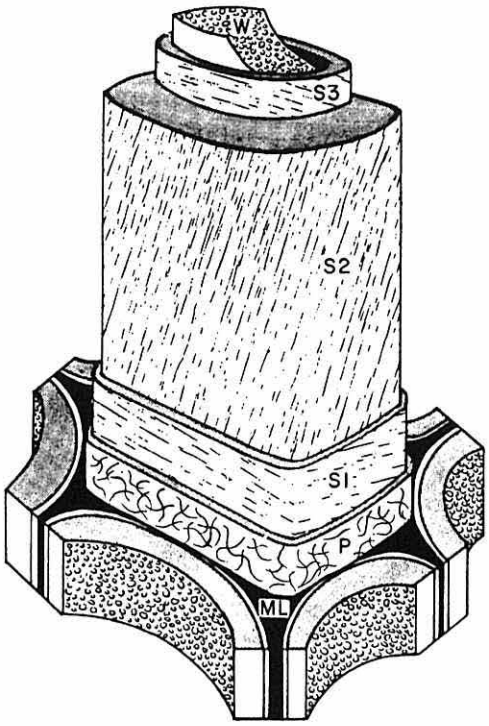

Key: ML = middle lamella; P = primary wall; S1 = secondary wall, 1st layer; S2 = secondary wall, 2nd layer; S3 = secondary wall, 3rd layer; W = warty layer

1.3. Wood chemistry

Wood is a complex matrix composed mainly of three polymers: cellulose, hemicelluloses and lignin. There is also a minor group of compounds called extractives, present in radiata pine sapwood at about 2-3% by weight (Uprichard, 1991). The three main groups of wood components have significantly different chemical structures (Figures 1.4, 1.6) and therefore different reactivity to acetylation.

In spite of the many differences between the three main groups of wood polymers, they do have some similarities; for example, the abundance of hydroxyl groups and the presence of ether linkages. The former feature gives rise to the affinity of wood for water and the latter feature to some of the difficulty of separating or selectively reacting lignin and carbohydrates.

While the basic structures of the wood polymers are reasonably well known, it is difficult with current techniques to describe the precise structure of each polymer. This is mainly because the individual polymers need to be extracted from the wood for them to be characterised. However, any extraction process changes the polymer to some extent.

The proportions of the polymers (or chemical composition) in wood can vary in different parts of the tree, from tree to tree, and from species to species. Softwoods commonly have 40-50% cellulose, 5-30% hemicelluloses and 25-35% lignin (Fengel and Wegener, 1989). Table 1.1 shows a range of softwood species and their chemical composition. The variability of chemical composition within a species adds to the complexity of any wood-based study.

Table 1.1 Chemical composition of softwoods (Timell, 1967).

Wood species	Chemical composition			
	Cellulose	Xylan	Glucomannan	Lignin
Balsam fir (*Abies balsamea*)	42	9	18	29
White spruce (*Picea glauca*)	41	13	18	27
Yellow pine (*Pinus strobus*)	41	9	18	29
Radiata pine (*Pinus radiata*)[1]	40	7	15	27
Eastern hemlock (*Tsuga canadensis*)	41	7	16	33
White cedar (*Thuja occidentalis*)	41	14	12	31

[1] Data from Uprichard, 1991

Extractives are low molecular weight compounds, which are extracted by water or neutral organic solvents. Softwoods contain around 2-5% extractives, with heartwood containing a higher extractive content than sapwood. Radiata pine extractives are mostly composed of mono- and di-saccharides, fatty acids, phenols and terpenes (Uprichard, 1991).

In this study, using pre-extracted wood for all studies eliminated the effects of extractives content. The main focus of the work was on the reaction of the cell wall components, and so the pre-extraction treatment was basically preparation of the cell wall before reaction.

1.3.1. Cellulose and hemicelluloses

Cellulose is a polymer derived from glucose monomers, which are joined by β-D-glycosidic bonds. These ether bonds are between the C1 and C4 carbons of neighbouring units (1:4 linkage). The glucose units are joined in an alternating fashion, as shown in Figure 1.4a, so that the repeating unit is cellobiose (2 consecutive glucose units). Polymeric strands of cellulose are hydrogen bonded to neighbouring strands so that the resulting structure is very strong, with low accessibility to reagents and therefore, low apparent reactivity. Cellulose in wood is highly crystalline, with a crystallinity index of 60-70% in wood pulps (Fengel and Wegener, 1989).

Figure 1.4. Partial structures of (a) cellulose, examples of (b) xylan and (c) glucomannan (Fengel and Wegener, 1989)

(a) Cellulose

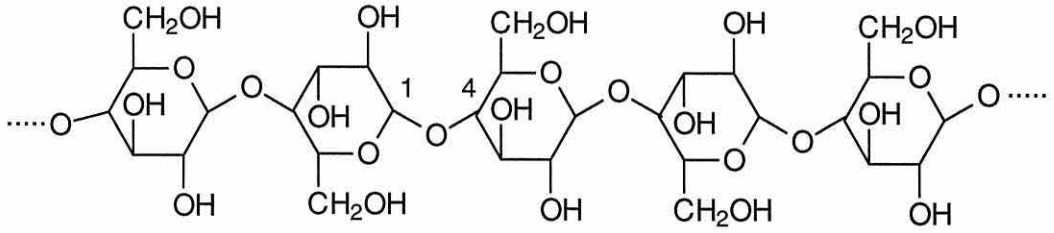

(b) Xylan

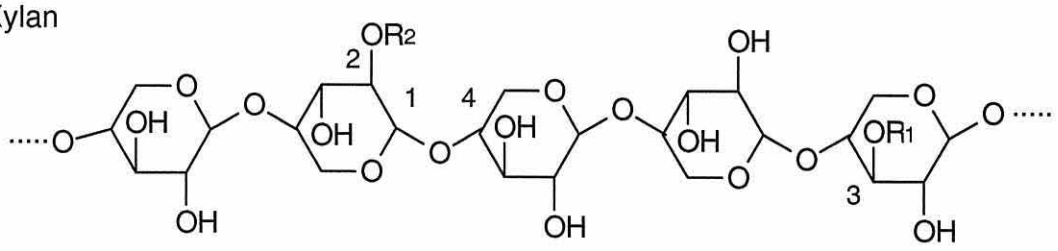

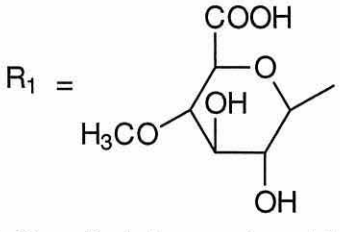

4-D-methylglucuronic acid

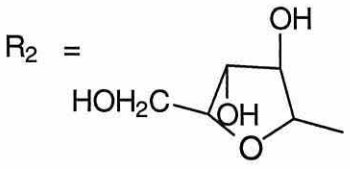

α–L-arabinofuranosyl

(c) Galactoglucomannan

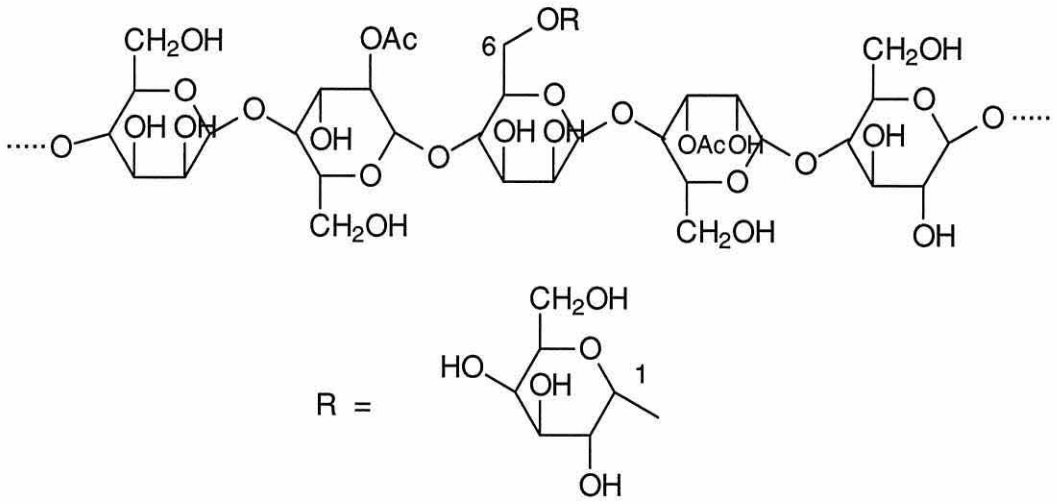

Hemicelluloses are polysaccharides derived from several types of monosaccharide units (for example; glucose, xylose, mannose) with additional functional groups (e.g. acetates), sometimes also incorporating uronic acids. They can be branched and have a much lower degree of polymerisation (DP) than cellulose.

Examples of the two main hemicelluloses, xylan and glucomannan, found in radiata pine, are shown in Figure 1.4b,c. Cellulose in wood is thought to have a DP of around 10,000, whereas hemicelluloses are thought to have DPs of up to 200 (Sjöström, 1981).

Xylan is made up of alternating β-D-xylose units with 1:4 ether linkages, with side chains of glucouronic acid units and arabinose units (Figure 1.4b). The α-D-glucouronic acid groups (R_1) are usually attached at the C3 carbon with a 1:3 ether linkage, and the α-L-arabinose groups (R_2) are attached at the C2 of a xylose unit with a 1:2 ether linkage (Uprichard, 1991; Fengel and Wegner, 1989). A xylan isolated and characterised from radiata pine was found to have a DP of 78, with an arabinose unit every 6.1 units of xylose on average, and a glucouronic acid group every 5.9 xylose units on average (Harwood, 1972).

The main chain in glucomannan is made up of glucose and mannose units, distributed randomly (Fengel and Wegener, 1989), also linked with 1:4 ether bonds. Some of the main chain units contain acetate groups, and some have side chains of galactose units. The acetate groups are on the C2 or C3 of a mannose or glucose chain unit. The α-D-galactose side units are probably bonded by a 1:6 linkage to a mannose or glucose unit (Uprichard, 1991). The ratio of mannose to glucose units is around 3 : 1 (Fengel and Wegener, 1989). Harwood (1973) found that an isolated glucomannan from radiata pine had an average DP of 45, with a ratio of mannose to glucose units of 3.7 : 1 and one galactose unit every 75 sugar chain units.

1.3.2. Lignin-carbohydrate complexes

Hemicelluloses have linkages to lignin polymers and are hard to completely separate from lignin when isolating. Björkman (1957a) gives a review of opinion of the evidence for native lignin-carbohydrate complexes (LCC), with the weight of the opinion then resting on the side that LCC do exist in wood. More recently, Liitiä *et al.* (2000a) examined residual lignin using solid state NMR spectroscopy and the results suggested the existence of LCC in wood. Whistler and Chen (1991) confirmed the existence of covalent bonds between lignin and hemicelluloses, although their nature remains uncertain.

Björkman (1957a) developed a method for extraction and isolation of LCC in DMF, as part of the milled wood lignin (MWL) extraction. He thought that it was likely that the LCC materials would be a mixture of various combinations of lignin and polysaccharides. Figure 1.5. shows the most frequently suggested types of LCC (Fengel and Wegener, 1989), where different types of linkages are shown; (a) benzyl ester, (b) benzyl ether and (c) phenyl glycosidic linkages.

Figure 1.5. The most frequently suggested lignin-carbohydrate linkages

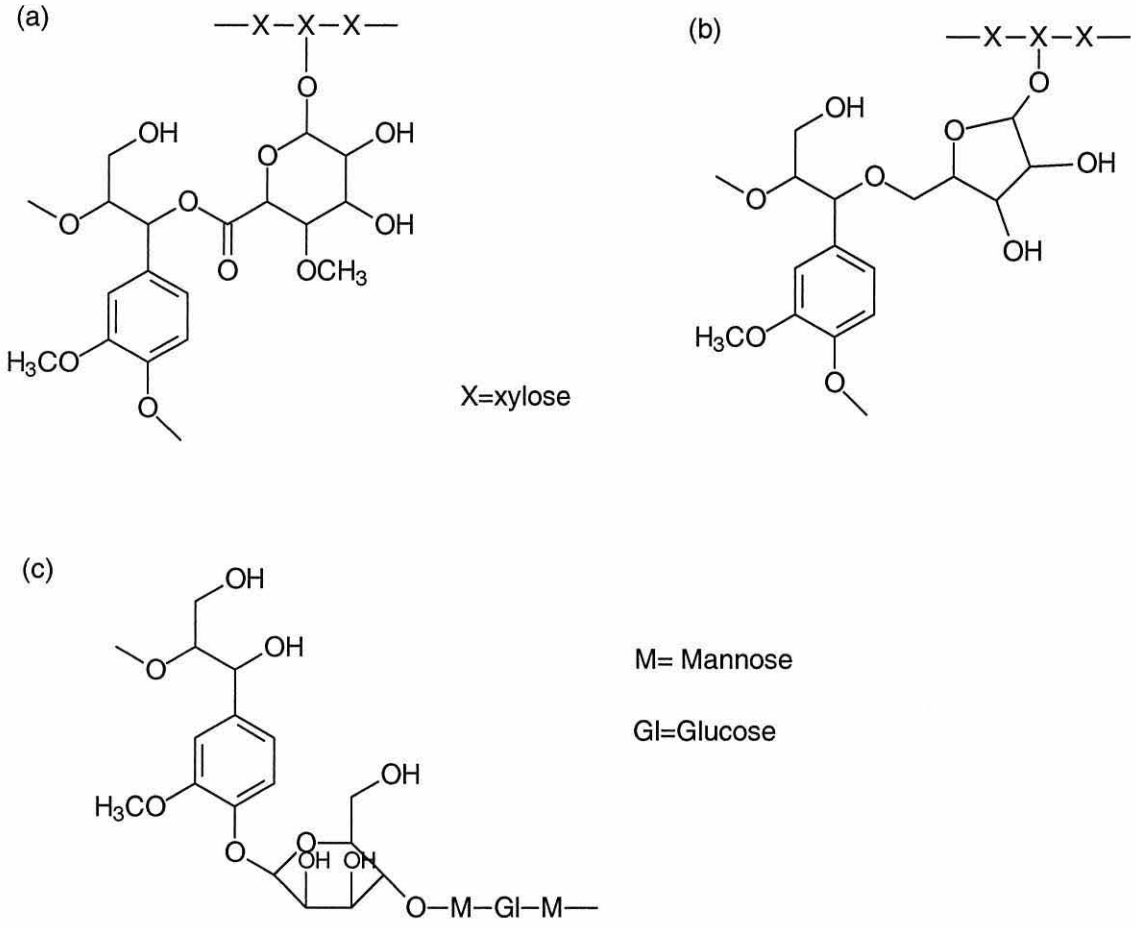

1.3.3. Lignin

Lignin has a very different structure to those of cellulose or hemicelluloses. The monomeric unit has a phenyl propanoid skeleton (Figure 1.6). However, due to it's extremely large size and the probability that it is formed among the carbohydrates *in situ*, lignin is extremely difficult to extract from wood without changing its structure.

Softwood lignin is mainly composed of the guaiacyl phenyl propane (G) units, as shown in Figure 1.6, with one methoxyl group on the aromatic ring. However, there are some aromatic groups that don't contain a methoxyl group, and these are called *p*-hydroxyphenyl propane (H) units. The lignin of hardwoods and grasses also contain syringyl phenyl propane (S) units, along with the other two types, G and H (shown in Figure 1.7). Lignins are

sometimes characterised by the ratios of these three groups. This is discussed in more detail in Chapter 5.

Figure 1.6. Basic phenyl propanoid (C9 unit)

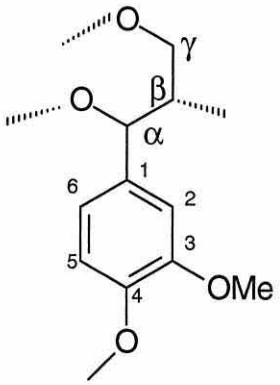

Figure 1.7. Different types of lignin units

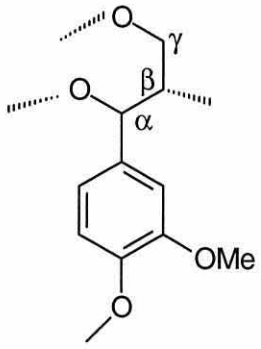

G unit

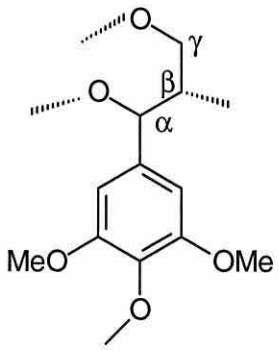

S unit

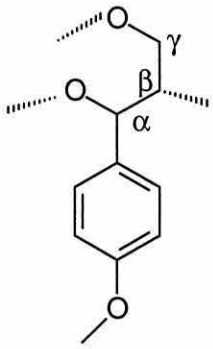

H unit

The proposed bonding types for lignin in softwood are shown in Figure 1.8 and are mostly from a review of Brunow (2001). However, some are based on the NMR analysis of softwood lignins (either RSCL or MWL; Ede and Brunow, 1992 or Kilpeläinen *et al.,* 1994, respectively). From these and other studies, Brunow (2001) has formed a model of softwood lignin, which is shown in Figure 1.9.

Linkages are named for the primary or first radical coupling reaction during lignin formation. The major bonding structures in softwood lignin, shown in Figure 1.8, are the β–O-4 linkage (**1**), and the cyclic β-5 (and α-O-4) linkage (**2**). The evidence for structure **3** (5-5-O-4) has recently been established

(Ämmälahti *et al.,* 1998) for both softwood and hardwood lignins. The bicyclic resinol β-β linkage (**4**) is a well-established structure, but is a more minor structure in terms of frequency.

Figure 1.8. Proposed bonding structures in softwood lignin (Brunow, 2001; Ede and Brunow, 1992; Kilpeläinen *et al.,* 1994)

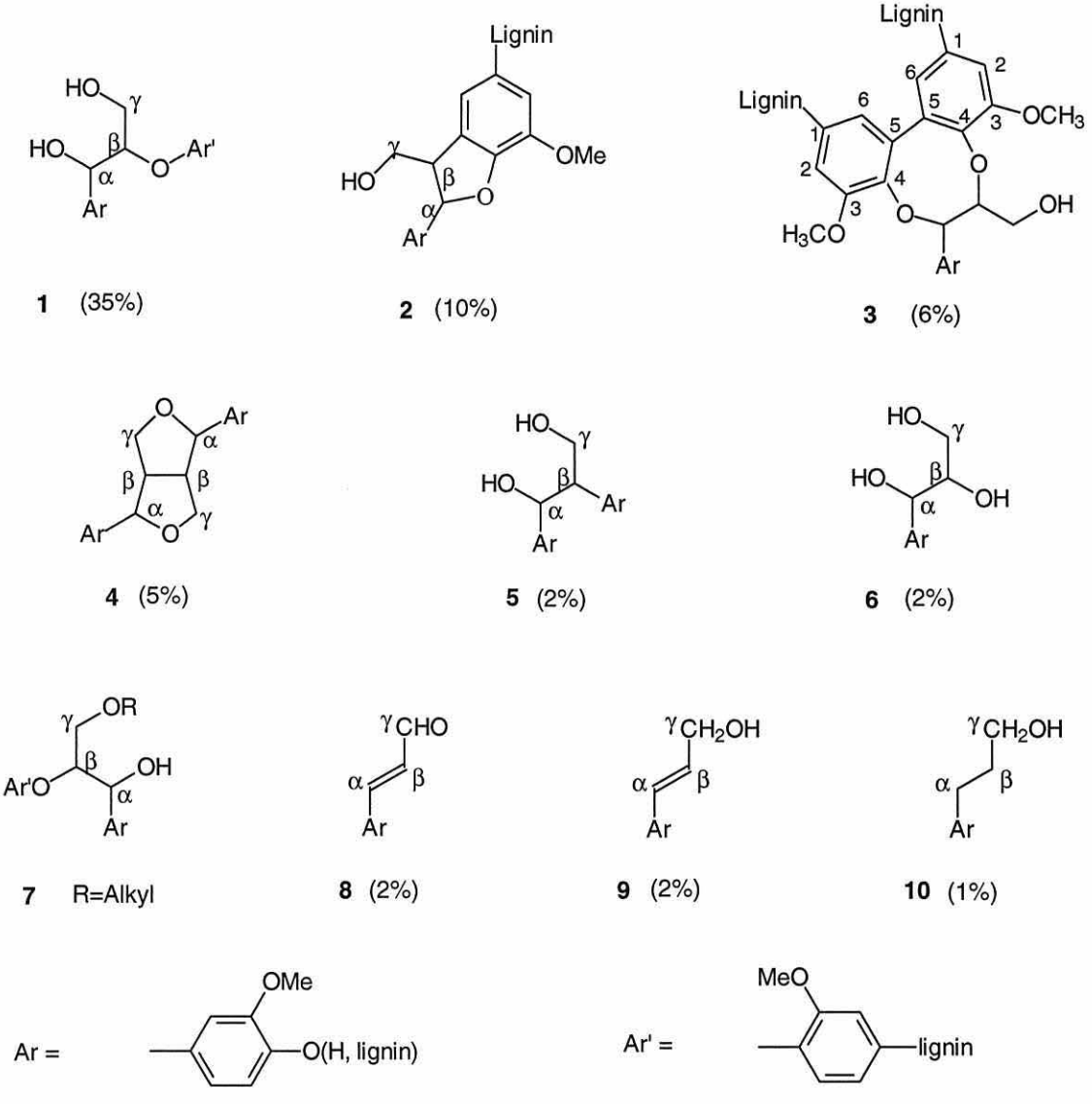

Adler (1977) estimated that there was around 2% of structure **4** in softwood lignins, but more recently Brunow (2001) has estimated these structures to be a little more prevalent at 5%. Ede and Brunow (1992) did not find much evidence for structure **5** (β-1 linkage), but a later study (Kilpeläinen *et al.,* 1994) did confirm its presence in softwood MWL. The presence of minor

structure **6** was confirmed (Kilpeläinen *et al.,* 1994). The evidence for structure **7** was reported to be obscured by that of structure **1**, but matches well data from the equivalent model compound (Kilpeläinen *et al.,* 1994).

Figure 1.9. Partial structure of softwood lignin (Brunow, 2001)

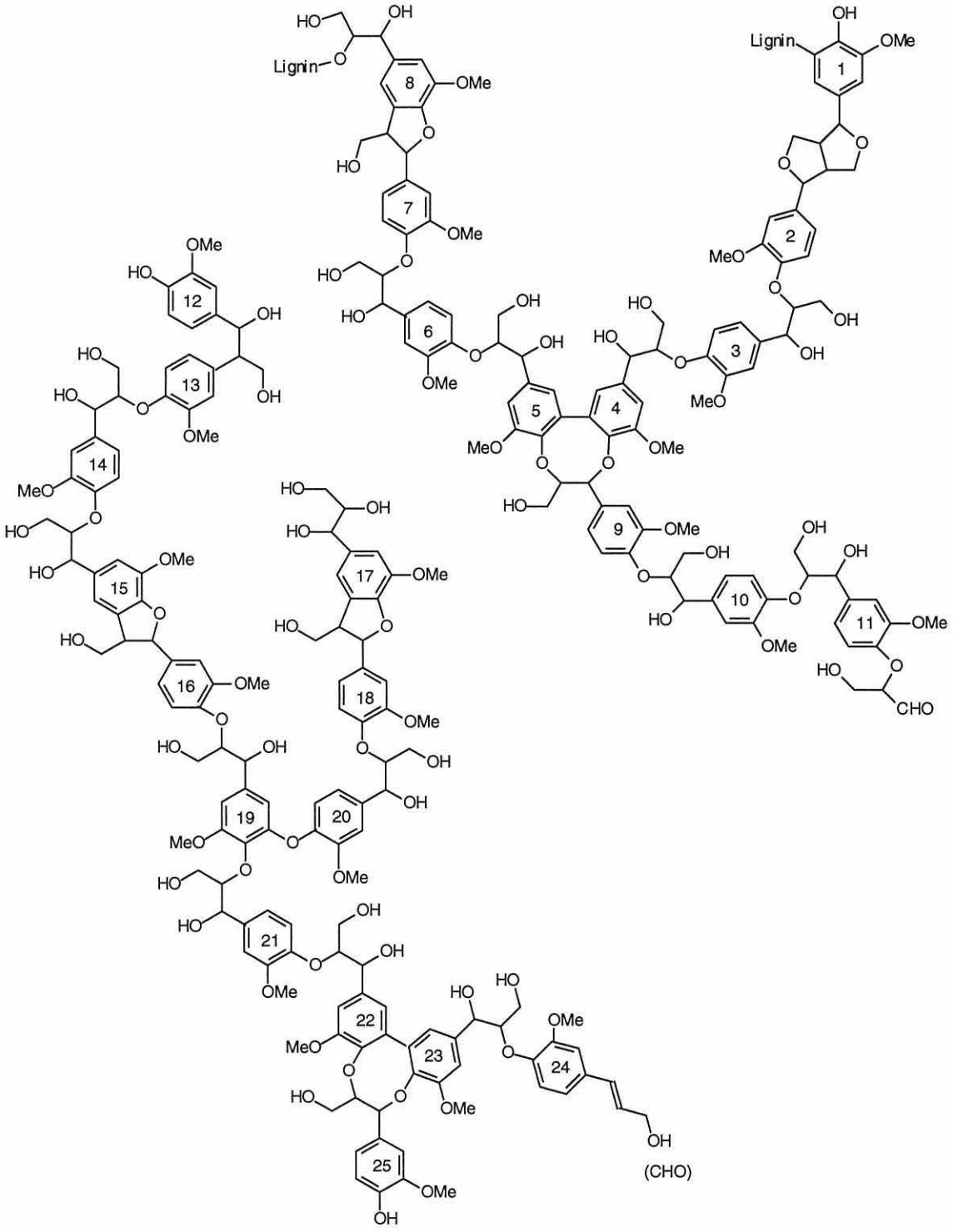

The model for softwood lignin from Brunow (Figure 1.9) has 25 aromatic groups (Ar), with the vast majority of the non-cyclic linkages shown to be of the β-O-4 type (for example, between aromatic groups 6 & 7, 5 & 6, 14 & 13 in Figure 1.9). The only form of the α-O-4 bond that appears in this model is as part of a cyclic linkage; for example, between Ar 16 and 15. In this lignin model, there are comparatively few phenolic hydroxyl groups (3 out of a total 42 OH), as these react to form the linkages between the Ar groups.

The methods used to isolate the wood components from wood need to be chosen very carefully, to obtain isolates that are as near to the native components as possible. This is particularly so for lignin. Acid hydrolysis methods give good yields, but significantly change the structure and properties of lignin, mainly by condensation (Fengel and Wegener, 1989), so these methods are generally used for estimating lignin content of a sample. There are milder methods of extraction which give rise to much lower yields, but do not change lignin as much. The different methods available and the choices made for this work are discussed in the appropriate results chapters (Chapter 5 for lignin).

1.4. Chemical modification of wood

All of the major wood components (cellulose, hemicelluloses, lignin) contain many relatively reactive hydroxyl (OH) groups, which are involved in many of the degradative reactions that wood undergoes; for example, colour change, surface erosion, biological decay, swelling and shrinkage (Rowell, 1983; Banks and Owen, 1987). One approach to limit these undesirable reactions is to substitute or derivatise these hydroxyl groups with less reactive groups (e.g. acetyl, urethane). A reaction of this nature with wood chemically changes or modifies the wood, so that it behaves differently in terms of performance. The extent of reaction is often reported in weight percent gain (WPG) units, which is convenient and easy to calculate. The oven-dried weight of the wood (or other substrate) is measured before and after the reaction and the difference is calculated over the original weight.

1.4.1. A review of literature

The use of chemical and other treatments to modify the wood and improve wood properties is not a recent area of research. Stamm and Baechler (1960) examined various treatments to improve decay resistance and dimensional stability, including acetylation. They found that all the treatments improved the decay resistance and dimensional stability to some extent. Kumar (1994) conducted an extensive review of the various ways in which chemical modification of wood can improve various properties. The chemical modification of the wood hydroxyls included formation of ethers with reaction of methyl iodide or dimethyl sulphate, formation of acetals from reaction with various aldehydes, formation of esters via acetylation with acetic anhydride, ketene gas or thioacetic acid, and formation of a urethane bond by reaction with isocyanates (Kumar, 1994).

Matsuda (1996) also reviewed the various chemical modification treatments of solid wood. The main modification methods were etherification, esterification and thermo-plasticisation of wood. Methods of etherification mentioned were benzylation (mainly on wood meal or the surface of blocks), allylation (for example, with allyl bromide and NaOH), cyanoethylation (with acrylonitile), acetalation (for example, with formaldehyde), and treatment with epoxides. Esterification included acetylation, treatment with higher aliphatic acid, acid anhydride or acid chlorides, treatment with cyclic dicarboxylic acid anhydrides (for example, phthalic, maleic or succinic anhydrides), and oligoesterifcation (where reactive carboxyl groups previously introduced reacted with epoxy groups).

Properties of wood can be altered (favourably or adversely) by reacting the hydroxyl groups. For example, dimensional stability is greatly improved on acetylation (Popper and Bariska, 1975). However, sometimes the mechanical properties can be reduced (Rowell, 1996).

Some property improvements induced by chemical modification have recently been found to be due to the physical effects of modification, rather than the

chemical changes introduced. Hill and Jones (1996) investigated the effect of chain length of linear anhydrides on dimensional stability. They found that the improved dimensional stability was primarily due to the bulking effect of the treatment, rather than how many hydroxyl groups were substituted. They found that even with differences in chain length (and thus number of hydroxyl groups changed for a particular WPG), WPG was a good indicator of dimensional stability.

Reaction of wood with ketene gas has been studied (Rowell *et al.,* 1986; Rowell *et al.,* 1991), and reasonable levels of reaction obtained. However, it was found that ketene-modified flakeboard particles (20 WPG) did not give the same level of dimensional stability as did particles reacted with acetic anhydride to the same level (Rowell *et al.,* 1986). However, acetylation of hydroxyl groups in wood is readily achieved by reacting wood with acetic anhydride (Rowell, 1983).

Acetylation of wood and wood-based products has been studied for many years, with much of the work focused on the property improvements achieved (Goldstein *et al.,* 1961; Imamura and Nishimoto, 1987; Vick *et al.,* 1991; Plackett *et al.,* 1992, Dunningham *et al.,* 1992, Takahashi *et al.,* 1989). In particular, dimensional stability and decay resistance are significantly improved. For example, a number of workers (Hill and Jones, 1996; Clermont and Bender, 1957) have found that wood that has been reacted to 20% weight gain shows about 70% improvement in dimensional stability (as measured by anti-shrink-efficiency, ASE). Decay resistance of acetylated wood towards white rot (*Coniphora versicolor*) and brown rot (*Serpula lacrymans*) was improved significantly compared to control samples. However, the level of acetylation needed to confer decay resistance varies with wood species and decay organisms (Takahashi *et al.,* 1989).

Weathering resistance has also been investigated by a number of workers (Plackett *et al.,* 1992, Dunningham *et al.,* 1992, Evans *et al.,* 2000). Wood exposed to accelerated weathering showed a reduction of surface erosion and checking, with some photo-protection (Plackett *et al.,* 1992). However, it

seems that at least in some cases the photo-protection does not last (Hon, 1995; Kiguchi, 1992), and the lignin on the surface of the acetylated wood is not photo-stable (Dawson and Torr, 1992). Acetylated wood exposed to natural weathering showed reduced amount of erosion and checking but not of color change (Dunningham *et al.,* 1992). It appears that acetylated wood is susceptible to stain and mould fungi colonisation, albeit at a slower rate than untreated wood (Wakeling *et al.,* 1991). Evans and others (2000) found that low levels of acetylation increased weight loss when samples were exposed to natural weathering.

Many different wood species show improved properties after acetylation, although some species are more readily treated than others (Goldstein *et al.,* 1961; Andersson and Tillman, 1989). Yano *et al.,* (1986) found that acetylation improved the acoustic properties of Sitka spruce.

1.4.2. The reaction mechanism of acetylation

The acetylation reaction with wood hydroxyls is shown in Equation 1.1. The reaction of acetic anhydride with an alcohol (or hydroxyl) is a nucleophilic substitution reaction, with respect to the reaction of the anhydride (Hill and Papadopoulos, 2002; Happer *et al.,* 1972), but with respect to the hydroxyl, the hydrogen is derivatised to form the acetate as the oxygen remains the same.

Equation 1.1. Reaction of wood with acetic anhydride

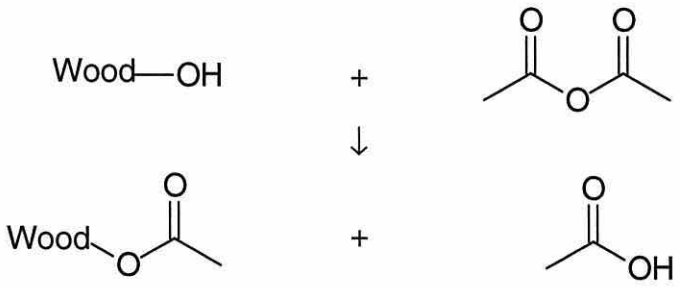

In summary, a bond is formed between one of the carbonyl carbons of the anhydride and the oxygen of the hydroxyl group, as the intermediate step in

the formation of the acetate (Equation 1.2). More specifically, the formation of this bond is facilitated by the addition of H^+; in this case, which the acetic acid by-product could provide. In this instance, the reaction could be said to be auto-catalysed. This possibility is discussed in more detail in section 1.5.5.

Equation 1.2 shows the various steps in the mechanism, each of which is reversible. The carboxyl oxygen of the anhydride can be protonated, forming an electrophilic centre at the carbon. This is then attacked by the oxygen atom of the alcohol, acting as a nucleophile (Wood *et al.,* 1968, using acetic acid as the example), forming the new bond between the oxygen and the carbon of the anhydride.

Equation 1.2. Reaction mechanism of the acetylation reaction

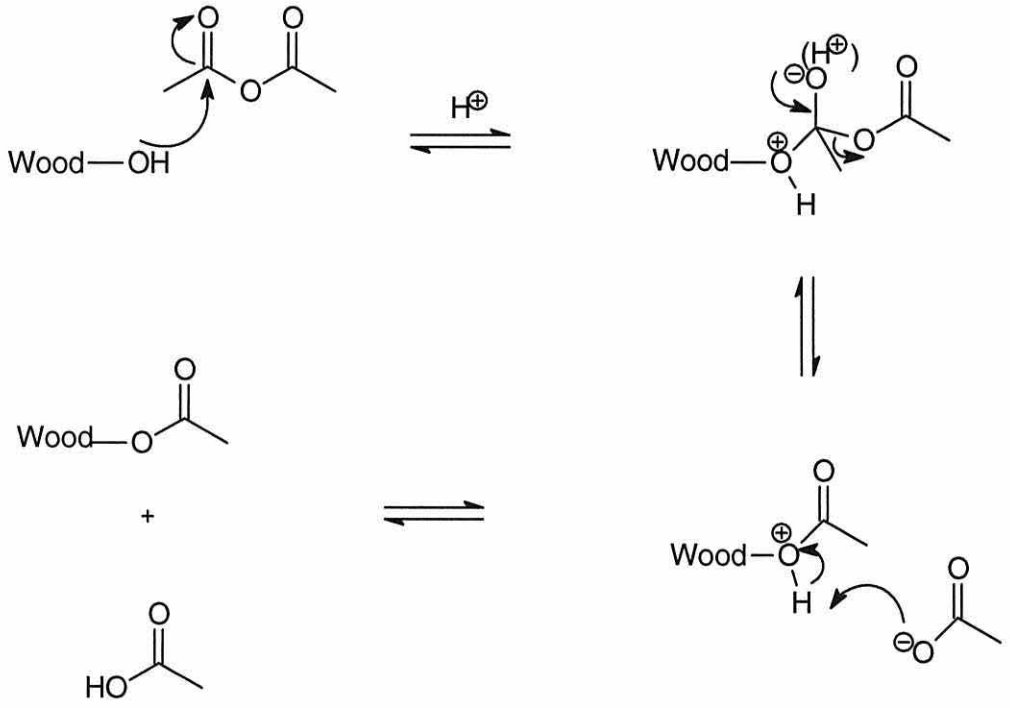

When this study commenced (1993), there had not been many kinetic studies that investigated the basic parameters that influence the rate of reaction, such as catalyst, swelling agents in combination with optimal time and temperature, nor investigated in a semi-quantitative manner the degree to which the cellulose, hemicelluloses and lignin had reacted. Since this time, there have

been a number of studies published since the practical work in this study was mostly completed. These are discussed in section 1.5.6.

1.5. Introduction to kinetics

Chemical kinetics is the study of the rates of chemical reactions. This generally involves the investigation of three variables: time, concentration and temperature. The reaction rate is a measure of how rapidly a reaction occurs; for example, the change of a reactant or product concentration with respect to time. Quantitative rate data can help in the elucidation of mechanism (Pilling, 1975). Most rate studies are based on reactions in one phase (liquid or gas), i.e. homogeneous reactions. The differences between homogeneous and heterogeneous reactions will be discussed later (section 1.5.4). The simplest case is where there is only one reactant, which reacts irreversibly to form the product(s). However, in the case of acetylation of wood, the reaction involves two reactants, which are converted to two products.

1.5.1. Reaction order

A rate law is an expression relating the rate of a reaction to the rate constant and the concentrations of the reactant(s) raised to the appropriate powers (Chang, 1981). The reaction order is the power to which the reactant concentration is raised (in the rate law). If the reaction is dependent on the reactant concentration to the first power, then the reaction is said to be first order. If the reaction is dependent on the reactant concentration to the second power (which is rare) or the reaction has two reactants and is dependent on each to the first power, then it is said to be second order. If it is not dependent on the reactant concentration, then it is zero order. More complex reactions can have fractional orders; for example, where A reacts with B, and the reaction is dependent on $[A]^1$ and $[B]^{1.5}$. This reaction would have the order of 2.5.

Most important reactions involve more than one reagent. The order of the reaction then is dependent on the sum of the power terms. If the reaction is

dependent on the concentrations of both reactants, it is often possible to make reactions quasi-1st order by keeping one of the two reagents in large excess so that the change in concentration of that reactant does not influence the rate. Commonly, reactions are first order with respect to each reactant, for homogeneous reactions.

Take a reaction expressed as in Equation 1.3 below, with A and B as the reactants, and P and Q, the products.

$$aA + bB \rightarrow pP + qQ \quad \text{..... Equation 1.3}$$

where a, b, p and q are the quantities of A, B, P and Q respectively consumed or produced in the reaction

The measured rate of reaction is usually observed to be dependent on the concentrations of the reactants (as in Equation 1.4); that is, the rate law. The rate constant (k) is not dependent on reactant concentration, but is usually dependent on temperature.

$$\text{Rate} = -d[A]/dt = k[A]^x[B]^y \quad \text{..... Equation 1.4}$$

where k is the rate constant; t is time; [A], [B] are the concentration of reactants A and B respectively; reaction order is x+y

The stoichiometry of a reactant consumed in the reaction (*a* or *b* in Equation 1.3) is not necessarily the same as the power of the reactant concentration on which the rate is dependent (*x* or *y* in Equation 1.4). For example, the decomposition of acetaldehyde (Aa), which is a second order reaction in the gas phase, consumes one mole of acetaldehyde from the balanced reaction (Equation 1.5), but its rate is dependent on $[Aa]^2$ (Chang, 1981).

$$CH_3CHO \longrightarrow CH_4 + CO \quad \text{..... Equation 1.5}$$

The homogeneous reaction of acetic anhydride and an alcohol would normally be a second order reaction, with the reaction rate dependent on both the anhydride and the alcohol to the first power. However, if one reactant (either the anhydride or the alcohol) is in a large excess over the other, then the reaction can be forced into a pseudo-first order situation. This can simplify the

kinetics since it enables one to focus on just one of the reactants, rather than both of them.

1.5.2. Reaction rate

The reaction rate can be given by the rate constant for a particular temperature. There are two types of rate constants that can be determined: the initial rate constant, and the first order rate constant. The latter assumes that the reaction is first order (or pseudo-first order). For the former method, one measures the initial slope of the reaction profiles to obtain the initial rate constants for each temperature. To determine the first order rate constant, the rate law (Equation 1.6, for a pseudo-first order reaction) is integrated (Equation 1.7) and this relationship plotted for each temperature.

$$-(d[A]/dt) = k_1[A]_o \quad \text{..... Equation 1.6}$$

$$\therefore -\int d[A]_t/[A]_0 = k_1.dt$$

$$\therefore \int d[A]_t/[A]_0 = -k_1.t + c$$

$$\ln([A]_t/[A]_o) = -k_1 t + c \quad \text{..... Equation 1.7}$$

where $[A]_t$ is the concentration of A at time, t; $[A]_o$ is the concentration of A at start (time=0); k_1 is the first order rate constant; and c is a constant.

In other words, the natural log (Ln) of (A_t/A_o) versus time is plotted and assuming linearity, the slope = $-k_1$ (the first order rate constant). Both types of rate constants can be used in the Arrhenius equation (Equation 1.8).

1.5.3. Activation energy

In order for chemical reactions to occur, the reactants need to be activated energetically. In other words, there is an energy barrier (the activation energy, Ea) to the reaction occurring (Figure 1.10). The implication of this energy barrier is that, given sufficient energy, the reaction may be reversible, and this is the case for many reactions.

Figure 1.10. The energy barrier between reactants and product(s)

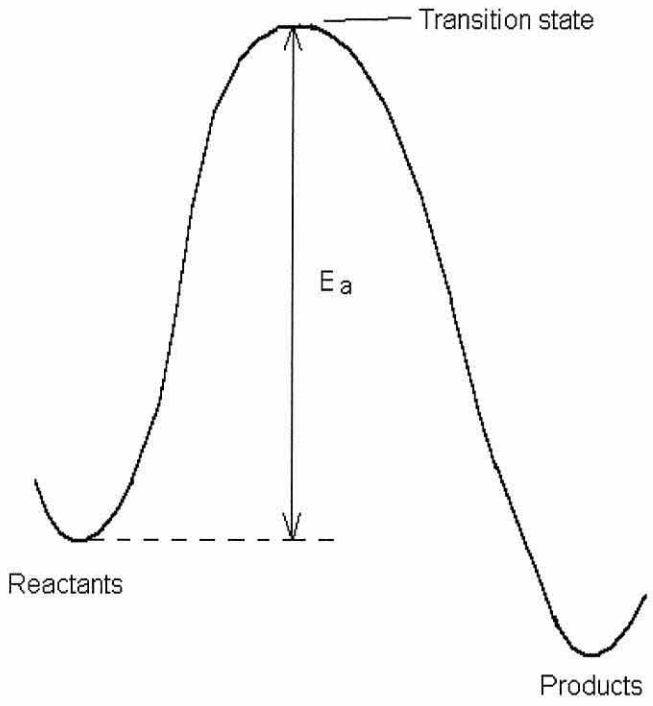

From the Arrhenius equation (1.8), it can be seen that activation energy, Ea, can be obtained by plotting Ln(k) against 1/Temperature, since the other terms in the equation are constants.

$k = A\, e^{-(Ea/RT)}$ ..... Equation 1.8 (Arrhenius equation)

where k = rate constant
A = pre-exponential constant
Ea = activation energy
R = gas constant
T = absolute temperature (in degrees Kelvin).

1.5.4. Homogeneous and heterogeneous reactions

A homogeneous reaction is a reaction where both reactants are in the same phase; for example, the reaction of two liquids that are miscible (or two substances dissolved in the same solvent). A heterogeneous reaction is a reaction where the two reactants are in two different phases; for example, reaction between a liquid and a gas, or between a solid and a liquid.

In a heterogeneous reaction between a solid (for example, a resin particle) and a substance dissolved in a liquid, then three steps may influence the rate

of reaction. These are (1) diffusion of the reactant in the liquid to the surface of the resin particle, (2) diffusion within the particle, and (3) chemical reaction in the solid particle (Walas, 1959). For ion-exchange reactions, the chemical reaction step is relatively fast, and thus these type of reactions (if in steady-state) are limited by diffusion in either the solid or the liquid.

The rate of a solid-liquid heterogeneous reaction can also be dependent on the amount of interfacial surfaces. For the reaction of wood, this would mean the size of the wood particles to be reacted.

1.5.5. Diffusion controlled reactions

Up until now, the rate of the reaction has been considered as dependent on the concentration of a reactant. This is referred to as being activation controlled and refers to the need of the reactant to be sufficiently activated for reaction to take place. However, if a reactant needs to diffuse through a matrix to a reaction site, and this diffusion process is slower than the activation of the reactant (or reactivity), then the reaction is said to be diffusion controlled. In this case, the diffusion is the rate-determining step, and the rate is not dependent on the reactant concentration (although the rate of diffusion is controlled by the concentration gradient). Therefore, the rate law will be a diffusion equation, such as Fick's diffusion laws.

Due to the heterogeneous nature of the wood acetylation reaction, the reactant (acetic anhydride) will need to diffuse through the wood structure (cell wall) in order to react with all accessible hydroxyl groups. The wood hydroxyl groups themselves do not have the ability to move freely through the reaction solution. The relative speed of this diffusion compared to the activation of the intermediate (transition state) will determine whether the wood reaction will be diffusion or activation controlled. In the former case, Fick's second law applies (Equation 1.9); that is, diffusion as a time dependent process.

$$(dR/dt) = D.(d^2R/dx^2) \quad \text{..... Equation 1.9}$$

where R is the reactant concentration at position x, time t
D is the diffusion coefficient
x is distance travelled.

The solution of this diffusion equation (Equation 1.9) with initial boundary conditions (all R_o solute particles are concentrated on the *yz*-plane at x=0) is shown in Equation 1.10. If one then substitutes the values of x for the root mean square distance ($x_m = (2Dt)^{1/2}$) into Equation 1.10, an equation for R (Equation 1.11) is obtained that is dependent on square root of time (Atkins, 1978). For a more complete treatment of these relationships, refer to Atkins (1978, pp836-9).

$$R = \{R_0/A.(\pi.D.t)^{1/2}\} .\exp(-x^2/4.D.t) \quad \text{..... Equation 1.10}$$

where R_0 is the concentration of the reactant at time=0
A is the cross-sectional area

$$R = \{R_0/A .(\pi.D.t)^{1/2}\} .\exp(-2/4) \quad \text{..... Equation 1.11}$$

If the reactant concentration at a particular place and time (i.e. the way it travels) is dependent on square root time ($\sqrt{t}$), and the extent of reaction is plotted against the $\sqrt{t}$, and the resultant relationship is linear, then this confirms that reaction is diffusion controlled. This would assume that the initial concentration (R_0), the diffusion coefficient (D), and the cross-sectional area (A) are constant. The latter assumption may not be true in the uncatalysed wood acetylation reaction (not pre-swollen), as the wood cell wall may swell upon reaction and upon contact with hot acetic anhydride. However, the change in the cross-sectional area may not be large enough to change this relationship.

Hill *et al.* (1998) developed a similar relationship when investigating the pyridine-catalysed acetylation of wood. They used an expression of Fick's law as described by Pannitier and Souchay (1967) to obtain Equation 1.12.

$m^2 = -2.D.r.S^2.c.t$ ..... Equation 1.12

where m is the mass of material diffusing
D is the diffusion coefficient
r is the density of the reagent
S is the surface area through which the reagent is diffusing
c is the concentration gradient
t is the time.

$m = a.t^{1/2}$ ..... Equation 1.13

where *a* is a constant related to the rate of diffusion.

If it is assumed that D, S, r, and c are constant, then the expression becomes Equation 1.13. The surface area (S) may not be constant with temperature (and other factors), but in the case of pre-swollen blocks using pyridine as Hill and others used (1998), it was a reasonable assumption.

The reaction of cotton and jute fibres with acetic anhydride was considered to be, at least partially controlled by diffusion, although the type of diffusion was influenced by whether the reaction was conducted in swelling or non-swelling conditions (Sen and Ramasway, 1957).

McKenzie and Higgins (1955a,b) studied the pyridine-catalysed acetylation of eucalypt α-cellulose and the effect milling or beating had on reactivity towards acetylation. They found that as the reaction progressed, there was an increase in soluble material, which could be precipitated in ethanol and water (1955b), and that the degree of substitution (DS) was much higher for the soluble material than it was in the residual cellulose fibres.

McKenzie and Higgins (1955b) also studied the kinetics of the acetylation of cellulose. They commented that the heterogeneous nature of the reaction relegated the relative reactivity of the OH groups to a less important position. They mentioned that earlier studies had found it impossible to determine the order of reaction due to the lower level of reactivity. However, McKenzie and Higgins (1955b) looked at the assumptions of diffusion control of different types. One of these was the Ostwald-Sakurada treatment which describe the kinetics of cellulose acetylation empirically in the form:

$x = k.t^n$ ..... Equation 1.14

where x is the quantity of material (cellulose) reacted in time, t and k, n are constants.

Therefore, by plotting log x against log t, a straight line is obtained. An assumption made in this relationship that the extent of reaction is proportional to the length of the diffusion path, and other workers (referenced in McKenzie and Higgins (1955b), but not cited here) found that this assumption was probably valid in micellar- or macro-heterogeneous reactions.

However, McKenzie and Higgins were not convinced as to the validity to other types of reactions, and with such little justification. They discussed another treatment from Crank, who had studied the penetration of dye in cellulose fibres. The idea of diffusion can be represented by a simple diffusion equation, with a diffusion co-efficient, which is dependent on concentration. McKenzie and Higgins (1955b) found that this approach was more applicable for a diffusion controlled reaction of cellulose, in which the reagent was consumed as fast as it reaches the site of reaction; for example, a Freundlich equation of the form given in Equation 1.15. The (variable) diffusion co-efficient related to the concentration of the dye in solution, c_p , as in Equation 1.16.

$x = k'.c_p^m$ ..... Equation 1.15

where x is the overall concentration of the dye adsorbed,
c_p is the concentration of the free dye in solution in the pores and capillaries per unit volume of water, and
k' and m are constants ($0 < m < 1$).

$$D_c = D_p.v.\frac{dc_p}{dx}$$ ..... Equation 1.16

where D_c is the variable diffusion co-efficient
D_p is the diffusion coefficient of the free dye along the pores with no adsorption (constant)
v is the volume fraction of water-filled pore space

If it is assumed that, for the application of this approach to acetylation of cellulose fibres, all the acetic anhydride absorbed by the fibre eventually

reacts, then the DS can be equated with the overall concentration, x. The kinetic data therefore refer to the overall concentration of material absorbed by the fibre at time t, rather than what has reacted with the hydroxyls (McKenzie and Higgins, 1955b). Note that this assumption is for theoretical purposes rather than for practical applications.

A solution of the diffusion equation for a cylinder by Crank, which can correspond to a fibre of circular cross-section, is given in Equation 1.17.

$$\frac{c_t}{c_\infty} = \frac{4\sqrt{D_p}.\sqrt{t}}{\sqrt{\pi}.r} \quad \text{..... Equation 1.17}$$

where c_t is the overall concentration at time t
c_∞ is the overall concentration at equilibrium ($t=\infty$)
D_p is the apparent diffusion co-efficient
r is the radius of the fibre

Equation 1.17 applies where only a small proportion of the reagent is consumed, and the absorption of the fibre does not exceed 50% of the saturation value. Then by substituting $c_t = v.c_p$ into Equation 1.1.7 and combining the constants to get K, one obtains Equation 1.18.

$$c_p = K.\sqrt{t} \quad \text{..... Equation 1.18}$$

All these various approaches to describing diffusion of a reactant in a solid second reactant arrive at a similar relationship; that is, the concentration of the material diffusing is proportional to the square root of time. If one assumes, as McKenzie and Higgins (1955b) did, that the amount of material that diffuses eventually reacts, then one can plot the extent of reaction against √time to determine if the reaction is diffusion controlled.

McKenzie and Higgins (1955b) noted that, although temperature, concentration of reagent, and degree of swelling may alter the mechanism and/or rate of the reaction of cellulose acetylation, it was more likely that such an alteration would be brought about by a change in fibre structure, rather

than the chemical process or conditions (because of the diffusion control of the reaction).

If a reaction is activation controlled, then the rate of the reaction will be directly dependent on one (or more) reactant concentration, and the activation energy of the reaction can be calculated from the k values obtained from the appropriate rate law (e.g. first or second order). However, if a reaction is diffusion controlled, the reaction activation energy has to be approximated from the initial rate constants (k_o), as a first or second order rate equation is not applicable. The activation energy values calculated from the initial rate constants will apply to the surface reaction, which occurs with little or no diffusion (Hill *et al.,* 1998; West, 1988). Thus, it won't describe the reaction once diffusion becomes a limiting factor. Therefore, the comparison of the activation energy from initial rate constants may be of limited value in diffusion controlled reactions.

However, the Arrhenius equation can also be applied to the diffusion process (Hill *et al.,* 1998), as diffusion can be considered to have an energy barrier associated with it. Thus, Equation 1.13 can be rewritten as Equation 1.19 by substituting the Arrhenius relationship for the constant (*a*), which in turn can be rearranged as Equation 1.20. (Hill *et al.,* 1998):

$$m = A.\exp(-Ea/RT).\sqrt{t} \quad \text{..... Equation 1.19}$$

$$\ln (m/\sqrt{t}) = \ln (a) = \ln (A) - Ea/RT \quad \text{..... Equation 1.20}$$

Therefore, the activation energy of diffusion can be calculated from the slope of the plot (assuming linearity) of the natural log of the *a* values (obtained from the diffusion plot for each temperature) against 1/Temperature (in degrees Kelvin). It is more likely that for a diffusion controlled reaction, the comparison of the activation energy of diffusion will give useful information on the effects of various reaction parameters and/or the influence of wood species.

1.5.6. Application of kinetics to wood

Classical kinetics are usually applied to simple reaction systems; for example, the gaseous reaction between O_2 and H_2 to form water. The reactants are in the same phase, and the reaction is readily monitored and quantified. However, wood is a complex natural product, which is composed of three main polymer groups. This means that wood samples are variable in their composition to some degree, and being complex are also difficult or impossible to definitively characterise. The reaction of wood with acetic anhydride is a heterogeneous reaction, between a solid and a liquid. This means that some of the assumptions that are made in classical kinetics are not exact. Nevertheless, it is possible to apply kinetic principles to this reaction and obtain some accurate information about the reaction, and in this case, the reactivity of the wood polymers *in situ*. One can make approximations about the acetylation reaction, so analysis is possible.

For example, one assumption that has been made is that there was only one population of hydroxyl groups in wood (and other samples), which reacted at the same rate, with the same mechanism. This is obviously not true, as was illustrated in section 1.3 on wood chemistry. It is clear that there are primary and secondary OH in the carbohydrates, as well as phenolic OH groups in lignin. However, if the reaction with wood is diffusion controlled, then this factor becomes less important. Another assumption is inherent in the application of the Arrhenius equation, which uses R, the gas constant. This would imply that the reaction system that the equation is being applied to is a gaseous system. However, it has been found that the Arrhenius equation does fit well for reaction systems in other phases.

A further assumption is that having a excess of acetic anhydride in which a solid wood sample is reacted, that there are not local concentration gradients that affect the rate of the reaction. However, when a solid is reacting with a liquid, the reactant contained in the solid is not free to move around in a random fashion, as would be the case with liquid or gas reactants. In addition, as the liquid reactant moves within the solid, its movement will probably also be restricted.

Hill and Papadopoulos (2002) discussed the effect of pore size and geometry in wood cell walls on the movement of molecules. They were investigating a range of anhydrides with increasing molecular size, and found that activation energy decreased as molecular weight (of the reacting anhydride) increased. However, the Hill and Papadopoulos (2002) study was conducted with pre-swollen blocks in pyridine which was also used as a catalyst, which they considered would still restrict movement of anhydride molecules through the wood cell wall. They suggested that the motion of acetic anhydride was not affected by the cell wall micropores, as the activation energy value they obtained for the uncatalysed reaction was 51 kJ/mol , similar to that of homogeneous reaction of acetic anhydride with ethanol (52-66 kJ/mol) in CCl_4, although the Ea values were higher (72-79 kJ/mol) when conducted in pure ethanol (Hill *et al.,* 1998). However, catalysis does lower the Ea value, which might put it in range of the activation energy of the homogeneous reaction.

Table 1.2. Comparison of activation energy values for various reactions with acetic anhydride

Sample	solvent	catalyst	Ea (kJ/mol)
Wood	none	none	51 [a]
Wood	pyridine	pyridine	37-43 [b]
Guaiacol	pyridine	pyridine	40-44 [b]
Ethanol [c]	Heptane	none	47
	Hexane	none	52
	CCl_4	none	58-66
	Ethanol	none	72-79

[a] Hill *et al.,* 1998
[b] Hill and Papadopoulos, 2002
[c] Values obtained from Hill *et al.,* 1998, original references not cited.

Activation energy values for a range of substrates are compared in Table 1.2. The reactions of guaiacol and ethanol would be homogeneous reactions, whereas the wood-acetic anhydride is a heterogeneous reaction.

Hill and Hillier (1999) have also applied percolation theory to the diffusion of molecules through wood cell walls. They considered a two-dimensional pore network (lattice) of the cross-section of a tracheid cell wall, made into a rectangle with the left and right edges joined as in Figure 1.11.

Figure 1.11. A cross-section of cell wall as a 2-D lattice (Hill and Hillier, 1999)

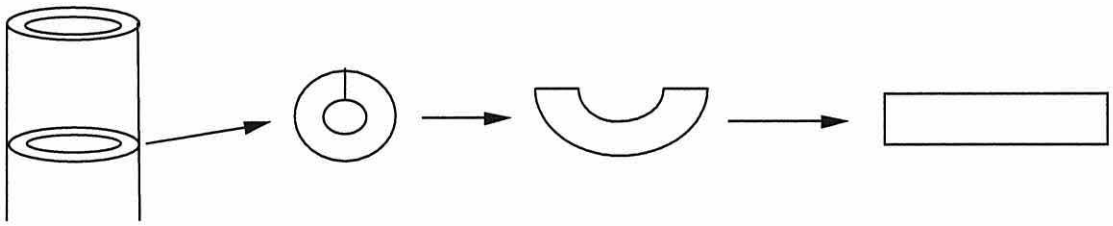

Figure 1.12. An example of a percolation network with values of ρ of 0.4 (a), 0.6 (b) and 0.8 (c) (Hill and Hillier, 1999)

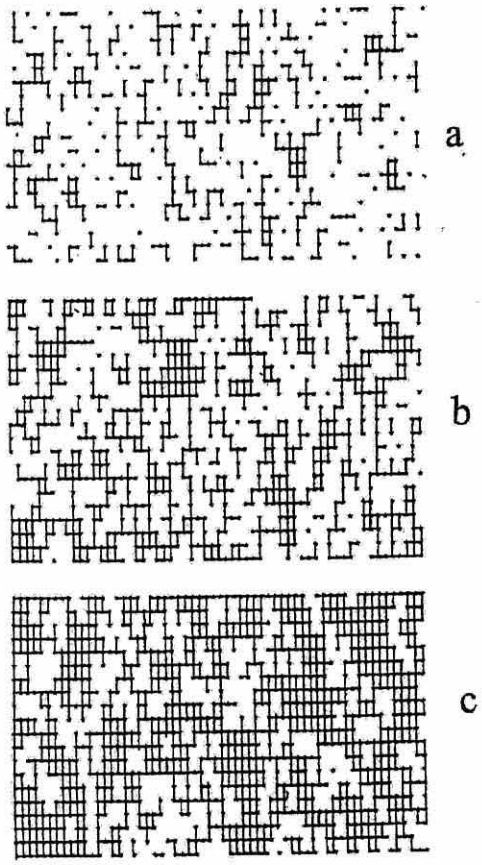

The rectangular lattice considered was 60 by 20 squares (as shown in Figure 1.12), with ρ being the probability that a single square was filled, and n the

total number of squares (or elements) within the lattice. The number of filled sites was ρn. If neighbouring squares were filled then they formed a cluster together. Applying this theory, they found that if diffusion was standard, where a single molecule travels average distance, A(t), then A(t) was proportional to $\sqrt{t}$ (Fick's 2nd law of diffusion).

Hill and Hillier (1999) found that the reaction data for carboxylic acid anhydrides and wood could be explained in terms of the percolation theory of diffusion through a porous network by altering r (the reaction probability of when the diffusing reactant anhydride collides with a wood hydroxyl), with ρ=0.6, which was close to the percolation threshold. They concluded that, because diffusion mechanisms dominated the reaction with acetic anhydride, the relative rates of reaction of the various OH groups in the wood matrix was of relatively little importance. In fact, wood density would be more influential, as the rate of diffusion was proportional to the inverse of density (Hill *et al.,* 1998).

The void spaces in the wood cell wall reduce as wood is dried, and this will reduce the accessibility of the cell wall (Hill *et al.,* 2000). In the study here, the wood was kiln-dried from green, which would lead to low cell wall porosity. When reaction of the OH groups occurs within the cell wall, there will be localised swelling at the reaction site, which will in turn allow for the easier ingress of the reactant to the next reaction site. Krässig (1985) shows a model where reaction at the ends of the fibre (cellulose in his case) widens the cellulose lattice, thus activating the cellulose towards reaction (Figure 1.13; original reference (Spurlin, 1938) not sighted). This is sometimes described as the zipper or unzipping model (Hill *et al.,* 2000). This can be applied to micro-fibril bundles, which are encased with hemicellulose and lignin. In the study here, the wood was not pre-swollen, and so most of the swelling of the cell wall would occur during reaction.

Figure 1.13. Reaction zone progressing along crystalline cellulose region, with retention of fibre structure (Krässig, 1985).

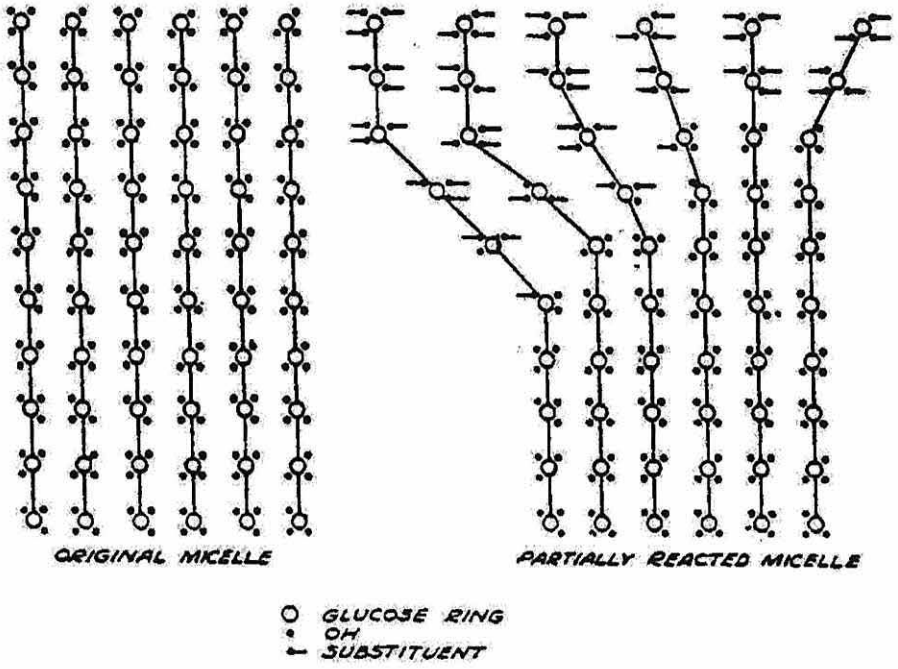

It is possible that the presence of acetic acid could facilitate the protonation of the carboxyl group of the anhydride, and thus act as a catalyst. However, it is likely that this autocatalytic effect is not a strong one. Turner and Harris (1952) noted that in the esterification of an alcohol with carboxylic acids, this autocatalytic effect is only marked with the stronger carboxylic acids (for example, halogenic acids or formic acid). Therefore, it seems likely that for esterification of wood with acetic anhydride that the autocatalytic effect of the acetic acid by-product may be present but is not likely to be strong.

Rowell (*et al.,* 1994) combined and summarised a number of groups work on the acetylation of various isolated wood polymers. Unfortunately, the various substrates used were not fully characterised, so the purity of the various substrates was not known. It also meant that for the delignified wood, the level of the acid soluble lignin was not known. However, it was shown using energy-dispersive X-ray analysis (EDXA) of chloroacetylated wood samples that, at low levels of acetylation (4.3 WPG), there was greater reaction in the secondary wall (SW) than the middle lamella (ML). At intermediate levels of

reaction (10.3 WPG), the level of reaction was approximately the same for the SW and ML, but a higher level of reaction (27.7 WPG), reaction was greater in the ML than for the SW. This latter observation was probably due to higher lignin content of the ML compared to the SW. This study showed that the probable relative rate of reaction of the wood polymers was lignin > hemicellulose > cellulose.

More recently, Ohkoshi and others (Okhoshi *et al.,* 1997; Ohkoshi and Kato, 1997) have looked at the acetyl distribution in wood components, after the acetylation of wood meal (makamba, *Betula maximowiczii*) in a mixture of acetic acid, trifluoroacetic anhydride and benzene. The acetylated wood samples were lightly delignified and then a portion was dissolved in MMNO/DMSO-d_6 (a cellulose solvent) for analysis using NMR spectroscopy. They found that cellulose was less reactive than xylan, although there were mono-, di- and tri-acetate cellulose subunits at low WPGs. The crystalline regions of the cellulose started to react above 20 WPG. However, all the hydroxyl groups were not reacted at 20 WPG for xylan in wood (Okhoshi *et al.,* 1997).

West (1988) examined the kinetics of the wood-isocyanate reaction. He found the uncatalysed reaction, which was reacted under non-swelling conditions, was slow and diffusion-controlled. Further, he found that reaction conducted under swelling conditions increased the reaction rate. From these results, he proposed that there was a need for the hydrogen bonds between hydroxyl groups to be broken before reaction could take place.

A model was also developed (West and Banks, 1986) which divided the initial stages of the reaction of n-butyl isocyanate with Scots pine into two parts: a fast part (due to the reaction of lignin) and a slower part (due to the reaction of holocellulose). The concept of this model was expanded into the attempt at forming an empirical model based on the reaction of lignin, hemicelluloses and cellulose, presented in Chapter 3 (section 3.3.3.3).

1.6. Scope of work

The aim of this study was to examine the (uncatalysed) wood-acetic anhydride reaction by studying the acetylation of wood substrates such as wood blocks, ground wood and MDF fibre. The acetylation of isolated wood polymers such as cellulose, hemicelluloses and lignin, were also examined. A lignin model compound was investigated in order to examine the relative rates of reaction of the different hydroxyl groups within it. The focus on the work was, however, on the acetylation of wood blocks and obtaining reliable kinetic data, which may help to understand the reaction in more depth. This data may help to manipulate this or similar chemical modification reactions of wood to obtain desired property improvement.

The general approach of investigating this heterogeneous reaction was to hold the acetic anhydride in large excess over the wood substrate being examined, so that the reaction was conducted in pseudo first order conditions (with respect to hydroxyl). So the acetylation reaction was conducted in pure acetic anhydride, with two or three replicates (depending on the sample). The oven-dry samples were reacted with excess acetic anhydride and the extent of reaction was primarily measured by the increase of weight due to the addition of acetyl (WPG). Acetylation reactions were undertaken at four different temperatures between 80-120 °C.

For the acetylation of the lignin model compound, the extent of acetylation was measured by ^{1}H NMR spectral analysis. Because acetylation was much faster under homogeneous conditions, the temperature range used was 60-90 °C. ^{13}C NMR spectroscopy was also used to determine the relative rates of reaction in both the model compound and milled wood lignin acetylated reaction products.

There is some repetition of information in the results chapters (3-6), as each has a short introduction and they were intended to stand, in part, by themselves. Chapter 2 gives the experimental details of the methods and analytical techniques used. Chapters 3 to 6 give the various results for the

fourteen different substrates investigated. Chapter 7 summarises the results and conclusions.

Chapter 3 gives the results of the acetylation reactions of solid wood blocks, MDF fibre, ground wood and three partially delignified ground wood samples, along with the kinetic information obtained from the reaction data. The ground wood was partially delignified to give a range of wood samples with decreasing lignin content. It was hoped to find a trend in the acetylation levels (and maybe kinetic data) obtained with the decreasing lignin content. This approach was utilised in an attempt to examine the effect of the reducing the amount of lignin in wood samples *in situ* (as opposed to studying isolated lignin).

Chapter 4 reports the acetylation of the wood carbohydrates, which included holocellulose, cellulose, and two isolated hemicelluloses, xylan and glucomannan. It was not possible to obtain reliable kinetic data from any of these samples. The two hemicelluloses reacted to lower than expected levels and so were reacted with two catalyst systems and the level of acetylation was investigated directly using FTIR spectroscopy.

Chapter 5 reports the reaction with acetic anhydride of three different lignin preparations. The first, milled wood lignin (MWL), was deemed to be a good representation of the native wood lignin from radiata pine used in this study. The second lignin preparation was a commercially obtained alkali lignin (AL) from a mixed softwood source. It was expected that the AL would give different reaction and kinetic results from the MWL, due to the chemical differences between the two samples. The third lignin preparation used was an organosolv bagasse lignin (BL), which is commercially available from an Indian supplier, and had been kindly donated for this study. This last lignin was not intended to be any kind of model for a softwood lignin, as it was from a member of the grass family rather than from wood. Further, BL may not be a good representative of lignins obtained from grasses, as it has a high p-courmaric acid content. However, as it was readily available, it was thought it might provide results in contrast to the softwood lignin samples.

Chapter 6 reports the acetylation of a lignin model compound. The model chosen was the β-O-4 model that contains a primary, secondary and phenolic hydroxyl group. More lignin models were not studied, due to the length of time that the reaction and analysis of results that one substrate requires.

Chapter 7 summaries the results, and gives some conclusions. Possible future work is also discussed.

CHAPTER 2: EXPERIMENTAL

2.1. Introduction

This chapter contains the methods used for most of the practical work in this thesis. It includes the details of the techniques used to characterise the untreated substrates and alternative methods to determine extent of acetylation.

There are numerous methods used to isolate wood components and the wood component isolates obtained vary with the method used. Therefore, the choice of appropriate isolation methods is very important. The range of methods available and the reasons for the final procedures chosen are outlined in the next section. They are discussed in more detail in the appropriate results chapter.

2.2. Discussion of choice of methods

2.2.1. Extractives

It was decided to remove the extractives from the wood-based samples prior to reaction. Extractive removal was done in order to eliminate the extractives as a variable and as sources of interference in the acetylation reaction. In addition, the removal of extractives would eliminate any loss of extractives during reaction which would affect weight calculations.

Removal of extractives before isolation of the major wood components is important. This is particularly so for lignin isolation, as some of the extractives are similar in structure to lignin and therefore would be difficult to separate (Browning, 1967). There are many methods for extractive removal, because extractives are diverse in nature, and the method chosen will depend on the species and the purpose (Browning, 1967). Usually, at least two solvents are used to remove the two broad range of extractives present. In this case, the two solvents chosen were dichloromethane and ethanol, used separately.

2.2.2. Lignin

Native wood lignin is a large and extremely heterogeneous polymer, due to its formation *via* a free radical enzyme mechanism. This type of mechanism means that the various monomer units, the phenyl propane groups, are bonded randomly with each other, in and around the hemicelluloses. There are therefore many different methods to extract lignin from wood, which vary in yield, purity and chemical composition. The choice of methods available and the background information on the lignin preparations used are discussed more fully in Chapter 5 (section 5.1).

Several lignin preparations were considered for use in this study: milled wood lignin (MWL), cellulolytic enzyme lignin (CEL), alkali lignin (AL), Kraft lignin, and organosolv lignin. For reasons of suitability or convenience, those eventually included in the study were MWL and AL. A donated sample of organosolv bagasse lignin (BL) was also included in the study.

An attempt was made to use CEL after the initial large scale MWL procedure gave very low yields (due to inefficient milling). However, although crude yields of CEL were good, much of this seemed to be lost during the purification stage, implying that much of the so-called crude lignin was in fact carbohydrates. A further disadvantage of using a CEL method is possible protein contamination from the enzyme.

2.2.3. Hemicelluloses and cellulose

Isolated hemicelluloses and cellulose from the same supply of radiata pine were required, so that comparison with the wood samples would be as accurate as possible. It is very difficult (if not impossible) to separate completely the different hemicelluloses from each other, as their structures are very similar. In addition, glucomannan is often associated with a variable amount of galactose units, and xylan is sometimes bonded to lignin. However, if fractions are obtained that are over 90% of one hemicellulose, then trends in the relative reactivities of the various hemicellulose fractions can be obtained.

The method selected was the Hamilton method (Beelik *etal.,* 1967), slightly modified, in which delignified wood meal was first slurried in barium hydroxide (2%) and then treated with sodium hydroxide (10%). An alternative method that uses borate instead of or as well as barium hydroxide was available. However, there have been problems reported of difficulty in completely removing boric acid from the hemicelluloses, so this was not used.

The xylan yield obtained in this work (5.6% of wood) is within the range obtained by other workers (Beelik *etal.,* 1967; Bicho, 1992). However, the initial glucomannan yield (2.8% of wood, first extraction) was lower than normally obtained, although an extra amount was re-extracted from the supernatant of the first extraction (giving a yield of 7.6%). If these results were corrected for their ash content, the yields were : xylan (4.5% of wood), glucomannan precipitate (2.5%, first extraction), glucomannan soluble (3.4%, second extraction). Although these yields were somewhat low, the amount of sample extracted was more than adequate to conduct the kinetic studies. The residue after the hemicelluloses were extracted was α–cellulose and the yield was 46.8% of wood.

2.3. Preparation of wood and MDF fibre samples

Solid wood samples of kiln-dried *Pinus radiata* (D.Don) sapwood from Kaingaroa forest, New Zealand were cut to dimensions 20 mm x 20 mm x 5 mm (radial x tangential x longitundinal), with the growth rings parallel to two edges (Figure 2.1). Samples were screened for defects, such as small knots, non-parallel or curvy grain, and splits or cracks. All samples were sanded and had extractives removed before use (see section 2.3.2.). Samples with abnormalities, such as high basic density (700-800 kg/m^3) or compression wood were also not used. There were four different sources of samples selected: that is, samples from four planks (and trees) of radiata pine sapwood. The samples selected for this study had even grain, average expected density and no defects. The details of each set of samples characteristics is given in Table 2.1.

Figure 2.1. Dimensions of the solid wood blocks used.

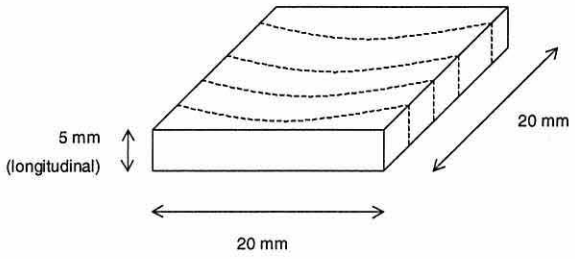

Fibre suitable for medium density fibreboard (MDF) manufacture was produced from the same batch of radiata pine sapwood, using the BioComposites Centre (Bangor, UK) MDF pilot plant. Lengths of wood were re-saturated in water before being chipped and screened to fall between 6 and 15 mm. A pre-heated pressurised refiner at 8 bar was used to refine the screened chips. The plates (single disc type D2A504) were about 30 cm in diameter and set 450-500 μm apart, with a running temperature of about 170 °C. The specific energy was 0.46 kW h/kg (oven-dried (OD) weight) and the through-put was about 54 kg/h (OD) for the MDF fibre sample used in the kinetic study. The moisture content of the MDF fibre after production and re-drying was 5.9%.

Table 2.1. Characteristics of the wood block samples

Sample [1]	No. of samples cut	Growth rings per block width [2]	Approximate density [3]
1 (4b)	93	2-3	445
2 (10b)	83	5	483
3 (23b)	92	2	499/525
4 (26b)	88	4-5	432/450

[1] Labels were to keep pieces of the same tree source separate, and 44 were assessed in total; a & b referred to two planks from the same tree.

[2] Width was 2.0 cm

[3] Density measured on source planks at room temperature and humidity, in kg/m^3

2.3.1. Preparation of wood meal

Lengths of wood were sawn to small pieces (< ~15 mm square) to fit into a "Christy" (hammer) mill. Before milling, each piece was dipped into liquid nitrogen for approximately five seconds in order to ensure the wood was not overheated during milling. Milled wood was sieved into three fractions: larger than 36 mesh (~0.425 mm square aperture), 36-60 mesh and smaller than 60 mesh (~ 0.250 mm aperture). The coarse fraction (larger than 36 mesh) and much of the middle fraction (36-60 mesh) was reground in order to ensure a good representation of the wider wood sample in the source of the MWL.

The middle fraction (36-60 mesh) was used for hemicellulose and cellulose isolation, as was the ground wood sample, and the finer portion (smaller than 60 mesh) was used for lignin isolation. Restricting the mesh size to 36-60 mesh for the hemicellulose and cellulose isolation was intended to limit the reduction of crystallinity of the cellulose. Using very finely ground wood meal for the lignin isolation was to ensure that the cell wall material was broken up, to allow lignin to be extracted more easily.

2.3.2. Removal of extractives

All samples of wood, MDF fibre and ground wood were soxhlet-extracted with dichloromethane for at least eight hours and air-dried. They were then extracted with 95% ethanol for a further minimum of eight hours. Weight loss due to removal of extractives from fine wood meal was about 4-5% wood (OD basis). This value is a little higher than the expected value for radiata pine sapwood of 2-2.5% (Uprichard, 1991). This was probably due to physical losses of the finely ground wood meal. The extractive loss was 1.8% on average for the wood blocks in this study.

2.4. Isolation of wood carbohydrates

Four separate types of wood carbohydrates were isolated: holocellulose (delignified wood meal), α-cellulose, and two hemicelluloses, xylan and

glucomannan. A modified version of the Hamilton procedure was used (Beelik *etal.,* 1967). A schematic summary of the carbohydrate isolation is shown in Figure 2.2. Results of the yields are given in Appendix A.

Figure 2.2. Schematic of isolation of the wood carbohydrates

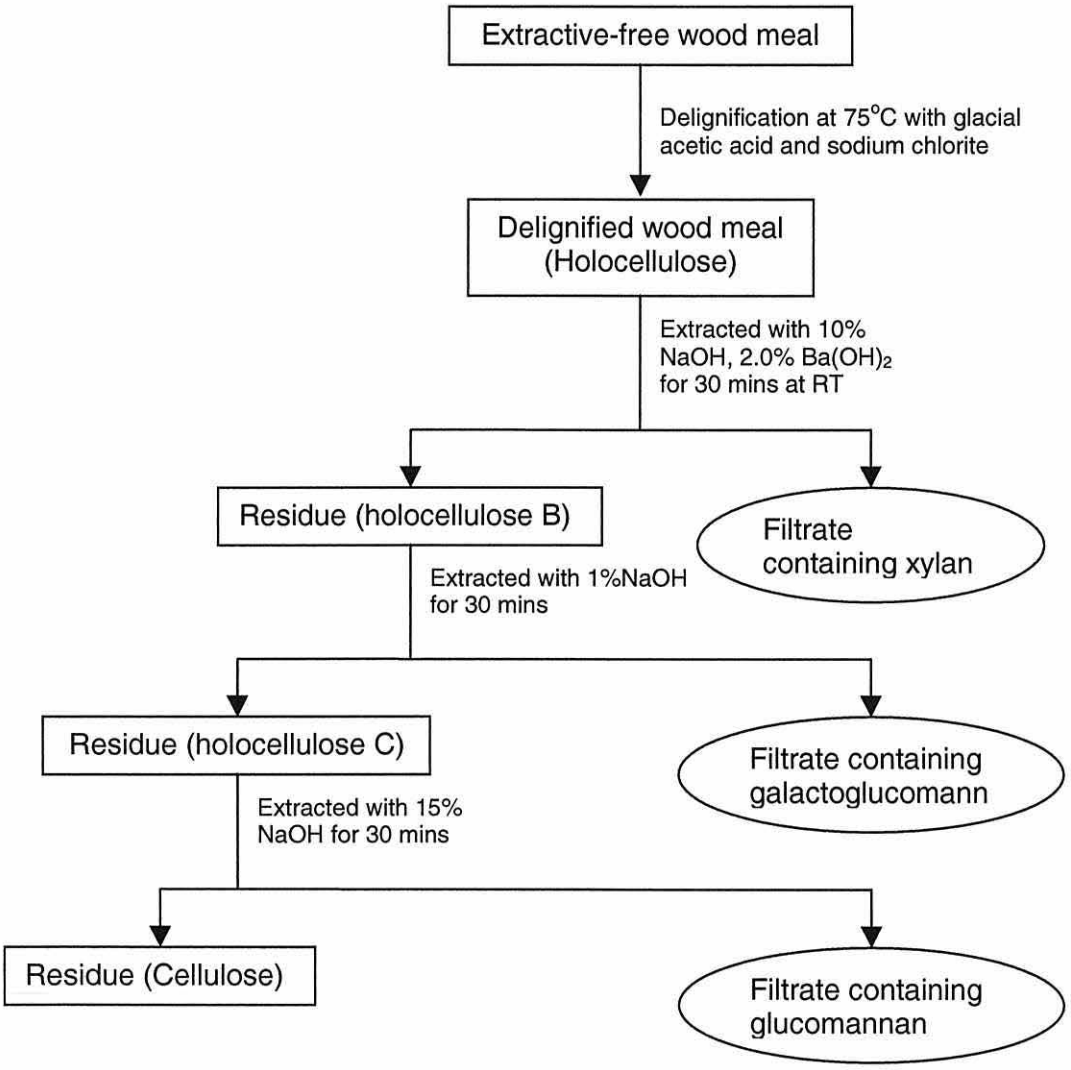

2.4.1. Delignification

The method used was the chlorite method described by Browning (1967), and is summarised below. Four batches were required in total.

Extractive-free wood (100 g, 36-60 mesh) was slurried in water (2.0 L) at 75 °C. Glacial acetic acid (10 ml) was added, then sodium chlorite (200 ml, 15%). This was repeated three or four times at hourly intervals. After cooling in an ice bath to 10 °C, the slurry was filtered and washed with ice-cold water,

washed once with ethanol, and then once or twice with acetone. The delignified wood (Holocellulose A) was then air-dried. A sample of this was kept and designated as 'holocellulose'.

2.4.2. Extraction of xylan.

Holocellulose A (50 g) was slurried at 8% consistency in barium hydroxide (4.4%, 625 ml) for 30 minutes. Then sodium hydroxide (750 ml,18.5%) was added (to give 10% NaOH, 2.0% $Ba(OH)_2$, and 3.6% consistency in final volume) and stirred for another 30 minutes at room temperature. The slurry was filtered and washed with a fresh volume (~500 ml) of solution containing 2.0% $Ba(OH)_2$ and 10% NaOH, and re-filtered. The filtrates (rich in xylan) were acidified to about pH 5.0 with acetic acid (1.2 L of filtrate required about 250 ml glacial acetic acid). The wood residue (Holocellulose B) was washed with water six times and stored in acetic acid (5%) at 2% consistency (or approximately 45 g wood residue in 2.25 L water with 112.5 g acetic acid).

2.4.3. Extraction of galactoglucomannan.

Although this hemicellulose was not intended to be used for kinetic studies, it was also extracted. Air-dried Holocellulose B was slurried at 4% consistency in NaOH solution (1%) for 30 minutes. The slurry was filtered and washed with fresh NaOH solution. Filtrate and washings were rich in galactoglucomannan. The wood residue (Holocellulose C) was washed until the filtrate was neutral, then air-dried.

2.4.4. Extraction of glucomannan and cellulose.

Holocellulose C was slurried at 4% consistency in NaOH (~1.0 L, 15 %) for 30 minutes at room temperature. The slurry was filtered and washed with fresh NaOH solution (thick, loose-webbed glass-fibre filter paper was required, Whatman GF-F). The filtrate was rich in glucomannan (GM). The wood residue (Holocellulose D) was washed to neutrality and air-dried. Holocellulose D was taken as α-cellulose. The overall yield for cellulose was 46.8% (of wood).

2.4.5. Purification of hemicelluloses

Purification of xylan or galactoglucomannan. Two volumes of ethanol (~3.0 L) were added to the acidified hemicellulose filtrate (~1.5 L) to precipitate the hemicellulose. The solution was centrifuged at 3000 rpm for 15 minutes and the supernatant decanted. Overall, the yield for xylan was 5.6% from wood (or 7.7% from delignified wood, including ash). The four batches of galactoglucomannan (GGM) were combined and purified together. However, only 2.98 g was obtained from a total of 234 g of holocellulose A used (1.27% yield).

The mineral content of the isolated xylan was reduced from about 20 % to 2.6% by passage through two ion exchange columns (anionic (Amberlite IRA-400 (Cl)) and cationic (Amberlite IR-120 (Na)). A dilute aqueous solution of xylan was passed through the anionic column first to exchange any unwanted anions with OH ions. Then the solution was passed through the cationic column to exchange any Na or Ba ions with H ions. The full method was as follows:

The columns were first prepared before use. This involved packing the wet resin into a glass column and removing the air bubbles. The anionic resin column (50 g, Amberlite IRA-400 (Cl)) was cleaned with distilled water (100 ml, DW), and then transformed to the OH^- form by passing NaOH (3-4 x 100 ml, 0.05 $mol.L^{-1}$, then 2 x 100 ml, 1 $mol.L^{-1}$) through the column. The column was washed again with DW until the eluant was neutral, before being degassed (CO_2-free) by placing under a vacuum for 1 hour.

The xylan solution (1 g in 100 ml DW, degassed) was passed through the column (flow rate 1-2ml/min). The filtrate was collected in aliquots, so that 1-2 aliquots (each 50-100 ml) would contain the highest levels of purified xylan. Smaller aliquots were then collected until the Molisch test for carbohydrates was negative. DW was used as the eluant to wash the remaining xylan off the column.

The aliquots taken off the anionic column were then put through the cationic column (Amberlite IR-120 (Na)). The cationic column was prepared in a similar manner to that of the anionic column, except that it was transformed and regenerated to the H^+ form by running 3% HCl solution through, then washing with DW until neutral. The xylan-containing aliquots which had passed through both columns were then freeze-dried.

Purification of glucomannan (GM). Barium hydroxide (500 ml, 4.4%) was added to the GM filtrate (~1.2 L) and stirred for 30 minutes. The solution was centrifuged (15 mins, 3000 rpm), the supernatant decanted and kept. The precipitate was dispersed in acetic acid (200 ml, 2 mol/L). It was re-precipitated by adding the solution drop-wise to three volumes of stirred ethanol (600-700 ml), and centrifuged. Overall, the yield of glucomannan was 2.8% of wood (including ash).

The first supernatant for glucomannan was found to contain significant amounts of carbohydrates (by the Molisch test (Bicho, 1992) see below), and was therefore re-extracted. The precipitate was dissolved in ~300 ml water, and added drop-wise to four volumes of stirred ethanol (~1.2 L). The solution was centrifuged and the precipitate dissolved in water. The solution was added to ethanol and centrifuged. Finally, the precipitate was dissolved again into water before freeze-drying. However, this second extraction of glucomannan contained a very high percentage of ash, which was found extremely difficult to reduce to acceptably low levels and so was not used.

Molisch test. This is a qualitative test for the presence of carbohydrates in solution. Reagent: 10% wt/vol α-naphthol in absolute ethanol. Recipe: 0.5 ml sample solution, 2 drops reagent, 1.0 ml conc. sulphuric acid. If carbohydrates are present, the solution will go red/pink within 3 minutes (Bicho, 1992; modified from Browning, 1967).

Further purification of glucomannan was attempted to reduce the ash content (8.9%). However, repeated precipitation into ethanol or methanol was not successful in substantially reducing the ash content, while still retaining most

of the carbohydrate. Glucomannan was only sparingly soluble in water and therefore ion exchange purification was not viable. Therefore, the glucomannan was used with a relatively high final ash content (6.2%).

The two isolated hemicelluloses were characterised after purification by analysing for monosaccharides, Klason lignin and acid soluble lignin (ASL) after acid hydrolysis, as well as with FTIR and NMR spectroscopy (reported in Chapter 4).

2.4.6. Ash content

Approximate ash contents of the wood carbohydrates (and other samples) were calculated from combustion of a small amount of sample. The standard Tappi method was modified to allow smaller samples to be used. The standard method requires duplicates of 3-5 g per sample and this amount of material was not available. Empty ceramic crucibles with lids were placed in a furnace pre-heated to 575 °C (± 25 °C) for 15 minutes. They were then removed and placed in a desiccator to cool for 45 minutes before being weighed. Samples (0.2-0.5 g) were weighed in to the crucibles and placed in the oven for 3.5 hours. They were cooled again for 45 minutes before being re-weighed.

Table 2.2. Ash contents of wood and wood components

Sample	Initial ash content (%)	Final ash content (%)
Extracted wood meal	1.2	1.2
Holocellulose A	1.9	1.9
MDF fibre	0.5	0.5
Xylan	20.9	2.6
Glucomannan (1)	8.9	6.2
Glucomannan (2)	55.3	16.3
Cellulose	0.9	0.9
Lignin, alkali	32.1	3.1

Note: where the ash content values were the same, no extra purification was attempted.

Wood, MDF fibre and lignin samples are included for comparison. Initial and final ash contents refer to the first ash content conducted on newly isolated components and the final one after several purification steps (Table 2.2).

For some of the samples initially isolated and purified, sodium and barium were measured by atomic absorption spectroscopy. All the ash was taken up in 50% nitric acid and diluted to 10 ml before being analysed by Flame Atomic Absorption spectroscopy for Ba and Na. Sodium was measured by emission at 589.1 nm in an acetylene flame, using standard solutions of sodium chloride (10-20 ppm). Barium was measured by emission at 553.6 nm in a nitrous oxide flame, using standard solutions of barium hydroxide (10-20 ppm). Some of the sample solutions required further dilution before analysis. Results are shown in Table 2.3. Ash contents of other samples are given in sections describing their extraction or purification.

Table 2.3. Concentration of sodium and barium in ash as analysed by Flame Atomic Absorption Spectroscopy

Sample	Amount in 10 ml solution (ppm)		Amount in ash (ppm)	
	[Na]	[Ba]	[Na]	[Ba]
Extracted wood meal	<0	0.5	<10-20	5
Holocellulose A	16.0	1.0	160	10
Xylan [a]	42.0	260	420	2600
Glucomannan (1)	3.9	126	39	1260
Glucomannan (2)	159.1	3200	1591	32,000
Cellulose	22.0	15.7	220	157

[a] Before further purification

The results showed that there were small amounts of Na, but only trace amounts of Ba in the holocellulose sample. However, for the hemicelluloses, xylan and GM (2), there were significant amounts of both Na and Ba present, with more Ba present than Na. The cellulose sample had small amount of both Na and Ba present.

2.5. Isolation of lignin

Two methods to isolate lignin from wood were compared in an effort to obtain sufficient quantities of purified isolated lignin: milled wood lignin (MWL), and cellulolytic enzyme lignin (CEL). For the MWL method, a large scale method was attempted initially, to obtain enough pure MWL in one batch. However, the milling in these larger pots (capacity of 3.5 L each) was not efficient enough to obtain reasonable yields. Therefore, many batches of the smaller scale MWL method was used instead (1000 ml capacity pots). In addition, a commercially available lignin was purchased (Aldrich Chemicals (37,095-9) Alkali lignin) to use as a comparison after purification to reduce ash content. The CEL method (based on that used by Glasser and Barnett (1979)) gave good crude lignin yields, but much of this increase was apparently carbohydrates, as the purification stage reduced the yield to very low levels.

2.5.1. Milled wood lignin

The MWL method used was based on Björkman's procedure (1956). Acetone was used instead of dioxane for dissolution of lignin from the finely ball milled wood meal. A larger scale method was attempted at first, using two 3.5 L capacity pots, allowing about 590 g to be milled at one time. However, the overall yield at the end of purification was very low (0.24%), making the method not viable. Therefore, many batches of a smaller scale method were used .

2.5.1.a Extraction

Extractive-free, air-dried wood meal (45-55 g, smaller than 60 mesh) was put into one 1.0 L capacity ceramic ball mill to make one batch. The ball charge (ceramic) weighed approximately 1460 g: the ceramic balls were of roughly the same size. The vibratory ball mill then ran for 4 days continuously. The finely ground wood meal was separated from the balls with aqueous acetone (400 ml, 80%), and stirred for 2 days. The slurry was allowed to settle before it was filtered through a sintered glass funnel. The residue was washed 3-4 times with fresh acetone solution (80%). The filtrate of acetone solution was then rotary evaporated (30 –40 °C) to remove the acetone before freeze-

drying. The product obtained at this stage was a light brown fluffy powder. The average crude yield (from 9 batches) was 1.8% of wood. This is yield lower than what others have obtained (eg 6% yield of lignin, Torr, 1994).

2.5.1.b Purification.

The crude lignin powder was dissolved in acetic acid (40 ml, 90%). This solution was added drop-wise to distilled water (~4 vols; 180 ml) to precipitate the lignin. The precipitate and solution were centrifuged for 15 minutes at 3000 rpm. The solution was decanted, the precipitate washed with water, and centrifuged again. This was repeated before the final precipitate was slurried in water prior to freeze-drying.

The powder obtained (0.87 g) was dissolved in dichloromethane/ethanol (40 ml, 2/1 vol/vol) by stirring overnight. The solution was filtered through a sintered glass funnel to remove undissolved particles (of which there seemed to be a significant amount). The filtered solution was added drop-wise to stirred ether (170 ml), after precipitation, the mixture was centrifuged for 15 minutes at 3000 rpm. Ether was poured off and fresh ether was added and centrifuged again. The final precipitate was added to petroleum ether (~2 vols, 80 ml, b.pt.= 40 -60 °C), stirred thoroughly and rotary evaporated at 30-35 °C to dryness. A total of 2.85 g of purified MWL was obtained from all the batches (0.75% yield).

2.5.2. Purification of alkali lignin

As-received alkali lignin (20 g, of Aldrich Chemicals (37,095-9) Alkali lignin, 100 g) was dissolved in distilled water (1.5 L) after addition of NaOH (70 ml, 10% w/v) while stirring. A solution of HCl (10% w/v) was added drop-wise until the pH of the lignin solution decreased (from pH 9 to pH ~3). This change was sudden and precipitation occurred simultaneously. The solution was then centrifuged (3000 rpm, 15 minutes), the filtrate was poured off, fresh water added, and re-centrifuged. The lignin precipitate was slurried with water and freeze-dried. The subsequent ash content was around 3% (see section 2.3.6, Table 2.2). This commercial lignin was sourced from a kraft pulping process of mostly Norway spruce, and thus contained some sulphur (as –SH). The

structure given in a later Aldrich catalogue is shown in Figure 2.3 (a) with the figure shown in (b) was given in technical information received from Aldrich (2001).

Figure 2.3. Structure given for the unpurified Alkali lignin (Aldrich 37,095-9)

(a)

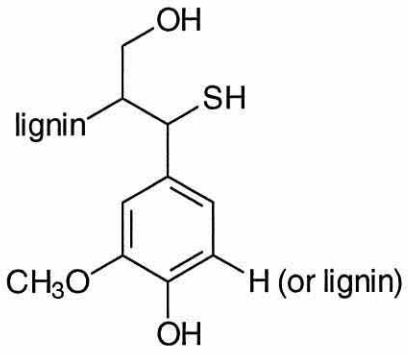

(b)

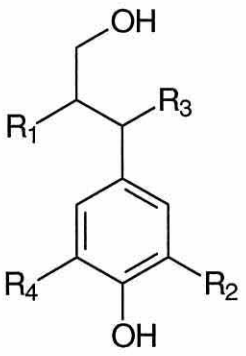

where R_1 = mostly H or other unit
R_2 = mostly OCH_3
R_3 = mostly SH or other unit
R_4 = mostly other unit.

Information received from Aldrich technical department (Aldrich, 2001) about this product was that there were almost no C=O groups (as shown by FTIR), and there was a predominance of phenolic over aliphatic OH group (from ^{1}H NMR). However, it appears from the ^{13}C NMR spectrum of the acetylated alkali lignin, that the number of primary OH groups were also reduced (Table 5.4, Chapter 5). The molecular weights were given as Mw = 14,200 gM^{-1} and Mn = 1750 gM^{-1}.

2.5.3. Source of bagasse lignin

Bagasse lignin was used as received from Dr A.J. Varma (National Chemical Laboratory, Pune, India). A commercial technique was developed to produce this lignin by Pudumjee Pulp & Paper Mills (Pune, India), using an organosolv method. The juice from the sugarcane stems was extracted using a crusher. The residue (bagasse) was dried and chopped to 1-2 mm in length. The bagasse was then extracted with aqueous ethanol (2% slurry) at 70 °C, while being stirred. The yield of lignin was about 12% (±2%) and no further purification was used. The molecular weight is < 1000, and the polydispersity

approximately 3. This lignin had a reported G:S:H ratio of 1.0:0.91:0.66, where G stands for guaiacyl phenyl propane units, S stands for syringyl phenyl propane units and H stands for *p*-hydroxyphenyl propane units. Information was kindly supplied by Dr Varma (1996). Further characterisation was conducted on the bagasse lignin, along with the other lignins used in this study (Chapter 5).

2.5.4. Cellulolytic enzyme lignin

Another method, cellulolytic enzyme lignin (CEL), to isolate lignin was evaluated. This method is similar to the MWL method, except an extra step of enzyme incubation was included. Wood residue previously used in the large scale MWL isolation was air-dried and reground finely. Wood residue (20 g) was stirred in an acetate buffer (800 ml, 0.05 mol/l) and one of two cellulase enzymes (15-20 g dried, Celluzyme (Novo) or from *Penicillium funiculosum*, (9012-54-8, Sigma)) at 45 °C for six days. The digested wood meal was extensively washed with water, before undergoing acetone extraction as in the MWL method (section 2.5.1a). The crude CEL lignin was then purified as previously described in the MWL method (section 2.5.1b).

An initial trial yielded 0.73 g (from 20 g residue) of crude CEL, or about 3.75 % yield. This is greatly improved over the large scale MWL at this stage. In addition, other workers (Chang *etal.,* 1975; Glasser and Barnett, 1979) found that the losses through the purification stage were much less for CEL compared to that of MWL. However, during purification 90-95% of the crude CEL obtained was lost, which was probably mostly carbohydrates. Therefore, this method was discarded as a viable method to produce isolated lignin. In more recent research, Adams (1999) found that a CEL method which used a combination of cellulases and hemicellulases was more effective than cellulase alone and gave good yields.

2.6. Partial delignification of ground wood samples

A mild chlorite delignification method (Uprichard, 1965) was used to partially delignify the ground wood samples for the delignified wood series. Ground

wood (air-dried, 36-60 mesh, 20 g) was slurried in an acetate buffer (800 ml, pH 4.5-5.0) at 75 °C. Sodium chlorite solution (20 ml, 27%) was added each hour, for as many times as necessary to obtain the target lignin content. The ground wood was filtered, washed thoroughly with water and once with acetone, before air drying. The acetate buffer (1920 ml) was made up from sodium hydroxide (48 g) dissolved in distilled water (500 ml), to which acetic acid (glacial, 144 g) was added slowly with stirring; the remainder of the volume was made with distilled water.

The total lignin contents of the samples were as follows (note: these values could contain some inorganics): ground wood (undelignified), 26.91% (or 100% of the total amount of lignin in wood); DWB, 18.87% (70 % of total lignin); DWC, 15.50% (56% of total lignin); DWD, 10.69% (40% of total lignin). The full characterisation for these samples are shown in Chapter 3, section 3.2.3.

2.7. Spectroscopic and analytical technique details

2.7.1. Fourier Transform Infra-red Spectroscopy (FTIR)

Spectra were obtained from ground wood samples (or fine hemicellulose or cellulose samples) in KBr pellets (of about 1% sample concentration) using 32 scans at a resolution of 4 cm^{-1} on a BioRad DigiLab spectrophotometer, with a SPC 3200 computer, with a background of pure KBr pellet (64 scans). Spectra were back-ground corrected if required. Lignin and delignified ground wood samples were run using the average of 64 scans.

2.7.2. Nuclear Magnetic Resonance Spectroscopy (NMR)

Samples for solution NMR were made up in deuterated acetone/water solution or deuterated chloroform (99.8%) with a 5 mm diameter probe. Spectra were initially run on a Bruker AC200 FT spectrometer at 50.1 MHz using either tetramethylsilane (TMS) or the central peak of the solvent for calibration. The ^{1}H NMR data are expressed as parts per million (ppm) as down field shift from the TMS signal at 0.0 ppm or acetone central peak at

2.05 ppm. For ^{13}C NMR, calibration was performed by using either the central peak of the $CDCl_3$ solvent at 77.04 ppm or the central acetone peak at 29.8 ppm.

Some of the later NMR analyses were done on an upgraded instrument which was a Bruker Avance 400 Digital NMR instrument with Silicon Graphics processing. The model compound spectra were run on the old instrument and converted for processing on the new instrument. Automatic integration was used on this system for the model compound acetylated products.

A number of wood and carbohydrate samples were run in solid state mode for ^{13}C NMR spectra on a Bruker DRX 200 Spectrometer at 50.33 MHz. They were run in a 7 mm rotor cup using a cross-polarisation (CP) program with a 1 second (s) contact time, 5000 Hz spin rate, 2 s pulse delay (recycle time), temperature of ~300 K (27 °C), acquisition time of 35 ms, line broadening of 20 Hz, with the number of scans between 2000-5000.

The lignin and model compound NMR spectra for relative rates of reaction were acquired on a Bruker Avance 400 NMR spectrometer operating at 50.33 MHz for ^{13}C spectra. Samples were dissolved in acetone-d_6 and run in 5 mm NMR tubes. For most quantitative spectra, an inverse gated decoupling sequence was used with 12 s relaxation delay (with no NOE generation), a 90 ° pulse width of 13 μs and decoupling only during acquisition of the FID. Approximately 10,-15,000 scans were acquired per spectrum with line broadening of 5.0 Hz being applied prior to Fourier transform. Spectra were referenced to the central acetone-d_6 peak. Integration was normalised with respect to the methoxyl peak at 56.2 ppm.

2.7.3. Acetyl analysis by GC and titration

A direct method for measuring acetyl in reacted wood was wanted, so that the WPG obtained from acetylation could be confirmed independently. Two methods were investigated for suitability and accuracy: acid hydrolysis followed by Gas Chromatographic (GC) analysis, and base hydrolysis, followed by back titration.

The GC method used involved mild acid hydrolysis before analysis for acetic acid, against standard acid solutions (an in-house method for the analysis of volatile fatty acids). Samples of ground wood (0.1 g for treated, 0.5 g for untreated) were mixed in a round-bottomed flask with hydrogen chloride (HCl, 50 ml for treated, 25 ml for untreated; 0.5 $mol.l^{-1}$) and refluxed for one hour. The solution was then cooled before filtering through a sintered glass filter and collected.

For the GC analysis, it was aimed to have all sample solutions in the range of 50-500 ppm acetic acid. For example, a sample (100 mg) reacted to 10 WPG would give 200 ppm acetic acid in 50 ml solution. Two types of standard solutions were run: volatile fatty acids (VFA) and a range of acetic acid standards (in HCl, same as the samples). The VFA standard was a solution of 250 ppm each of acetic acid, propionic acid, iso-butyric acid and n-butyric acid. An internal standard of 1000 ppm of valeric acid was added to all the sample and standard solutions. The settings for the integrator and the temperatures used are given in Appendix B.

The GC traces of a typical standard and a sample and shown in Figures 2.4 and 2.5, where the peak at 8.78 minutes was acetic acid, and the peak at 21.88 minutes was valeric acid which was used as the internal standard. The other peaks in the standard are those of other acids that were analysed for with this method, but were not of interest here.

The titration method used was based on that of Nevell and Zeronian (1962) and involved mild alkaline hydrolysis, neutralisation of excess alkali with acid, then back titration. Samples of ground wood (or other finely divided substrate) were oven-dried (OD, 0.1-0.2 g) and accurately weighed into a stoppered conical flask. Potassium hydroxide in 50 % ethanol (KOH, 25 ml, 0.4 mol/L) was added to the sample and left for 18 hours (overnight) at RT. Then sulphuric acid (H_2SO_4, 25 ml, ~0.2 mol/L) was added and left for a further 30 minutes, stirring occasionally. Hydrolysis solutions were filtered before duplicate aliquots (15 ml) were taken and titrated against sodium hydroxide

(NaOH, 0.1 mol/L), with phenolphthalein as an indicator. As a control, a blank (replicate without any sample) was measured. Stock solutions of KOH and NaOH were standardised against a primary stand solution of oxalic acid (0.5 mol/L).

Figure 2.4. GC trace of the VFA standard used for calibration

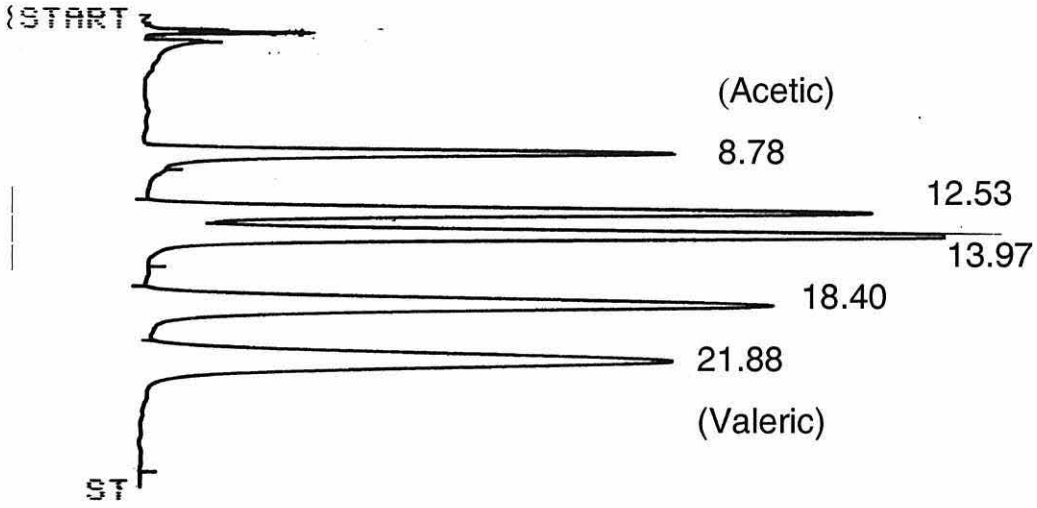

Figure 2.5. GC trace of a hydrolysed sample of acetylated wood

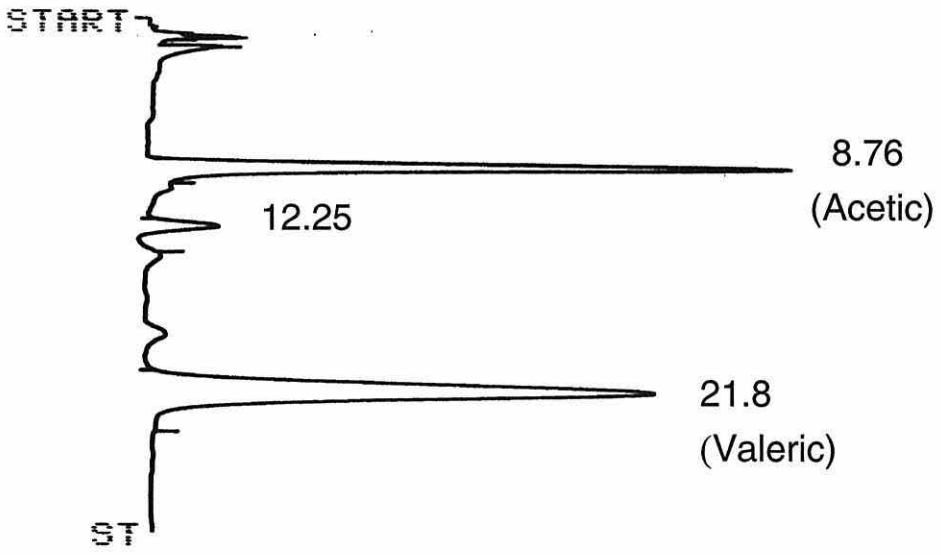

There were significant problems is getting the GC method to work: the base line was unstable, and the instrument itself took a great deal of time to give reproducible results. Because of these problems, it was decided to compare

the results obtained from both methods. In the case of the results reported (Table 2.4), both were analysed from the base hydrolysis of samples.

The comparison of results of the two methods that had been investigated (Table 2.4) showed that the titration method seemed to be the more reliable and accurate over the range of %acetyl (w/w) that was needed. The results from the titration method gave very close values for %acetyl as did the values from the WPG measure of the acetylation reaction. Therefore, this suggests the use of the WPG measure is appropriate for the measurement of extent of reaction.

Table 2.4. Comparison of titration and GC methods of measuring acetyl

Sample	WPG	Titration [1] (% acetyl)	GC (% acetyl)
Untreated wood	- [2]	1.98	1.99
	- [2]	1.53	1.73
Acet. wood (W14c) [3]	5.23	6.30	9.19
Acet. wood (W13c) [3]	7.86	6.71	11.53
Acet. wood (W22c) [3]	12.67	12.28	17.92
Acet. wood (GW2a) [4]	14.99	14.81	22.95
Acet. wood (GW2b) [4]	14.99	15.33	23.53
Acet. wood (W17c) [3]	16.20	17.23	23.04

[1] Each value is the average of duplicate titrations
[2] Untreated wood has 1-2% of natural acetate
[3] These samples were acetylated as wood blocks (from the kinetic study), and were ground up for the acetyl analysis
[4] These samples were acetylated as ground wood in a trial reaction.

2.7.4. Monosaccharide and Klason lignin analyses

These analyses were performed at NZ FRI (now Forest Research) by Analytical Laboratory staff using standard methods. Samples that were not already extractive-free were extracted with dichloromethane prior to analysis. Klason lignin and acid soluble lignin were determined by methods based on TAPPI test methods (TAPPI (1996) and TAPPI (1991) respectively). The Klason lignin method involves the determination of acid-insoluble residues

after hydrolysis in 72% sulphuric acid. Samples of 250 mg were hydrolysed in 3 ml of 72% H_2SO_4 and reacted for 1 hour at 30 °C with intermittent stirring. The moisture content of the sample was determined on a separate sample. The reacted sample was diluted with distilled water (DW) to make 3% H_2SO_4 and a 5 ml aliquot of internal standard solution (fucose) was added. Sample flasks were covered and cooked in a pressure cooker at set pressure (~15 psi) for 30 minutes or at 120 °C for 60 minutes. Flasks were allowed to cool before being removed and the solution filtered. The filtrate was retained for carbohydrate and acid soluble lignin analyses. The insoluble residue (Klason lignin) was washed with DW and dried before weighing.

The acid soluble lignin (ASL) was measured in the retained filtrate of the Klason lignin method using UV/visible spectrometry at 205 nm, against a blank reference solution of 3% H_2SO_4. This is to account for the solubilisation of smaller fragments of lignin which don't condense in the acid fraction during digestion (Maekawa *etal.,* 1989). Total lignin in a sample is usually expressed by the sum of Klason lignin and ASL.

Carbohydrates in the filtrate obtained after lignin analysis were analysed by anion exchange chromatography using a Dionex DX-300 Ion Chromatography system, following a method of Pettersen and Schwandt (1991). Standard solutions of monosaccharides (arabinose, galactose, glucose, xylose and mannose) were prepared which also contained the fucose internal standard and enough 72% H_2SO_4 to make 3% acid in the final volume. These standard solutions underwent the secondary hydrolysis in the pressure cooker along with the other samples.

Measured volumes (20µl) were injected into a Dionex DX-300 ion column. A standard solution containing the five sugars of interest, plus the fucose internal standard, was used to determine the response factors. The full details of the system, including column types, run rates and program details are given in Appendix C.

2.7.5. Elemental analysis

Elemental analysis of carbon, hydrogen, nitrogen and sometimes sulphur (CHNS) were carried out on lignin and model compound samples by staff at the Campbell Microanalytical Laboratory (University of Otago). The technique is based on the complete and instantaneous oxidation of the sample by "flash combustion" which converts all organic and inorganic substances into combustion products. The samples were analysed for CHNS on a Carlo Erba instrument (EA1108 Elemental Analyzer). The moisture content was detected at room temperature under vacuum. In each case, a few mgs of sample was weighed out accurately into a small tin capsule and burnt at 1020 °C, with a catalyst and copper present. The helium gas carrier is enriched with oxygen and after the quantitative combustion reaction has been completed, the products are detected by thermal conductivity. Blanks of the tin capsule were also done as controls. The methoxyl content was determined using the Zeisel reaction where the ether is cleaved with refluxing hydriodic acid to give the relatively volatile alkyl iodide, which is then titrated against sodium thiosulphate.

2.7.6. Shive analysis

Shive analyses were done on the MDF fibre sample used in the study, another MDF fibre sample produced from same material (coarser), and some commercial samples for comparison, as part of the characterisation of substrates. The analyses were carried out using a STFI Shive Analyzer 3000L (Tellusond, H.E. Messer Ltd), located in the BioComposites Centre, Bangor. The principle of this technique is to measure individual fibre length and width into 17 different pre-set categories by using infrared beams. Two beams are set 90 degrees to each other and each fibre is counted as it breaks the beams when it goes through the detector. The length of time a beam is broken corresponds to the length or width of the fibre.

A diagram of the apparatus used is given in Figure 2.6. While water (90 L total) is pumped in through valve 1, the sample (1.7 g OD dispersed in 2.0 L water) is added to the main vessel. When the upper level has been reached, the sample is ready for measurement. The suspension is pumped through the

detector (D) and to waste through point 3, until the lower level is reached, after which the remainder is pumped directly to waste (through 2).

The data are categorised into 17 sizes: fines (< 0.075 mm wide, < 0.3 mm long), which cannot be properly measured by the instrument but can be counted, and 16 other combinations of width and length as shown in Table 2.5. Six replicates of each MDF fibre sample was measured and the results were averaged. MDF fibres are considered to be shives if they have a width of > 0.3 mm and/or a length of > 3 mm (Elias, 1994).

Figure 2.6. Diagram of the Shive Analyser

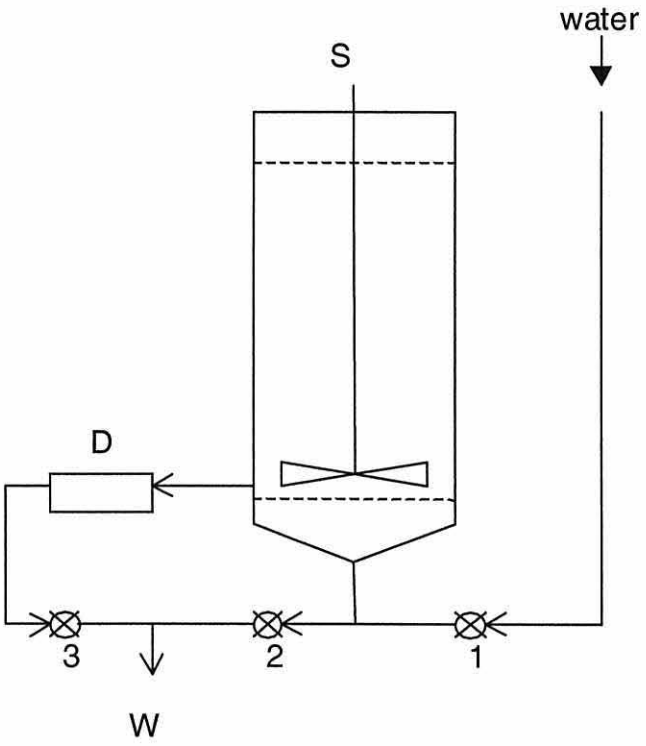

Key: S = Stirrer, D = Detector, W = Waste

The shaded areas in Table 2.5 are the channels of fibre numbers which are considered shives (channels 3, 4, 7-16). The true "fibres" are considered to be the remaining channels (1, 2, 5, 6), not including the fines which are given separately.

Two samples were produced from the refiner, as the first sample of MDF fibres produced were very coarse. The second batch were much finer and

deemed to be suitable for experiments. However, the measurements made on the coarse sample was also reported in the Chapter 3. Total number of MDF fibres measured were 11-16,000 for these two samples.

Table 2.5. Size distribution of the measured MDF fibres of the Shive instrument.

Channels	Length (mm)			
Width (mm) ↓	0.3	1.5	3.0	6.0
0.075	1	2	3	4
0.15	5	6	7	8
0.3	9	10	11	12
0.6	13	14	15	16

Note: Shaded areas are the shive channels of fibre measurement.

2.8. Kinetic experiments

2.8.1. Reaction of wood and wood-based substrates

This section describes the method used for the acetylation of wood (solid, ground), MDF fibre, cellulose, holocellulose, and delignified ground wood. Other substrates required modified procedures due to their solubility in the reaction solution.

Wood blocks of the dimensions 20 mm x 20 mm x 5 mm (radial x tangential x longitudinal respectively), were used in the solid wood experiments. More finely divided substrates (all ground wood samples, MDF fibre, holocellulose, cellulose) were reacted in smaller amount (300 mg), in duplicate, which were in separate flasks, and not vacuum impregnated. All samples were oven-dried at 105 °C overnight. Blocks (~1 g each, 3 blocks in one flask) were vacuum impregnated for 15 minutes at room temperature (RT) with acetic anhydride. The excess anhydride was poured off before flask was placed in the holder with the other flasks. The holder (Figure 2.7), containing up to eight round-bottom flasks with four on each side, was placed over the pre-heated oil bath (either 80, 100, 110, or 120 °C) so that each flask was immersed.

Pre-heated acetic anhydride was introduced into each flask via the top of the condenser immediately after being placed in the oil bath (< 1 minute). For wood blocks, 35 mls of hot acetic anhydride was used, giving a wood liquor ratio of approximately 1g wood/11.67ml anhydride (not including any anhydride absorbed during vacuum impregnation). For the other substrates, 25 ml of acetic anhydride was used, giving a ratio of 300 mg/25 ml or 1 g/83 ml. Timing of the reaction started when the last flask had received the anhydride. It took approximately 80 seconds to deliver acetic anhydride to eight flasks.

Figure 2.7. Holder for condensers and reaction flasks.

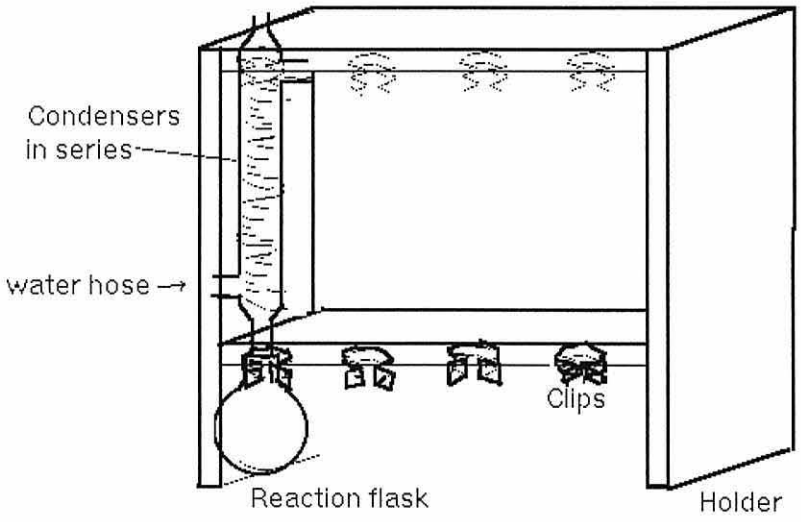

When the reaction time was completed, the holder and flasks were removed and immersed in an ice bath to quench the reaction (Moore, 1957). Each reaction time was conducted in a separate experiment. For example, the range of substrates (wood block, MDF fibre, holocellulose and cellulose, using 7 flasks) were reacted at 100 °C for 60 minutes reaction time, making one experiment. Once the samples were cooled (about 10 minutes), flasks were removed one by one and the anhydride removed. For blocks, the anhydride was simply poured off into a storage jar.

Samples were rinsed with acetone which was also collected and the excess solvent was allowed to evaporate in a fume hood. The other samples were filtered through sintered glass crucibles (porosity 2 or 3) and washed with acetone. The samples were replaced in the flasks with fresh acetone and refluxed for three hours. Samples were re-filtered, washed with fresh acetone and oven-dried at 105 °C (overnight). Samples were weighed (after cooling in a desiccator) before and after the acetylation reaction to determine the weight gain due to chemical add-on, on an oven-dried basis.

Solutions of anhydride and acetone were collected so that if any wood substance had dissolved during reaction or washing, it could be analysed and the weight gain corrected. Therefore, selected solutions were dried under reduced pressure, then further oven-dried before being weighed, to determine the mass of dissolved substrate or acetylated product. It was found that dissolution was only moderately significant for MDF fibre samples, although at longer reaction times, there was some dissolution for holocellulose samples.

The extent of reaction by acetylation at a given temperature was generally determined from the increase in weight of the initial sample of the substrate, expressed as a percentage. This was denoted as weight percent gain (WPG) and was calculated as follows:

$$\text{Weight percent gain (WPG)} = [(w_2 - w_1) / w_1] \times 100 \quad \text{.....Equation 2.1}$$

where w_1 is the weight of the OD sample before reaction
and w_2 is the weight of the OD sample after reaction.

This mass increase was converted into moles (actually milli-moles, mmol) of OH reacted per gram of wood for the reactions plots. This was calculated as follows, as the moles of acetate produced is the same as OH groups reacted:

$$\text{mmol OH reacted per g} = \{ [(w_2 - w_1) \times 42] / w_1 \} \times 1000 \quad \text{.....Equation 2.2.}$$

where 42 is the molecular weight difference of the added acetyl group

For the integral method (first order rate equation), Ln $[OH]_t/[OH]_0$ is plotted against reaction time to give a straight line if the reaction is first order with

respect to OH. This was calculated as in Equation 2.3, where $[OH]_t$ is the initial concentration of OH ($[OH]_0$) minus the amount reacted at time t (calculated from mol OH reacted).

$$[OH]_t/[OH]_0 = [\ (w_1 \times mole_{OH/wood}) - ((\ w_2 - w_1\ ) \times 42) / w_1\ ]\ /\ (w_1 \times mole_{OH/wood})$$

.....Equation 2.3.

where $[OH]_t$ is the concentration of OH groups at time, t
$[OH]_0$ is the concentration of OH groups at time=0
$mole_{OH/wood}$ is the number of moles of OH in wood per g, which was calculated as being 0.01366 for radiata pine sapwood

The data were fitted to curves using a simple exponential function in an EXCEL spreadsheet in the form, $y = a.\ (1 - b^x)$, where *a* is the asymptote and *b* is the degree of curvature. This form of the exponential curve was used for convenience as it was useful in practice. The curves were fitted on the lowest residual sum of the squares (SS) solution, and the co-efficient of variance (CV%) was given for that solution. Equation 2.4 shows how this was calculated.

$$CV\% = \frac{\text{Total SS} - \text{Residual SS}}{\text{Total SS}} \times 100 \quad \text{..... Equation 2.4}$$

where Total SS = variance $(y_1 \ldots y_i)$. (n-1)

$$= \frac{n\Sigma y_i^2 - (\Sigma y_i)^2}{n.(n-1)} . (n-1)$$

$$= \Sigma y_i^2 - \frac{(\Sigma y_i)^2}{n}$$

$$\text{Residual SS} = \Sigma(y_i - y_i^p)^2$$

$y_1 \ldots y_i$ or y_i = individual data points
y_i^p = predicted data points
n = number of data pairs

The initial rate constant (k_o) was calculated as the derivative of the exponential equation at 10% of the asymptote for each curve. In some cases (for example, the reaction at lower temperatures of significantly delignified wood), a sigmoid curve may better describe the data. Where this was true, there was an attempt to fit to both types of curves so that more accurate k_o values could be obtained. A second method was used to determine k_o values,

which used the linear regression of the first two reaction data points and zero. This latter method was thought to be more reliable as sometimes the initial data did not fit the exponential curves well.

An alternative method (using the first order integral rate equation) was used to obtain k values (rate constant) with wood acetylation data. This was accomplished by plotting the natural logarithm of the ratio of reactant consumption ($Ln[OH]_t/[OH]_0$) against the reaction time (Equation 2.3). Assuming linearity, the slope was the rate constant of the reaction at that temperature. However, using a first order integrated rate relationship to obtain rate constants assumes that the acetylation reaction is controlled by first order kinetics (ie activation controlled). When the reaction is proven to be diffusion controlled, then this method is not appropriate. The natural log of these rate constants were plotted versus the inverse of absolute temperature (in degrees Kelvin) to obtain the activation energy via the Arrhenius equation (for further details, see Chapter 3).

2.8.2. Reaction of hemicelluloses with catalysts

Acetylation reactions were carried out for the two isolated hemicelluloses, xylan and glucomannan, in the same way as for the MDF fibre, holocellulose and cellulose (that is, oven-dried before and after reaction with acetic anhydride). After the initial experiments showed a very reduced acetylation level, reactions with catalysts were conducted. The reaction solution used was 50% (by volume) of pyridine in acetic anhydride, or 30% acetic acid in acetic anhydride for the two catalyst systems used. It was found that for the acetic acid-catalysed reaction, significant amount of the hemicelluloses had dissolved during reaction. Therefore, these solutions were dried under reduced pressure to give additional weight for the WPG calculations.

2.8.3. Reaction of lignin preparations

The three lignin preparations were reacted using a smaller scale due to the low amount of MWL obtained. Lignin samples (50 mg, duplicate) were weighed into tared round bottom flasks (50 ml) for oven-drying (105 °C, overnight). The flasks were re-weighed (after cooling in a desiccator) very

carefully (as weighing errors could add up significantly with this small scale). The pre-heated acetic anhydride (8 ml each flask) was introduced into the flasks as before, giving a sample to liquor ratio of 1 g/160 ml anhydride. After the reaction time was reached, sample flasks and the holder were removed in the same way as previously described and quenched in an ice bath. After approximately 5 minutes, chilled distilled water (10-12 ml) was introduced via the top of the condenser. Samples were removed from the ice bath and the contents of each flask were transferred to a larger round-bottom flask (250 ml, tared) for rotary evaporation with acetone. The product was washed twice with distilled water before being oven-dried (105 °C, overnight). The solid product was recovered and stored.

A control reaction of lignin with acetic acid was conducted in exactly the same way as with the anhydride, except the acetic anhydride was replaced with acetic acid. This was to determine how much, if any, acetylation took place with acetic acid.

CHAPTER 3: REACTION OF WOOD AND WOOD-BASED SUBSTRATES

3.1. Introduction

The variation in the uncatalysed acetylation rates of wood and wood-based substrates with temperature are described in this chapter. Solid wood blocks, MDF fibre, ground wood, and three samples of partially delignified ground wood were examined. The acetylation of chlorite holocellulose, isolated cellulose and hemicelluloses are reported in Chapter 4. Studies on the acetylation of lignin samples and those of a lignin model compound are in Chapters 5 and 6 respectively.

This wide range of substrates was chosen in order to relate the acetylation of wood to that of its individual wood components, and the physical structure of the material studied. The primary idea was to attempt to build an empirical model of the kinetics of the solid wood reaction from the reaction of its polymer groups; that is, cellulose, hemicelluloses and lignin. The MDF fibre used in these experiments came from the same sample of radiata pine used for the preparation of wood blocks and ground wood.

For convenience in discussion, these experiments on wood and its components are said to be "uncatalysed". However, during acetylation of wood (and other substrates) with acetic anhydride, the acetic acid produced as a byproduct can act as a catalyst. The reaction therefore could be said to be auto-catalysed. The possible effects of acetic acid released during the acetylation reaction were not separately considered during studies on reaction rates, nor during the attempts to construct a mathematical model of the process. The possible catalytic effect was not thought to be strong (Turner and Harris, 1952) and it is impossible to eliminate acetic acid during acetylation.

In the studies on reaction kinetics, the initial rate method was generally used to obtain the kinetic data, rather than the integral method (ie using the

integrated first order rate equation), since the latter assumes the reaction is activation controlled (see Chapter 2, section 2.8.1 for details). However, both methods were used in the study of wood blocks for comparative reasons.

The extent of reaction by acetylation at a given temperature was generally determined from the increase in weight of the initial sample of the substrate, expressed as a percentage. This was denoted as weight percent gain (WPG). This mass increase was converted into moles (actually milli-moles, mmol) of OH reacted per gram of wood for the reactions plots. The calculations are given in Chapter 2 (section 2.8.1).

For the integral method (first order rate equation), Ln $[OH]_t/[OH]_0$ is plotted against reaction time to give a straight line if the reaction is first order with respect to OH.

The accuracy of the WPG measurement was compared with wet chemistry techniques for analysing acetyl content and found to be consistent with % acetyl measured. Samples were oven-dried (OD) before and after reaction in order to obtain accurate weight measurements. However, the results obtained with air-dried samples were compared with those obtained using OD samples. Duplicate or triplicate samples were used with these substrates, but this was not possible for the reactions of the lignin model compound.

The choice of wood blocks as the main form of wood used in this study was deliberate. With solid wood blocks, there are no changes in components caused by milling, grinding or an isolation process. The choice of wood blocks also meant that diffusion through the cell wall structure could well be influential in the kinetic information obtained. The wood blocks chosen were small and were vacuum impregnated to minimise any problems of diffusion through the gross wood structure itself.

Refined fibre (MDF or high temperature mechanical pulp (HTMP) fibre) that was used in this study is substantially different in structure from solid wood but not much different in chemical composition. For example, the cell structure

has been cleaved in the middle lamella (ML) zone, so that many of the fibres are coated with ML lignin (Walker, 1993; p469).

Ground wood was expected to be different from the wood blocks used in the main experiment, its greater surface area to volume ratio, perhaps allowing diffusion at a faster rate. Therefore, any differences in reactivity between the ground wood and the wood block could be attributed due to the effect of the difference in physical structure.

Some samples of ground wood were delignified by a mild method, in an attempt to minimise any effects on the substrate of the delignification process. Examining delignified ground wood samples was another way of obtaining a picture of the effect of reducing lignin content, without (hopefully) having changed the remaining substrate much from the original and using a different means other than using an isolated lignin. Three samples of ground wood (36-60 mesh) were delignified to obtain a range of samples with reduced lignin content.

3.1.1. Discussion of the choice of methods used

The wood used came from New Zealand and all substrates examined were extracted from the same supply of radiata pine, with the exception of the two of the lignin samples (alkali and bagasse) and the model compound. The wood samples were from a number of different planks, which were from different trees, to ensure the applicability of the results to radiata pine, rather than one tree. This meant that there was more variability in the results than there would have been from wood sourced from one tree.

Wood blocks were chosen to have the dimensions of 20 mm x 20 mm x 5 mm, (radial x tangential x longitudinal) to ensure reasonable access by treatment liquid (average tracheid length normally around 3-4 mm). It was decided to also use MDF (or HTMP) fibre as a substrate, to investigate the effect of the different form of wood (individual fibres) which has a similar composition to the solid wood used.

Figure 3.1. Diagram of a MDF fibre

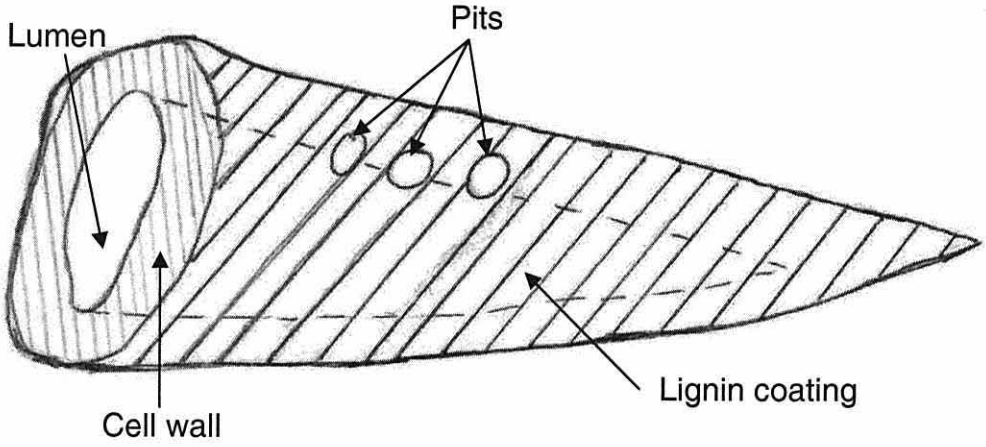

The surface of the MDF fibres is coated with lignin from the middle lamella, which is a major difference from the wood blocks or particles (Figure 3.1). The lignin coating might be expected to react faster, as it is completely accessible, although the coating could also act as a barrier to the fibre cell wall it covers. However, this lignin coating would not be expected to significantly affect diffusion into the fibre itself, as the pits along the MDF fibre length are open, with no visible torus (photos in Thumm and Grigsby, 2001). The pits would allow the quick ingress of the anhydride to the lumen and from there through the cell wall. It appears that many of the MDF fibres are single tracheids, although a few fibres are still in small bundles (Kerr and Goring, 1976)

The temperatures chosen for reaction were: 80, 100, 110 and 120 ^{o}C. The upper temperature of 120 ^{o}C was so chosen because thermal degradation of the wood is known to occur at temperatures greater than this. Reaction at temperatures lower than 80 ^{o}C is slow, and excessively long reaction times are required to give reasonable weight gains. The swelling coefficient of acetic anhydride at 25 ^{o}C is 1.5 in comparison to water at 10.0 (Rowell, 1983). This means that in the vacuum impregnation step, the anhydride would not react and would not significantly penetrate the wood cell wall.

The whole reaction profile was not intended to be studied, as rate constants were to be calculated from the initial reaction. This choice was to shorten the length of time needed to gain kinetic data from a range of substrates. However, extra (longer) reaction times were investigated for wood blocks to

sketch out a greater portion of the reaction, as solid wood was the focus of the study. A maximum level of acetylation (for these conditions) would be arrived at after a sufficiently long reaction time (days or months depending on the temperature), and this is expected to be the same for all temperatures, unless there is significant wood degradation.

3.1.1.1. The effect of oven-drying and vacuum impregnation

Extra reactions were carried out on wood blocks to determine what effect vacuum impregnation and oven drying had on the extent of reaction (Table 3.1). The longer reaction time (120 °C, 60 minutes) without vacuum impregnation (VI) gave a slightly higher WPG than with VI. This effect was expected to be greater with a shorter reaction time. However, the results did not show this when compared to four batches of three replicates in each reaction. The between batch or run variation seemed to be greater than the effect of vacuum impregnation. The variability of the wood reaction results was investigated more extensively and is discussed in section 3.5.

Table 3.1. Reaction of wood blocks, with and without vacuum impregnation or oven drying.

Reaction type	Reaction at 120 °C, 60 mins WPG (s.d.)	Reaction at 120 °C, 10 mins WPG (s.d.)
Normal (OD, VI)	14.14 (0.11)	6.06 (0.31)
		7.75 (0.63)
		6.63 (0.47)
		6.99 (0.40)
No OD (but with VI)	14.64 (0.20)	
No VI (but with OD)	15.32 (0.26)	7.82 (0.64)

Note: three replicates for each value given. s.d. = standard deviation

The samples that had not been oven-dried (OD) before reaction reacted to approximately the same extent, as did the OD samples, with a similar variability. However, the moisture contents were relatively low (~8%), which may have reduced any effect (more details, see Appendix D). Beckers and

Mililtz (1994) reported that, as the moisture content increased above 15%, the WPG decreased, with limited acetic anhydride. Samples were vacuum impregnated before being drained of anhydride and reacted in a separate reaction vessel. Therefore, samples with varying moisture content were not reacted with a high excess of liquid anhydride (as in this study), so the hydrolysis of the anhydride with water limited the level of reaction obtainable. In addition, some of the acetylation of the blocks may have occurred with vapour-phase acetic anhydride, which would change the reaction process.

The source planks had been kiln-dried from green before samples for this study were taken. The temperature and rate of drying wood affects the porosity and permeability of the wood cell wall (Siau, 1984). For example, if pits are aspirated (closed), this significantly reduces the permeability of liquids through the wood structure (Siau, 1984).

3.2. Characterisation of the wood and wood-based substrates

The information in this section describes, spectroscopically or chemically, the samples that were used in the kinetic studies. The techniques used to examine the samples were Fourier Transform Infrared spectroscopy (FTIR), Nuclear Magnetic Resonance (NMR) spectroscopy, both carbon and proton and, for a few samples, solid state NMR spectroscopy, and wet chemistry techniques that included monosaccharide and lignin analysis. The MDF fibre sample was also analysed for its size distribution (length and width) by a shive analyser.

3.2.1. Fourier transform Infrared spectroscopy

The experimental details for the FTIR technique used are given in Chapter 2, section 2.7.1. Spectra are given in two sections: the first of wood and MDF fibre and the second of the delignified ground wood samples. FTIR spectra give a summary of functional groups present in the sample, and can be used as "fingerprints". As with all natural products, there are variations between samples even from the same tree, but a sample of wood from the same species will give generally the same pattern, with only small variations.

3.2.1.1. FTIR spectra of wood and MDF fibre

FTIR spectra of wood and MDF fibre are shown in Figures 3.2 and 3.3, and a summary of the main peak assignments is given in Table 3.2. There are many similarities in the spectra shown, such as the strong band at about 3300 - 3400 cm^{-1} due to the abundant hydroxyl groups present in all the samples. There was a small peak at 1735 cm^{-1} in the wood and MDF fibre sample due the naturally occurring acetyl. The native acetyl content is probably in the glucomannan (Uprichard, 1991).

Table 3.2. Main peak assignments of FTIR spectra of wood and wood-based substrates

Assignment of FTIR peak[1] (cm^{-1})	Maximum of peak in sample (cm^{-1})	
	Wood	MDF Fibre
3350-3420, ν_{O-H}, bonded	3356	3416
2890-2950, ν_{C-H}, CH_2/CH_3	2899	2903
1735, $\nu_{C=O}$, unconjugated [2]	1736	1734
1630-60, $\nu_{C=O}$, conjugated	1655	1653
1510, $\nu_{C=C}$, (aromatic), characteristic of lignin	1510	1510
1400-1470, δ_{C-H}	sm	sm
1375, δ_{C-H}, $-CH_2$	sm	sm
1220-1275, ν_{C-O-C}	1270	1268
1020-60, ν_{C-O-C}, ethers, ring saccharide skeleton [3]	1032	1032
1000-670, group frequency in polysaccharides	sm	sm

Key:

sm A small peak (unpicked) is present.

1 The symbol ν means a stretch frequency and δ means a bend (scissor/wag etc) frequency, with the subscript denoting the type of bend or stretch.

2 Most likely acetyl, but also could be carboxyl, ketone

3 This peak is one of two at maximum, and a band from 1150-918 cm^{-1} is assigned to the saccharide skeleton.

The assignments made in Table 3.2 were generally in agreement with those from Faix and Böttcher (1992), who also compared results from FTIR spectra using KBr pellets (as used here), diffuse reflectance (DRIFT), transmission through a thin section of wood and direct reflectance of the wood surface. They found that using high concentrations of wood in a pellet decreased the apparent absorption of some peaks. Otherwise, the KBr pellet method gave very high correlation coefficients.

Figure 3.2. FTIR spectrum of ground wood

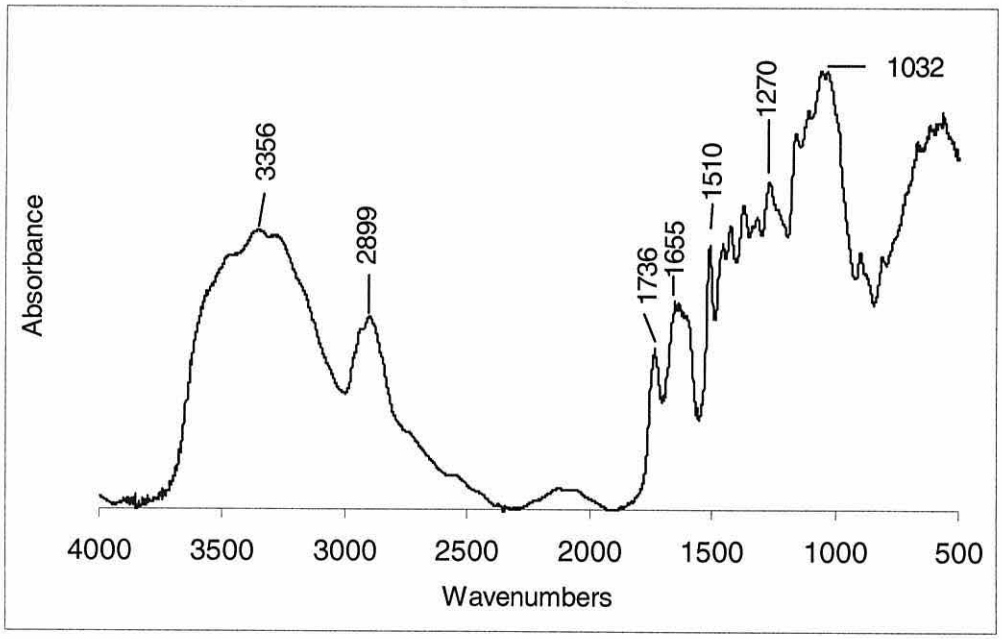

Figure 3.3. FTIR spectrum of MDF fibre

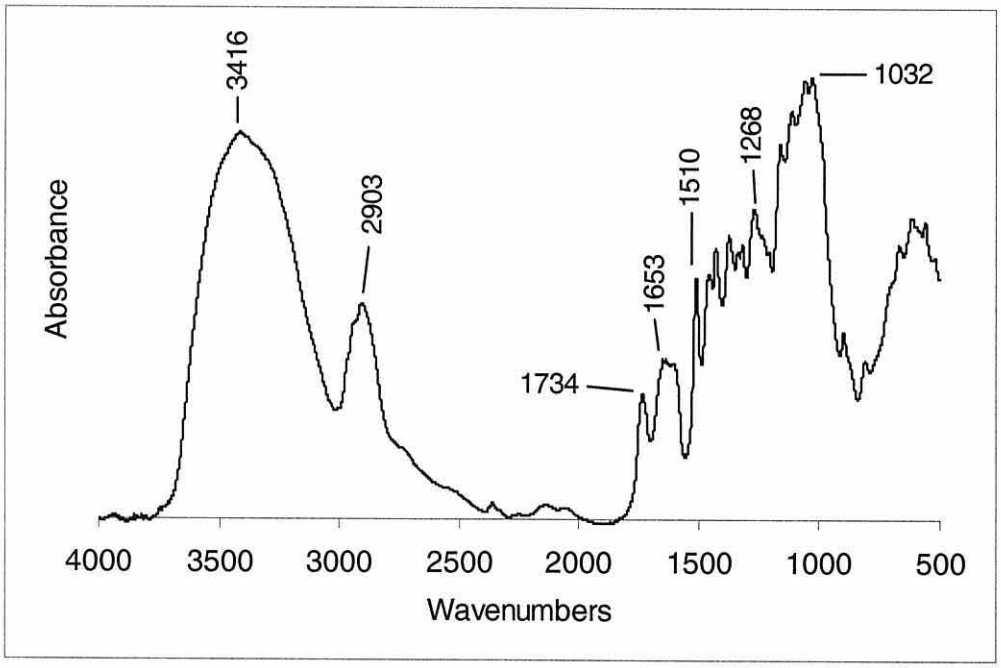

Zanuttini *et al.* (1998) applied the DRIFT technique to the analysis of acetyl in wood and found that it gave a good correlation with values obtained by GC. However, the internal standard used was the lignin characteristic peak of 1510 cm-1, and as lignin was not present in any quantity in some of the samples used here (eg holocellulose or cellulose), this technique could not be used. In addition, they measured relatively low levels of acetyl (0-3%), and the use of this method at the higher levels obtained by acetylation of wood would need to be further validated.

3.2.1.2. FTIR of the delignified ground wood

FTIR spectra of the partially delignified ground wood were done to characterise changes introduced in the substrate by the delignification method. Figure 3.4 shows a summary of the changes going from the non-delignified ground wood (Figure 3.4a) to the increasingly delignified ground wood samples. Figures 3.5-3.7 show the delignified ground wood samples, DWB, DWC and DWD respectively. The untreated (not delignified) ground wood (26.9 % total lignin content) has been given in Figure 3.2.

Figure 3.4. FTIR spectra of ground wood samples, increasingly delignified, a-d

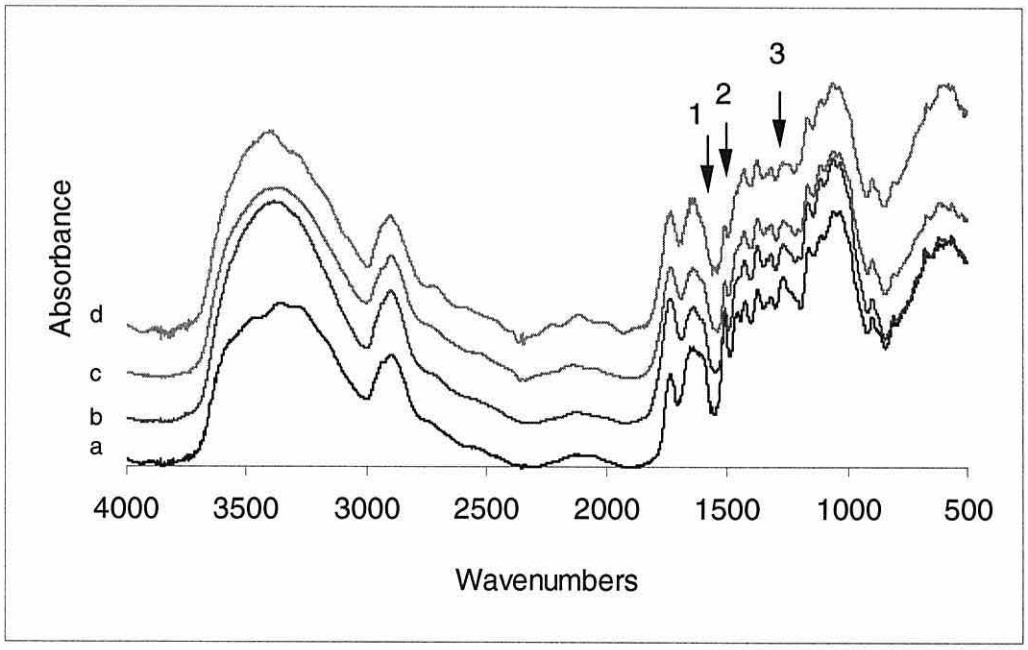

Table 3.3 shows the assignments of the FTIR peaks in the ground wood series of samples. The small sharp peak at 1510 cm^{-1} is characteristic for

lignin, and one can see this decrease with decreasing lignin content (point 2, Figure 3.4), as well as the shoulder at around 1599-1605 cm^{-1} (point 1). The small peak at 1250-70 cm^{-1} has also decreased slightly with decreasing lignin content (point 3). This was assigned to an ether linkage, which may have been lost through the delignification process.

Figure 3.5. FTIR spectrum of delignified wood sample B (DWB 18.9% lignin)

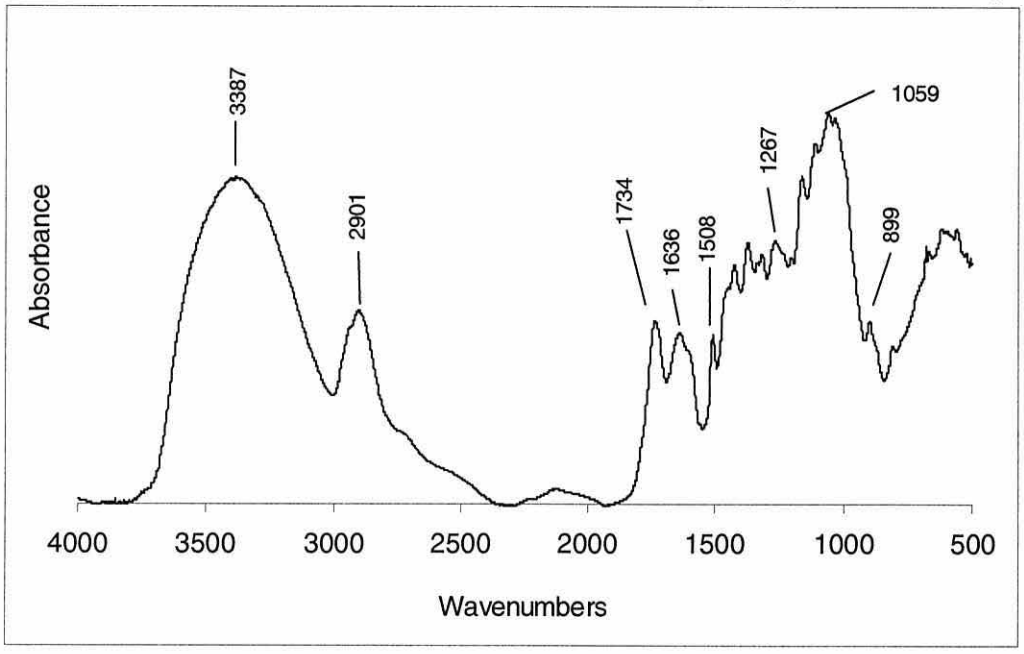

Figure 3.6. FTIR spectrum of delignified wood sample C (DWC 15.5% lignin)

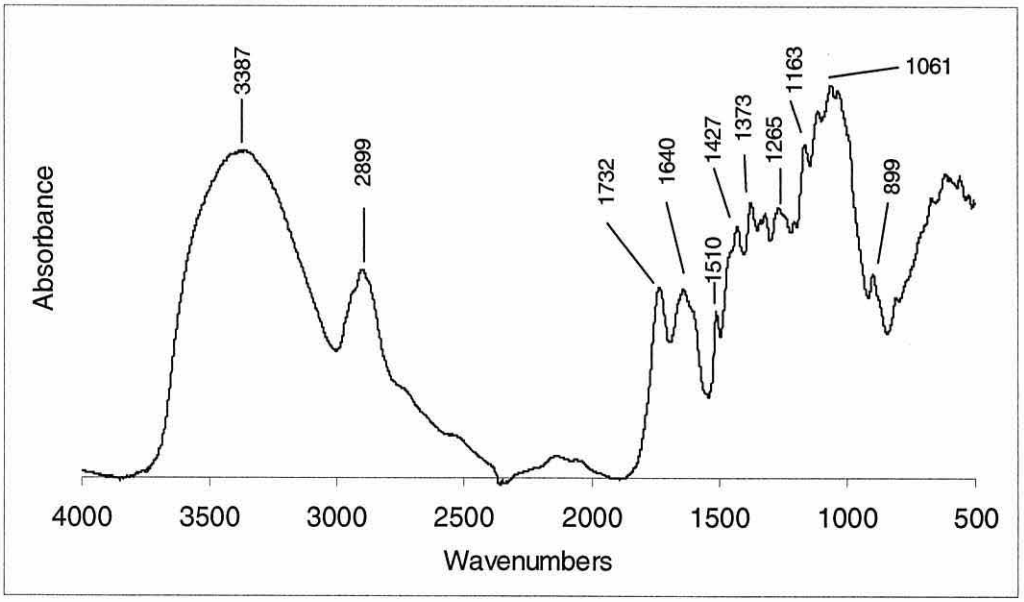

Figure 3.7. FTIR spectrum of delignified wood sample D (DWD 10.7% lignin)

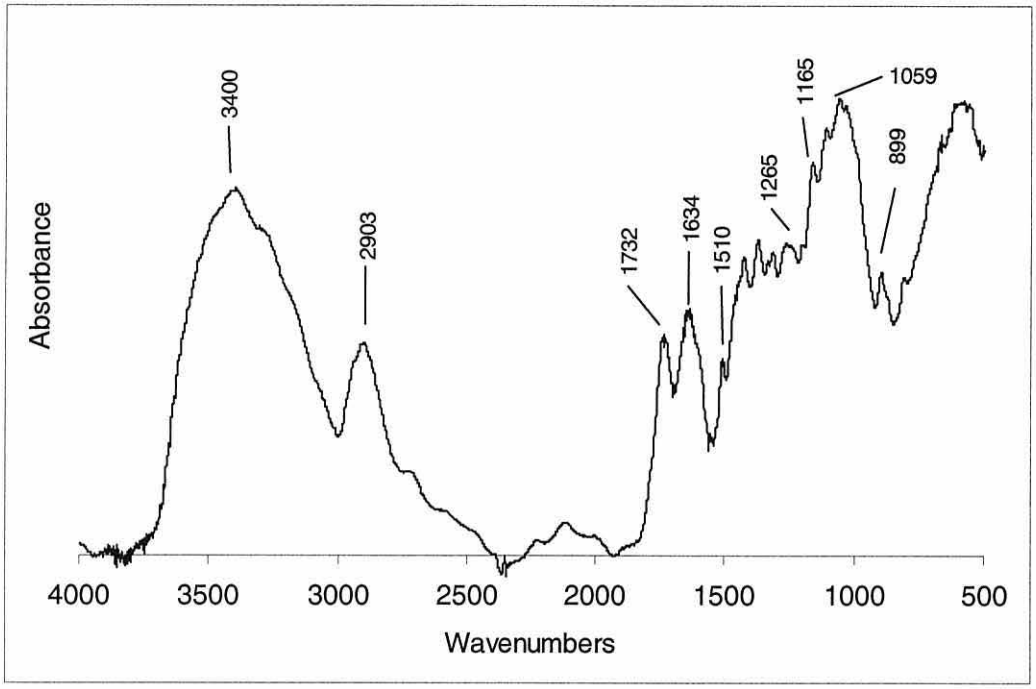

Table 3.3. Assignments of FTIR spectra of the delignified ground wood series

Assignment of FTIR peak[1]	Maximum of peak in sample (cm^{-1})			
(cm^{-1})	Grd wood	DWB	DWC	DWD
3350-3420, ν_{O-H}, bonded	3356	3387	3387	3400
2890-2950, ν_{C-H}, CH_2/CH_3	2899	2901	2899	2903
1735, $\nu_{C=O}$, acetyl, carboxyl,	1736	1734	1732	1732
1630-60, $\nu_{C=O}$, conjugated	1655	1636	1640	1634
1510, $\nu_{C=C}$, aromatic	1510	1508	1510	1510
1400-1470, δ_{C-H}	sm	√	1427	1427
1375, δ_{C-H}, $-CH_2$	√	√	1373	1373
1220-1275, ν_{C-O-C}	1270	1267	1253	1265
1020-60, ν_{C-O-C}, saccharide ring[2]	1032	1059	1061	1059
1000-670, polysaccharides	√	899	899	899

Key: sm A small peak (unpicked) is present. √ Peak present but unpicked.

[1] The symbol ν means a stretch frequency and δ means a bend (scissor/ wag) frequency, with the subscript denoting the type of bend or stretch.

[2] This peak is one of two at maximum, and a band from 1150-918 cm^{-1} is assigned to the saccharide skeleton.

Ratios of two peak areas in a FTIR spectrum of wood can give some semi-quantitative data on the extent of reaction. The reference area chosen was that of the carbohydrate skeleton (sugar units) of between 918 - 1188 cm^{-1}. The lignin peak is at 1510 cm^{-1}, and so the area of interest was between 1493 cm^{-1} and 1535 cm^{-1} for this series of samples. This peak area was ratioed with the reference peak area for each of the spectra and the results are shown in Figure 3.8. The wood samples' lignin content is given in Table 3.8, in the next section. The relationship between the total lignin content and the peak area ratio appeared to be curvi-linear, rather than linear.

In fact, when the various types of lignin content (total, Klason lignin (KL), and acid soluble lignin (ASL)) were plotted against the ratio, ASL had the most linear relationship (negative slope, r^2=0.997) with the characteristic lignin peak at 1510 cm^{-1}. The r^2 values for KL (positive slope, r^2=0.937), and total lignin (positive slope, r^2=0.871) were both lower. These plots, their regression values and equations are shown in Appendix E.

Figure 3.8. Comparison of total lignin content with FTIR peak area ratio

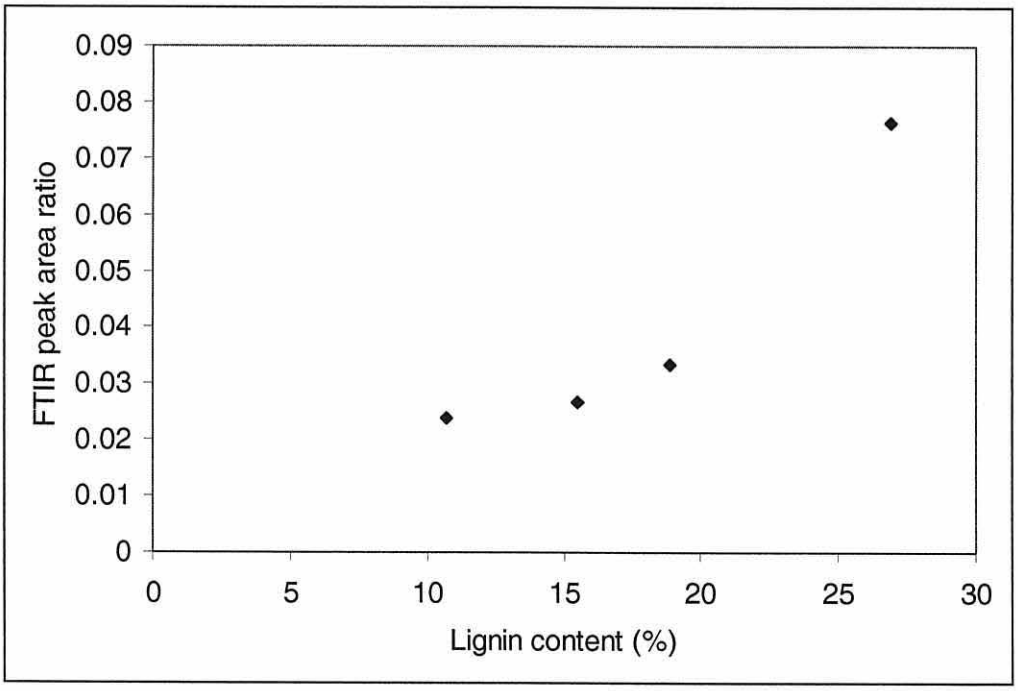

Ratio = area (1535-1493)/area (918-1188)

3.2.2. Nuclear magnetic resonance spectroscopy

This section contains the solid state NMR spectra of untreated (Figure 3.10) and acetylated wood (17.6 WPG, Figure 3.11). In the untreated wood spectrum, the peaks between 110-160 ppm (peaks 2, 2a, 2b) are assigned to the aromatic ring carbons of lignin (Haw *et al.,* 1984). The slight broadening at the lower frequency side (to the right) of peak 3 (105 ppm) was probably indicating the presence of hemicelluloses (Haw *et al.,* 1984).

The two peaks at 4 & 5 (89, 84 ppm), assigned to C4 of the glucose unit, are further assigned to the inside and surface respectively of crystalline cellulose chains in the microfibril. The two peaks at peak 8 (62-65 ppm) in the untreated wood spectrum are assigned to the inside (65 ppm) and the surface of crystalline cellulose chain for C6 (Newman, 1999). There were small peaks in the untreated wood spectrum at both points 1 & 10, which indicated the small amount of natural acetyl contained in glucomannan. The carbon numbering of the glucose units of cellulose is shown in Figure 3.9.

Figure 3.9. The numbering of carbon atoms in the cellulose glucose unit

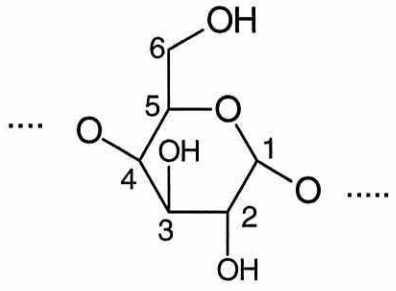

The assignments of the ^{13}C NMR spectra of untreated and acetylated wood, are given in Table 3.4, and are in agreement with those of Newman (1994) and Haw *et al.* (1984).

Figure 3.10. Solid state ^{13}C NMR spectrum of untreated wood

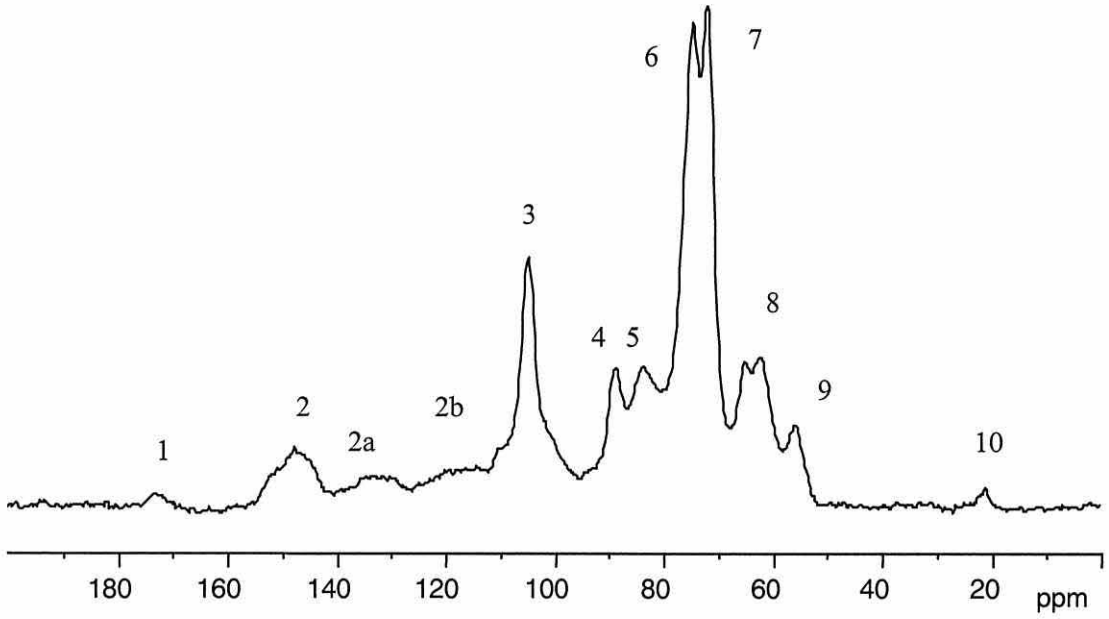

Figure 3.11. Solid state ^{13}C NMR spectrum of acetylated wood, 17.60 WPG

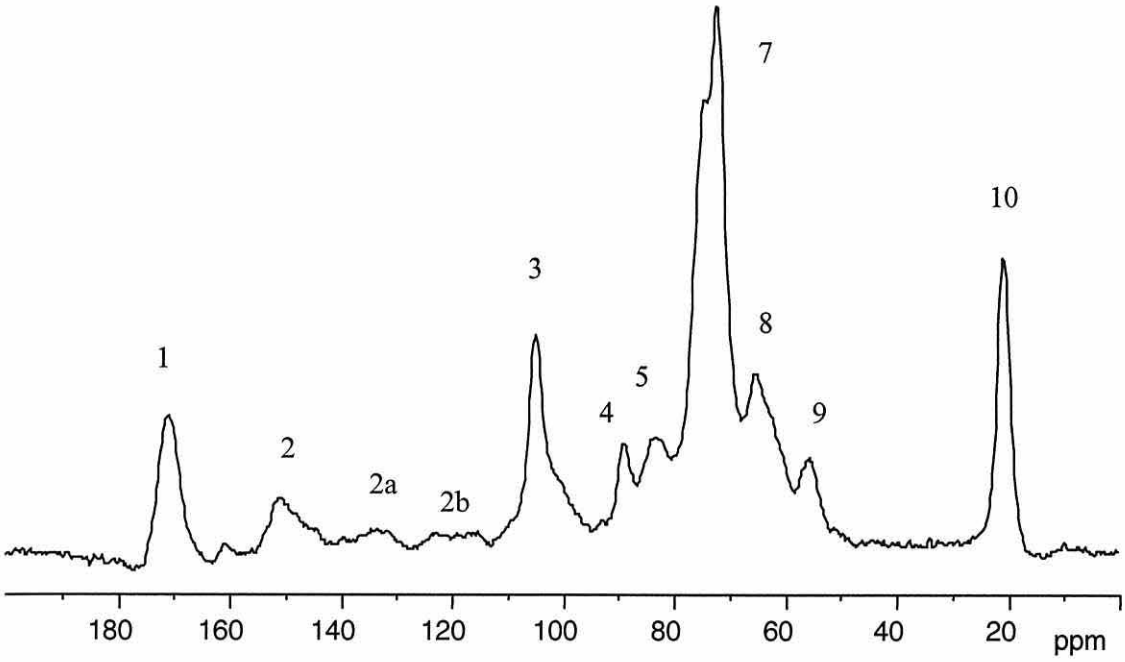

The peak at 62 ppm (8b in Table 3.4) in the acetylated wood spectrum (Figure 3.11) was significantly reduced. It is probably the hydroxyl attached to C6 on the surface of the crystalline regions that does react, as various researchers have reported that the OH on C6 position reacts fastest (Miyamoto *et al.*, 1984; Wu, 1980, on studies of commercial cellulose powder). This is confirmed by an examination of the spectra of the untreated holocellulose and

cellulose (Chapter 4, section 4.2.3). The two peaks (8 a &b) are clearly visible in the holocellulose spectrum, but only peak 8b (63 ppm) appears in the cellulose spectrum. In general, a primary hydroxyl (such as is attached to C6) is more reactive than a secondary hydroxyl (such as is attached to C2 or C3).

Table 3.4. Assignments of main peaks for solid state ^{13}C NMR spectra of wood

Peak assignment	Untreated wood (ppm)	Acetylated wood (ppm)
1 C of C=O in acetate	sm	172
2 Aromatic C attached to O	148 (br)	151 (br)
2a Aromatic C attached to C	br	132-137 br
2b Aromatic C attached to H	br	115-125 br
3 C1 of polysaccharide skeleton	105	105
4 C4 of polysaccharide skeleton	89	89
5 C4 of polysaccharide skeleton	84	84
6 C2,3,5 of polysaccharide skeleton	75	sh
7 C2,3,5 of polysaccharide skeleton	72	72
8a,b C6 of polysaccharide skeleton	65, 62	65, sh
9 C of OCH_3 of lignin	56	56
10 C of $-CH_3$ in acetate	21	21

Key:
sh Shoulder of peak present
br Broad peak
sm Small peak present

However, the reactivity of the various positions on cellulose ring may be dependent on cellulose source as well as method of reaction. Okhoshi *et al.* (1997) commented that cellulose in wood has a different reactivity to that of pure cellulose, due to the presence of lignin and hemicelluloses in the wood matrix. They found that OH groups at positions C2, C3 and C6 of cellulose in wood did not seem to have any difference in relative reactivity when makamka wood was acetylated using acetic acid, trifluoroacetic anhydride and benzene at low levels (5.7 WPG). However, in an earlier study, Ohkoshi and Kato (1993) found that the OH group at C6 in cellulose reacted to a greater extent

than those at either C2 or C3 in the uncatalysed reaction of wood (19.0 WPG). It must be noted that the studies by Ohkoshi and others, the ^{13}C NMR spectra were run on solubilised acetylated wood samples (DSMO or MMNO/DMSO).

The irregular peak 2 also has shifted slightly (148 ->151 ppm) in the acetylated wood spectrum (Figure 3.11), compared to that in the untreated wood spectrum, probably due to the acetylation of phenolic hydroxyls in lignin sub-units.

Another two acetylated wood samples were analysed by solid state NMR, and spectra were integrated (spectra not shown). The core spectra (40-160 ppm) was used as a reference and set to 100. Two acetate regions were examined: the methyl carbon of the acetate around 21 ppm (13-33 ppm) and carbonyl carbon of the acetate around 171 ppm (163-185 ppm). Figure 3.12 shows the comparison of the two acetate peak areas from the NMR spectra and extent of reaction as measured by WPG (solid).

Figure 3.12. NMR estimation of acetate in acetylated wood

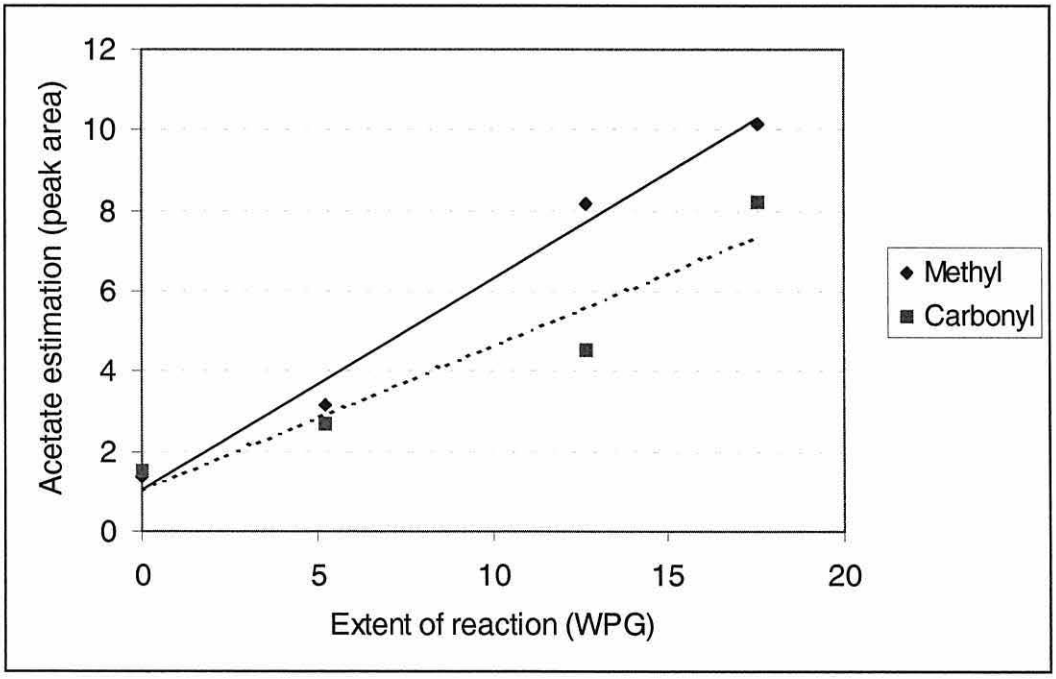

The methyl region seemed gave a better correlation (r^2=0.9851) to extent of reaction as measured by WPG compared to that of the carbonyl region

(r^2=0.9176). This could be a quick and easy way to estimate extent of reaction for acetylated wood, which has not had extent of acetylation measured. However, validation with a much greater number of samples would need to be done to confirm this method.

3.2.3. Monosaccharide and Klason lignin analyses

The results are given in two sections: the first with the source substrates (wood blocks, MDF fibre and ground wood) and the second with the delignified ground wood samples.

3.2.3.1. Analyses for wood blocks, MDF fibre and ground wood

The monosaccharide and Klason lignin analyses are given in Table 3.5 for the different wood blocks, MDF fibre and ground wood. Ground wood sample 2 was the one used in the partially delignified wood trial. This sample had a slightly different chemical composition, although some of these differences may be near to experimental error. Often these analyses do not add to 100%, as there can be losses over the three or more analysis methods used.

The three samples of the wood blocks originated from different planks of wood, and might be slightly different in composition, so were analysed separately. Slight differences were observed: for example, wood sample 1 had more lignin, more galactose and less mannose than wood sample 3. This could be due to the fact that the samples were sourced from different logs, which came from separate trees. For the reaction experiments, there were four separate source planks for the samples. Three different samples were used for each of the reaction experiments.

The MDF fibre sample, by contrast, had significantly less arabinose than any of the wood block samples, indicating that the arabinose branch units had split off the xylose chain. As the MDF fibre was made from a combination of all the wood used in this experiment, these changes were probably due to the high temperature (~170 °C) of the refining process.

Table 3.5. Monosaccharide and Klason lignin analyses of wood-based samples

Sample	Klason Lignin %	Ara %	Gal %	Glu %	Xyl %	Man %	total [c] %
Wood 1 [a]	29.4	1.20	3.10	44.8	4.90	11.4	94.80
Wood 2 [a]	28.7	1.19	1.69	46.6	4.49	12.3	94.97
Wood 3 [a]	26.8	1.15	1.52	50.6	4.87	12.3	97.24
Average	*28.3*	*1.18*	*2.10*	*47.3*	*4.75*	*12.0*	*95.67*
Grd wood 1	27.7	1.27	1.79	46.9	5.34	12.4	95.40
Grd wood 2	26.8	0.96	1.50	48.0	5.04	13.0	95.30
Average	*27.25*	*1.12*	*1.65*	*47.5*	*5.19*	*12.7*	*95.35*
MDF fibre [b]	29.6	0.38	1.66	48.5	5.09	12.1	97.33

[a] Ash content for a similar wood sample was 1.2%
[b] Ash content was 0.5% for MDF fibre
[c] Total does not include ASL
* Below detection limit: 0.04% Ara; 0.25% Gal; 0.11% Xyl
Grd wood 1 = Ground wood to smaller than 60 mesh
Grd wood 2 = Ground wood to between 36 and 60 mesh

3.2.3.2. Analyses of delignified ground wood

The lignin levels (Klason lignin and acid soluble lignin) and monosaccharides of the delignified wood samples are shown in Table 3.6. It seems that the mild method of delignification chosen did not greatly change the overall level of xylose, mannose, galactose or arabinose (a slight loss of Ara and Gal), although there was an increase in the amount of glucose (cellulose) as expected when reducing the overall lignin content.

The level of lignin in the delignified wood samples is shown in Table 3.7 (not corrected for ash), along with the percentage of the original amount of lignin. It was interesting to note the significant level of ASL generated even using this mild method of gradual delignification, and that this increased with increasing treatment times (B ->D). This level of ASL would probably affect the overall lignin reactivity, which may make the kinetic information from these samples less relevant.

Table 3.6. Monosaccharide and Klason lignin analyses of delignified wood samples

Sample	Klason lignin	ASL	%Ara	%Gal	%Glu	%Xyl	%Man	% total
Grd wood [1]	26.5	0.41	1.31	2.31	46.4	5.34	12.9	95.17
DWB [2]	13.8	5.07	1.38	1.87	50.5	5.53	12.3	90.45
DWC [3]	9.81	5.69	1.17	1.62	52.5	5.71	12.8	89.30
DWD [4]	4.95	5.74	1.22	2.14	56.5	5.43	13.4	89.38

[1] Ash content of less than 0.32 % (detection limit)
[2] Delignified wood sample B, ash content of 0.9 %
[3] Delignified wood sample C, ash content of 0.9%
[4] Delignified wood sample D, ash content of 1.5%

Table 3.7. Total and percentage lignin for the delignified ground wood

Sample	Klason lignin	ASL	Total lignin	% of original lignin
Grd wood	26.5	0.41	26.91	100.00
DWB	13.8	5.07	18.87	70.12
DWC	9.81	5.69	15.50	57.60
DWD	4.95	5.74	10.69	39.73

3.2.4. Shive analysis of MDF fibre samples

Shive analyses were conducted on the MDF fibre samples in this study to further characterise them. The results were compared to two commercially produced MDF fibre samples, to ensure that the MDF fibre used here were of a similar nature to a commercially produced MDF fibre. There were two batches produced from the refiner, as the refining variables were modified. The first batch produced a rather coarse fibre sample, so another batch of finer fibre was produced. Both the coarse and fine fibre samples (Figures 3.13 and 3.14) were analysed for interest, on samples of 1.7 g OD weight, although the coarse sample was not used in reaction experiments. Experimental details are given in Chapter 2 (section 2.7.6).

Fine MDF fibre numbers (fibres < 0.075 mm wide, or < 0.3 mm long) were not measured but were counted, and are given as a percentage of the total number of fibres counted. However, "fibres" and shives are given as a percentage of measured MDF fibres (those shown in plot). Shives are considered to be those MDF fibres that have length ≥ 3.0 mm and width ≥ 0.3 mm (Elias, 1995).

These two commercial samples (Figures 3.15 and 3.16) were selected of five commercial MDF fibre samples analysed and represented the two extremes. The shive analysis of the fine MDF fibre sample used in this study resembles that of commercial sample #1, while the coarse sample (Figure 3.14) is nearer that of commercial sample #2 (Figure 3.15). Therefore, the fine fibre sample used in this study resembled a commercially produced MDF fibre, in terms of its size distribution.

Figure 3.13. Shive analysis of the fine fibre sample
(60% fines, not measured)

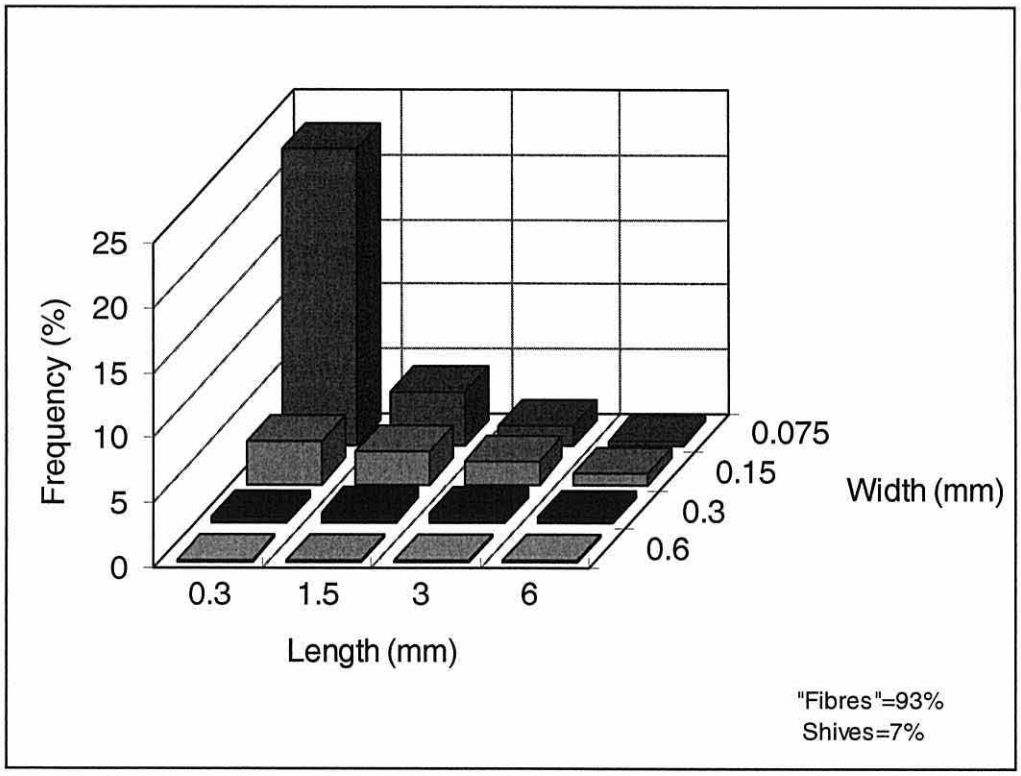

Figure 3.14. Shive analysis of the coarse fibre sample
(40% fines, not measured)

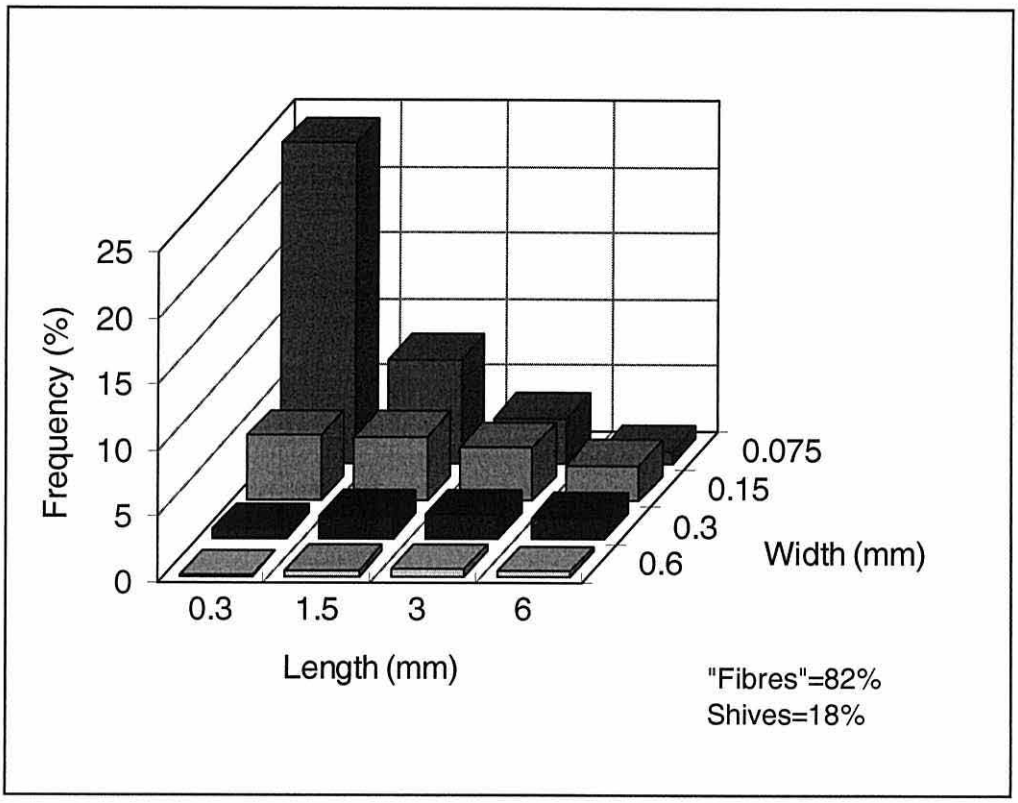

Figure 3.15. Shive analysis of commercial sample #1
(55% fines, not measured)

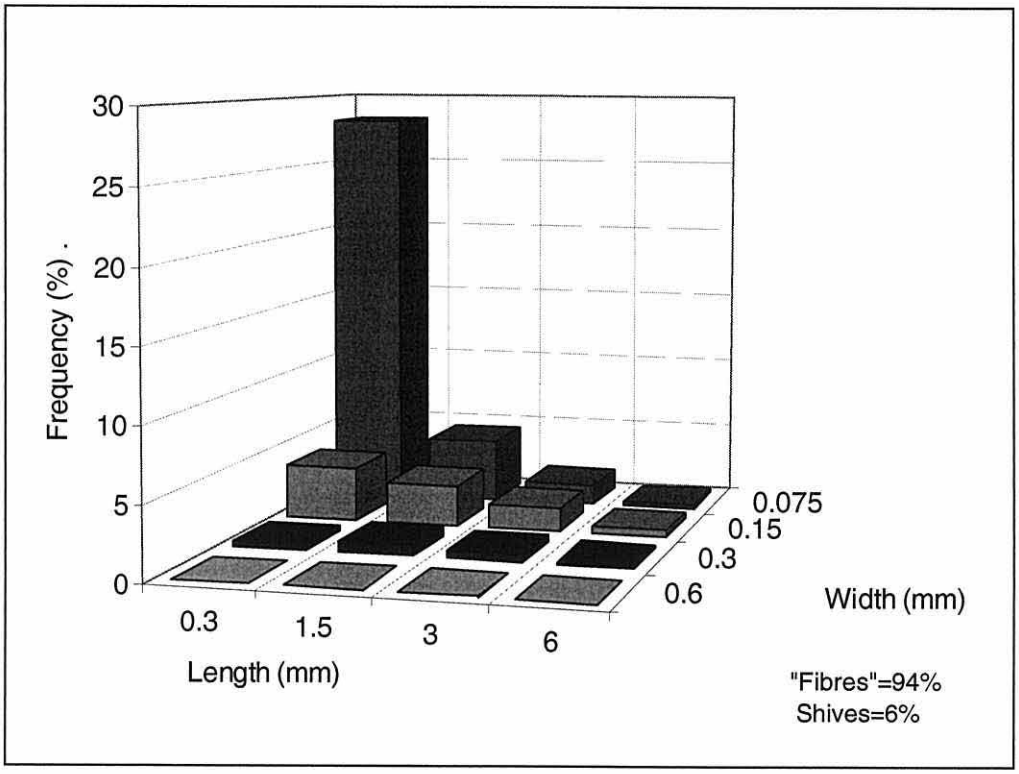

Figure 3.16. Shive analysis of commercial sample #2
(40% fines, not measured)

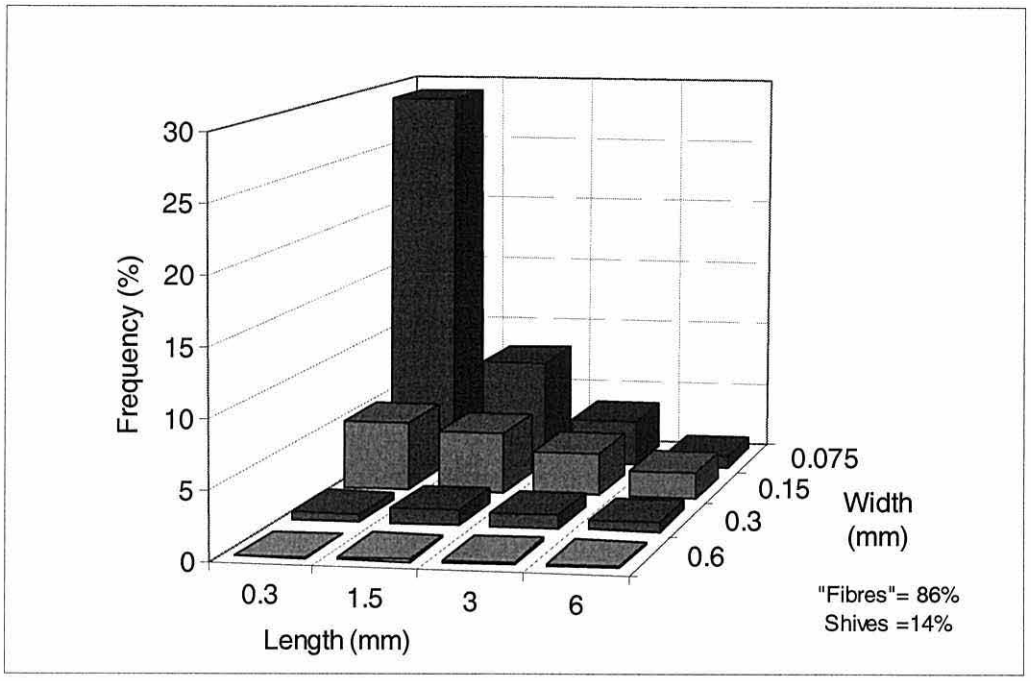

3.3. Reaction of wood, MDF fibre and ground wood

Reaction profiles were generated for each substrate at four temperatures (80, 100, 110, 120 °C) and at least four reaction times per temperature. Extra experiments conducted with longer reaction times at three temperatures were used to ascertain whether the apparent asymptote sloped to join a common maximum level of reaction for these conditions. The reaction solutions of each substrate were analysed to check whether there had been dissolution of part of the substrate. This was only significant for the MDF samples, although there were very small amounts dissolved for the other substrates.

A series of experiments were conducted to ascertain the variability in the acetylation levels obtained in wood blocks at three difference time and temperature combinations. Results are presented and discussed in section 3.5.

3.3.1. Reaction profiles

Reaction profiles are given in mmoles of wood hydroxyl (OH) reacted per gram of wood (OD) for reaction with wood blocks, MDF fibre and ground wood (Figures 3.17-3.21). Delignified ground wood samples are shown in a separate section (3.4). The extra y-axis with WPG is shown on the plots for reference.

The data were fitted using a simple exponential function of the form, $y = a.\ (1 - b^x)$, where a was the asymptote and b was the degree of curvature. The initial rate constant (k_o) was calculated either as the derivative of the exponential equation at 10% of the asymptote for each curve, or using the first two reaction data points and zero. This level for the former method was chosen so that not too much reliance was placed on the first reaction data point. Degree of fit and other raw data are given in Appendix F. All reaction profile plots have fitted curves as follows:

120 °C —— 110 °C - - - - 100 °C -—-— 80 °C — —

These simple exponential curves fitted the data in the main, although some cases did not have a flat asymptote; for example, reaction of wood blocks at 100, 110 and 120 °C. However, for the purpose of obtaining the initial rate constants, the simple curves shown were sufficient. For more extensive examination of the reaction profiles, more complex functions would need to be used.

The reaction profiles for MDF fibre are shown in Figures 3.18 and 3.19. The reaction data at 120 °C in Figure 3.18 was fitted twice: the light solid line included all the data; the dark solid line excluded reaction for 120 minutes (which was abnormally low). However, the two lines gave very similar initial rate constants. Solid WPG refers to the weight gain measured in the MDF fibre immediately after reaction. Total WPG included the small amount of dissolved substances in the reaction liquor.

Figure 3.17. Reaction of solid wood blocks

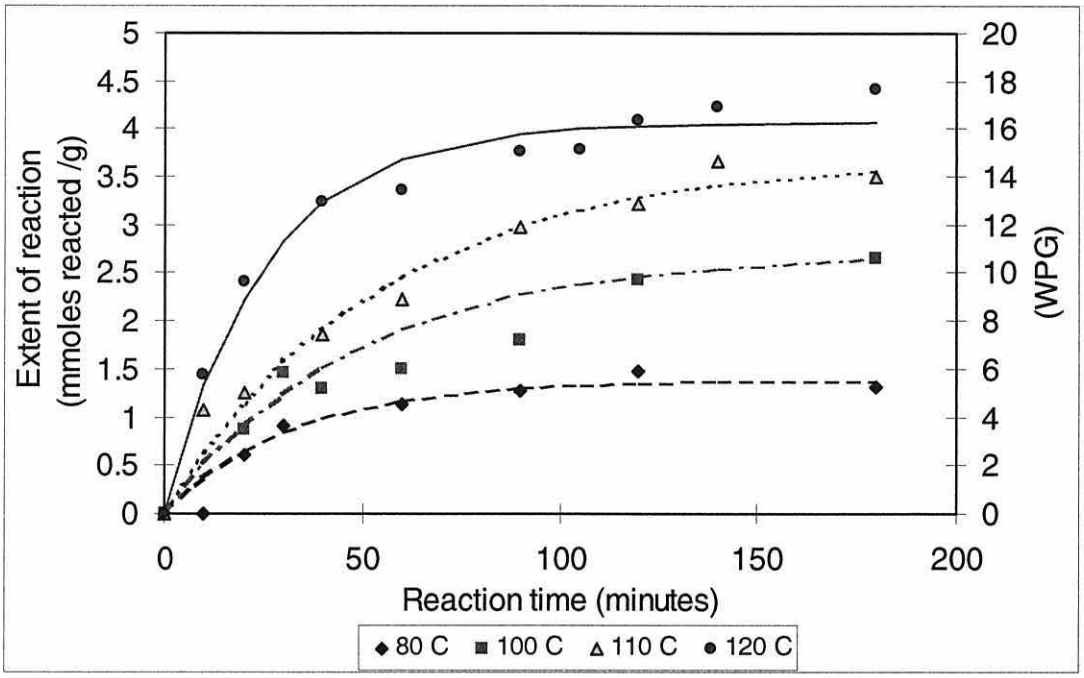

Figure 3.18. Reaction of MDF fibre (solid WPG)

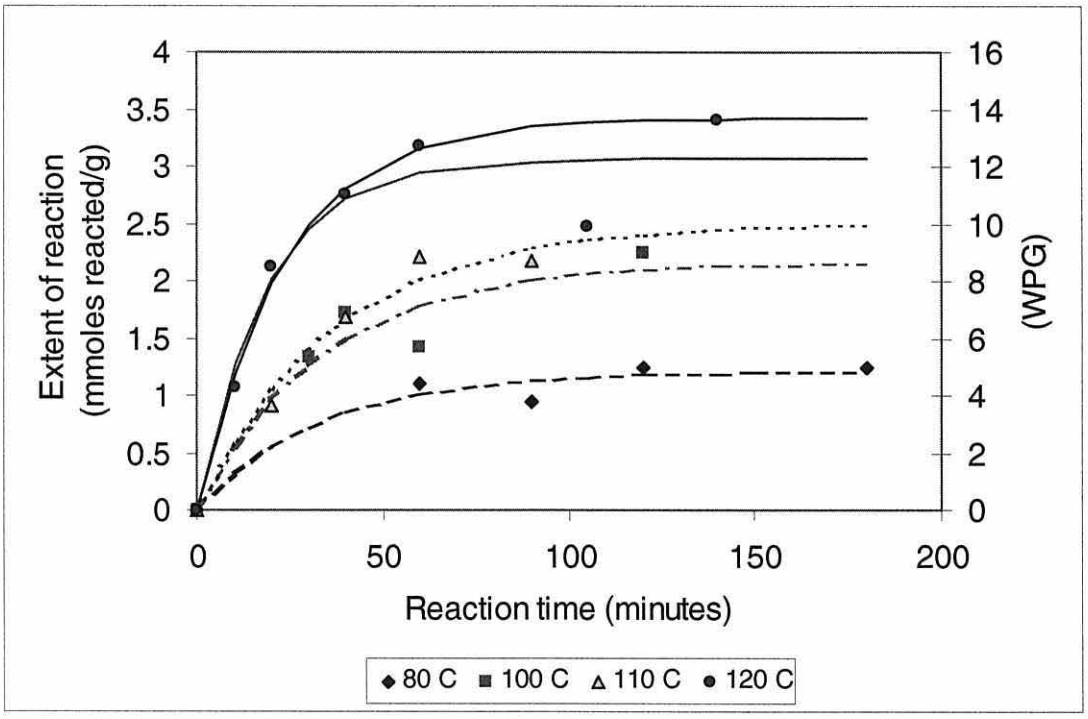

Figure 3.19. Reaction of MDF fibre (total WPG)

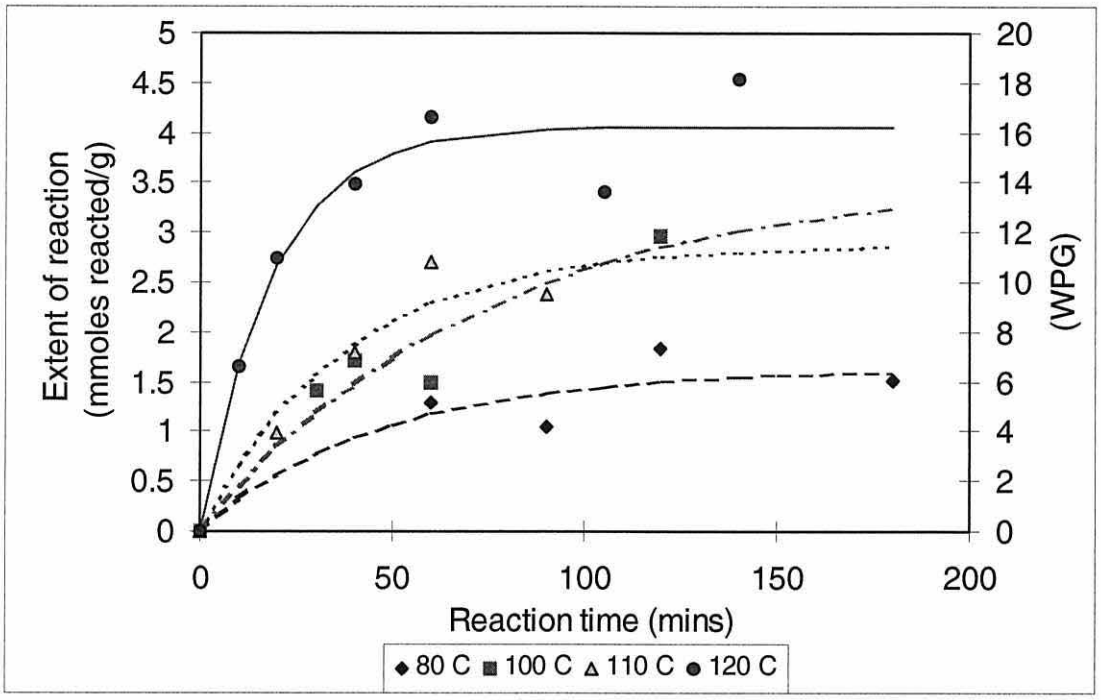

Figure 3.20. Reaction of ground wood

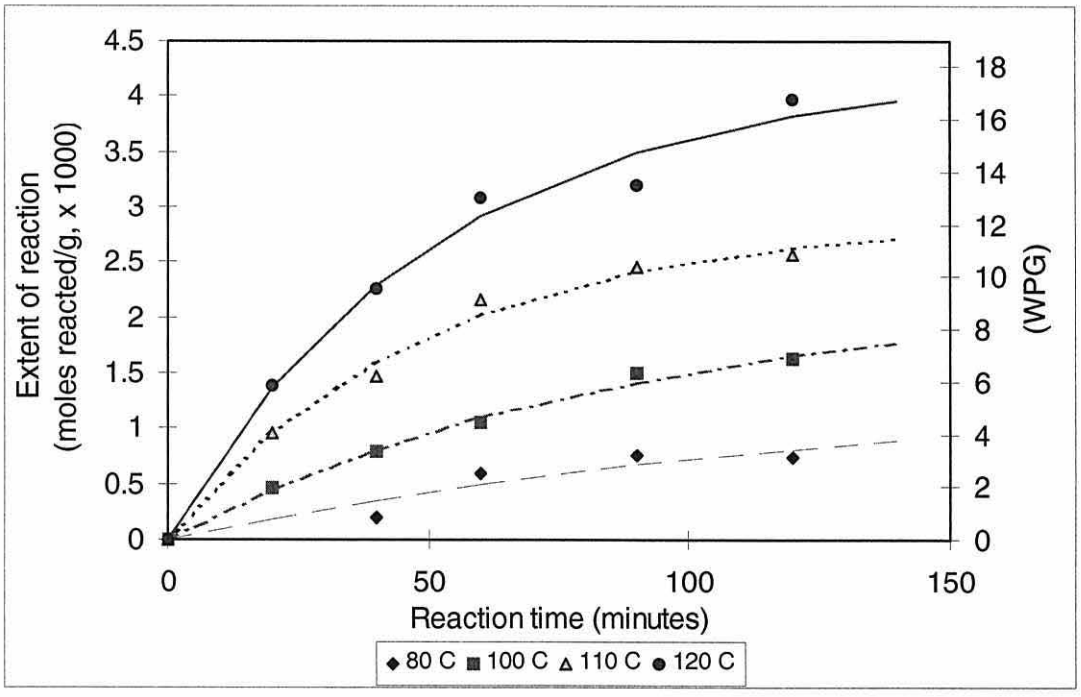

The data for MDF fibre reactions at 100 and 110 ^{o}C were similar to each other and could reasonably be described by one curve. It is difficult to know why this was so. In addition, the measurement of the small amount of dissolution of

MDF fibre into the reaction medium and/or washing solution has a reasonably high error associated with it and could have led to over or under estimation of the extent of reaction (as measured by weight added).

The ground wood (Figure 3.20) reacted to a lesser extent than did the wood blocks. This was particularly true for the reaction at 80 °C. This was surprising, as one might have predicted that the ground wood would be more accessible to the anhydride for reaction, and therefore react to a greater extent or, at least, more quickly. However, this was not observed.

Figure 3.21. Acetylation of wood blocks with longer reaction times

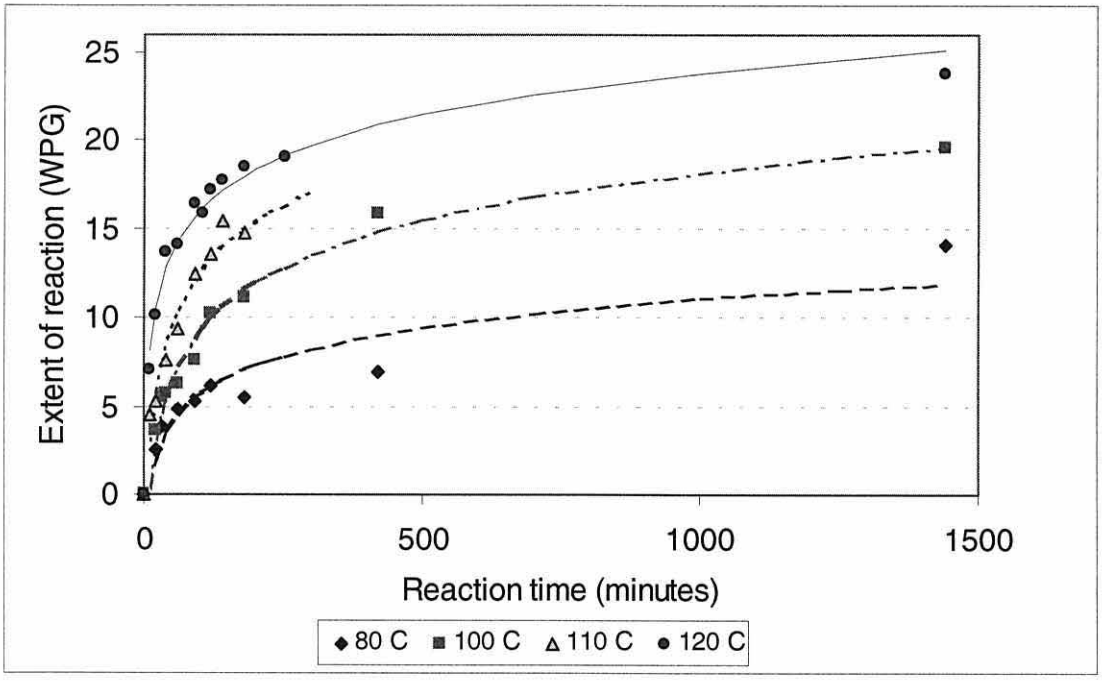

Longer reaction times for wood block reactions at 80 and 100 °C (and 120 °C) were conducted to ascertain if their apparent asymptotes converged at the same level. The reaction level did slope up to near the maximum level indicated from the reaction at 110 and 120 °C (Figure 3.21), when the data was fitted with curves (logarithmic) that did not have a flat asymptote.

Therefore, the asymptotes of the fitted exponential curves were not representing the full reaction at that temperature, but more the best fit to the data within the limits of that type of curve. It appears that under these reaction

conditions (with no added catalyst) that full reaction is around 25 WPG for radiata pine sapwood. It was interesting to note that the reaction at 80 °C seemed to rise rapidly at longer reaction times, but more data would need to be collected to model this accurately. This could be due to swelling from reaction opening up more reaction sites in the cell wall. The logarithmic curve for 120 °C might indicate that the total reaction level for these conditions might be a little higher, but no data was collected for reaction times over 24 hours (1440 minutes). It is possible that with very long reaction times, wood degradation could occur, producing new OH groups.

3.3.2. Kinetic data

Kinetic data for each substrate were calculated using the initial rate method. This involved obtaining an initial rate constant (k_o) for each temperature with each substrate (see section 3.3.1.). The natural log of k_o was then plotted against inverse temperature (in Kelvin), to see if the data fitted the Arrhenius equation (see section 1.5.2. in Chapter 1). The linear regression data obtained are shown in Table 3.8, along with standard errors, r^2 values and statistical significance.

The activation energy (Ea) values for wood blocks obtained from the initial rate method (using k_o values from 10% of the exponential asymptote) did not fit the Arrhenius equation very well (Figure 3.22a). However, the alternative initial rate method (using the first two reaction data points and zero) yielded k_o values that fitted the Arrhenius equation better. These values are compared in Table 3.8, along with results obtained from the integral method.

Table 3.8. Activation energy values from the initial rate and integral methods

Sample	Initial rate method		Initial rate (with zero) [d]		Integral method (first order)	
	Ea, kJ/mol (std error)	r^2 (significance) [c]	Ea, kJ/mol (std error)	r^2 (significance) [c]	Ea, kJ/mol (std error)	r^2 (significance) [c]
Wood blocks	33.07 [b] (13.57)	0.7480 (NS)	34.08 (9.04)	0.8765 (0.1)	39.10 (3.43)	0.9848 (0.01)
MDF fibre (solid) [a]	38.32 (11.71)	0.8426 (0.1)	47.85 (11.12)	0.9025 (0.05)	36.48 (12.23)	0.8165 (0.1)
MDF fibre (total) [a]	48.00 [b] (17.55)	0.7889 (NS)	62.54 (12.41)	0.9311 (0.05)	36.47 (10.19)	0.8649 (0.1)
Ground wood	62.13 (6.40)	0.9792 (0.02)	52.68 (4.19)	0.9875 (0.01)	42.51 (3.14)	0.9892 (0.01)

Key:

[a] Sometimes significant amounts of samples dissolved into the reaction solution, so this was measured. This gave a solid WPG (initial weight), and total WPG (including dissolved sample).

[b] These results of given for comparison purposes only, as they did not fit the Arrhenius equation.

[c] Probability of the r^2 being significant is determined using |r| values and Pearson's correlation coefficient tables, with ν=n-2, where n=number of data pairs.

[d] These values were calculated with the first two reaction data points as well as zero to obtain k_o values which were then used to obtain an Ea value

Figures 3.22a and 3.22b. show the Arrhenius plots for wood blocks as examples, for the two initial rate constant methods. The regression data for the k_o and k (first order) values for the wood reaction, and the Arrhenius plots for the other substrates are given in Appendices G, H, and I.

Figure 3.22a. The Arrhenius plot for wood blocks using the initial rate data from 10% of exponential asymptote

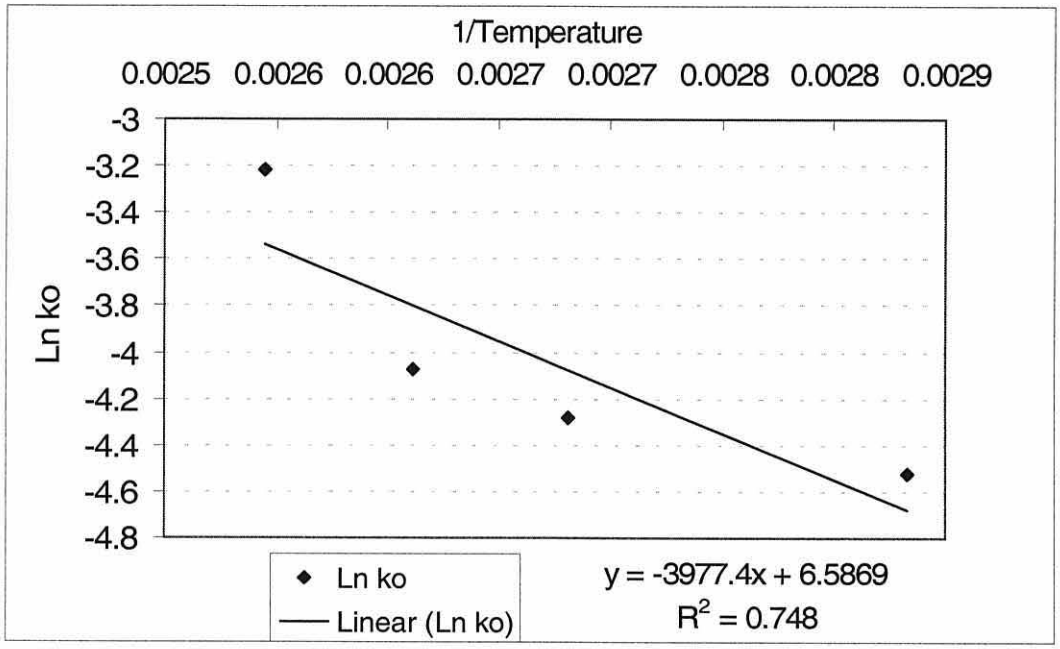

Figure 3.22b. The Arrhenius plot for wood blocks using the initial rate data from the first two reaction data points and zero.

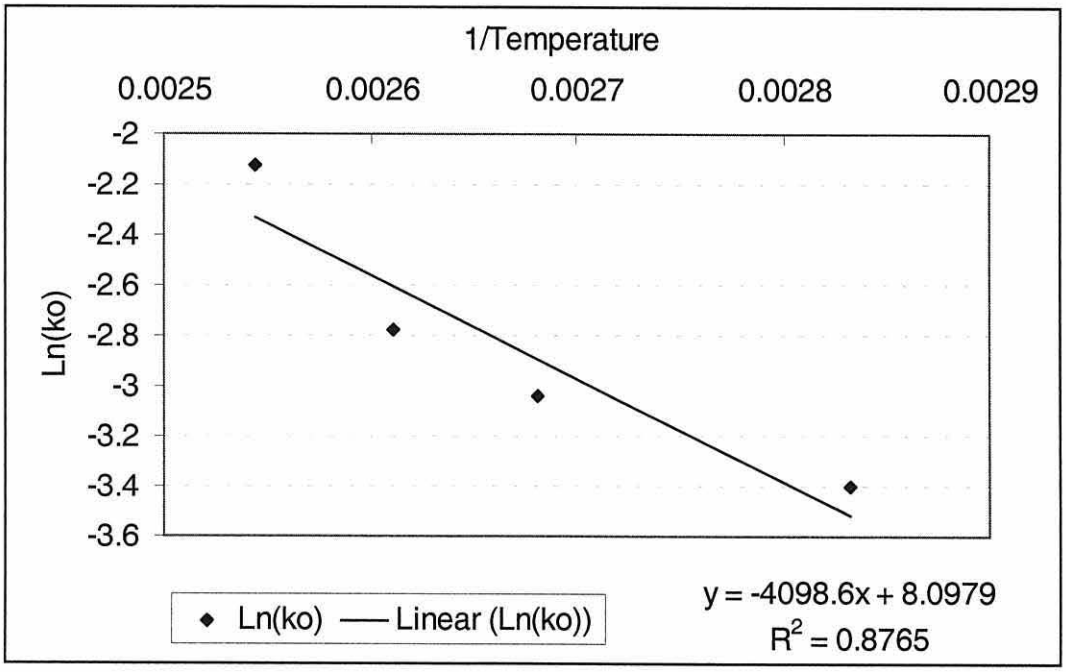

The data obtained from the reaction of the wood blocks showed that both the initial rate methods derived very similar Ea values (33.07 and 34.08 kJ/mol), with the value obtained with the integral method (first order) a little higher at 39.10 kJ/mol. As the reaction was found to be diffusion controlled (see section 3.3.3), the values for Ea obtained by the initial rate method are likely to be more accurate, at least for the initial part of the reaction.

The comparison Ea values for MDF fibre (solid) was similar or higher than for wood blocks, with 38 kJ/mol (k_o values from 10% exponential asymptote) and 48 kJ/mol (first two data points and zero). The latter is likely to be the more accurate value. However, the Ea obtained from the integral method k values (first order) was 36 kJ/mol (around the same level as for wood blocks). For MDF fibre (total), the first initial rate method gave a higher value (48kJ/mol) than that of wood blocks, which did not really fit a straight line, and the second initial rate method gave a higher value still (63 kJ/mol), which did fit well. However, the data was so variable, with the reaction level being ascertained by WPG due to varying amount of the substrate dissolving into the reaction solution. More work would need to be done to definitively determine kinetic data.

3.3.3. A closer look at the solid wood reaction

It was initially assumed that the rate of the solid wood (block) reaction would be dependent on Wood-OH concentration in the first order (ie to the power of one). It had been thought that the vacuum impregnation of the blocks and their dimensions (5 mm thick in the longitudinal direction) would allow the acetic anhydride to diffuse through the wood structure. However, when the data was tested using the first order (and second order) rate equation, and then the diffusion control test, it was found that the reaction data for the wood blocks fitted the diffusion equation better than either a first or second order rate equation.

When a solid reacts with a liquid, the liquid reactant will need to diffuse through the solid to other reaction sites once the surface reaction sites have reacted. When the diffusion through the solid is slower than the activation of

the reaction sites, then the reaction is said to be diffusion controlled. It appears that the diffusion of the acetic anhydride through the wood cell wall is slower than the reactivity of the OH reaction sites within the wood. The results are fitted to the diffusion equation and then the first order integrated rate equation for comparison.

3.3.3.1. Diffusion control plots for the solid wood reaction

The solid wood reaction was found to be diffusion controlled (Figure 3.23, using individual data points), when the extent of reaction was plotted against the square root of reaction time. This relationship was developed by Fick and others, as described in Chapter 1 (section 1.5.4). The relevant equation is shown below, as developed by Hill and others (1998).

$$m = a.\sqrt{t} \quad \text{..... Equation 3.4}$$

where m = mass of material diffusing
a = a constant (if the surface area is constant)
t = reaction time

If the extent of reaction (formation of the product) is proportional to the √time, then the rate of reaction is the same as the rate of diffusion, which means that diffusion is the rate-determining step (and slower than the activation of the reagent). However, the rate of diffusion is dependent on the concentration difference of the diffusing agent (anhydride) between the inside and outside of the cell wall, although not dependent on the concentration of OH.

The r^2 values for the regressions of the reaction data in the diffusion equation are shown in Table 3.9, and a better fit was obtained than for either the 1st or 2nd order plots for obtaining k values (Appendix H). The data in Table 3.9 was calculated using the regression on the individual data points, including the longer reactions times for 80 and 100 °C but not 120 °C (although the values for all the 120 °C data are also shown). The fit was not as good when the longer reaction times at 120 °C were included. It is important to fit these relationships on individual data points, rather than averaged data, as then the influence of one outlying data point is diminished.

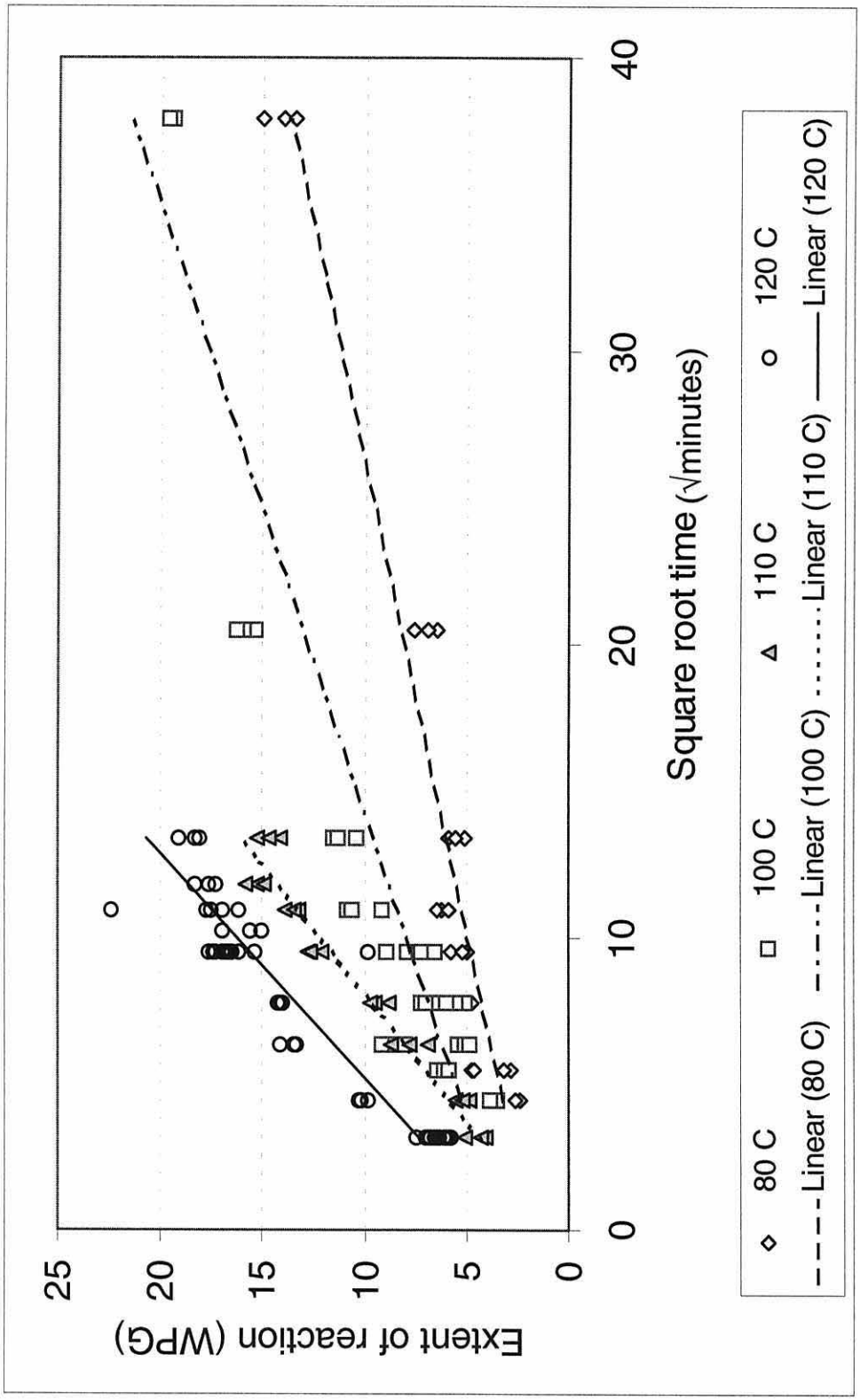

Figure 3.23. Diffusion control plot for the reaction of solid wood.

Table 3.9. Wood reaction diffusion control plot data

Temperature (°C)	n	r^2
80	27	0.9292
100	42	0.8726
110	24	0.9543
120 (up to 180 min)	48	0.8747
	Average	0.9077
120 (all data)	54	0.6080

Note: all these regression values were significant to < 0.001

A reaction can be completely diffusion controlled, which can happen when the separation of the two reactants is slow (or constrained) or the activation energy is low. As the other end of the scale, a reaction can be highly activation controlled, when the reaction rate is determined by the equilibrium concentration of the encounter pair of the two reactants (Pilling, 1975), and their passage. In this case, the activation energy is large.

Between these two extreme reaction types, there are reactions that are intermediary; for example, being diffusion controlled only under certain reaction conditions or between certain temperature ranges. There may be a small initial phase of the acetylation reaction when the surface (or readily accessible) sites are reacted, which could be controlled by first order kinetics. However, this is not particularly obvious from the diffusion plots.

If the wood is impregnated with pyridine before reaction with acetic anhydride, then only diffusion controlled reaction kinetics are observed. (Hill *et al.,* 1998). However, if there is no pre-swelling of the wood blocks, then the reaction was found to be diffusion-controlled after around 20 minutes (Hill *et al.,* 2000). When the data here were re-calculated to exclude reaction data with 20 minutes or less reaction time, the linear regression fit was not improved for the diffusion plots. This implies that there was no obvious initial phase

controlled by first order kinetics, as opposed to diffusion for radiata pine blocks in this study.

For the highest temperature studied here (120 °C), the r^2 values for the linear regression apparently improves from 0.6080 to 0.8747 (although both were significant to $P<0.001$), when data from the two longer reaction times (240 and 1440 minutes) were excluded. It appears that the longer the reaction goes at 120 °C, the more the reaction does not seem to fit the diffusion control relationship. This may be because of the expansion of the wood cell wall, which means that the cross-sectional area would not be constant, as assumed in the diffusion equation used. Alternatively, it could be simply because the available OH groups have been reacted.

The reaction of wood in this case is further complicated in that one of the products, acetic acid, can catalyse the reaction (this is called auto-catalysis), although this effect was not thought to be a strong one. A catalyst can change the activation energy, by changing the mechanism of the reaction (Walas, 1959).

So in summary, it appears that the overall reaction of solid wood blocks with acetic anhydride is diffusion controlled, despite the inclusion of a vacuum impregnation step. The rate determining diffusion is through the cell walls, rather than the wood macro-structure itself. Impregnation with acetic anhydride at room temperature would not swell the cell wall very much, although there would be some penetration of the cell wall. It is possible that the reaction of wood is initially first order, then diffusion controlled, as the anhydride present due to impregnation is used up.

It was found that the ground wood reaction was diffusion controlled between 100 and 120 °C, which would support this explanation. The reaction at 80 °C seemed to have a lag phase. It was expected that, due to the greater surface area to volume ratio in the ground wood, there would be a greater number of reaction sites available initially (and thus the initial reaction would be faster than for wood blocks). In fact, a study by Haque and Hill (1998) found that the

extent (and rate) of reaction increased as particle size decreased, and that the reaction of the smaller particles (63 - 211μm) showed first order kinetics for longer than the larger particles (500 μm – 1mm). When results here are compared, ground wood (0.250 – 0.425 mm) reacted less than wood blocks in general, which does not agree with what Haque and Hill found. However, a range of particle sizes was not investigated.

An activation energy (Ea) value of 34 kJ/mol was obtained for the acetylation of wood blocks using the initial rate constants. This is a relatively low value. Pilling (1975) indicated that reactions with low activation energies (<20 kJ/mol, for homogeneous reactions in water) tended to be diffusion controlled, and reactions which had higher activation energies tended to be activation controlled. This may be further evidence that the reaction is not purely diffusion controlled, but rather a mix of first order and diffusion control, with the latter being the dominant rate-determining step.

To kinetically characterise the whole wood reaction is difficult to do any more definitively than this, as there could be a number of other influences that have not been formally considered here. The possible diluent effect of acetic acid, the auto-catalytic effect of the acetic acid by-product, and the effect of the swelling of the wood cell wall upon reaction or increase in temperature. In particular, the swelling of the cell wall would mean that the cross-sectional area would not be constant, as is assumed in the diffusion equation used. Even the degradation of wood to produce new OH group could be a factor, although this is unlikely to happen to any significant degree under these reaction conditions.

As described in Chapter 1, diffusion can be considered as an activated process (Hill *et al.,* 1998). This means that the Arrhenius equation can be used to describe the activation needed for diffusion to take place. The activation energy of diffusion calculated for the wood block reaction was 42-44 ± 10 kJ/mol (full details shown in Table 3.10). These values are higher than

that found by Hill and others (1998) for the uncatalysed acetylation of Corsican pine (34.2 ± 1.0 kJ/mol), although within the higher error value.

Table 3.10. Comparison of activation of diffusion for different substrates

Sample		Ea (diffusion)[4] (± std err, kJ/mol)	r^2 (P)	n
Radiata pine wood blocks[1]:	Case 1	42.0	0.8991	4
		(10.4)	(0.1)	
	Case 2	44.4	0.9069	
		(10.0)	(0.05)	
Radiata pine ground wood		33.5	0.9869	4
(0.250-0.425 mm)		(2.7)	(0.01)	
Radiata pine MDF fibre [2]:	Case 1	30.1	0.9473	4
(based on solid WPG)		(5.0)	(0.05)	
	Case 2	33.3	0.9873	
		(2.7)	(0.01)	
Corsican pine wood blocks [3]		34.2	0.982	6
		(1.0)	(0.001)	

[1] Case 1 included all data for 120 °C reaction except that of 1440 min to generate the *a* values in the diffusion equation. Case 2 included only reaction data up to 180 minutes for the 120 °C reaction

[2] Case 1 includes all data. Case 2 excludes one outlier (120 °C, 105 min)

[3] Data from Hill *et al.* (1998) for the uncatalysed acetylation of wood blocks

[4] The data in this study are calculated from *a* values (Equation 3.4) which do not included the origin. However, for wood blocks the Ea (diffusion) is very similar (40.49 ± 10 kJ/mol), but for ground wood the value was a little higher (44.07 ± 1.41 kJ/mol)

Hill and others (1998) also obtained an equivalent Ea (diffusion) for the pyridine-catalysed reaction (20.5 ± 0.9 kJ/mol), which was expected to be lower than for the uncatalysed reaction. They examined six temperatures over the range 50 –110 °C, which would partly account for the lower errors and may explain the lower values obtained for the uncatalysed reaction. It was interesting to see from a comparison of Ea (diffusion) values obtained for other substrates in this study (Table 3.10), the Ea (diffusion) value for the ground wood was lower than that of the wood blocks from this study. This

would be expected, with the activation of diffusion having a lower barrier for the ground wood.

3.3.3.2. Comparison of first order integrated rate equation

The reaction of the wood blocks did not fit the first order integral rate equation particularly well (in other words, the plots sometimes fitted curves better than straight lines) for the four temperatures studied. In fact, when the second order calculations were made, the same data seemed to fit equally well as the first order equation, indicating that the data did not really fit either well (Appendix H).

For the record, the results are briefly recorded here, so that a comparison can be made to the fit of the diffusion-controlled relationship. For reaction data fitting a first order rate equation, the relationship, Ln $\{[OH]_t/[OH]_0\}$ is plotted against reaction time. Activation energy values are also given from the k values obtained. Although the k values obtained from the linear regression of the first order plots did not have a good fit to the reaction data, they fitted the Arrhenius equation reasonably well. The activation energy values obtained from these k values was 39.1 ± 3.4 kJ/mol ($r^2 = 0.9848$).

Table 3.11. Comparison of individual data of the wood reaction for both first order and diffusion plots

Temperature (°C)	Diffusion control		First order	
	n	r^2	n	r^2
80	27	0.9292	27	0.9009
100	42	0.8726	42	0.7246
110	24	0.9543	24	0.8806
120	48	0.8747	51	0.7007
Average	35	0.9077	36	0.8017

The equivalent data for the individual data points for first order is compared to that of diffusion controlled in Table 3.11. In each case, the fit is better for the

diffusion control than for the first order relationship, although for the 80 °C data, the difference was not great.

Figure 3.24 shows the first order plot for the reaction of solid wood, with regression lines (up to 180 minutes reaction time, using averaged points for clarity). For one or two of the temperatures, the data could fit a straight line, but the others seem more to be gentle curves for each of the plots, indicating that the overall reaction of wood was not controlled by first order kinetics. However, when individual data points were examined, it appears that the wood reaction could be first order initially (the first 2 points), although the diffusion plots did not indicate this. Therefore, this plot is showing the poor fit for the reaction data to a first order rate equation.

Figure 3.24. First order plot for the reaction of wood

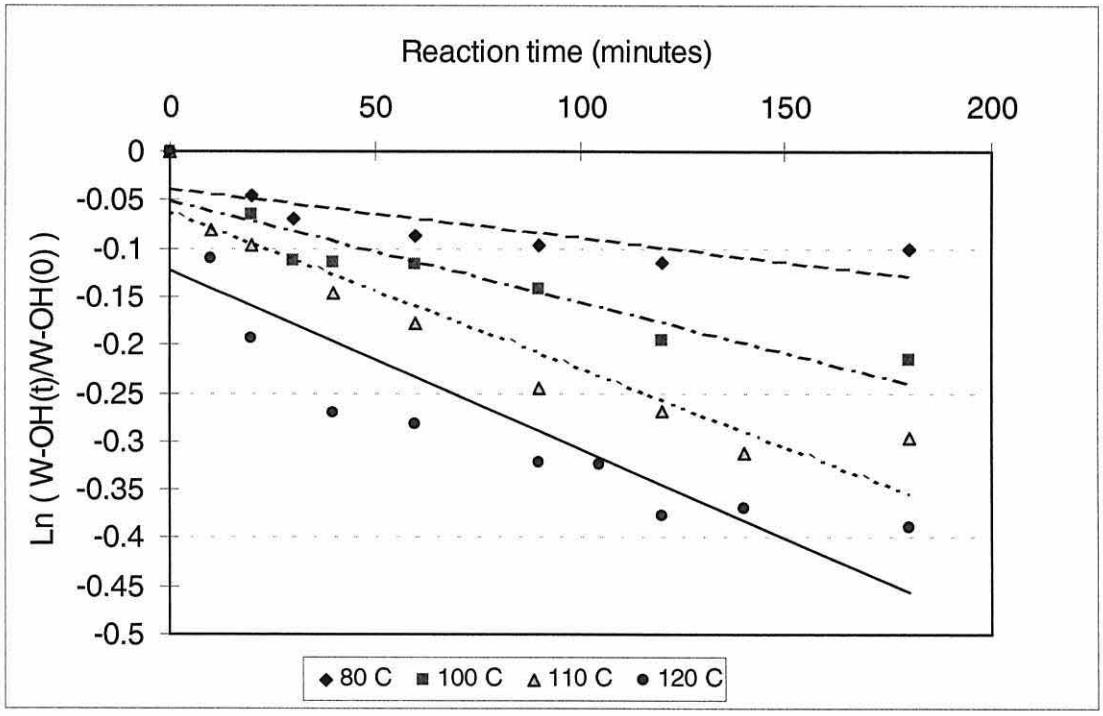

3.3.3.3. Calculation of an empirical model for wood reaction

It is difficult to develop a model of kinetics for a complex natural polymer system, particularly that of a multi-component system. However, it was decided to attempt to form a mathematical relationship between the reaction of the isolated wood components and the reaction of the solid wood. West and

Banks (1986) found that the wood-isocyanate reaction could have a double exponential equation fitted to it. They further assigned one of the exponential terms to the lignin reaction and the other to the holocellulose reaction. This type of approach was extended in this study to the three polymer groups, lignin, hemicellulose and cellulose.

As the reaction of wood with acetic anhydride was found to be diffusion controlled, then the reactivity of the individual components are not as important, as the wood ultra-structure is more influential. Therefore, this model is recorded here to illustrate the limitations of thinking of wood reactivity towards acetylation purely in terms of the reactivity of its isolated components.

The empirical model was made of the form:

$$W(x) = p.L(x) + q.H(x) + r.C(x) \quad \text{Equation 3.5a}$$

where W(x) = wood reaction, in WPG units
L(x) = lignin reaction in WPG units
H(x) = hemicellulose reaction, in WPG units
C(x) = cellulose reaction, in WPG units
p, q, r = pre-function terms (not equal)
x = reaction time at a specified temperature (between 80-120 °C)

It was decided to split the values, p, q, and r, into two parts: the first part being the proportion of that wood component in the wood, and the second part being the dominance of that wood component in the wood reaction. Thus the proposed equation would look as follows:

$$W(x) = PL.DL.L(x) + PH.DH.H(x) + PC.DC.C(x) \quad \text{Equation 3.5b}$$

where PL = proportion of lignin in wood sample
PH = proportion of hemicellulose in wood sample
PC = proportion of cellulose in wood sample
DL = dominance of the lignin reaction in the wood reaction
DH = dominance of the hemicellulose reaction in the wood reaction
DC = dominance of the cellulose reaction in the wood reaction.

The values DL, DH and DC were found to be dependant on temperature, and so predicted wood reaction curves made from the combination of the lignin, hemicellulose and cellulose reactions were investigated for three

temperatures, 80, 100 and 110 °C. This was due to the fact that the lignin reaction was run only up to 110 °C, with an extra temperature of 90 °C, so there were only three temperatures in common.

The functions L(t), H(t) and C(t) were all exponential functions of the form:

$$y = a \cdot (1 - b^{t}) \quad \text{..... Equation 3.6}$$

where a is the asymptote
b is the degree of curvature.
t is the reaction time in minutes
y is the extent of reaction

The values for DL, DH, DC and sum of the squares are given in Table 3.12 (for fitted curves, see Appendix J).

Table 3.12. Equation variables for the empirical model of the wood reaction

Temperature (°C)	DL	DH	DC	Sum sq
80	0.5312	1.896	0	0.7438
100	0	4.263	0	11.03
110	0.4199	3.8461	1.8717	3.326

This simple model implies (based on the least sum of the squares solution) that at 80 °C, the most dominant reaction is that of the hemicelluloses then the lignin to a lesser extent. For 100 °C, the hemicelluloses were indicated to be more dominant, and for 110 °C, the order was hemicelluloses, cellulose and then lignin. However, this is not what one would expect intuitively. When one looks at the comparison of the lignin and wood reaction (Chapter 5, section 5.4.1), then it is obvious that lignin models the wood reaction well in the initial stages for at least reaction at 80 °C, and therefore would be the most dominant reaction. The comparison of the predicted wood reaction with the observed wood reaction at each temperature is shown in Appendix J.

This means that a simple mathematical model that only takes the chemical composition and reactivity of the isolated wood components into account is not adequate to describe the reaction of the whole wood. This kind of model assumes that there is equal accessibility to all the components

simultaneously, yet this is obviously not true. For example, there is a significant amount of lignin in the middle lamella, rather than the S2 layer of the cell wall. The micro-porosity of the middle lamella will be different to that of the cell wall proper.

Several important aspects are not taken into account with this model, which is one based purely on the chemical composition of wood components in the wood sample and the observed reactivity of the isolated wood polymers. Firstly, the diffusion control of the solid wood reaction was in contrast to the probable activation control of the lignin (MWL) reaction, with the latter probably due to the homogeneous nature of the lignin reaction. Secondly, the swelling of the wood cell wall upon reaction (or upon contact with hot acetic anhydride), making available parts of the wood which were previously inaccessible.

This simple model was overall not a good one possibly for the above reasons, and also possibly because of the low levels of reaction (and thus high errors) of both the cellulose and holocellulose (and therefore the hemicelluloses). It was thought that it was worthwhile recording the attempt at a model of this kind to show the limitations of thinking of wood in purely chemical terms, as there are obviously physical aspects of the wood structure that play an important part in how it reacts.

A confirmation of the shortcomings of this approach for the acetylation reaction was made when a comparison was conducted of the approach of West and Banks (1986). They reported reaction data from one temperature (100 °C) of the pyridine-catalysed reaction of n-butyl isocyanate with Scots pine. The data fitted a double exponential of the form shown in Equation 3.7.

$$WPG\ (ISO\text{-}wood) = A - B.\exp(-K.t) - C.\exp(-L.t) \quad \text{Equation 3.7}$$

where A, B, C, K and L are positive parameters, with the assumption that as the curve must pass through the origin, then A = B + C
WPG (ISO-wood) is the extent of reaction for wood reacted with isocyanate

West and Banks (1986) found that this type of equation fitted the reaction data well ($r^2 < 0.999$). However, when the acetylation reaction data in this study of wood blocks for 100 °C was fitted to this type of equation, a fit could not be made. However, when C equalled zero (ie taking out the third term), a good fit was made (Figure 3.25). The equation that fitted the data is shown in Equation 3.8.

WPG (Acet-wood) = 19.72 – 15.97.exp(-0.0034.t)..... Equation 3.8

This indicated again that the wood-acetylation reaction could not be divided so simply into the reaction of the components, in the way that the catalysed wood -isocyanate reaction at 100 °C was. The acetylation reaction data at 120 °C was also investigated and also could not be described by a double exponential equation (as in Equation 3.7). Moreover, a single exponential equation (as in Equation 3.8) did not give a very good fit.

Figure 3.25. The fit of the wood-acetylation data at 100 °C using the West and Banks approach (single exponential only)

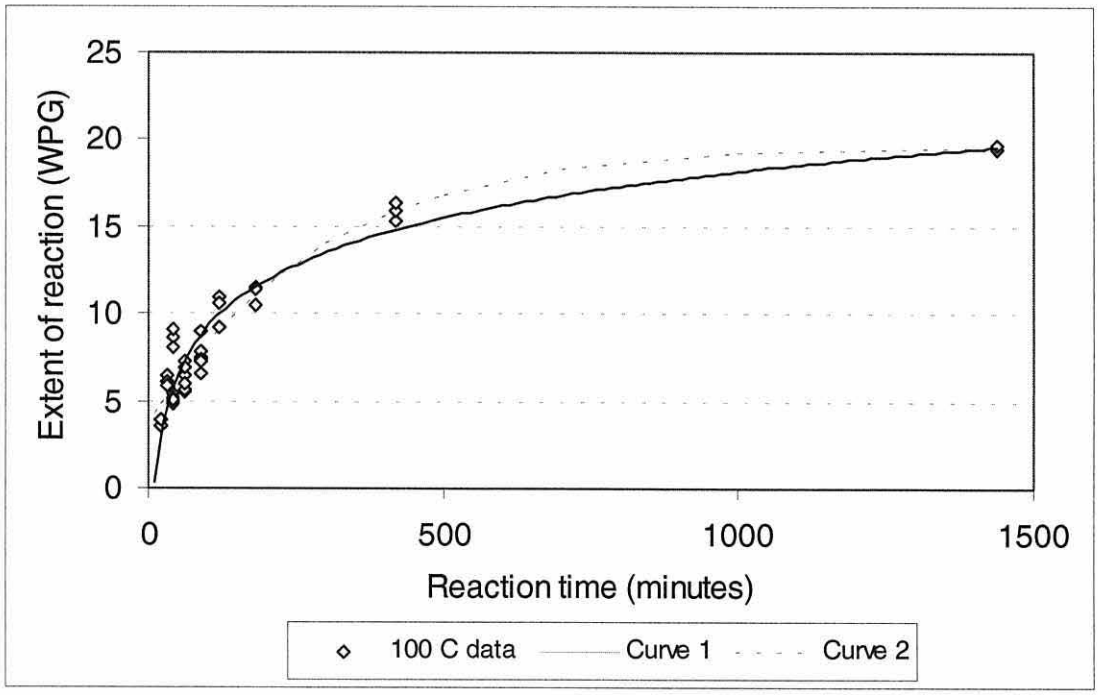

Key: Curve 1 is the exponential equation originally fitted in the reaction profile
Curve 2 is the exponential from the West and Banks (1986) approach

The curve for the reaction data at 100 °C obtained from the West and Banks approach (Figure 3.25), albeit with C=0 (Curve 2) fitted the data slightly better than the exponential curve obtained originally (Curve 1).

3.3.3.4. A mathematical model for wood reaction

It was decided to develop a mathematical equation based on reaction temperature and time to describe the reaction of wood blocks. The individual data points of extent of reaction in WPG (with the longer reaction times) at each of the four temperatures were fitted to a non-linear model with non-homogeneous variance. The following equation is the model arrived at:

$$\text{Wood reaction} = A + (A - B).\exp(-\exp(C_1 + C_2.T).t) + (D_1 + D_2.T).\sqrt{t} \quad \text{Equation 3.9}$$

where A, B, C_1, C_2, D_1, D_2 are all unknown parameters; estimates given in Table 3.13.
Wood reaction is in WPG units
T= temperature (°C)
t= reaction time (minutes)

Table 3.13. Parameter estimates for Equation 3.9, a mathematical model for wood reaction data

Constant	Value	Std error	P-value
A	15.62	0.6888	<0.0001
B	28.24	1.284	<0.0001
C_1	-15.50	0.7009	<0.0001
C_2	0.09899	0.006501	<0.0001
D_1	-0.06565	0.08788	0.4563
D_2	0.00218	0.000882	0.0144

The fit of the data to Equation 3.9 is shown in Figure 3.26, with the fit values of 467.1 and 494.0 for AIC and BIC respectively. AIC stands for the Akaike Information Criterion, which is the lowest predicted error on future data, and BIC stands for the Bayesian Information Criterion, which is the approximate probability of model to be true. The fit is very good, considering the spread of some of the data, although this is not surprising given the number of

parameters fitted and the limited number of temperatures studied. For the last term in Equation 3.9, other variations were also tried; instead of $\sqrt{t}$, t^2 and t were also tried. It was found that $\sqrt{t}$ was the better fit of these three options (lower AIC and BIC values). It was interesting to note that the latter term was dependent on the square root of time, giving confirmation of the diffusion control of the reaction.

Figure 3.26. The fit of the mathematical equation to the wood reaction data

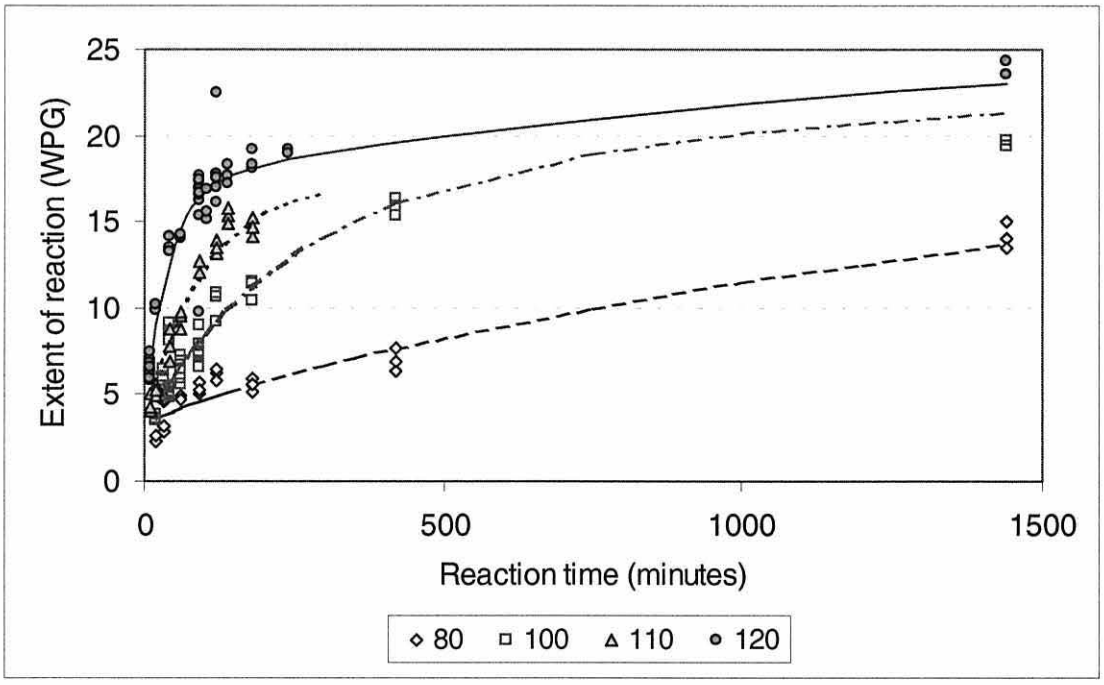

The summary of the standardised residuals is shown in Figure 3.27, and shows a reasonably even spread of error over the data range. There were two obvious outliers, but as they were in opposite directions, neither biased the model/equation significantly.

This model is only applicable to the uncatalysed reaction of liquid acetic anhydride reaction of small radiata pine blocks. However, it may also predict the approximate reaction level for similar wood species under the same reaction conditions. The wood species would need to be of similar treatability and permeability to that of radiata pine. In addition, the equation would only apply within the temperature range used here (80-120 °C). It is probable that

an equation of the same form, but slightly different parameters would be suitable for other species.

Figure 3.27. The standardised residuals for the equation of wood reaction.

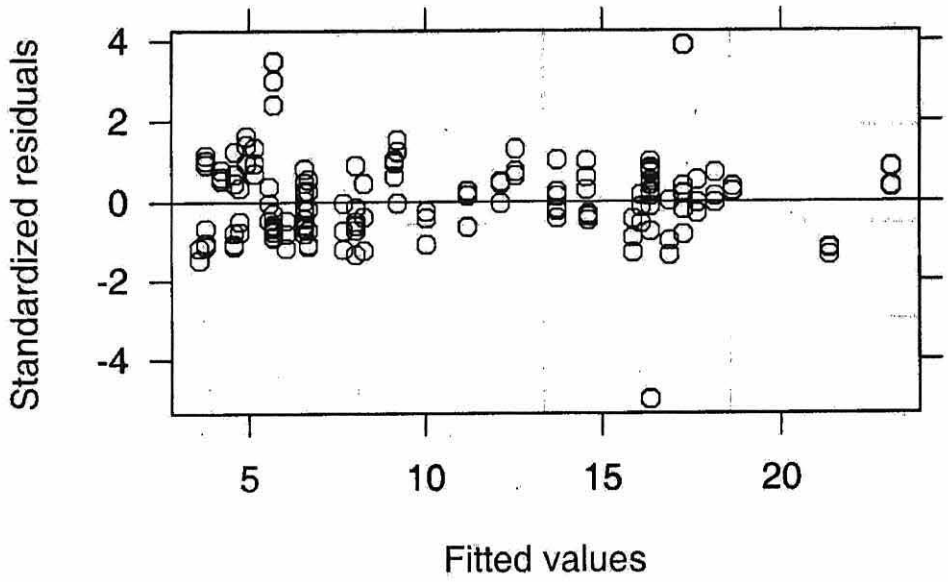

The equation was applied successfully, with small adjustments to two parameters, to the reaction of ground wood (section 3.3.4.1). However, for both of these cases (blocks and ground wood) reactions were quenched quickly at the end of the reaction time, so that accurate kinetic data could be obtained. Generally, when acetylation of wood is undertaken for property improvement, this is not a consideration, Without such quenching, this model will under-predict the level of reaction that would be reached at any given time and temperature.

3.3.4. Comparison of ground wood and wood block reaction

The ground wood samples generally reacted to a lesser extent and less rapidly than did the solid wood blocks. Possible reasons could include better acetone washing for ground wood, the vacuum impregnation of the solid wood blocks so that the anhydride has slightly penetrated the cell wall and thus not needing to diffuse for the initial reaction. For reaction at 80 °C, there was significantly lower reaction for ground wood (Figure 3.28), with the difference reducing as the temperature increased. In fact, there wasn't much difference

between reaction level obtained for ground wood and wood blocks at 110 and 120 °C (Figures 3.30 and 3.31).

Figure 3.28. Reaction of ground and solid wood at 80 °C

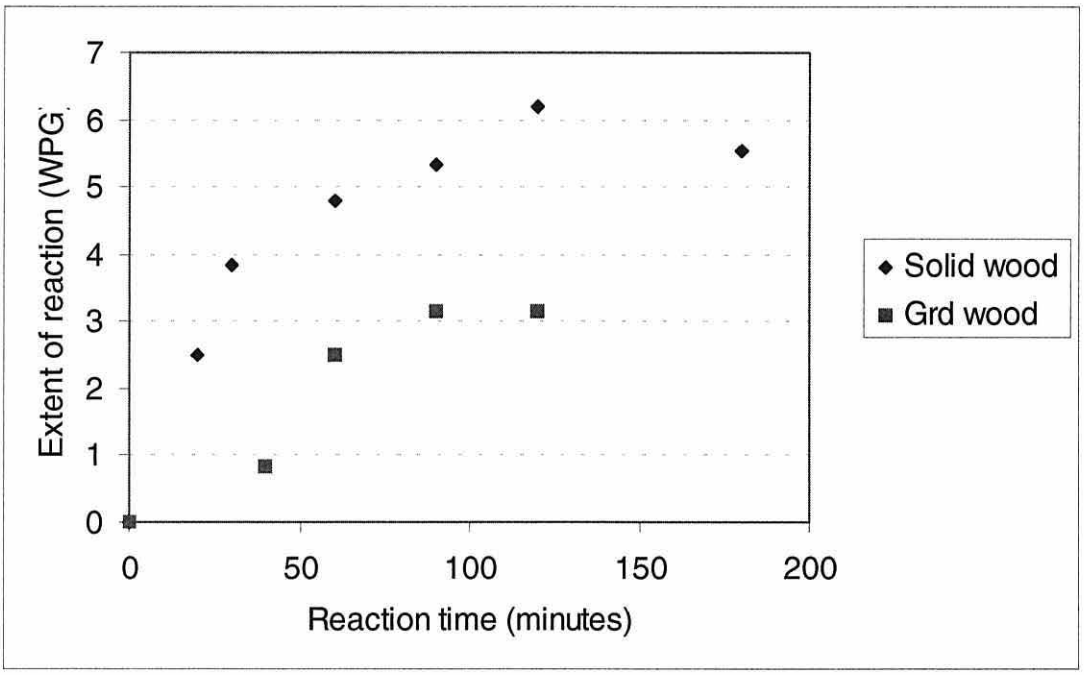

Figure 3 29. Reaction of ground and solid wood at 100 °C

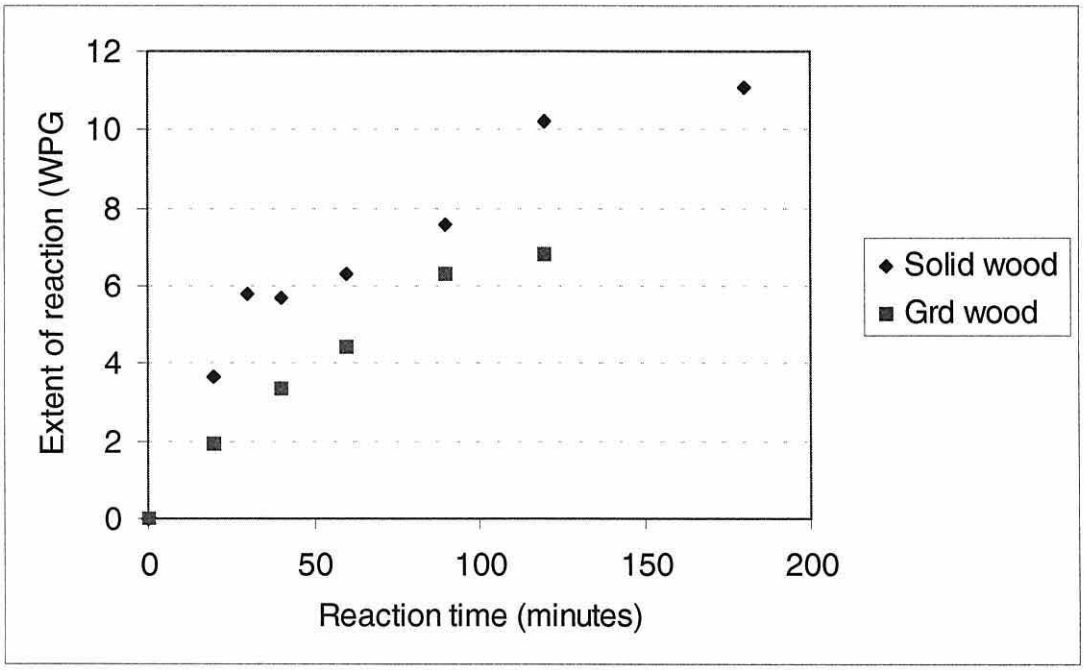

Figure 3.30. Reaction of ground and solid wood at 110 °C

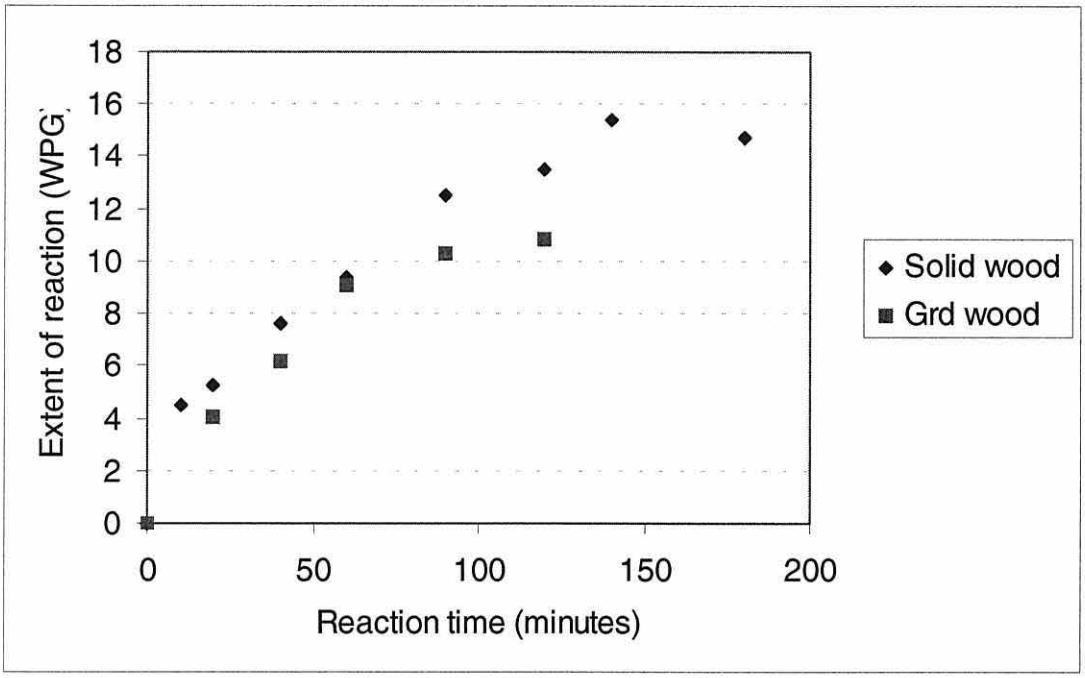

Figure 3.31. Reaction of ground and solid wood at 120 °C

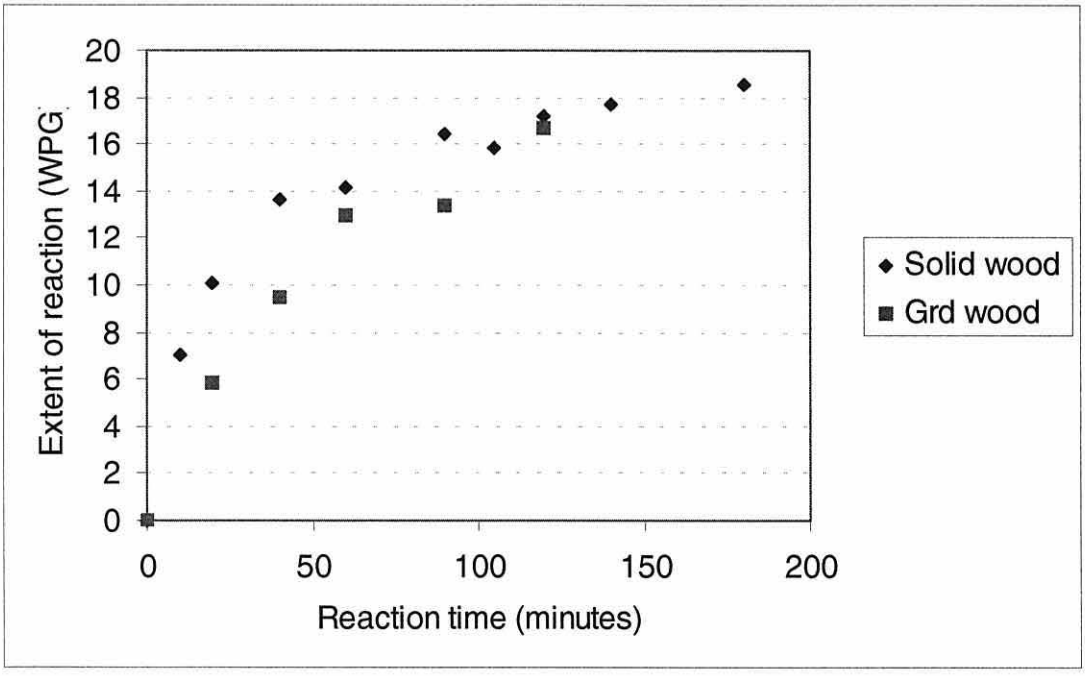

If diffusion were a major limiting factor for the ground wood reaction, one would think that it would have a lower Ea than wood blocks (even though the latter was vacuum impregnated). However, this was not observed. The Ea value (from initial rate constants) for wood blocks was around 34 kJ/mol,

whereas the Ea value for ground wood was higher (53 kJ/mol). These values imply that the reaction with ground wood exhibited greater temperature dependence than solid wood. This could also be due to the initial reaction being more controlled by first order kinetics than diffusion, with the anhydride already slightly penetrated into the cell wall due to impregnation for wood blocks. However, the ground wood did have a smaller Ea (diffusion) value (34 kJ/mol) than wood blocks (42-44 kJ/mol), which would support the dominant influence of diffusion in the ground wood reaction (see Table 3.10 for details).

Figure 3.32. The diffusion control plot for ground wood

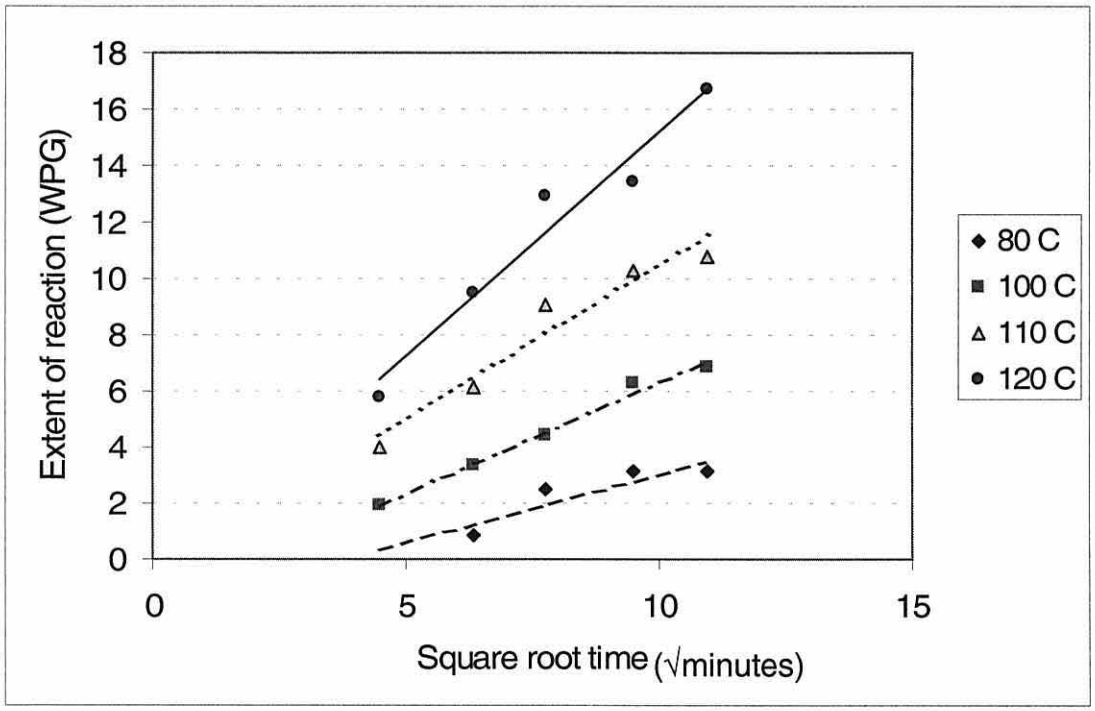

However, the ground wood reaction was found to be diffusion-controlled, when extent of reaction was plotted against $\sqrt{t}$ (Figure 3.32), at least for the temperature range 100°-120 °C. The reaction data at 80 °C did not fit a straight line so well. The regression results are given in Table 3.14 and were calculated on the regression of individual data points rather than the averaged data shown on Figure 3.32. The P value of 0.01 for the reaction at 80 °C in Table 3.14 does not mean that the data fit a straight line well; in fact, these data fitted a curve much better.

It was surprising initially that the ground wood reaction was also diffusion controlled for much of the temperature range studied. However, this evidence supports the idea that the rate-determining diffusion occurs through the wood cell wall, rather than the wood macro structure.

Table 3.14. Regression data for the diffusion control test of the ground wood reaction

Reaction level	n	r^2	|r|	P
80 °C	8	0.763	0.874	0.01
100 °C	14	0.934	0.966	<0.001
110 °C	10	0.930	0.964	<0.001
120 °C	10	0.953	0.976	<0.001

It was thought it might be interesting to see whether the empirical model fitted the ground wood reaction to a better or worse extent than it did for wood blocks. However, the model seems unlikely to have a better fit to ground wood data, given the similarity between the kinetic results; that is, that the reaction for both wood blocks and ground wood was found to be diffusion controlled. In fact, the same kinds of problems were encountered for ground wood that had been for solid wood.

The predicted curves of best fit (lowest sum of squares) implied that the reaction of cellulose was dominant for the ground wood reaction at 80 °C (regression plots and variables are given in Appendix K). In the same way, it implied that the reaction of hemicelluloses was dominant for the reaction at 100 °C, and that the reaction of cellulose was slightly more dominant than that of the hemicelluloses for the reaction at 110 °C. Since there was approximately the same level of lignin in ground wood as the wood blocks, and that lignin comprises the larger part of the acetylation reaction achieved in wood, these results do not accord with other observations. Therefore, the empirical model attempted did not fit ground wood reaction any better than it fitted the wood block reaction.

3.3.4.1. Application of the mathematical model to ground wood

The reaction data for ground wood was plotted against the mathematical equation obtained for the reaction of wood blocks (Figure 3.33).

Figure 3.33. Ground wood reaction data compared to the predicted wood block reaction (mathematical model)

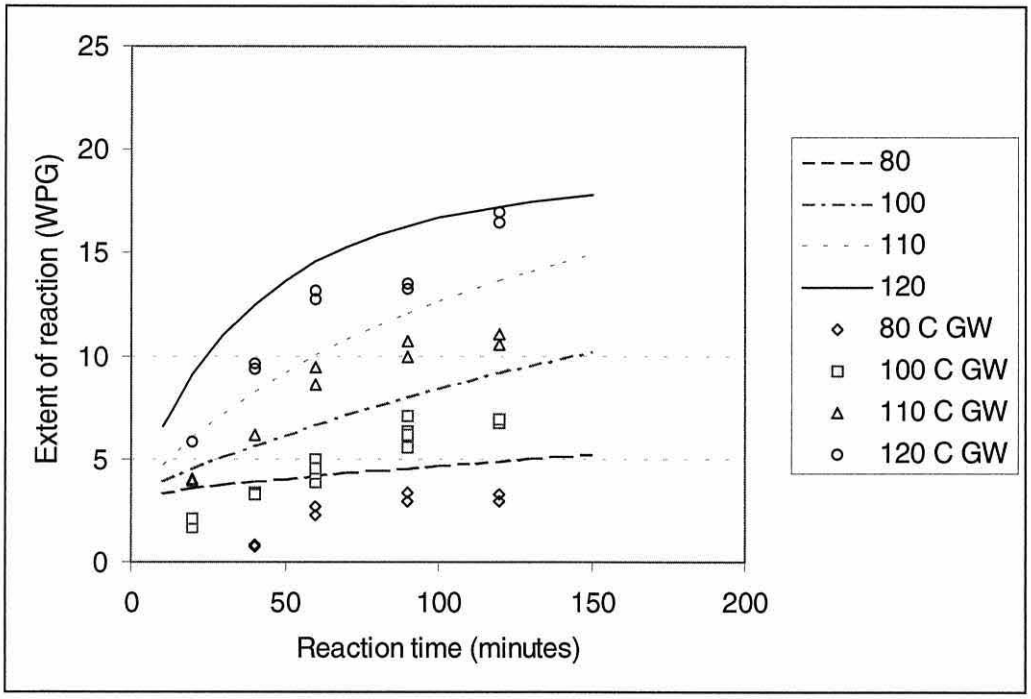

Figure 3.34. Ground wood reaction data with adjusted parameters for mathematical equation

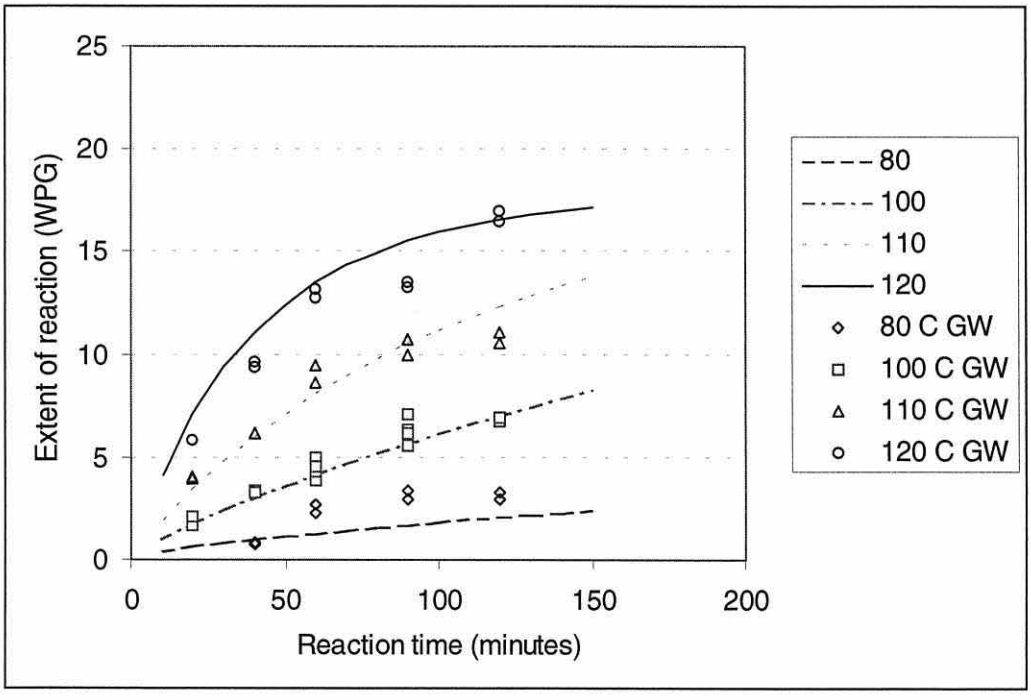

The predicted wood block reaction level from the mathematical model over estimates the extent of reaction for ground wood, as would be expected. However, if just two parameters (A and B) are adjusted, the fit is much better, particularly for data from reactions at 100-120 °C (Figure 3.34). The parameter A was changed from 15.62 to 15, and B from 28.24 to 30.

3.3.5. Discussion

The purpose of obtaining kinetic data for a wide range of wood-based or wood-derived substrates was to compare the effect on the rate of reaction that the substrate changes brought. However, there can be difficulties when applying classical reaction kinetics to complex natural polymer systems such as wood. Nevertheless, some useful points of comparison were noted.

When the wood reaction was found to be diffusion controlled, calculations were also carried out on the MDF fibre (total WPG) data. These showed that the MDF fibre reaction could be diffusion controlled, rather than first order with respect to hydroxyl concentration, but it was difficult to be definitive with such variable data (Appendix L). When the equivalent calculations were done for the MDF fibre (solid WPG) reaction data, the data showed an even better fit to the diffusion equation. This implies that diffusion through a single cell wall is still influential in the acetylation of MDF fibre. It would be interesting to pursue this in greater depth for future work and confirm this.

The initial rate method of obtaining the activation energy (Ea) was probably the most accurate that was obtained for wood blocks, as the reaction was diffusion-controlled and a first order rate equation could not be used. The Ea values obtained here for wood blocks are compared with literature values, obtained under a variety of reaction conditions and wood species (Table 3.15).

Hill and others (Hill *et al.,* 1998; Hill and Papadopoulos, 2002) found that the effect of pyridine catalysis was to lower the activation energy for the reaction. However, the value that they obtained for the uncatalysed reaction (51 kJ/mol) was higher than the value found here (34 kJ/mol), but the temperature range they used was wider and lower than that of this study.

Table 3.15. Comparison of activation energy values for reaction of wood

Sample	Ea, kJ/mol (std err)	Acetylation method	Reference
Radiata pine	34 (9)	Uncatalysed acetic anhydride (80-120 °C) blocks	This study
Corsican pine	51 (3)	Uncatalysed acetic anhydride (50-110 °C) blocks	Hill *et al.*, 1998
Southern yellow pine	42 (8)	} Uncatalysed acetic anhydride } in xylene (100-140 °C)	Ramsden and Blake, 1997
Larch	107 (2)	} 2 ml cubes [2]	"
Corsican pine	42 (8)	Pyridine-catalysed (50-110 °C) blocks [1]	Hill *et al.*, 1998
Corsican pine	37 (5)	} Pyridine-catalysed } (60-120 °C) blocks }	Hill and Papa-dopoulos, 2002
Scots pine	43 (11)		
Cotton	71	} Perchloric acid-catalysed	Sen and Ramaswamy, 1957
Jute	54	} (25-36 °C, 3 Ts only)	

[1] Samples were vacuum impregnated with pyridine, and then brought to temperature before introducing anhydride (ie pre-swollen)

[2] Samples were not vacuum-impregnated and k values were calculated from zero-order rate equations

The effect that wood species has on such data is not known. Ramsden and Blake (1997) looked at four different wood species and found that activation energy values (calculated from zero order rate constants) varied from species to species. Unfortunately, they only examined three temperatures (100, 120 and 140 °C) and did not consider diffusion control. Further, extractives were not first removed before reaction, and so could have significantly effected the results obtained.

It is possible that wood species influences Ea values obtained for acetylation, with properties such as wood density, permeability and degree of wood

collapse contributing to observed differences (as these are factors that might alter diffusion). However, more work would need to be done to confirm or deny the influence of such property differences. It is more likely that differences in reaction conditions, inclusion of a solvent (swelling or non-swelling), the temperature range and number of temperatures studied, and size and orientation of wood block (or substrate) investigated will have a greater influence on the apparent activation energy of the reaction.

Due to the expected dominance of lignin in the reaction of wood as a whole, lignin and a lignin model compound were studied in more depth (Chapters 5 and 6), and compared to the whole wood reaction. However, it was realised that by isolating the lignin from the wood structure, not only was the isolated lignin chemically changed from the native lignin, but it would also be in a completely different physical environment during reaction, which could also change the results. It was for the latter reason that it was attempted to obtain kinetic results from partially delignified ground wood using a mild delignification method. These results are presented and discussed in the next section.

3.4. Reaction of partially delignified ground wood

Ground wood samples were delignified with a mild method (buffered), to minimise any changes to the remaining lignin and to minimise the dissolution of hemicelluloses. The details of the method used is given in Chapter 2 (section 2.6). The isolated lignin was known to have changed during the isolation and purification process. In addition, the isolated MWL was a powder and therefore would dissolve during reaction with acetic anhydride, making the reaction homogeneous. The examination of increasingly delignified ground wood was an attempt to quantify the reducing effect of lignin on extent and rate of reaction, and thus build up a picture of the native lignin reaction. Another way this could be obtained, without using isolated lignin, would be to subtract the reaction of holocellulose (delignified ground wood) from the ground wood reaction. However, due to the low level of reaction of the

holocellulose, much longer reactions times would be needed, so that most of the reaction profile is examined.

Three partially delignified ground wood samples were reacted, along with untreated ground wood to obtain kinetic information from these substrates. The partially delignified ground wood samples had total lignin contents of: 18.9% (DWB), 15.5% (DWC) and 10.7% (DWD), in comparison to the non-delignified ground wood samples which had a total lignin content of 26.9%. Details of the lignin analyses of these samples are given in section 3.2.3.2.

The acid soluble lignin (ASL) content increased with increasing delignification. Half of the lignin content of sample DWD was ASL rather than Klason lignin, out of a total lignin content of 10.7%. In comparison, the untreated ground wood sample had an ASL content of only 0.4%. Acid soluble lignin was produced by the delignification and therefore was one significant change from the original sample. It appears that ASL has less methoxyl content than KL, and could contain lignin carbohydrate complexes (Yasuda & Murase, 1995). However, not much work has been done on characterising ASL. The work of Yasuda and Murase (1995) was conducted with simple lignin model compounds, which reacted with carbohydrates in 72% sulphuric acid.

The ground wood samples in this study were not in contact with sulphuric acid, but were treated with chlorite as part of the delignification process. If the principle that Yasuda and Murase (1995) found holds for this study, then that it could mean some of the residual ASL could be newly formed lignin carbohydrate complexes (LCC) that weren't present originally in the wood. This would mean that the ASL has an altered reactivity and number of potential reaction sites. Therefore, the ground wood samples that have been partially delignified might give erroneous impression about the reactivity of the residual lignin, if a significant proportion was ASL.

However, there is some debate about where what is measured as ASL is derived from. For example, as well as low molecular weight lignin and chlorinated lignin, there could also be modified carbohydrates present and

measured as ASL (Swan, 1965; Schöning and Johansson, 1965). The latter workers found that the amount of ASL increased for a bisulphite pulp with increasing yield of cooking up to around 4% ASL (at ~70% yield).

3.4.1. Reaction profiles

Reaction profiles from partially delignified ground wood (Figures 3.36-3.39) at the lower temperatures used seemed to have a lag phase, for reasons which are unclear. The ground wood (not delignified) reaction profile is shown for comparison (Figures 3.35). The profile for ground wood showing only exponential curves is shown earlier in Figure 3.20 (section 3.3.1). Therefore, the exponential curves successfully used for the other substrates did not fit some data as well as a sigmoid curve fitted, and so both are shown.

Figure 3.35. Reaction of ground wood, 26.9% total lignin content (with sigmoid curve for 80 °C)

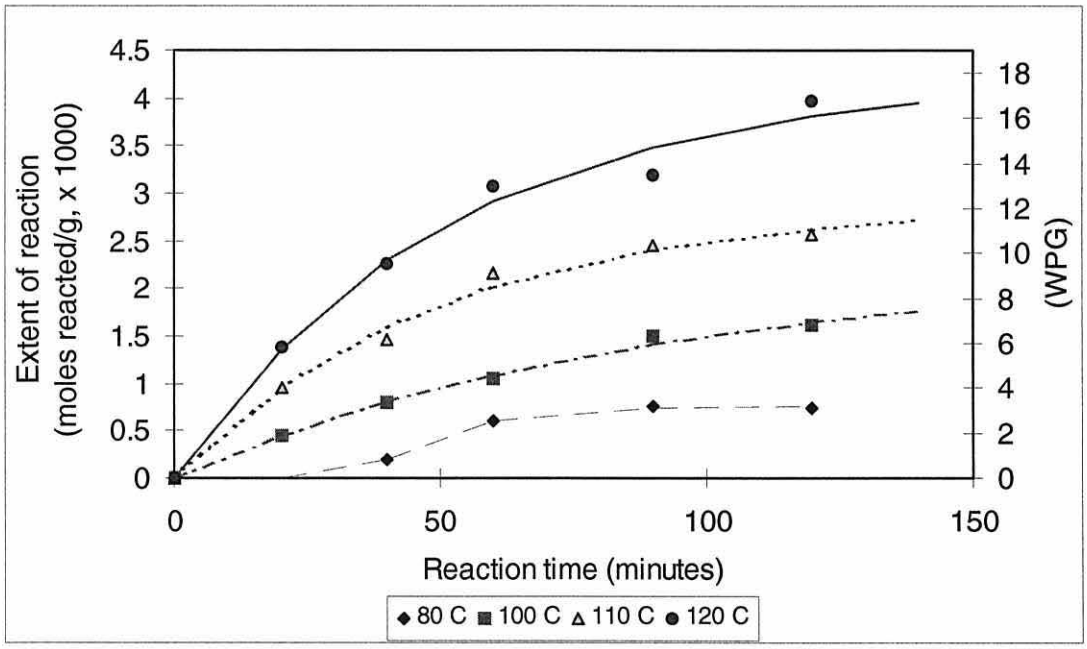

Figure 3.36. Reaction with delignified wood sample, DWB, 18.9% lignin (sigmoid curves for 80 and 100 °C)

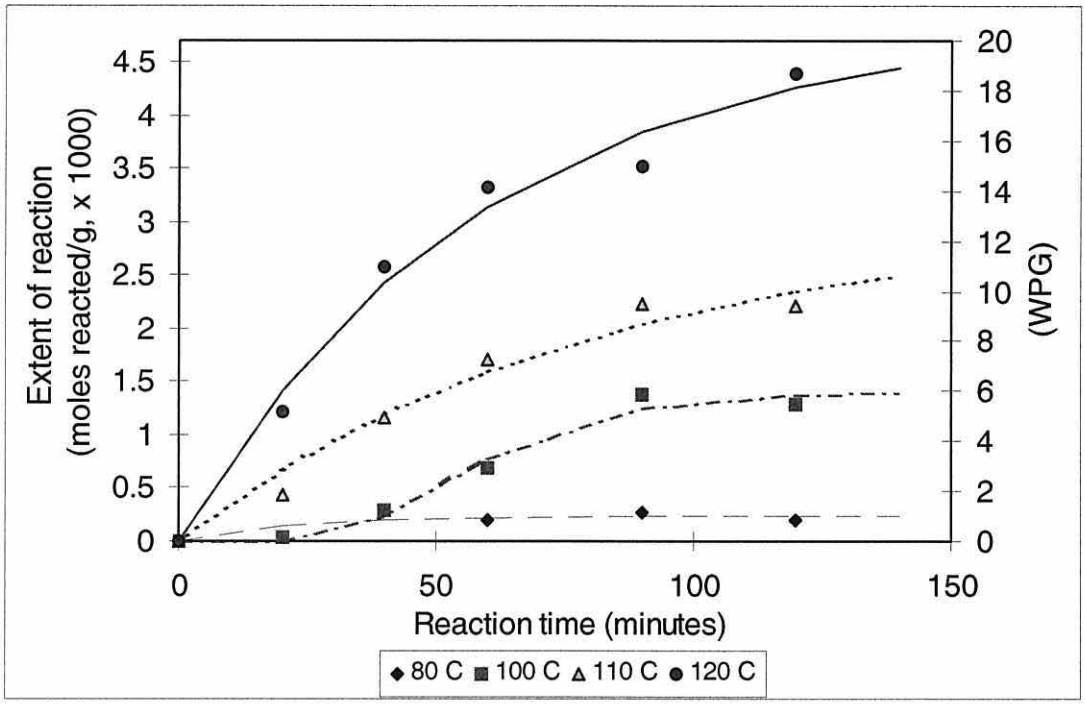

Figure 3.37. Reaction with delignified wood, DWC, 15.5% lignin (sigmoid curve for 100 °C)

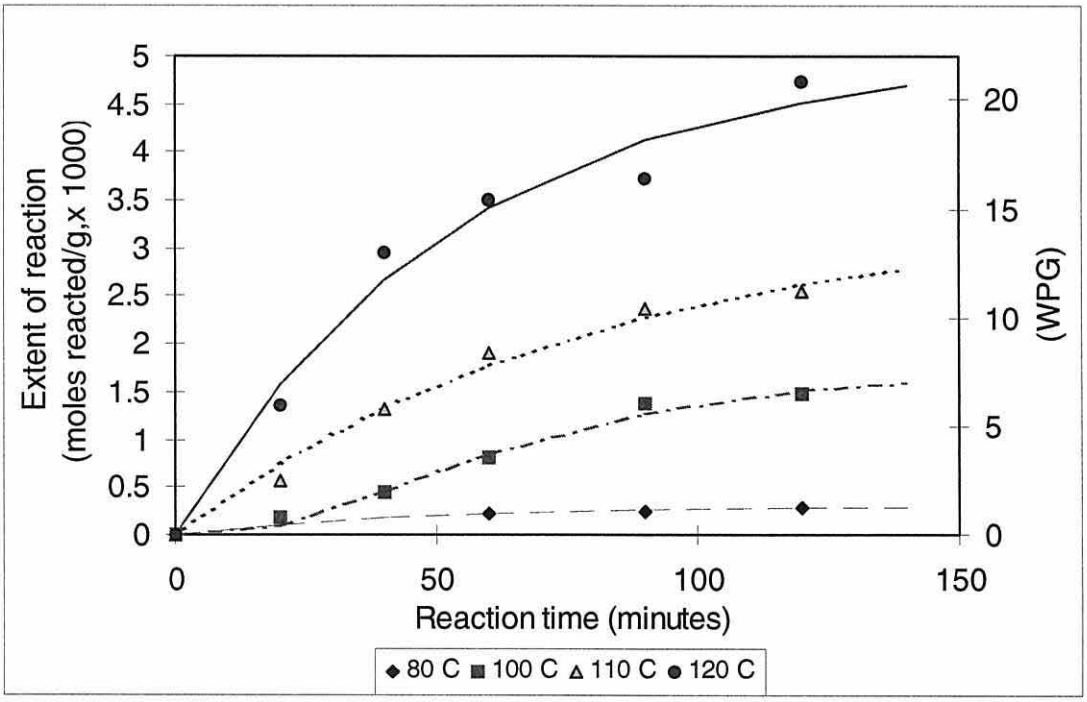

Figure 3.38. Reaction with delignified wood, DWD, 10.7% lignin (all sigmoid curves)

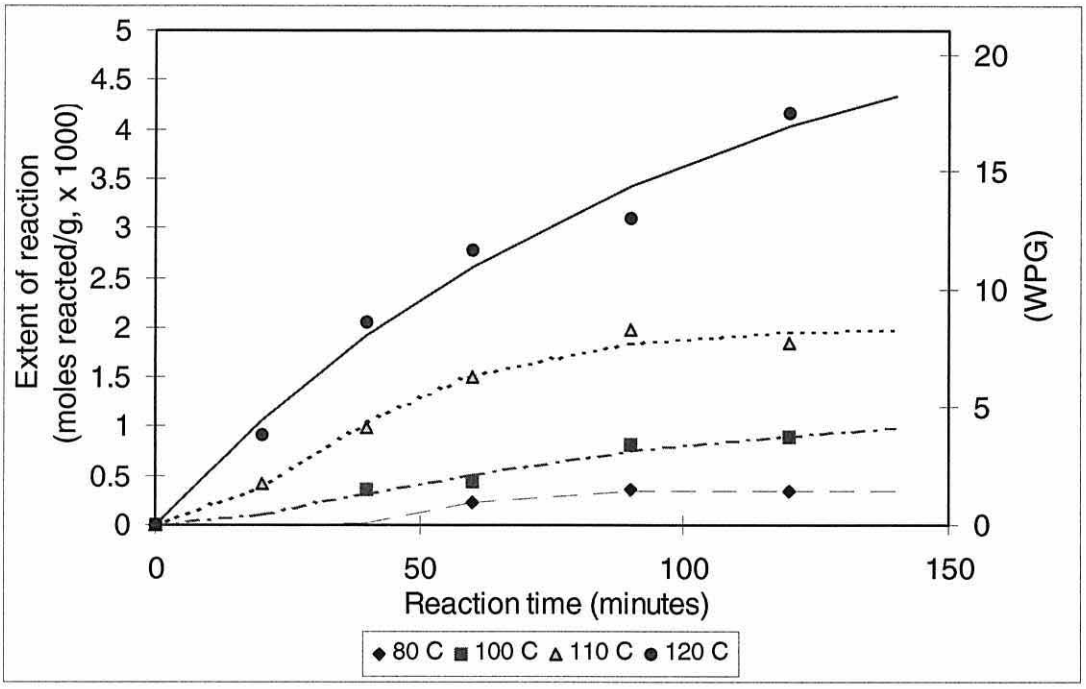

Figure 3.39. Reaction with delignified wood, DWD, 10.7% lignin (all exponential curves)

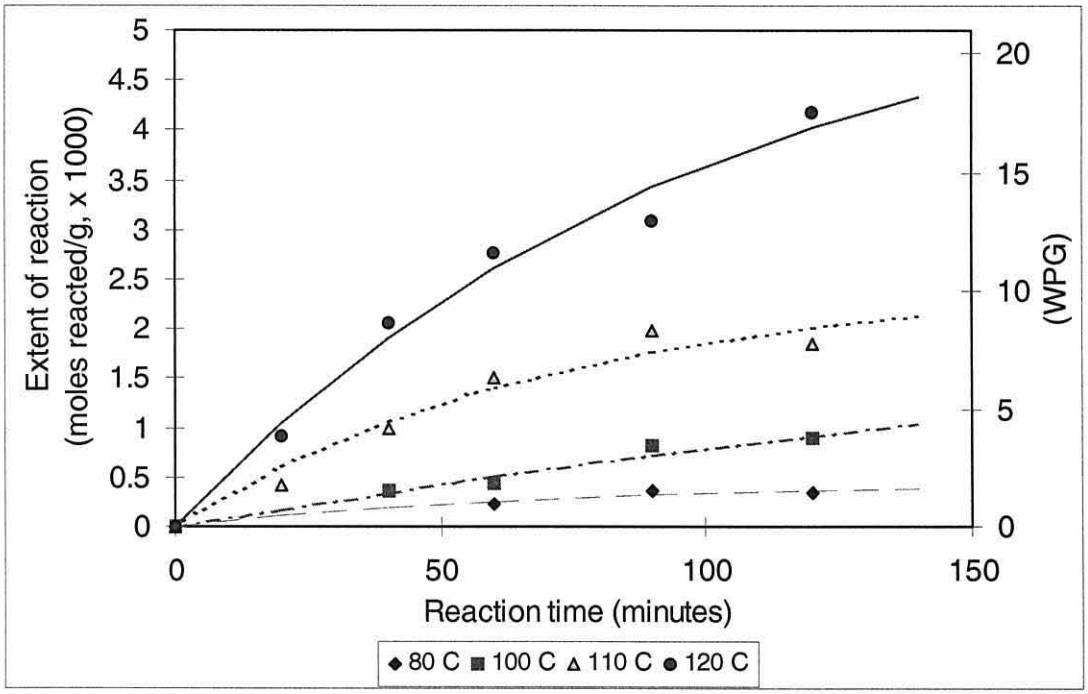

For sample DWD, sigmoid curves rather than exponential curves gave a better fit for reaction data at both 80 and 100 °C. In fact, the sigmoid curves generally fitted almost as well as did the exponential curves for sample DWD. Degree of fit and other raw data are given in Appendix M. The solutions of all the ground wood (delignified or not) were investigated to see if any of the wood substance had dissolved during reaction. However, there was not any significant dissolution of any of the ground wood samples.

The presence of an apparent lag phase might be explained by the reduction in lignin content, which normally reacts very quickly, and there was less to do so. However, it does not seem to explain all that was observed. Possibly, the presence of a lag phase may be reflecting the diffusion of the anhydride through the wood ultra-structure and cell wall (as ground wood samples were not pre-impregnated).

Some of the delignified ground wood samples (DWB, DWC) reacted to a greater extent than did the ground wood samples at 120 °C (for all times except 20 minutes). This could be due to the increased amount of the more reactive ASL present. It is also possible that with the removal of some lignin, the porosity of the cell wall was increased, thus allowing the anhydride to diffuse more quickly to reaction sites within the cell wall.

Comparison of initial rates (k_o) was inconclusive (Figure 3.40), with the expected trend of GW>DWB>DWC>DWD only found at two temperatures (100 and 110 °C). It had been expected was that with less lignin in the material being acetylated, the more delignified samples would react more slowly than the less delignified samples.

The k_o values (from the exponential or sigmoid curves) followed the same general trend, which was to increase as shown over the temperature range studied. The k_o values from the alternative method (using the first two data points and zero) did not give any consistent trend between the ground wood samples. The raw data and regression values are given in Appendix N for all the initial rate constants.

Figure 3.40. Comparison of initial rates of ground wood (partially delignified)

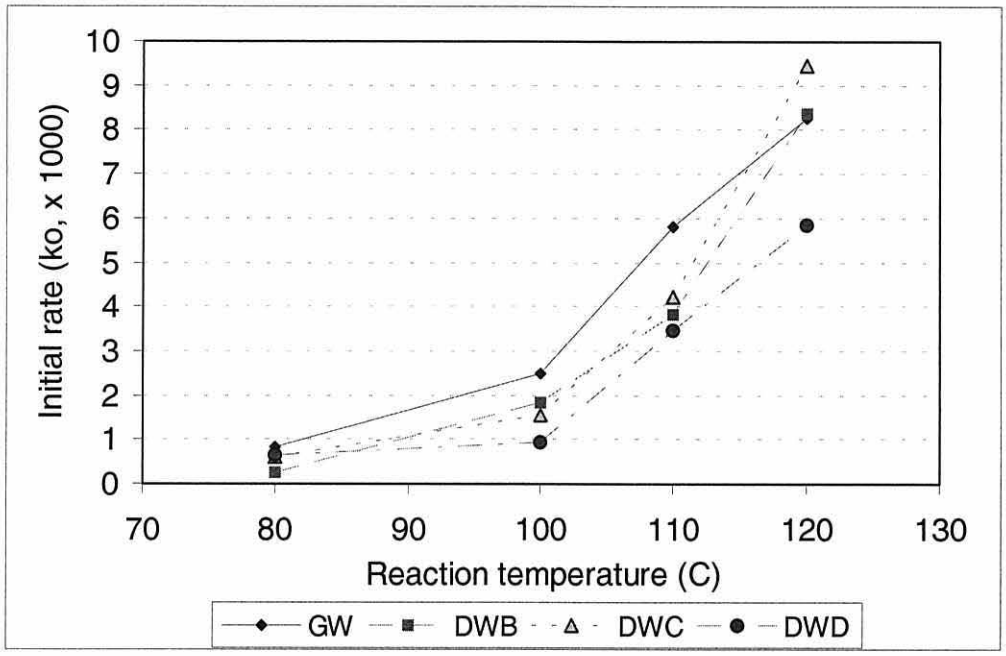

3.4.2. Kinetic data

The activation energy (Ea) values of the partially delignified ground wood samples were calculated using k_o values from the initial rate method and were illustrated in two ways: raw data given in Table 3.16, and plotted against total lignin content (Figure 3.41). As explained in the previous section, some of the reaction curves for samples gave a better fit to a sigmoidal curve, rather than an exponential curve. Calculations were made using initial rates from exponential curves only and from a mix of exponential and sigmoid curves (whichever best fitted), as well as the alternate method, involving the initial reaction data and the origin (see Appendix O for detailed data).

Table 3.16 shows three sets of activation energy values. The first set (1) was calculated from the initial rate values (k_o) obtained from exponential curve fitting (at 10% of exponential asymptote). The second set (2) were some (or one set of) data using sigmiodal curves and some using exponential curves, whichever was the best fit for the individual temperature data for each sample. The third set (3) was calculated from the initial rate constants obtained from taking the slope of the line fitted through the first two reaction data points and

zero. The curves of best fit are shown in the reaction profiles (Figures 3.35, 3.36, 3.38) and the degrees of fit are shown in Appendices N and O.

Table 3.16. Activation energy values for delignified ground wood

Sample	Ea, kJ/mol (std err)		
	1	2	3
Ground wood	62.1	79.5	52.7
	(6.4)	(7.7)	(4.2)
Delignified wood B	56.0	102.6	90.4 [a]
	(9.6)	(4.1)	(16.7)
Delignified wood C	75.4	77.5	95.6 [a]
	(5.5)	(11.6)	(7.6)
Delignified wood D	65.00	56.2	74.7 [a]
	(18.7)	(22.1)	(17.1)
Holocellulose	3.4		97
	(21.5)		(25)

1 = Exponential curve fit
2 = Sigmoid or exponential curve fit (curve of best fit)
3 = Initial rate values calculated from 1st two reaction data points & zero
[a] These values were calculated excluding negative WPG values obtained

The data in Table 3.16 shows that the method of obtaining initial rate constants influenced the Ea value obtained. The Ea values obtained using the initial rate constants calculated from first two reaction data points and zero (method 3) are probably the most accurate, and are in agreement for each sample (within standard error). Two of the delignfiied samples (DWB, DWD) had large errors for Ea, which means that the k_o values did not fit the Arrhenius equation very well. Figure 3.41 gives the trend for Ea values (method 3) for the ground wood samples with reducing total lignin content. There seemed to be a general downward trend in Ea value with increasing lignin content (r^2=0.479). If sample DWD (10.7% lignin) was omitted, then the negative correlation was stronger (r^2=0.680), although still not statistically significant.

Given the trends of activation energy for wood blocks (~34 kJ/mol) and lignin, AL or MWL (~80 kJ/mol), it might have been expected that the more heavily delignified samples would give a lower Ea. However, this was the opposite that was observed. The picture was somewhat complicated by the possible but unknown affect of the presence of acid soluble lignin, and the large error margins for some of the Ea values. It is possible that be that the reduction of lignin content in ground wood does not give an observable trend in activation energy values.

Figure 3.41. Activation energy versus lignin content for the ground wood samples

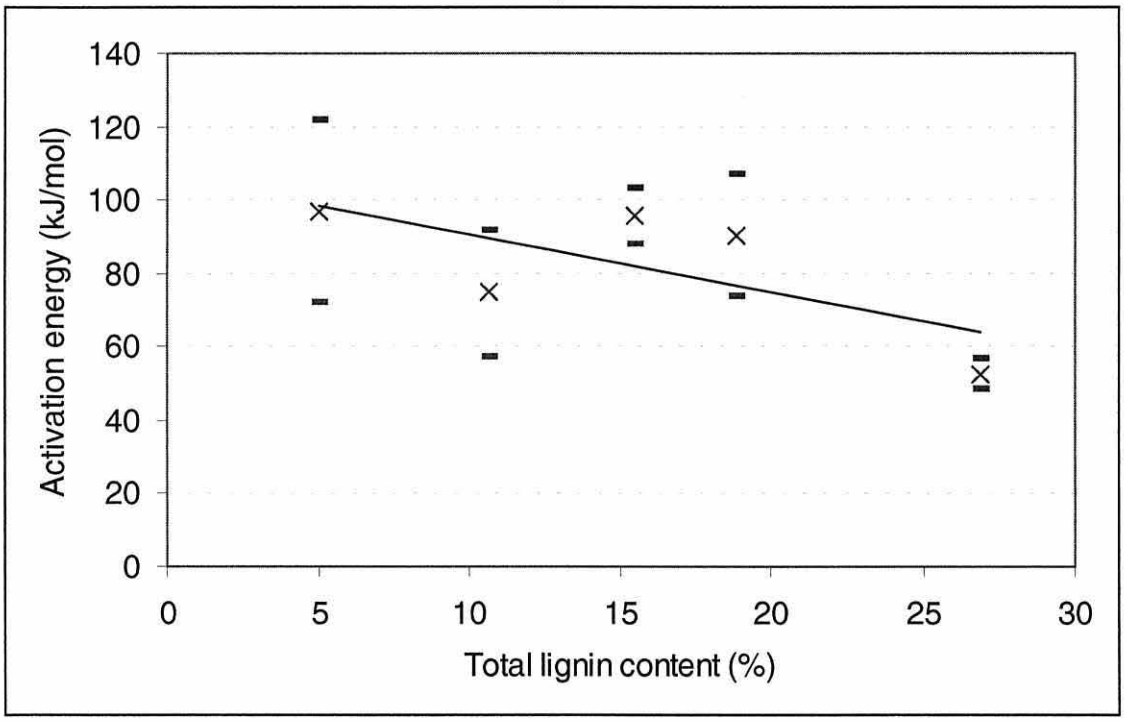

Note: Ea values are those calculated using the initial rate constants obtained by using the first two data points plus zero.

However, any results or conclusions from these samples are significantly compromised by the large increase of ASL in the delignified samples. For example, the most delignified sample (DWD) had a total lignin content of 10.7%, half of which was ASL. The reactivity of ASL would probably be different from native lignin. The holocellulose sample had a total lignin content of 5.0%, of which 3.17% was ASL.

The reaction of the delignified ground wood samples, like ground wood reaction, were largely diffusion controlled. Again, the reaction at 80 °C had a lower compliance to the diffusion equation than did the higher temperatures (regression data shown in Appendix P).

As discussed earlier in this chapter (section 3.3.3.1), diffusion can be considered to have an energy barrier associated with it, and can therefore be applied to the Arrhenius equation. The activation of diffusion values are shown for the ground wood samples (delignified and not) in Figure 3.42. It appeared to have the opposite trend of the activation energy values from the initial rates; that is, a positive correlation of lignin content to Ea (diffusion). The linear regression was made excluding ground wood (which had not been delignified at all), and had a r^2 value of 0.9269 (details are given in Appendix Q).

Figure 3.42. Activation of diffusion values for the ground wood series

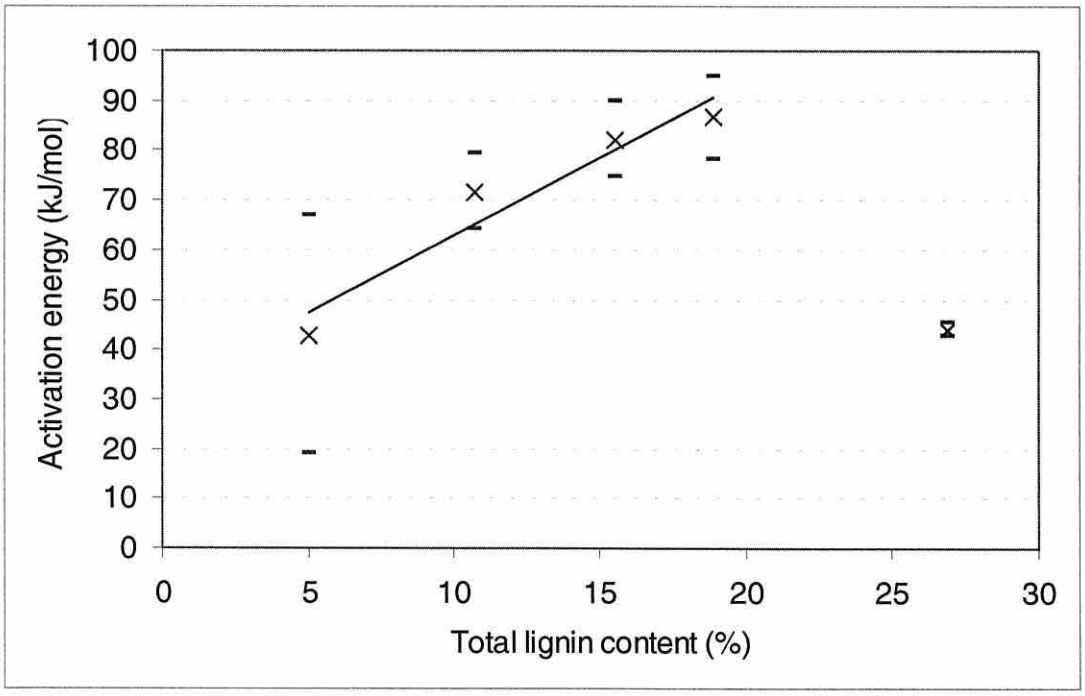

The trend shown in Figure 3.42 supports the theory that diffusion is aided by the removal of lignin in the cell wall, as the Ea (diffusion) decreased with increasing delignification (or decreasing lignin content). However, the standard error was large for the sample with lowest total lignin content (holocellulose), which may put this apparent trend in doubt. It is possible that the removal of

lignin created larger pores in the wood cell wall, thus allowing diffusion to happen more rapidly and easily.

The problem with any chemical method of delignification is that it will make some changes to the residual lignin, as the native lignin needs to be depolymerised to some extent to remove it from the wood structure. However, delignification involving chlorite has also been found to modify the carbohydrates and reduce the cellulose viscosity, which other methods do to a lesser extent (Leopold, 1961).

3.5. Variability of reaction with wood blocks

A trial was conducted to ascertain the variability of the reaction data of wood. The variablility was assessed between the three wood block samples in each flask, between flasks reacted at the same time, and between runs at different times. There were three different temperature and time combinations: 120 °C for 90 minutes, 120 °C for 10 minutes and 100 °C for 40 minutes. This was to investigate if the variability at shorter reaction times was greater than for longer times, and if a lower temperature also affected the variability.

It was found that the variability at the run level was higher than for the flask level, but the residual variability (which includes between sample variability) was between these two levels, and all were at a reasonable level. This means that from day to day, the experimental error was higher than when experiments were run at the same time, but in different flasks.

Figure 3.43 shows the three temperature/time combinations as trt1, trt2 and trt3 (120 °C, 90 mins; 120 °C, 40 mins; and 100 °C, 40 mins respectively). Three flasks were reacted at one time, for each run, with nine runs (three for each treatment level). The key for these figures are as follows: the horizontal axis shows 1/1, 1/2, 1/3 and so on, which is the treatment number/run number, and the open circles indicate outlying data points. This figure is a box plot, where the line within the box indicates the mean, and the box contains 50% of the data points, with the bars compassing at least 95% of the data.

The aim is to have the residuals for each run within around the same relatively low range as each other.

Figure 3.43. The residuals from Model 1 for the three treatments of wood blocks

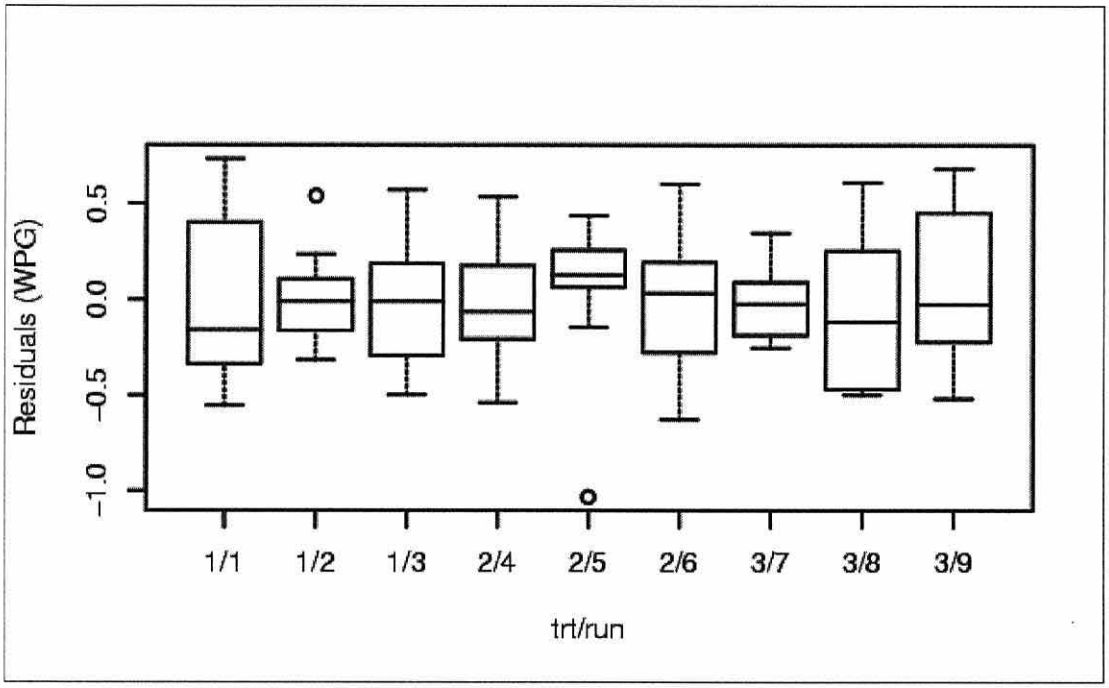

The selected model (Model 1) was a simple one and had the best fit of the four models tested, according to the AIC or BIC indices (Table 3.17). It assumed that the variance was the same for all runs, and pooled data at each level. Three other models were tested which allowed for different variance for each treatment combination and independent random variables. However, none of these fitted as well as Model 1. The AIC and BIC indices both show the model of best fit at the lowest value. These indices are used for comparing different models and do not have an absolute scale, as they can be calculated in different ways.

There was no evidence of different levels of variability for different treatment combinations, although run 7 may have lower variability than the other runs (there was not really enough replication to be sure). Table 3.18 shows the components of the variability at the different levels. If two individual data points (or means) were randomly compared, in a treatment combination from

the same run and flask, then only the residual variance would contribute to the standard error of difference. However, if they came from different runs and flasks, then all three variances would contribute.

Table 3.17. Comparison of fit for four different models of analysis

Model	Degrees of freedom	AIC	BIC
1	6	136.6	150.7
2	8	139.2	158.1
3	10	140.4	163.9
4	16	152.4	190.1

Key: Model 1 = same variance for each treatment
Model 2 = different variance for run level but same at flask level
Model 3 = different variance at each level
Model 4 = different variance at each level and allows random effects to be dependent
AIC = Akaike information criterion, lowest predicted error on future data
BIC = Bayesian information criterion, approximate probability of model to be true

Table 3.18. Components of variability for WPG of wood blocks

Level	Symbol	Est. variance	Std. dev.	95% confidence limits
Run	σ^2_R	0.40	0.63	0.12 - 1.38
Flasks	σ^2_F	0.05	0.22	0.014 - 0.210
Residual	σ^2_e	0.16	0.40	0.111 - 0.237

So in conclusion, there was an increase in variability between runs conducted on different days, but not a large one when compared with the total variance of 25.7. If one wanted to reduce the overall level of variability in the experimental design, the most effective way to do this would be to increase the number of runs per treatment.

3.6. Summary

It was found that the reaction profiles of solid wood blocks with pure acetic anhydride fitted reasonably well (at least for the first 200 minutes) to simple exponential curves between temperatures studied of 80-120 °C. The reaction

of wood blocks was found to be diffusion controlled, rather than first order with respect to wood hydroxyl concentration. The Ea value obtained by using the initial rate method was relatively high for a diffusion controlled reaction (34 ± 9 kJ/mol), although the reaction of wood blocks was possibly activation controlled (first order) for the first part of the reaction.

MDF (HTMP) fibre was also reacted with acetic anhydride and it was found that small but significant amounts of the substrate dissolved into the reaction solution. This made accurate assessment of the true extent of reaction difficult. The MDF fibre reaction showed the same general trends as the wood block reaction, including the possible diffusion control of the fibre reaction. The Ea values obtained for the MDF fibre reaction (solid WPG) were similar or a little higher (38 ± 12 kJ/mol), to that of the wood block reaction, when the initial rate constants were obtained using 10% of the exponential asymptote. However, when the Ea value was calculated using the alternative method of initial rate constants calculated by a linear regression of the first two reaction data points and zero, then the Ea value was higher (48 ± 11 kJ/mol). This latter value is probably the more accurate one. Unfortunately, the results for the total WPG of the MDF fibre (solid WPG and weight from dissolved substances) were highly variable.

It was found that ground wood reacted more slowly (and to a lesser extent) than solid wood blocks, especially at 80 °C, where a lag phase was visible in the reaction profiles. The slower reaction might have been due to better acetone washing, or the lack of vacuum-impregnation. It was also found that the ground wood reaction was diffusion controlled, for at least reaction at 100-120 °C. This indicates that the rate-determining step was diffusion through the wood cell wall, which was present in the ground wood sample as well as the wood blocks. The Ea values obtained for the ground wood reaction were higher (53-62 kJ/mol) than for the wood blocks, which might be because the reaction was less diffusion-controlled. A comparison of the activation energy of diffusion values (Ea (diffusion)) gave an expected trend, given the structural differences of the substrates. This was that wood blocks had the highest Ea

(diffusion) values (42-44 kJ/mol), then ground wood (34 kJ/mol), which was around the same as MDF fibre (30-33 kJ/mol).

The reaction of the partially delignified ground wood had been devised to examine *in situ* the influence lignin had on the wood acetylation reaction. Therefore, three samples of partially delignified ground wood, which had decreasing total lignin content, were reacted and kinetic data were produced. However, reaction levels were variable and no obvious trends were found. It was thought that the increase of acid soluble lignin (ASL) in the increasingly delignified samples might have changed the overall reactivity of the samples. Ea (diffusion) values (excluding non-delignified ground wood) decreased with decreasing total lignin content. This would support the theory that the removal of lignin may have created more micropores in the cell wall, which improved diffusion through the cell wall to new reaction sites.

It was not possible to form a model of the wood reaction from the reaction of the isolated wood components. However, a mathematical equation that related the acetylation level of the wood block reaction to temperature (T) and time (t) fitted the observed data well. With slight adjustment of two of the equation parameters, the equation could also model the ground wood reaction. The equation for wood blocks was:

$$\text{WPG (blocks)} = 15.62 + (15.62 - 28.24).\exp(-\exp(-15.50 + 0.09899.T).t) + (-0.06565 + 0.00218.T).\sqrt{t}$$

This could be a useful approach when trying to predict the level of acetylation in an uncatalysed reaction, although dimension of the wood samples, as well as the lack (or inclusion) of a quenching step will influence the results obtained.

CHAPTER 4: REACTION OF THE WOOD CARBOHYDRATES

4.1. Introduction

This chapter reports results from the reaction of acetic anhydride with the wood carbohydrates examined, namely, holocellulose, cellulose and two isolated hemicelluloses, xylan and glucomannan. The purpose of these experiments was to quantify the kinetic effects of the different polymer groups separated from each other. The holocellulose is delignified ground wood, and the cellulose used was the α-cellulose that is the end product of removing sequentially the lignin and then the hemicelluloses. Xylan and glucomannan are the two main hemicelluloses present in radiata pine (Uprichard, 1991). However, when the isolated hemicelluloses underwent preliminary reactions, they did not react to the expected level. Therefore, they were further investigated using FTIR and then reacted with catalysts to check the reaction level possible.

Both holocellulose and cellulose were extracted from wood to provide very close models of the native wood carbohydrates. Restricting the mesh size to 36-60 mesh (0.250-0.425 mm) for the hemicellulose and cellulose production was intended to limit the reduction of crystallinity of the cellulose.

The isolated hemicelluloses had been intended to elucidate more about the reactivity of wood carbohydrates, but it was obvious that the hemicelluloses had been changed significantly during the isolation process, such that their reactivity was much lower. This meant that it was difficult to measure their reactivity from under similar conditions to the other substrates. It is now thought that the hemicelluloses hornified during the freeze-drying after the second purification process.

Hornification is an irreversible process that happens when carbohydrates are dried from water (Whistler, 1945), and involves intra-molecular hydrogen bonding. This could have been avoided if the hemicelluloses had been precipitated into ethanol then dried without any water present. However, the

hemicelluloses were reacted with two different catalysts and the reaction products were examined by FTIR spectroscopy to give any further information that might be useful.

During isolation of holocellulose and cellulose, a few changes will have occurred to the remaining substrate. In particular, any residual lignin will be different in structure to the original native lignin. There may be less of the more water-soluble components, such as xylan. There may also be small changes to the cellulose itself, for example, to the crystallinity due to grinding the wood (Browning, 1967; Vol. II p503). Chlorite delignification causes some oxidation to cellulose (Leopold, 1961), increasing the carboxyl content and lowering the DP. In general, isolated wood components may not exhibit the same reactivity as when they do within the unmodified wood.

4.2. Characterisation of the carbohydrates

FTIR and NMR analyses were conducted on holocellulose and cellulose. FTIR analysis was done of the untreated hemicelluloses, xylan and glucomannan. The results are included in the reaction section of this chapter (4.3) for comparison with the partially acetylated hemicelluloses. It was difficult to obtain NMR analyses on the isolated hemicelluloses because of the lower solubility of glucomannan in D_2O. However, some solution spectra were attempted for comparison purposes. Solid state NMR spectra were run on the two hemicelluloses (as well as the holocellulose and cellulose).

4.2.1. NMR analysis

Two solution state NMR spectra of the isolated xylan and glucomannan (proton only) were examined (Figures 4.1 and 4.2). It was not possible to get a worthwhile carbon spectra from these samples. It was necessary to use NaOD to get the glucomannan sample into solution. However, this made it very difficult to optimise the instrument, thus the peaks were rather broad and less-resolved in the ^1H NMR of the glucomannan (Figure 4.2), with a very broad solvent peak.

Figure 4.1. ^{1}H NMR spectrum of untreated xylan (solution NMR)

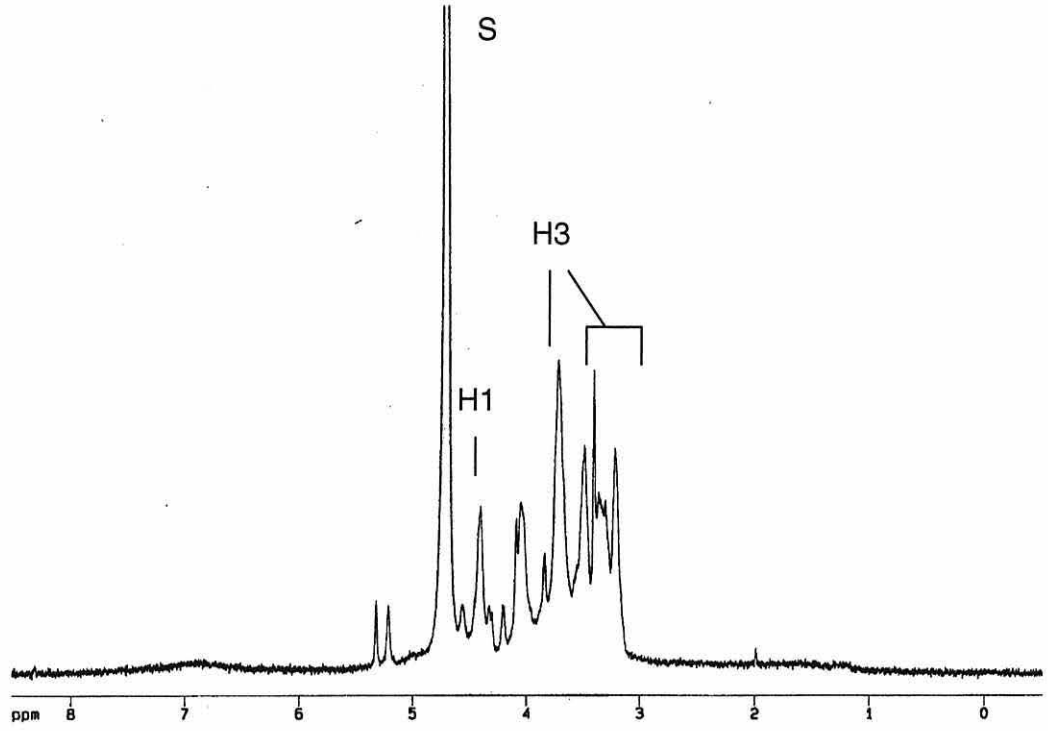

Figure 4.2. ^{1}H NMR spectrum of untreated glucomannan (solution NMR)

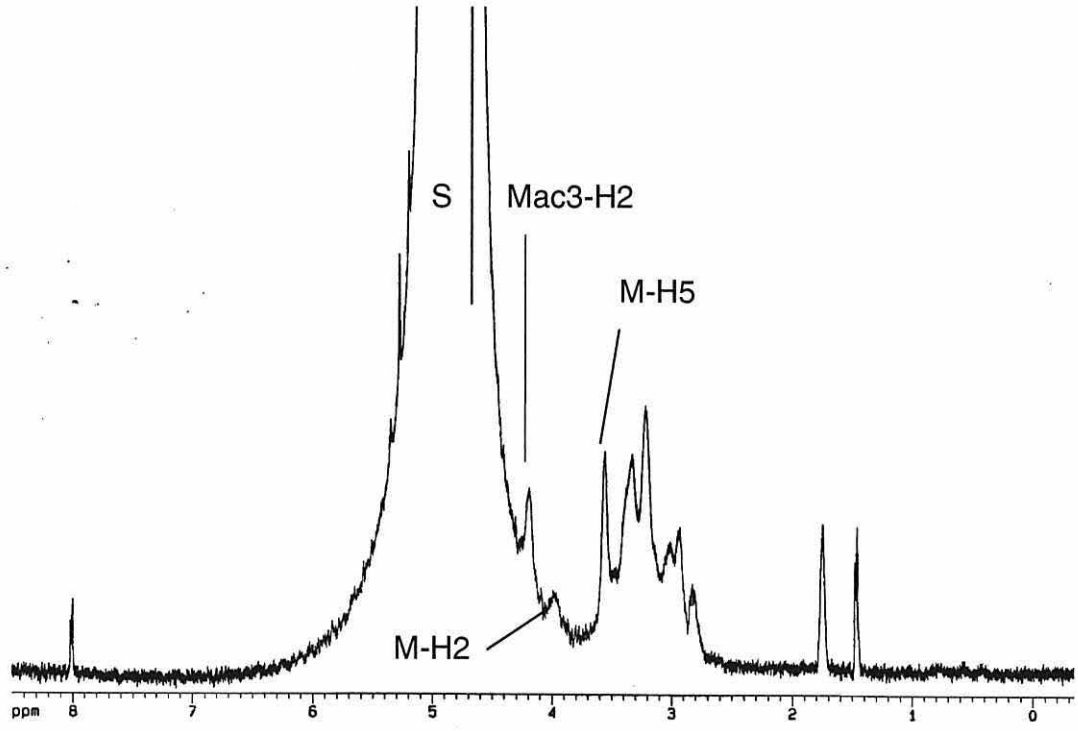

Basic assignments only have been given for the ^{1}H NMR spectra of the two hemicelluloses. For the xylan spectrum, van Hazendonk *et al.* (1996) gave the assignments for hemicelluloses isolated from flax (*Linum usitatissimum* L.). This flax xylan is acetylated naturally, unlike the xylan from radiata pine. The probable assignments of the protons attached to the main xylose chain are shown in Figure 4.1, where H1 is the proton attached to C1 of the xylose unit and so on.

For the glucomannan spectrum (Figure 4.2), many of the peaks of interest are obscured by the large solvent band (S). The assignments marked are also from van Hazendonk *et al.* (1996), where Mac3-H2 refers to the proton attached to C2 on a mannose unit, which is acetylated at position C3, and M-H2 refers to an unacetylated mannose unit's C2 proton and so on . McDonald *et al.* (1999) gave the additional general assignments of mannosyl residue of water-soluble fraction of MDF fibre (Table 4.1). Some of these were not obviously present, or were obscured in the glucomannan spectrum.

Table 4.1. Peak assignments for the ^{1}H NMR spectra of mannose or xylose residues

Residue	H1	H2	H3	H4	H5	H6	Reference
Mannose (general)	4.74	4.11	5.48	3.87	3.58	3.75	1
Mannose (non-acet.)	4.6-4.7	4.0-4.1					2
Mannose (acet.)	4.8-4.9	4.1-4.2 5.3-5.4	4.0 5.0				2
Xylose (non-acet.)	4.44	3.28	3.54				2
Xylose (acet.)	4.5-4.6	3.3 4.6	3.5 4.9				2

Reference 1 = McDonald *et al.* (1999)
2 = van Hazendonk *et al.* (1996)

The solid state ^{13}C NMR spectra (CPMAS) of the untreated samples are shown in Figures 4.3-4.6 (holocellulose, cellulose, isolated xylan and glucomannan respectively), with assignments of the main peaks given in Table 4.2. For some of them, NMR spectra of the acetylated samples have been shown for comparison. The solid state NMR spectra of the holocellulose and cellulose samples were done through Dr Noel Owen at a facility in the USA. Spectra were run on a CMX Infinity spectrometer at 50 MHz, with samples packed in 7.5 mm zirconia rotors and spun at 4-5 kHz. These spectra were acquired with contact time of 2 ms, pulse delay of 1 s, and 1000 - 4000 scans. For other NMR spectra, the experimental details used are given in Chapter 2, section 2.7.2.

The holocellulose spectrum (Figure 4.3) showed the characteristic peaks of the monosaccharide ring. The natural acetate in the glucomannan would have been lost during the isolation process, so this does not show in the holocellulose spectrum. The shoulder in the cellulose spectra (Figure 4.4) at around 106 ppm (peak 3) was probably showing the presence of I_β form of crystalline cellulose, with the stronger peak being assigned to I_α form (Newman, 1994). The spectra in this study are not well enough resolved to produce ratios of the two crystalline forms.

Newman (1994) also commented that some of the hemicelluloses in radiata pine wood seemed to be well-ordered such that they would have NMR relaxation times similar that of cellulose. In his estimation, around 5 % of wood hemicelluloses were well-ordered. Newman assigned a small shoulder at 102 ppm (faintly visible in the holocellulose spectrum, Figure 4.3, on the right side of peak 3) to the C1 of well-ordered hemicellulose (probably gluco-mannan).

Figure 4.3. Solid state ^{13}C NMR spectrum of untreated holocellulose

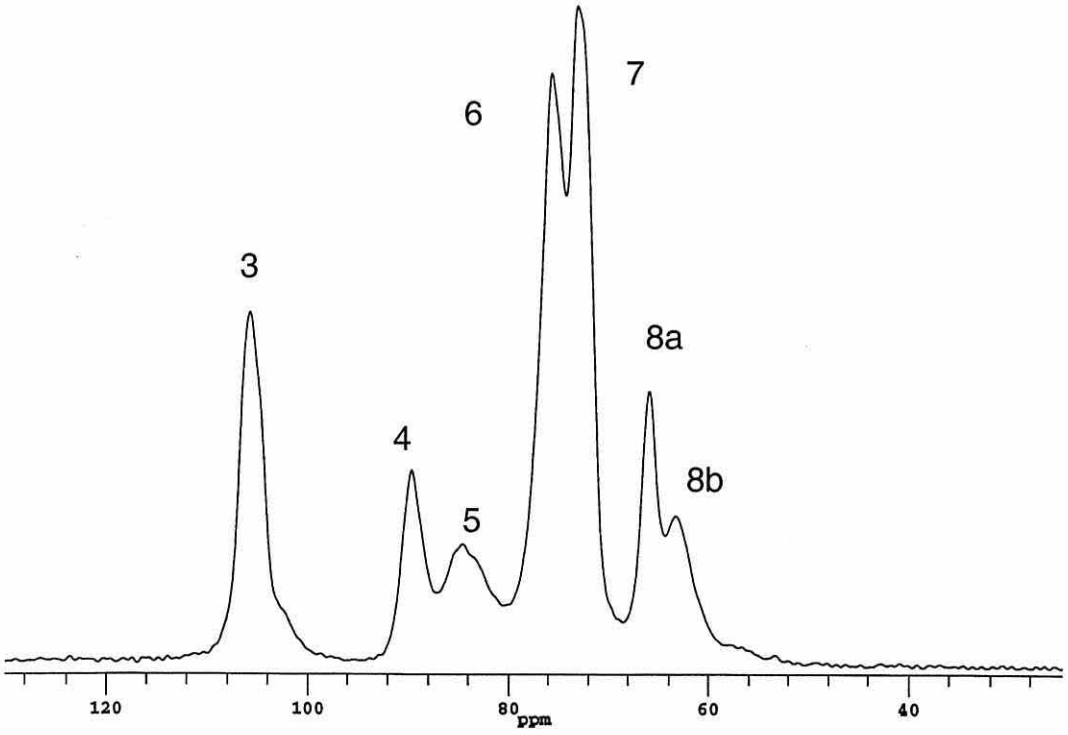

Figure 4.4. Solid state ^{13}C NMR spectrum of untreated cellulose

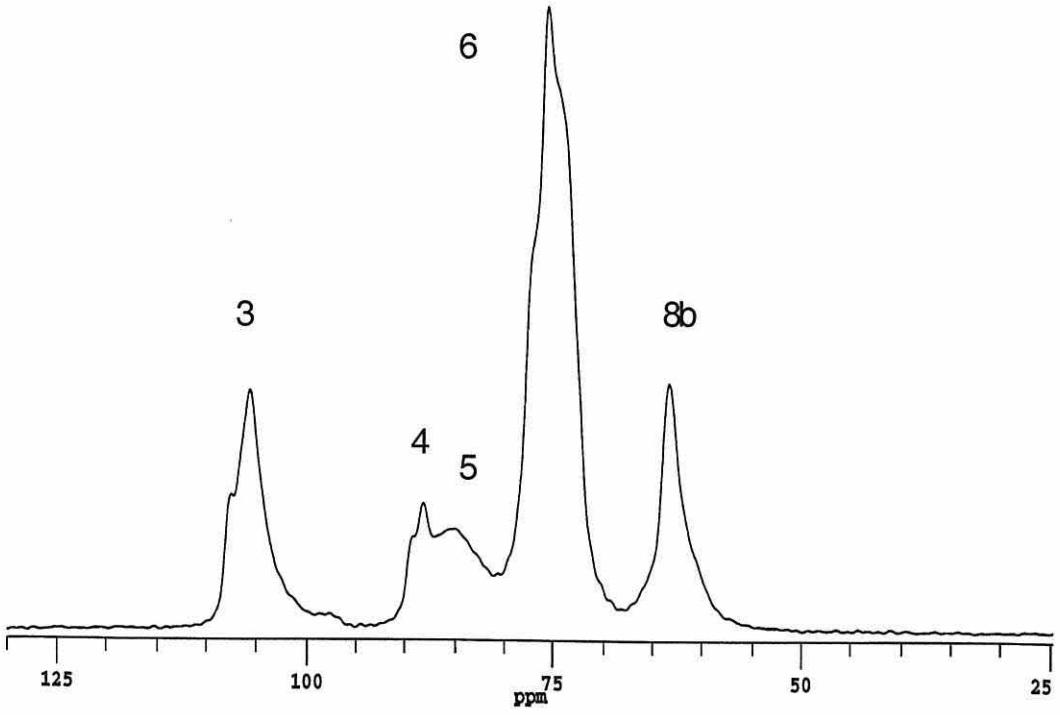

Figure 4.5. Solid state ^{13}C NMR spectrum of untreated xylan

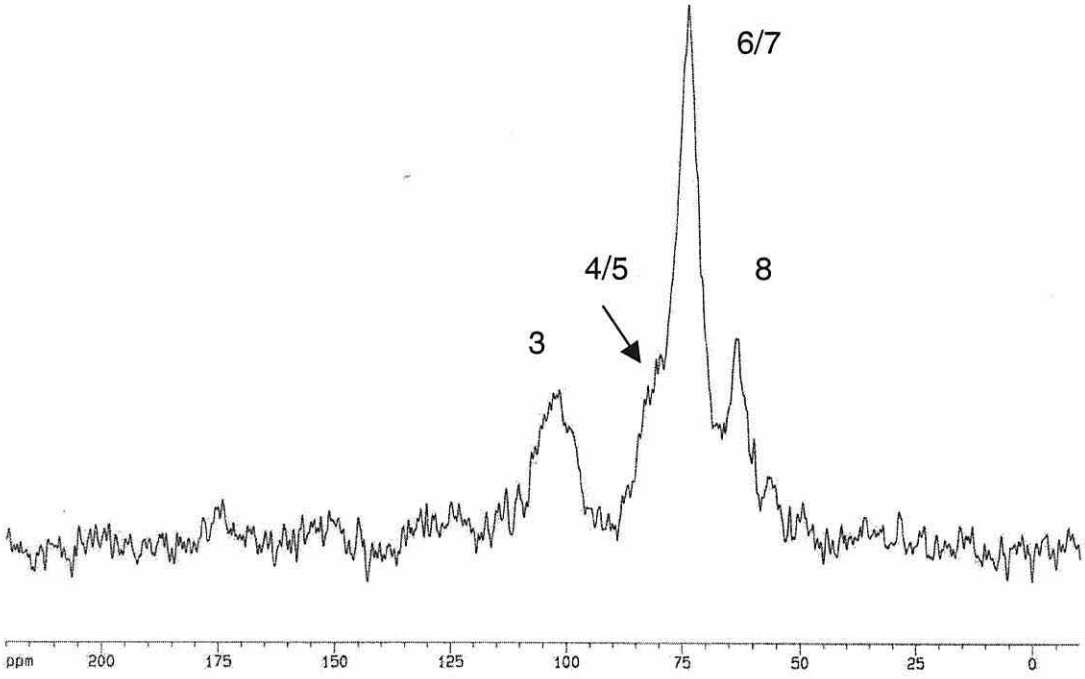

Figure 4.6. Solid state ^{13}C NMR spectrum of untreated glucomannan

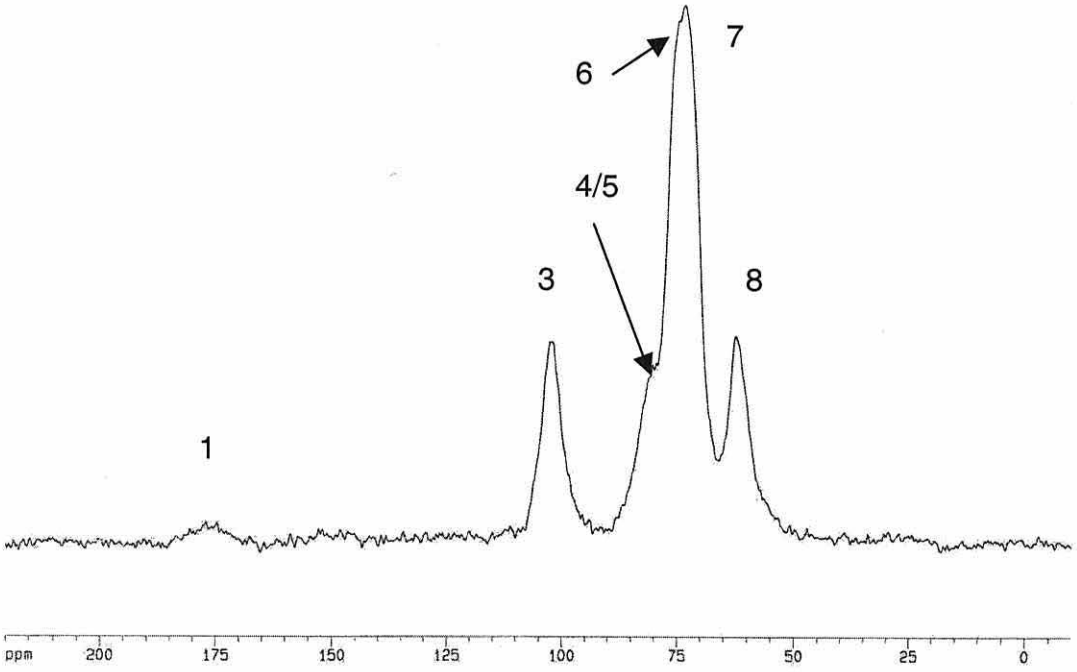

Table 4.2. Assignments of main peaks for solid state ^{13}C NMR spectra of untreated carbohydrates

Peak assignment	Wood (ppm)	Holocellulose (ppm)	Cellulose (ppm)	Xylan (ppm)	Glucomannan (ppm)
1 C of C=O in acetate					177 br
2 Aromatic C attached to O	148 br				
2a Aromatic C attached to C	br				
2b Aromatic C attached to H	br				
3 C1 of polysaccharide skeleton	105	106	sh, 106	102 br	102
4 C4 of polysaccharide skeleton	89	90	sh, 89	sh	sh
5 C4 of polysaccharide skeleton	84	84 br	85 br	sh	sh
6 C2,3,5 of polysaccharide skeleton	75	76	sh, 76	74 br	sh
7 C2,3,5 of polysaccharide skeleton	72	73	Sh	74 br	73
8a,b C6 of polysaccharide skeleton	65, 62	66, 63	63	64 br	62
9 C of OCH_3 of lignin	56				
10 C of $-CH_3$ in acetate	21				

Key:

sh Shoulder of peak present
br Broad peak

Figure 4.7. Solid state NMR spectral comparison of untreated and acetylated cellulose and holocellulose (a) acetylated holocellulose, 5.52 WPG, (b) acetylated holocellulose, 3.04 WPG, (c) untreated holocellulose, (d) acetylated cellulose, 1.55 WPG, (e) untreated cellulose.

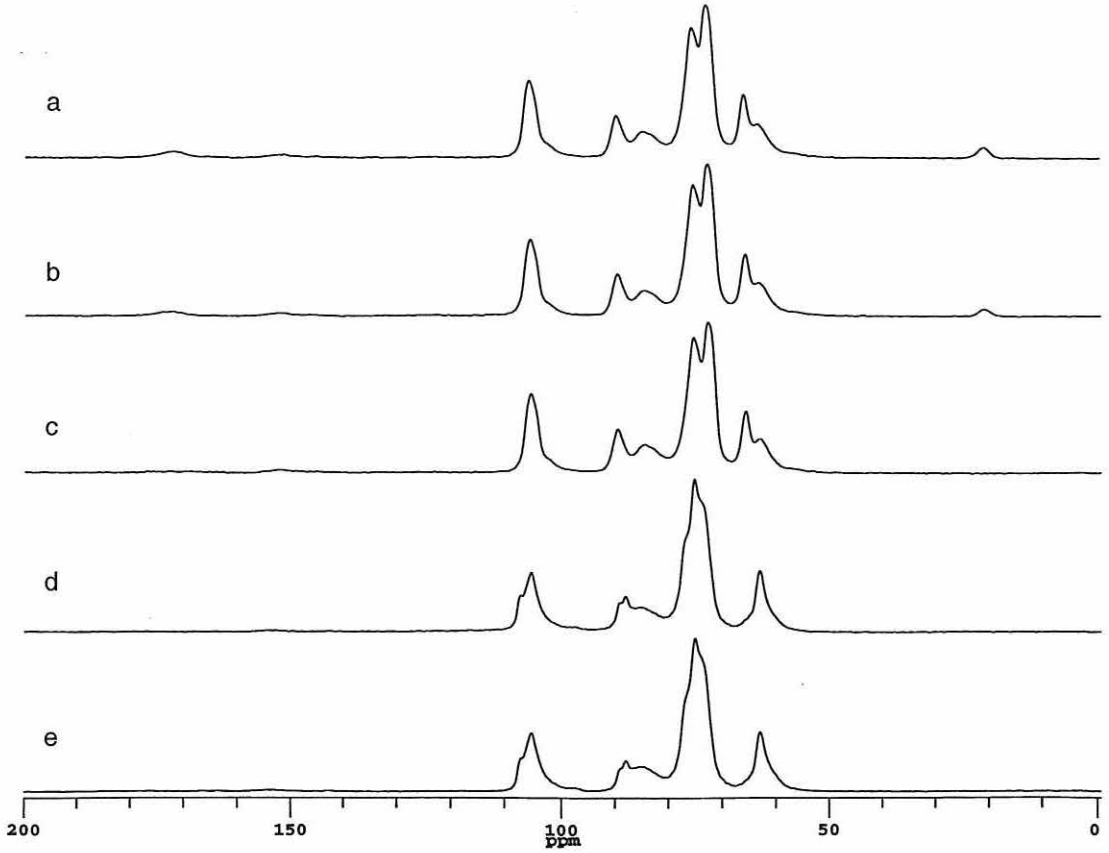

Liitiä *et al.* (2000a) further assigned peaks 4 and 5 (at 89-90 ppm and 84-85 ppm) to crystalline and amorphous C4 of cellulose of kraft pulp respectively (Figures 4.3 and 4.4). In the spectra in this study, it might have been useful to be able to resolve peaks 4 and 5 to give a clearer idea of the portion of crystalline to amorphous cellulose present in each sample. However, to get this level of resolution requires lengthy NMR experiments under specific conditions (such as relaxation times; Newman, 1994; 1999). In an earlier study, Newman and Hemmingson (1990) reported a value for the degree of crystallinity of cellulose in radiata pine of 0.54 (mean cellulose crystallites) from NMR examination.

The solid state ^{13}C NMR spectra of the isolated hemicelluloses (Figures 4.5 and 4.6) were less resolved than the holocellulose or cellulose spectra. For example, the peaks assigned to the C4 carbon of the monosaccharide ring only showed as a shoulder on the side of the nearby larger peak assigned to C2, C3 and C5 at 73 ppm. However, in general, these spectra showed similar features to those of the holocellulose and cellulose. One of the acetyl peaks (at 177 ppm, peak 1), which is naturally occurring in the wood, was just visible in the glucomannan spectrum (Figure 4.6).

Figure 4.7 shows a spectral comparison of two acetylated holocellulose samples (5.52 and 3.04 WPG), with the untreated holocellulose, and an acetylated cellulose sample (1.55 WPG) and untreated cellulose. Samples b and d were reacted under the same reaction conditions (100 °C, 240 minutes). It is clear from spectra d and e that very little cellulose reacted, as there was no apparent difference between these spectra, although a WPG was recorded. This means that a significant amount of the reaction in holocellulose, sample b, was due to the hemicelluloses. Solid state ^{13}C NMR was not sensitive to such small levels of reaction, so it seems that the detection limit for this technique is around 2.0 WPG for this reaction.

4.2.2. Monosaccharide and Klason lignin analyses

Table 4.3 shows the Klason lignin and monosaccharide analyses of holocellulose, cellulose, and the hemicelluloses, glucomannan and xylan (compared with wood blocks, average of three samples). These results give some idea of how pure the sample was. However, one cannot take the percentage glucose in the cellulose sample, for example, as the level of purity as there could be some glucomannan also in the sample, which would contribute to the glucose units measured. Often these analyses do not add to 100 %, as there can be losses over the three or more analysis methods used.

Table 4.3. Monosaccharide and Klason lignin analyses of carbohydrates

Sample [a]	Klason lignin	ASL	%Ara	%Gal	%Glu	%Xyl	%Man	% total
Wood (ave)	28.3	0.5	1.18	2.10	47.3	4.75	12.0	96.2
Holo-cellulose	1.83	3.17	0.70	0.53	76.5	5.40	10.0	98.1
Cellulose	0.9	0.7	*	*	94.9	*	2.04	98.5
GM	10.5	1.0	0.3	1.2	19.5	1.5	54.2	88.2
Xylan	12.5	5.5	6.8	2.1	3.6	43.0	0.5	74.0

[a] Ash contents were 1.9 % (holocellulose), 0.9 % (cellulose), 6.2 % (glucomannan, GM), and 2.6 % (xylan) and not subtracted from analyses

The holocellulose sample had around 5 % total lignin content, with around 6 % xylan, 14 % glucomannan (using the proportions obtained for isolated glucomannan), and 73 % cellulose. The isolated cellulose still had about 1.6 % lignin present and probably some glucomannan (about 3 %), but was about 92 % pure cellulose, indicating this was a good wood cellulose model.

The xylan sample had a relatively high level of total lignin after isolation (18 %, not corrected for ash). This was after an extensive purification process, including ion exchange to reduce the mineral content. It is thought that xylan may have linkages with lignin within wood (Fengel and Wegener, 1989), and

these results seem to bear this out. This was also illustrated on close inspection of the FTIR spectra of untreated or acetylated xylan (Figures 4.13-4.16, section 4.4.1.), where a small peak at around 1510 cm^{-1} was present. It was more obvious in the most acetylated xylan spectrum (Figure 4.16), although it was still visible in the untreated xylan spectrum as the small spike on the side of the larger peak at 1415 cm^{-1}. This relatively high level of lignin in the xylan sample makes the low level of reaction obtained even more striking. This high level of lignin in the isolated xylan sample is abnormal, and was not found by other workers (Uprichard, 1991).

The total summation of the analysis for xylan was very low, and the analyses were repeated to check. However, the results were reproducible. The reason for this very low value was not known, but could possibly be the presence of some entity that was not included in the analyses (for example, uronic acid).

Uronic acid does not hydrolyse fully in the analysis and it is possible that some xylose units were still attached to the unhydrolysed uronic acid units, and thus also not measured (Whisler and Chen, 1991). This would lead to an under-estimation of the xylose in the sample. The uronic acid content of a radiata pine xylan was found to be a little higher than that of arabinose (Uprichard, 1991), which would be around 7 % for the xylan here.

The apparent high KL content of the glucomannan was probably mostly ash, as it (the KL analysis) is a gravimetric measurement, which does not correct for mineral content. Therefore, the real total lignin content for the glucomannan would probably be around 5 %

4.2.3. FTIR of holocellulose and cellulose

The FTIR spectra of holocellulose and cellulose are shown in Figures 4.8 and 4.9; the spectra of the isolated hemicelluloses are shown in section 4.4.

The characteristic peak of lignin (1510 cm^{-1}) was not present in either holocellulose or cellulose, although there is a residual few percent of lignin present (5.0 or 1.6 % respectively).

Figure 4.8. FTIR spectrum of holocellulose

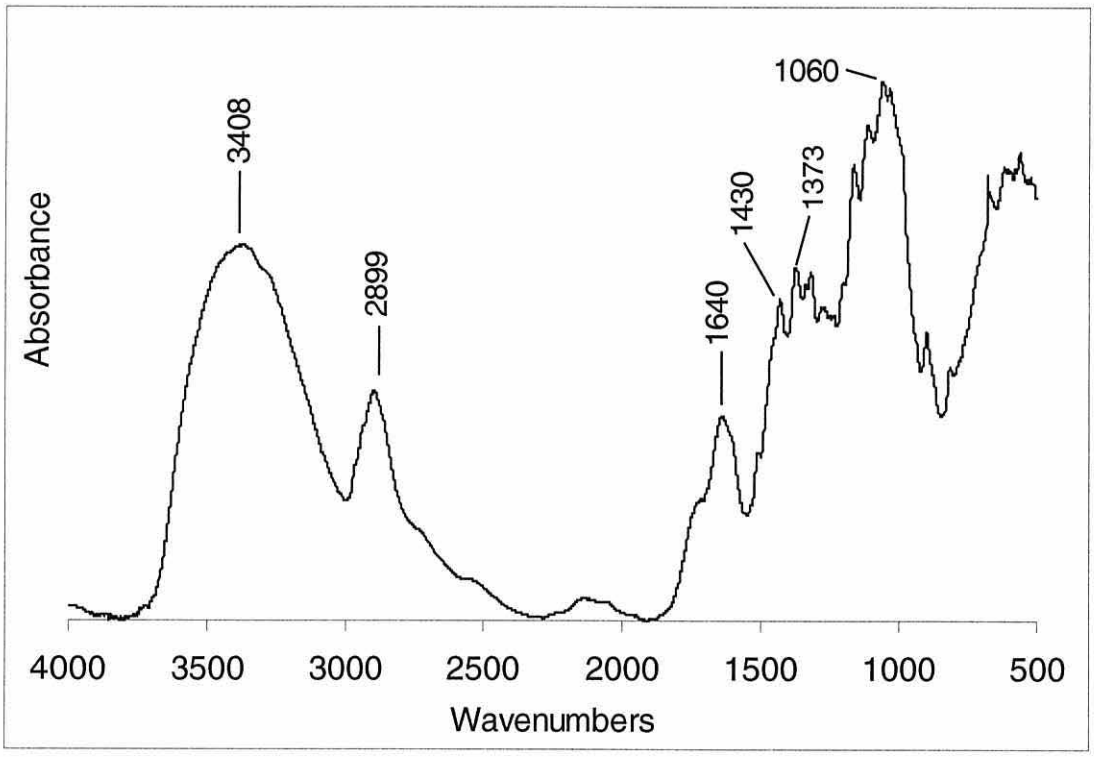

Figure 4.9. FTIR spectrum of cellulose

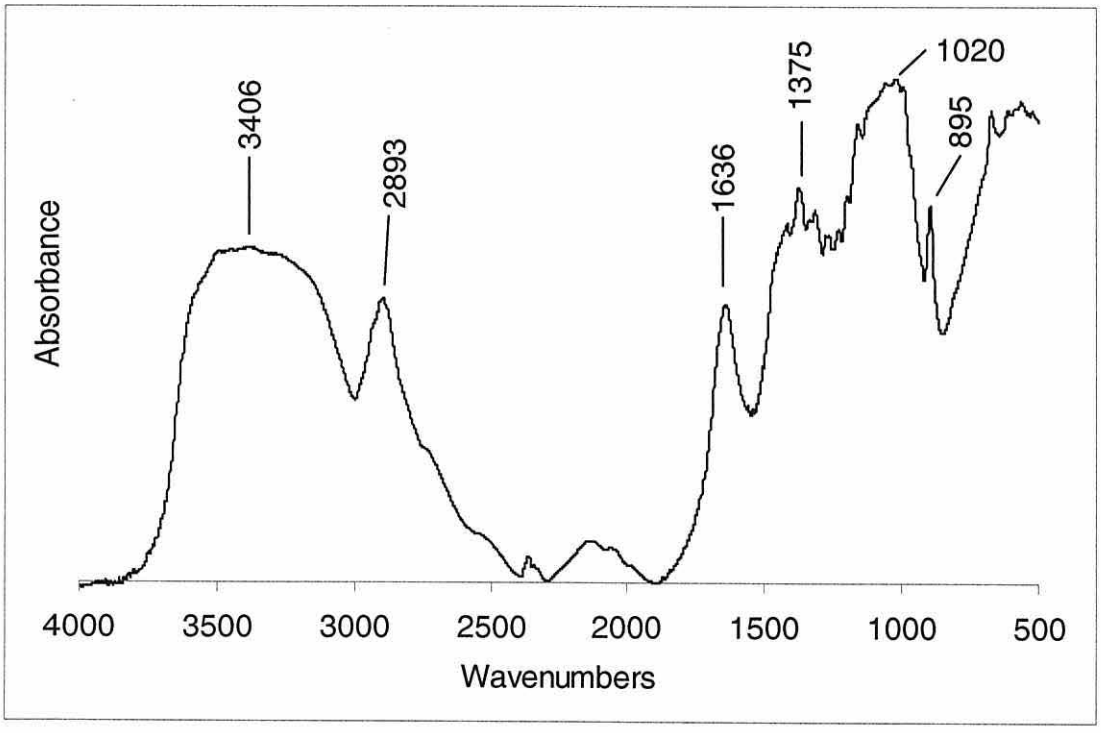

There was a small peak at 1735 cm^{-1} in the wood spectrum, which was only a shoulder in the holocellulose sample, due the naturally occurring acetyl. The native acetyl content is probably in the glucomannan (Uprichard, 1991). However, through the isolation process, these acetyl groups would largely have been removed and therefore are not present or greatly reduced in the isolated hemicelluloses and the holocellulose.

Table 4.4. Main peak assignments of FTIR spectra of holocellulose and cellulose

Assignment of FTIR peak[1] (cm^{-1})	Maximum of peak in sample (cm^{-1})		
	Wood	Holocellulose	Cellulose
3350-3420, ν_{O-H}, bonded	3356	3408	3406
2890-2950, ν_{C-H}, CH_2/CH_3	2899	2899	2893
1735, $\nu_{C=O}$, unconjugated [2]	1736	sh	
1630-60, $\nu_{C=O}$, conjugated	1655	1640	1636
1510, $\nu_{C=C}$, (aromatic), characteristic of lignin	1510		
1400-1470, δ_{C-H}	sm	1430	sh
1375, δ_{C-H}, $-CH_2$	sm	1373	1375
1220-1275, ν_{C-O-C}	1270		
1020-60, ν_{C-O-C}, ethers, ring saccharide skeleton [3]	1032	1060	1020
1000-670, group frequency in polysaccharides	sm	sm	895

Key:
sh A shoulder is present in this region
sm A small peak (unpicked) is present.
1 The symbol ν means a stretch frequency and δ means a bend (scissor/wag etc) frequency, with the subscript denoting the type of bend or stretch.
2 Most likely acetyl, but also could be carboxyl, ketone
3 This peak is one of two at maximum, and a band from 1150-918 cm^{-1} is assigned to the saccharide skeleton.

Assignments of the main peaks in each spectrum have been made and are shown in Table 4.4, and compared to those in the wood spectrum. There are many similarities in the spectra shown, such as the strong band at about 3300-3400 cm^{-1} due to the abundant hydroxyl groups present in all the samples.

4.3. Reaction of the holocellulose and cellulose

The acetylation data of the holocellulose and cellulose are given, along with the kinetic data obtained. However, as the reaction levels were low, the data are reported for interest, rather than for comparison with data for other components. The raw data of the reaction profiles are given in Appendix F (d and e).

4.3.1. Reaction profiles

The acetylation reaction profiles of holocellulose and cellulose are shown in Figures 4.10 and 4.11 respectively. The level of reaction was very low, and the initial rates obtained from these plots did not give rise to meaningful activation energy values. Shorter reaction times would have enabled more accurate initial rates values to be calculated. However, it was not possible to reliably gain reaction data of times less than 10 minutes.

The reaction plot of holocellulose (Figure 4.10) showed that at longer reaction times (> 150 minutes) the reaction level apparently dropped. However, it seems that a greater amount of sample may have dissolved into the reaction solution. Two longer reaction times (240, 1440 minutes) were examined to confirm that, given enough time, the hemicelluloses in the wood were accessible and reactive under these conditions (results presented later, Figure 4.12)

Figure 4.10. Reaction of holocellulose

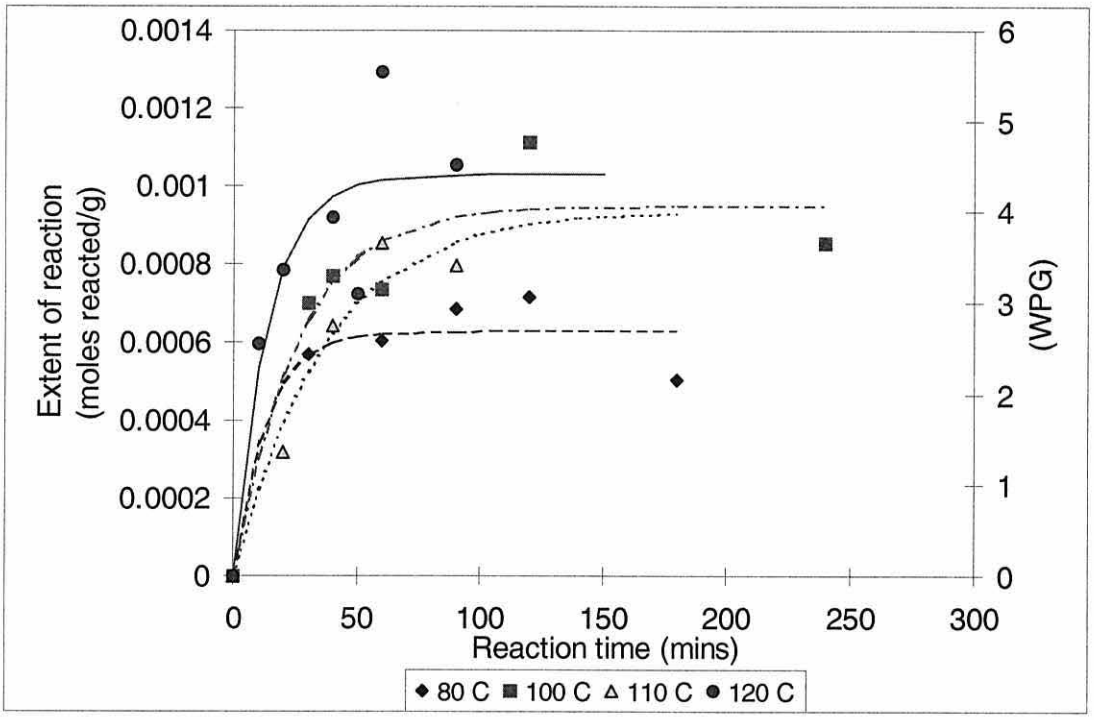

Figure 4.11. Reaction of cellulose

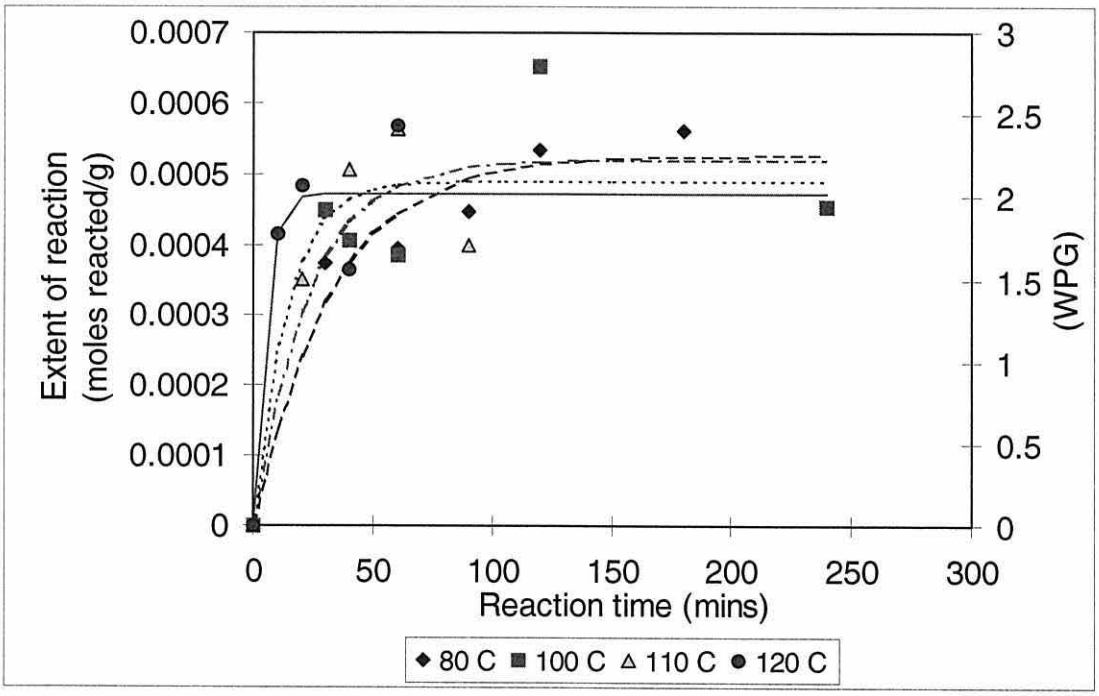

Figure 4.11.b. Reaction of cellulose at the wood reaction scale

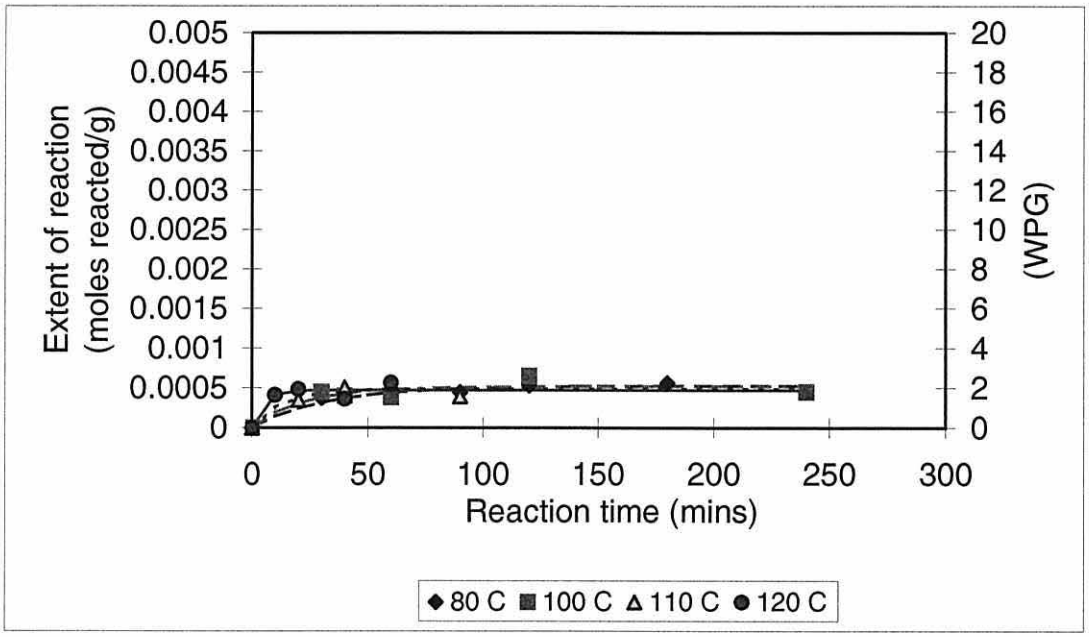

Cellulose did not react very much under these conditions as expected (Figure 4.11). In fact, when looked at on the same scale as the wood reaction (Figure 4.11b), all the cellulose reactions could almost be described by one curve after the first 20-30 minutes of the reaction. Figure 4.12 shows a comparison of reaction of cellulose, holocellulose and wood blocks at 120 °C. It is clear that the initial part of the reaction is dominated by lignin, as both the cellulose and holocellulose react only at a lower level, in comparison with lignin. Holocellulose reacted more than cellulose, as the small amount of cellulose that reacted seemed to do so within 20-30 minutes.

There seemed to be a slower phase of reaction (Figure 4.12), after the initial part of the reaction of wood (the first 60 minutes). This could be the reaction of newly accessible regions of the wood cell wall due to swelling from previous reaction. It is clear from Figure 4.12 that the native hemicellulose react significantly at longer reaction times, and that cellulose does not react to a greater extent with longer times. It appears that the reaction of holocellulose might be diffusion controlled at the higher temperatures studied (110-120 °C), but it is thought that with the lower reactivity of the hemicelluloses, the activation of the OH groups to acetylation might be the rate-determining step.

More extensive study of holocellulose reaction would be necessary to confirm this. In addition, the results shown in Figure 4.12 are the solid WPG values. It was found that at longer reaction times, a greater proportion of the substrate dissolved into the reaction solution. This aspect would also need to be more fully investigated to understand the holocellulose reaction more completely.

Figure 4.12. Comparison between cellulose, holocellulose and wood - reaction at 120 °C.

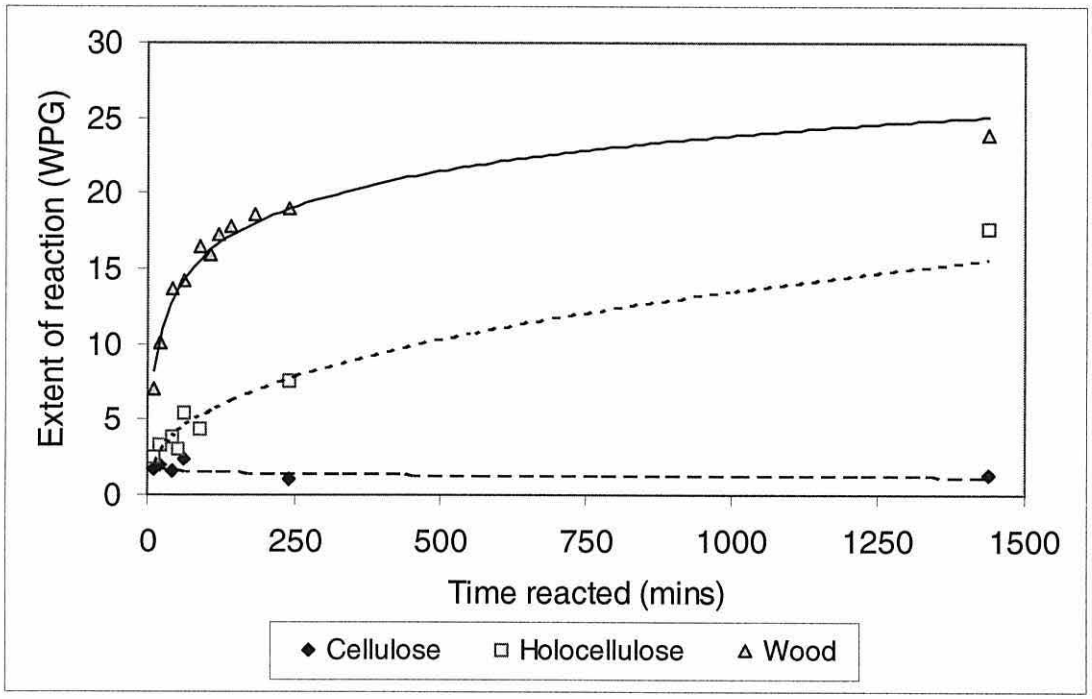

Reaction of the cellulose was expected to be low under these reaction conditions. The highly crystalline regions in cellulose (the majority of the sample) would not be reactive under these conditions. This leaves the surface of the crystalline regions, and the non-crystalline cellulose potentially available for reaction. However, probably both inaccessibility and low reactivity under these conditions influenced the level of reaction obtained.

Okhoshi *et al.* (1997) found that, even using significantly more reactive conditions (reaction with mixture of acetic acid, trifluoroacetic anhydride and benzene), there was a significant number of unreacted OH groups in non-crystalline cellulose within wood meal (makamba) above 20 WPG. They found that above this level of reaction that the crystalline cellulose within wood

started to react. It had been thought that position C6 in cellulose sub-units were more reactive than other positions. However, Okhoshi *et al.* (1997) found that at very high WPG (>40) all positions in cellulose seemed to be equally substituted.

4.3.2. Kinetic data

Data for the acetylation of holocellulose and cellulose are given in Table 4.5: the values for ground wood are given for comparison. Reaction rates obtained for holocellulose and cellulose were very low and differences between temperatures were small or out of order (initially). This low level of acetylation obtained and the relatively high variability made these results difficult to interpret.

Table 4.5. Kinetic data for holocellulose and cellulose

Sample	Initial rate (exp)		Initial rate (with zero) [b]	
	Ea, kJ/mol (std error)	r^2 (significance) [a]	Ea, kJ/mol (std error)	r^2 (significance) [a]
Holocellulose[c]			97 (25)	0.8871 (0.1)
Cellulose	48.18 (16.36)	0.8120 (0.1)		
Ground wood	62.13 (6.40)	0.9792 (0.02)	52.68 (4.19)	0.9875 (0.01)

[a] Probability of the r^2 being significant is determined using |r| values and Pearson's correlations coefficient tables, with ν=n-2, where n=number of data pairs.

[b] These values were calculated with the first two reaction data points as well as zero to obtain k_o values which were then used to obtain an Ea value.

[c] The values for the initial rate (exponential method) were not meaningful nor significant (Ea = 3.43 ± 21.5 kJ/mol, r^2=0.0125, P=NS).

The Ea calculation from the rate constants from the integral method (first order) for the holocellulose reaction (Ea = 50 ± 19 kJ/mol; r^2=0.7742, P=NS)

showed the data fitted the Arrhenius equation better, although they still weren't statistically significant.

When the diffusion equation (Chapter 3, Equation 3.4) was examined for the holocellulose reaction, the data at 120 °C fitted well when the longer times were included (using solid or total WPG). However, solid WPG data for holocellulose at the other temperatures (particularly the lower temperatures, 80 and 100 °C) did not really fit the diffusion equation well. Therefore, it seems likely that the rate of diffusion is faster than the rate of activation of the available OH groups, and the reaction of the holocellulose is probably controlled by first order kinetics (except possibly at 120 °C). To ascertain with more reliability whether the holocellulose reaction fitted a first order rate equation or a diffusion equation, the reaction would need to be investigated in more depth for all temperatures studied and with longer reaction times, so that around 90 % of the reaction profile was covered. However, the relative dominance of these two factors can change over reaction time, as well as over a temperature range.

The equivalent data using the k values from the integrated rate equation for the cellulose reaction was an Ea value of 23 ± 6 kJ/mol with r^2 of 0.8821 (P=0.1). Surprisingly, the data from cellulose did fit a straight line, but this could have been coincidence rather than reliable values.

4.4. Reaction of the isolated hemicelluloses, with catalysts

Two hemicelluloses, xylan and glucomannan, were isolated from radiata pine, along with the other substrates used. However, it was found from the initial reactions that the reactivity of the isolated hemicelluloses was much lower than expected from the holocellulose and cellulose reaction levels. The approximate level of reaction was obtained by the subtraction of the cellulose from the holocellulose reactions. From the sample analyses in section 3.2.3, approximately 75 % of the holocellulose sample was cellulose (actual figures in Equation 4.1).

Holocellulose = 73.5 % cellulose + 13. 5% GM + 6.1 % xylan + 5 % lignin ...
..... Equation 4.1

The cellulose reaction level was corrected for the amount that lignin contributed to the WPG observed (cellulose samples used here had 1.6 % lignin present). This corrected amount was then subtracted from the holocellulose reaction (which has also been corrected for lignin), then the combined hemicelluloses (about 20 % of holocellulose sample) contributed 2.86 WPG for reaction at 120 °C for 60 minutes (data in Table 4.6). Therefore, a sample of pure hemicellulose (approximately 2:1 GM:xylan) should react by about 14 WPG at 120 °C for 60 minutes. Likewise, the equivalent calculations at 100 °C for 90 minutes were an expected reaction level of 7.4 WPG for the combined hemicelluloses. However, the uncatalysed reaction (at 100 °C for 90 minutes) of the xylan and GM gave 2.92 and 3.02 WPG_{tot} respectively.

Table 4.6. Reaction of wood carbohydrates when reacted with catalysts [1]

Sample	Reaction with no catalyst	Reaction with pyridine		Reaction with acetic acid	
	WPG_s [2]	WPG_s [2]	WPG_{tot} [3]	WPG_s [2]	WPG_{tot} [3]
Xylan	*0.74* [4, 5]	4.84	6.34	8.52	18.63
		(0.61)	(0.77)	(1.00)	(0.30)
Glucomannan	*1.28* [4, 6]	1.93	7.18	6.32	16.90
		(0.43)	(2.57)	(0.54)	(2.03)
Holocellulose	5.43	15.11	17.35	5.91	7.47
	(0.13)	(1.23)	(2.56)	(0.66)	(0.26)
Cellulose	2.39	2.35	2.35	2.22	2.22
	(0.35)	(0.22)	(0.22)	(0.04)	(0.04)

1 Reaction was at 120 °C for 60 minutes. Values are duplicates averaged with (standard deviation)
2 Solid weight percent gain: as measured initially.
3 Total weight percent gain: initially measured + amount that was dissolved in reaction solution (as measured by evaporating solutions down).
4 Reaction was at 100 °C for 90 minutes; in italics, for comparison only
5 Total WPG for xylan was 2.92 WPG_{tot}
6 Total WPG for glucomannan was 3.06 WPG_{tot}

Therefore, the two hemicellulose samples, xylan and glucomannan, were reacted with two different catalysts (pyridine and acetic acid) to check that the isolated hemicelluloses did actually react. Holocellulose and cellulose were also reacted with the catalysts to check levels of reaction in these samples for comparison. The samples were then examined by FTIR spectra to directly measure the extent of reaction semi-quantitatively, independently from weight measurement. The same samples were also briefly examined by solid state NMR spectroscopy. The levels of reaction obtained are shown in Table 4.6.

It was found that when acetic acid was the catalyst, significant amounts of the isolated hemicellulose samples dissolved during reaction. This means that the true level of reaction is much higher than originally measured, as shown by the WPG_{tot} values. The hemicelluloses, which were most effectively catalysed with acetic acid (17-19 WPG), did not react that much above the predicted level of the uncatalysed reaction of the combined hemicelluloses (14 WPG). This confirmed that the isolated hemicellulose were significantly changed by the isolation process, and were therefore of reduced value from which to obtain kinetic information. In addition, the holocellulose reaction was catalysed more effectively with pyridine, which was another indication that the hemicelluloses in the holocellulose sample were different at least in their reactivity to the isolated hemicelluloses (as cellulose wasn't catalysed effectively by either catalyst under these reaction conditions).

The reason for the observed low level of reaction for the isolated hemicelluloses was probably reduced reactivity due to hornification during drying.

4.4.1. Reaction of the isolated xylan

A comparison of the different levels of reaction as shown by the FTIR spectra is shown in Figure 4.13, with arrows showing the main differences due to acetylation.

The FTIR spectrum of unreacted xylan is shown in Figure 4.14 for reference, and the FTIR spectra of reacted xylan, uncatalysed (reacted at 100 °C for

90 minutes) and catalysed (reacted at 120 °C for 60 minutes) are shown in Figures 4.15-4.17. In the unreacted xylan spectrum, there is a significant change in the region 1200-1500 cm^{-1} from that of wood or holocellulose, as in the latter two spectra, there are many compounds contributing to this region.

Figure 4.13. Comparison of acetylated and untreated xylan FTIR spectra

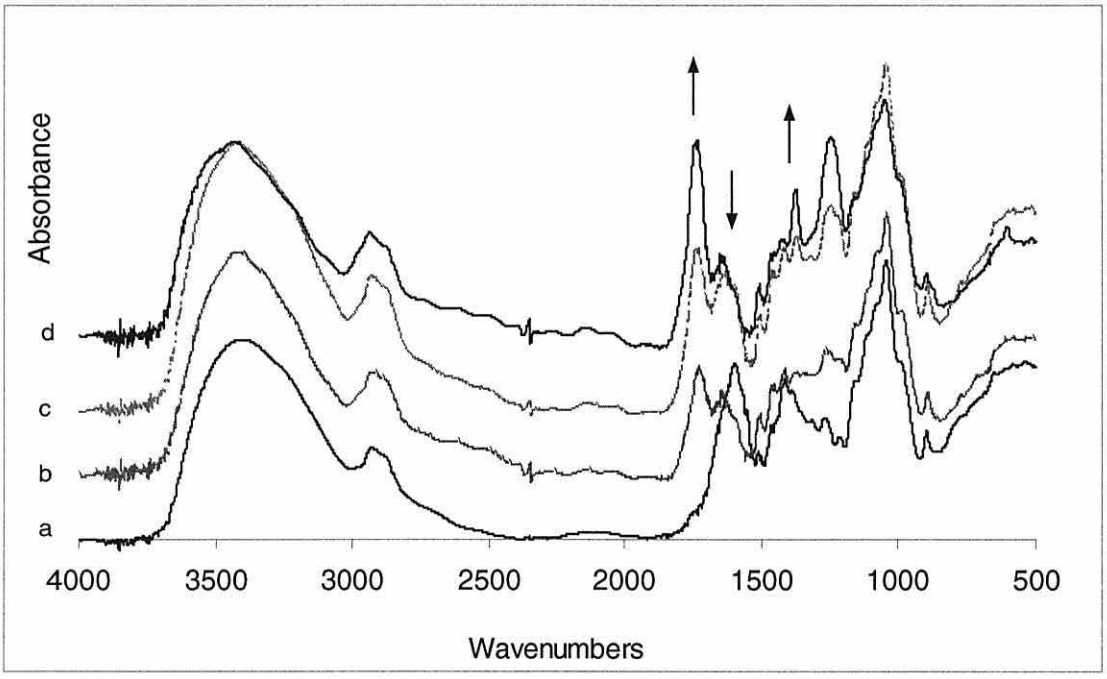

Key: a = Untreated xylan
b = Acetylated xylan uncatalysed (1.5 WPG_{tot})
c = Acetylated xylan, catalysed with pyridine (5.8 WPG_{tot})
d = Acetylated xylan, catalysed with acetic acid (18.4 WPG_{tot})

There were three main areas of increase in the spectra of acetylated xylan (Figures 4.15-4.17) compared to the untreated spectrum (Figure 4.14). However, all three can only be seen clearly at high levels of reaction. These areas were carboxyl (C=O), at 1732-37 cm^{-1}, carbonyl (C-O) at about 1244-50 cm^{-1}, and methyl (CH_3) of the acetate at 1375 cm^{-1}. There was one obvious area of decrease in the spectra on acetylation, apart from a reduction in the broad OH region at 3410-3435 cm^{-1}. This was the region at 1415 cm^{-1} possibly due to loss of acid during reaction. Assignments of the main FTIR peaks for unreacted and reacted xylan are shown in Table 4.7.

Figure 4.14. FTIR spectrum of unreacted xylan

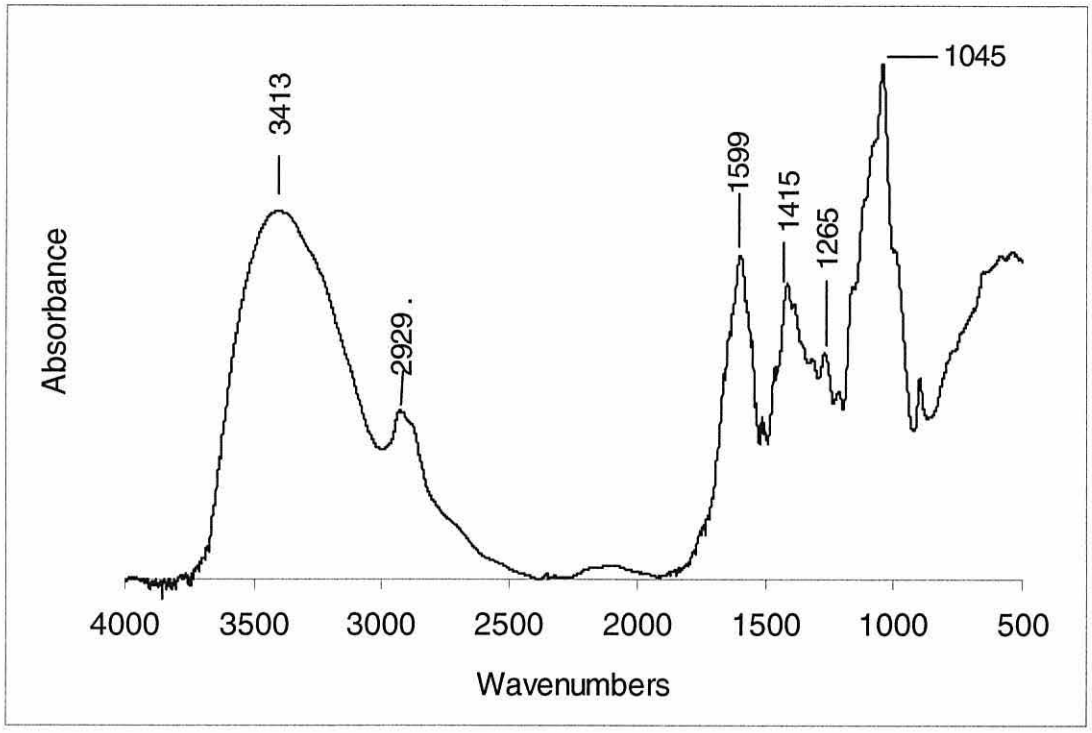

Figure 4.15. FTIR spectrum of acetylated xylan, uncatalysed ($0.46\ WPG_s$, $1.54\ WPG_{tot}$)

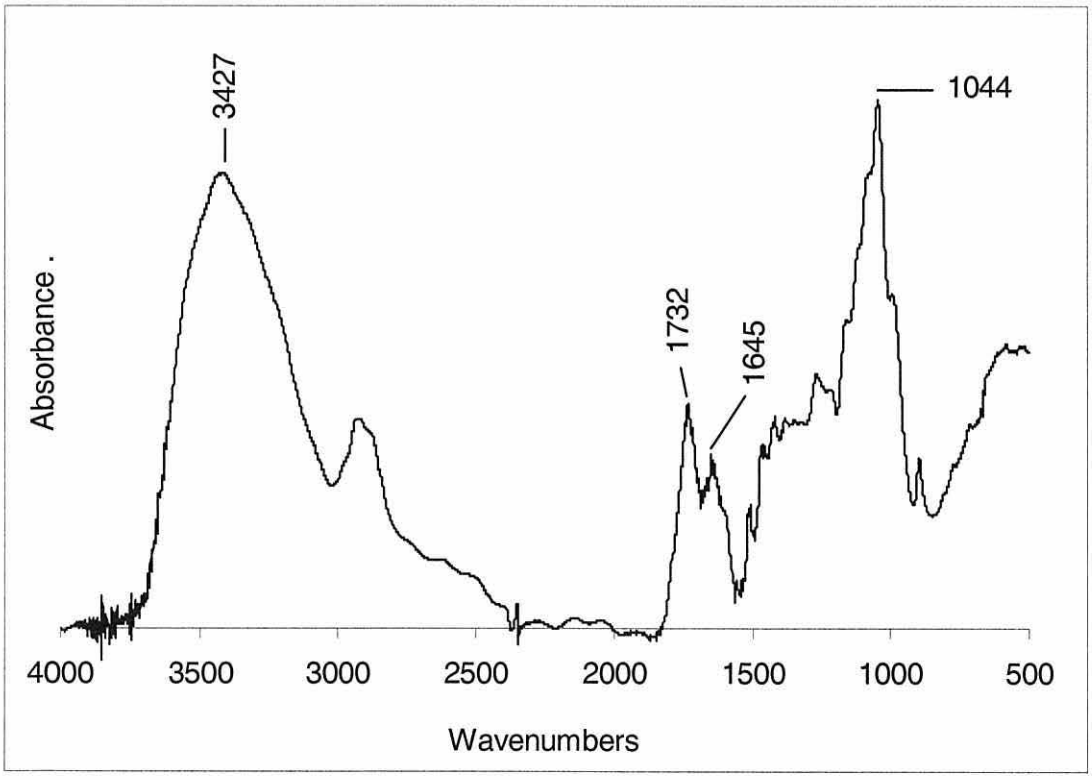

Figure 4.16. FTIR spectrum of pyridine-catalysed xylan
(5.27 WPG_s, 5.79 WPG_{tot})

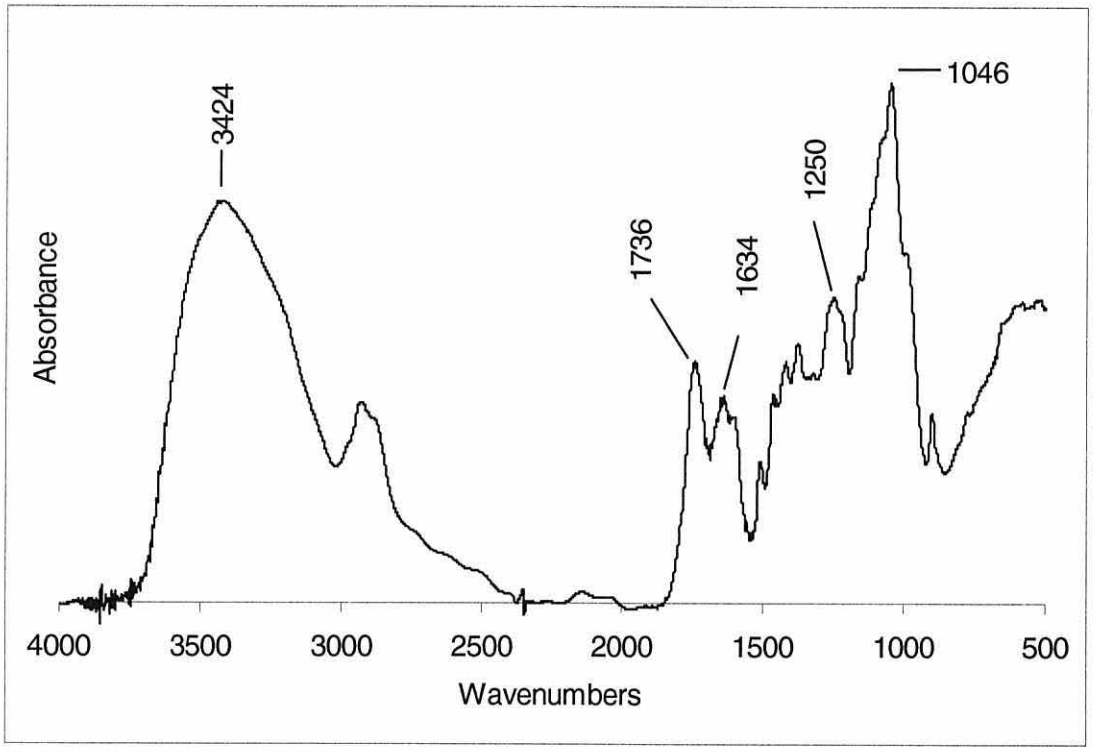

Figure 4.17. FTIR spectrum of acetic acid-catalysed xylan
(9.32 WPG_s, 18.42 WPG_{tot})

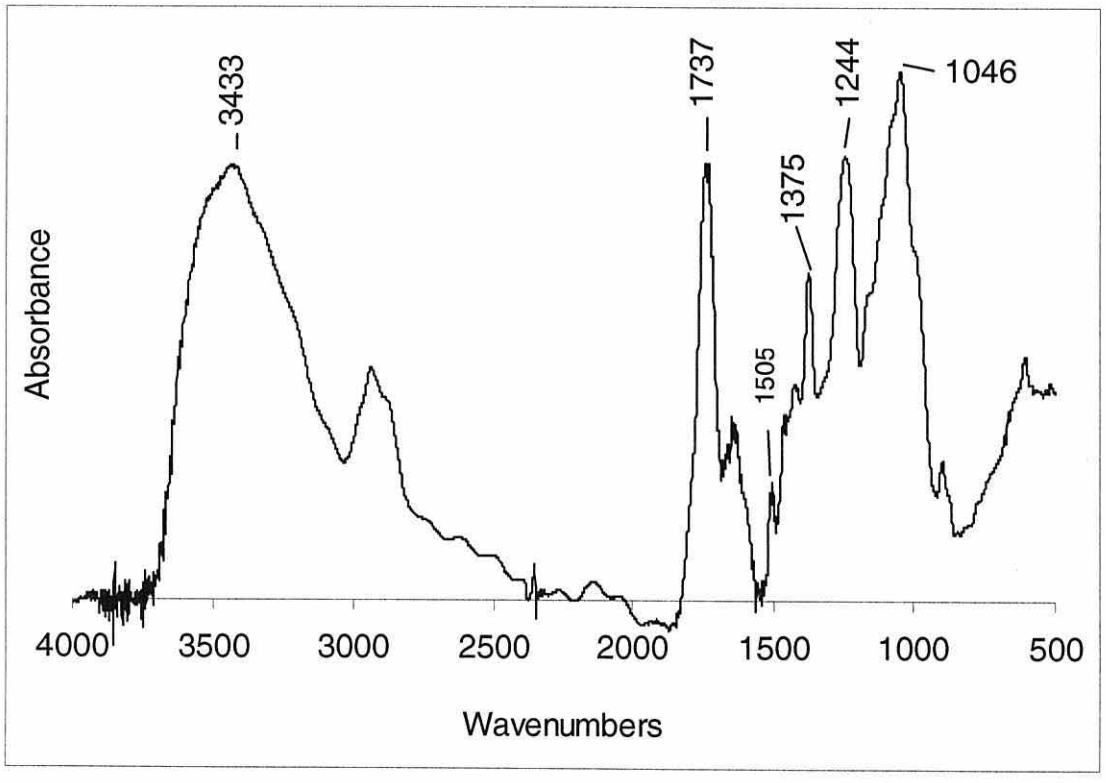

Table 4.7. FTIR peak assignments for treated and untreated xylan (in wavenumbers, cm^{-1})

Peak assignment (maxima)	Untreated xylan	Acetylated xylan, uncatalysed	Acetylated xylan, catalysed with pyridine	Acetylated xylan, catalysed with acetic acid
3410-40, ν_{O-H}, bonded	3413	3427	3424	3433
2930, ν_{C-H}, CH_3/CH_2	2929	√	√	√
1735, $\nu_{C=O}$, unconjugated,		1732	1736	1737
acetyl, carboxyl, ketone				
1635, $\nu_{C=O}$, conjugated, acid	sh	1645	1634	√
1599, $\nu_{C=C}$, (aromatic)	1599	sh	sh	sh
1400-1470, δ_{C-H}	1415			
1375, δ_{C-H}, $-CH_3$			sm	1375
1220-1275, ν_{C-O-C},	1265 (sm)	√ (sm)	1250	1244
1020-60, ν_{C-O-C}, ethers, ring				
saccharide skeleton	1045	1044	1046	1046
1000-670, δ_{C-H}, group	√	√	√	√
frequency in polysaccharides				

Key: √ indicates peak was present but was not picked out
sh indicates that a shoulder of a peak was visible
sm indicates that a small peak was present

Figure 4.18. Comparison of FTIR peak area ratios of xylan (solid WPG)

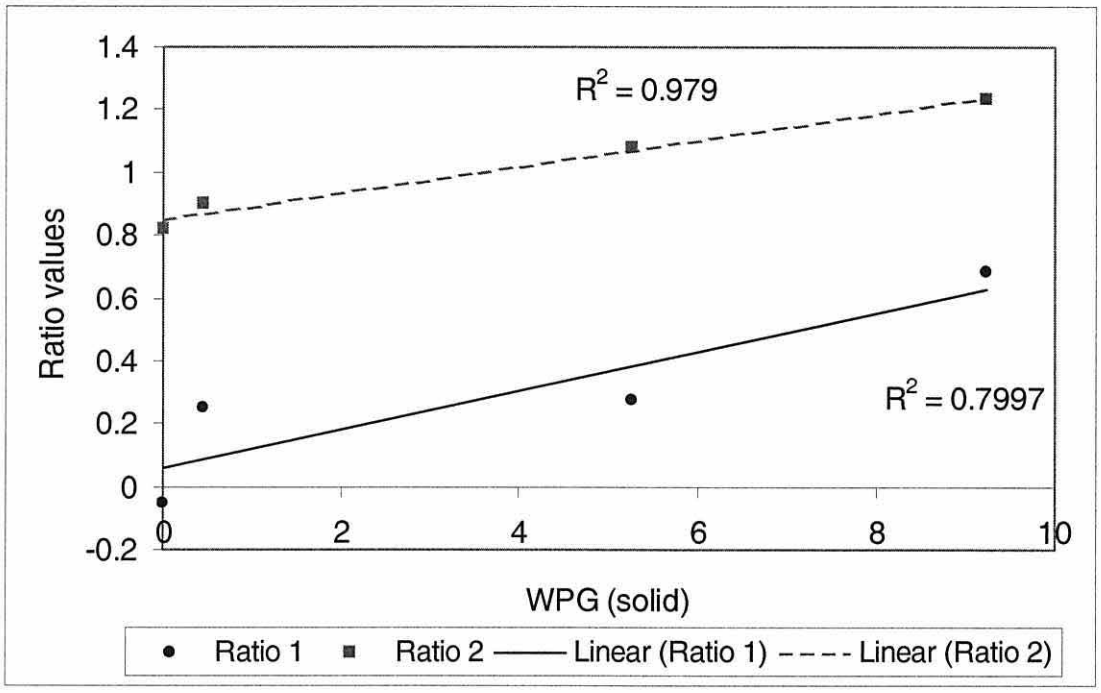

Figure 4.19. Comparison of FTIR peak area ratios of xylan (total WPG)

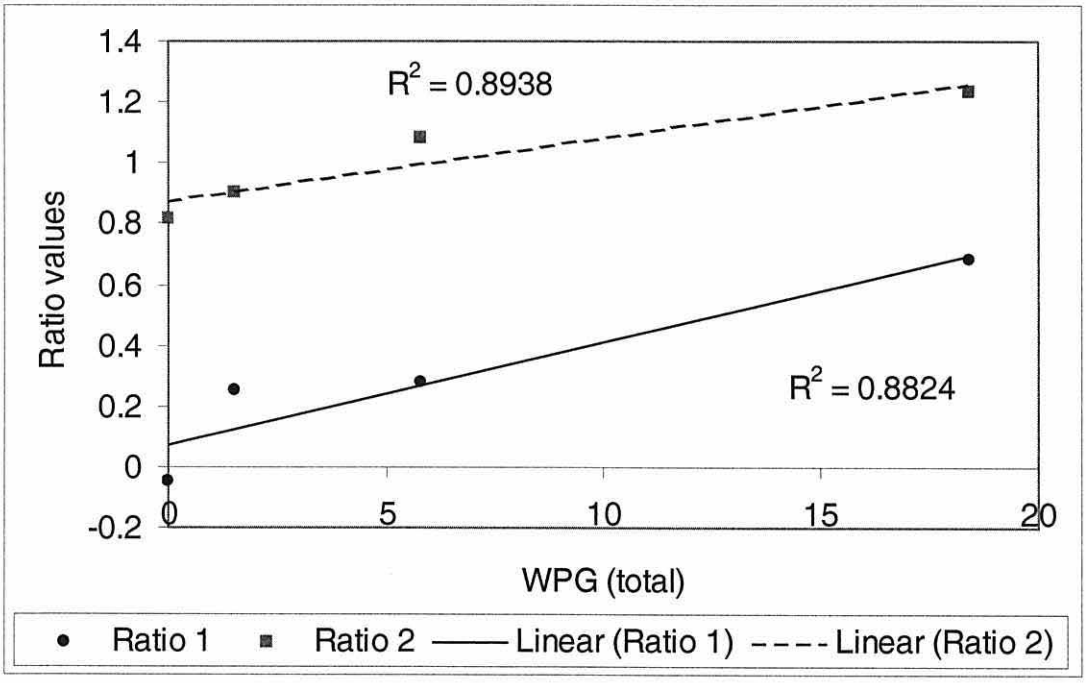

Note: The xylan values at different WPGs were untreated, reacted uncatalysed, reacted pyridine-catalysed, and acetic acid-catalysed xylan respectively.

A peak characteristic of lignin (1505 cm^{-1}) is most visible in the most acetylated xylan sample (Figure 4.17), indicating that the abnormally high apparent lignin content (as measured by Klason lignin and acid soluble lignin, Table 4.3) is probably real, rather than an artefact.

Ratios of two peak areas can give some semi-quantitative data on the extent of reaction. The reference area chosen was that of the carbohydrate skeleton (sugar units) of between 918 - 1150 cm^{-1}. There were a number of peak areas that can be used to monitor the growth of the acetate from the reaction. Two are reported: C=O at about 1735 cm^{-1}(Ratio 1); and C-O at about 1245 cm^{-1} with a slightly different reference peak area (Ratio 2). Each of these peak areas was ratioed with the selected reference peak area and are shown in Figures 4.18 and 19. The value for 0 WPG was that for the untreated xylan sample.

These ratios were as follows:

Ratio 1 = area (1688-1855)/area (918-1150)

Ratio 2 = area (1191-1304)/area (918-1142)

Ratio 1 seemed to describe the level of reaction better than Ratio 2, especially at lower levels of reaction (as no acetate is present in untreated xylan), although the r^2 values were lower than those of Ratio 2. The use of FTIR techniques for the analysis of wood has been developed (Pandey and Theagarajan, 1997; Tolvaj and Faix, 1995; Zanuttini *et al.,* 1998). However, when one is using only part of the wood sample, for example, an isolated hemicellulose, finding a reliable reference area and validating it can be difficult and time consuming. Therefore, the use of FTIR in these studies was only indicative, and full validation of the use of FTIR quantitatively with these samples would need to be carried out. However, this was outside the scope of this study.

A solid state ^{13}C NMR spectrum of one acetylated xylan sample (7.81 WPG_s) was included to illustrate the possibility of using this technique to estimate extent of reaction directly (Figure 4.20). This figure shows the integration

areas used: the core sample between 40 and 135 ppm (used as reference), and two areas to probe the acetate, the methyl carbon at 10-25 ppm (maximum 21 ppm, Acet1) and the carbonyl carbon at 163-190 ppm (maximum at 173 ppm, Acet2). The wider range was used to ensure that the integral trails were horizontal along the baseline (as there was a lot of noise). The equivalent spectrum of the untreated xylan sample is shown in section 4.2.1 (Figure 4.5).

Solid state NMR spectra of samples are easy to run, and the technique is non-destructive, so that if there is limited sample available then this is a suitable technique. For wood-based samples, it can be useful method to give an estimate of extent of acetylation, as the acetate peaks are well separated from peaks of the substrate itself. A range of acetylated wood samples was run and the results are discussed in Chapter 3, section 3.2.2.

Figure 4.20. Solid state ^{13}C NMR spectrum of acetylated xylan (7.81 WPG_s, acetic acid-catalysed reaction)

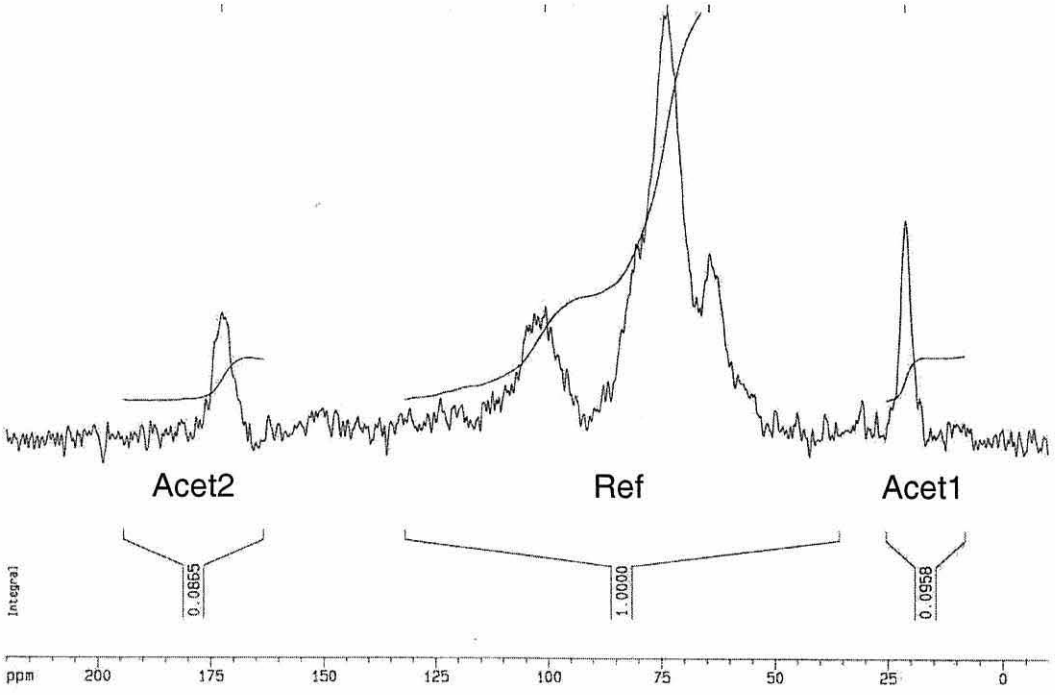

It was likely that even the native xylan in the wood samples would not have been completely acetylated under these reaction conditions, even at the

longest times and highest temperatures. Okhoshi *et al.* (1997) found, using much more reactive conditions than used here, that xylan in wood (makamba) was not completely acetylated at wood WPG level of 29.0 %, but seemed to be at 41.3 WPG.

4.4.2. Reaction of the isolated glucomannan

The FTIR spectrum of unreacted glucomannan is shown in Figure 4.21 and the FTIR spectra of acetylated glucomannan, uncatalysed (reacted at 100 °C for 90 minutes) and catalysed (reacted at 120 °C for 60 minutes) are shown in Figures 4.22-4.24. There were significant differences between the untreated xylan and untreated glucomannan spectra. The xylan spectrum had a sharp, large peak at 1599 cm^{-1} (characteristic of lignin) and a significant peak at 1415 cm^{-1}, indicating more carbonyl groups. The glucomannan spectrum had a smaller ill-defined peak, which had a maximum at 1634 cm^{-1}, and much smaller band at 1415-18 cm^{-1}. The glucomannan spectrum also contained at peak at 812 cm^{-1}, which was absent in the xylan spectrum, and would indicate some unsaturated carbons were present.

As for the acetylated xylan, there were also three main areas of increase in the spectra of the acetylated glucomannan (GM): carboxyl (C=O), at 1740-50 cm^{-1}, carbonyl (C-O) at about 1242-4 cm^{-1}, and methyl (CH_3) of the acetate (O-C(=O)-CH_3) at about 1375 cm^{-1}. In the latter case, there was already a small peak at 1381 cm^{-1}, which slightly masked the increase at this point due to acetylation.

For the GM spectra, there was not a decrease in the region 1415-8 cm^{-1}, as GM does not contain uronic acid as the xylan does, but instead contains natural acetyl, most of which would be lost during the isolation process. There was a small decrease (apart from the OH region) at around 1597 cm^{-1}, but only for one acetylated sample, that of the acetic acid-catalysed GM (Figure 4.24). Assignments of the main FTIR peaks for unreacted and reacted GM are shown in Table 4.8.

Figure 4.21. FTIR spectrum of unreacted glucomannan (GM)

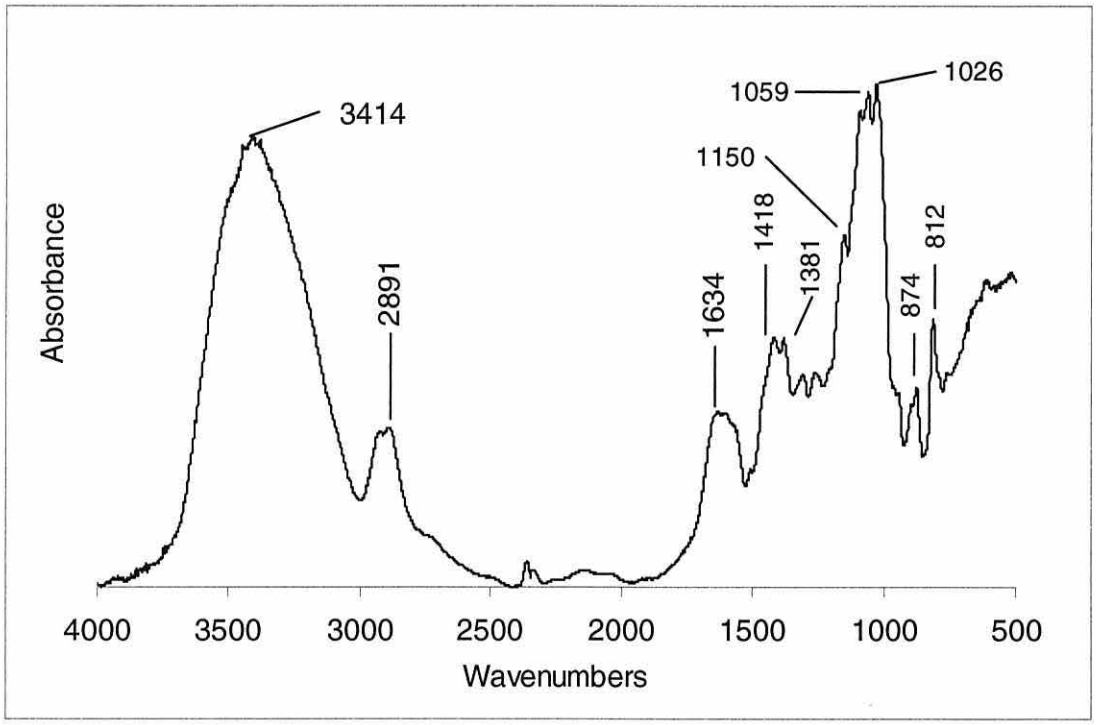

Figure 4.22. FTIR spectrum of acetylated GM, uncatalysed
(1.28 WPG_s, 3.34 WPG_{tot})

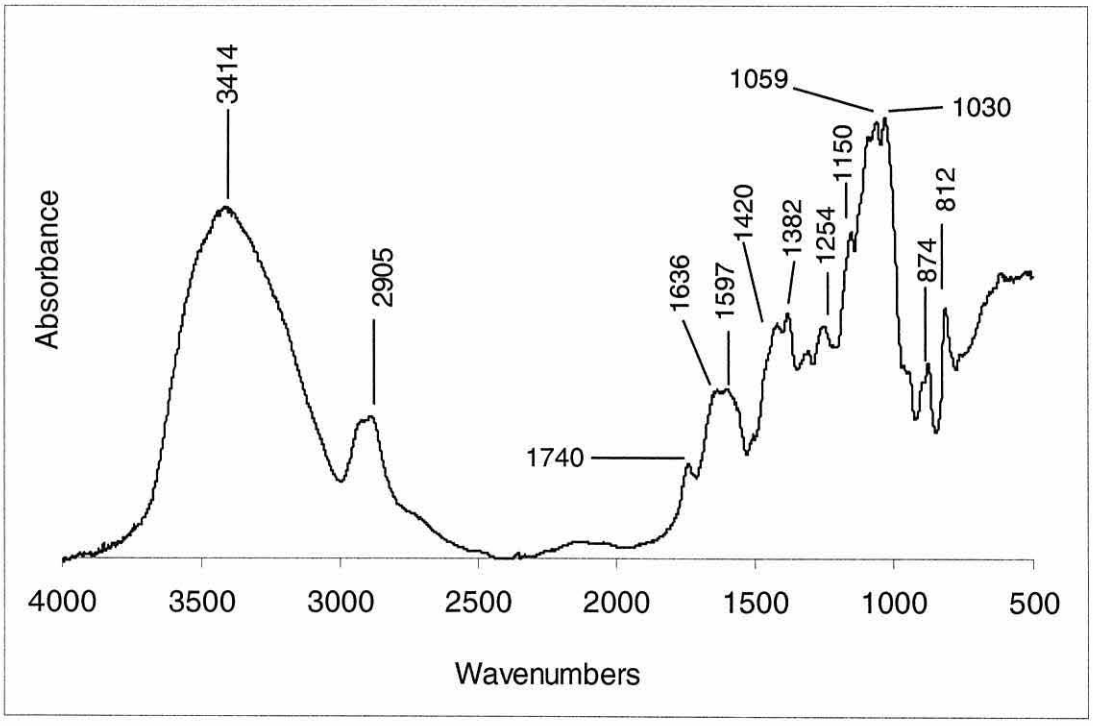

Figure 4.23. FTIR spectrum of acetylated GM, pyridine-catalysed ($2.23\ WPG_s$, $5.36\ WPG_{tot}$)

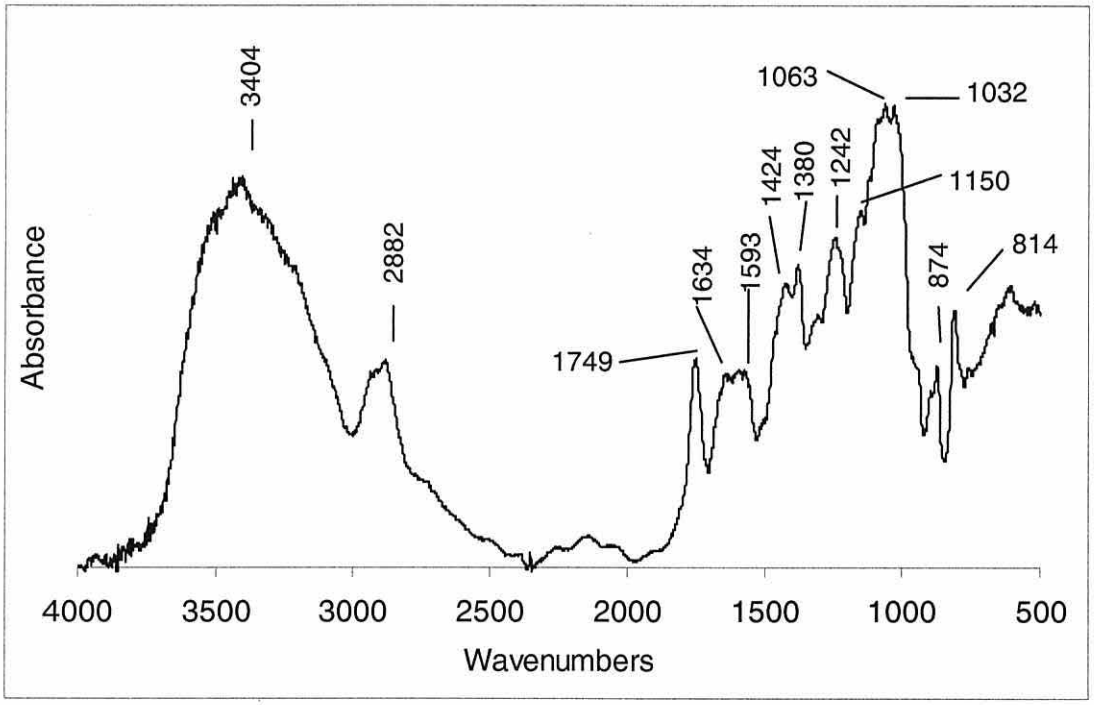

Figure 4.24. FTIR spectrum of acetylated GM, acetic acid-catalysed ($6.61\ WPG_s$, $15.46\ WPG_{tot}$)

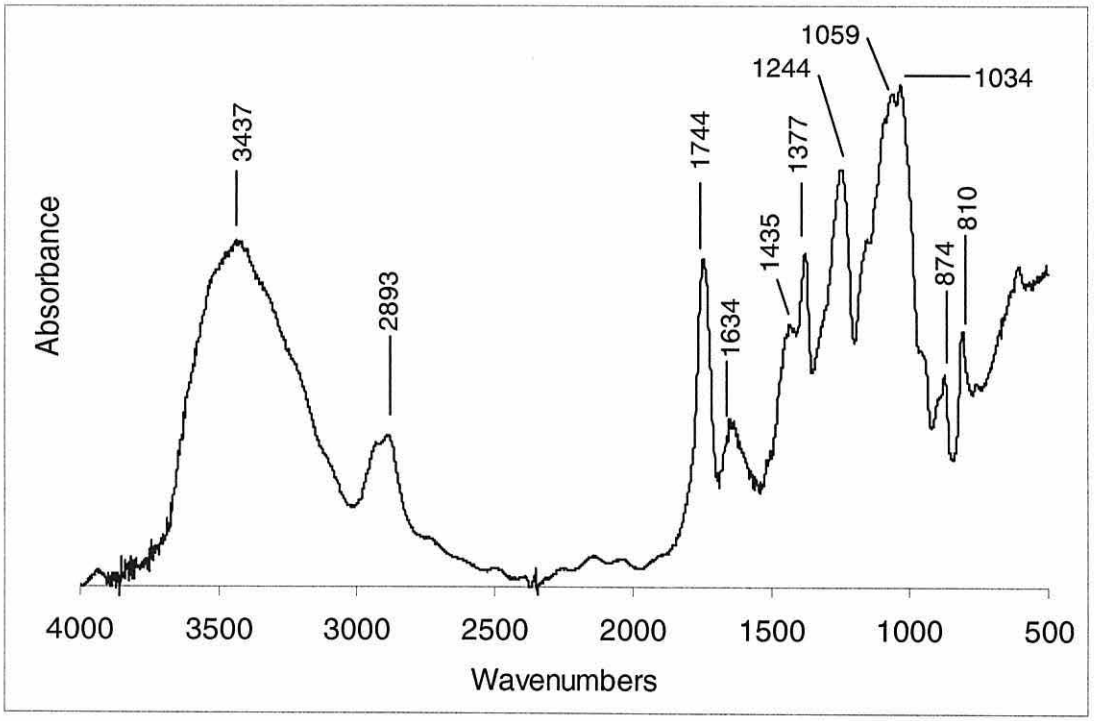

Table 4.8. FTIR peak assignments for treated and untreated glucomannan, GM (in wavenumbers, cm^{-1})

Peak assignment (maxima)	Untreated GM	Acetylated GM, uncatalysed	Acetylated GM, catalysed with pyridine	Acetylated GM, catalysed with acetic acid
3400-40, ν_{O-H}	3414	3414	3404	3437
2930, ν_{C-H}, CH_3/CH_2	2891	2905	2882	2893
1735, $\nu_{C=O}$, acetyl		1740	1749	1744
1635, $\nu_{C=O}$, acid	1634	1636	1634	1634
1599, $\nu_{C=C}$, (aromatic)	sh	1597	1593	sh
1400-1470, δ_{C-H}, - CH_2-CO-	1418	1420	1424	1435
1375, δ_{C-H}, -CH_3	1381	1381	1380	1377
1220-1275, ν_{C-O-C}		1254	1242	1244
1020-1140, ν_{C-O-C}, ethers, saccharide skeleton	1150,1059, 1026	1150, 1059, 1030	1150, 1063, 1032	1152, 1059, 1034
1000-670, δ_{C-H}	874, 812	874, 812	874, 812	874, 810

Key:
sh Indicates that a shoulder of a peak is visible

Figure 4.25. Comparison of FTIR peak area ratios of glucomannan (solid WPG)

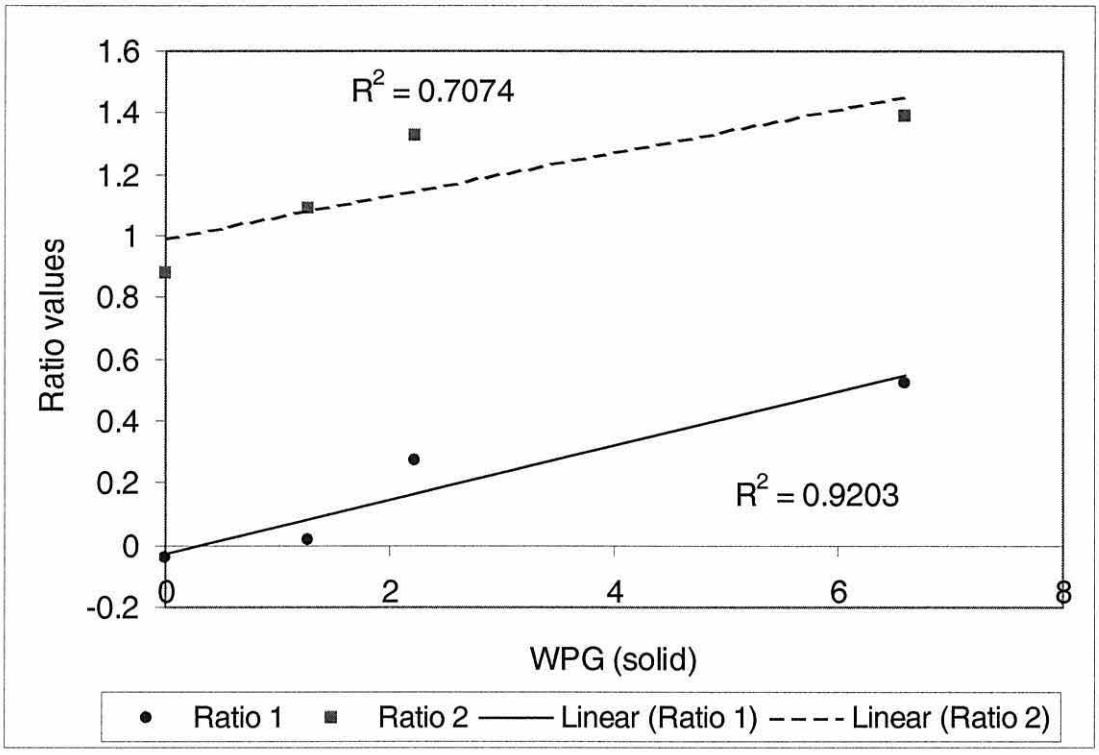

Figure 4.26. Comparison of FTIR peak area ratios of glucomannan (total WPG)

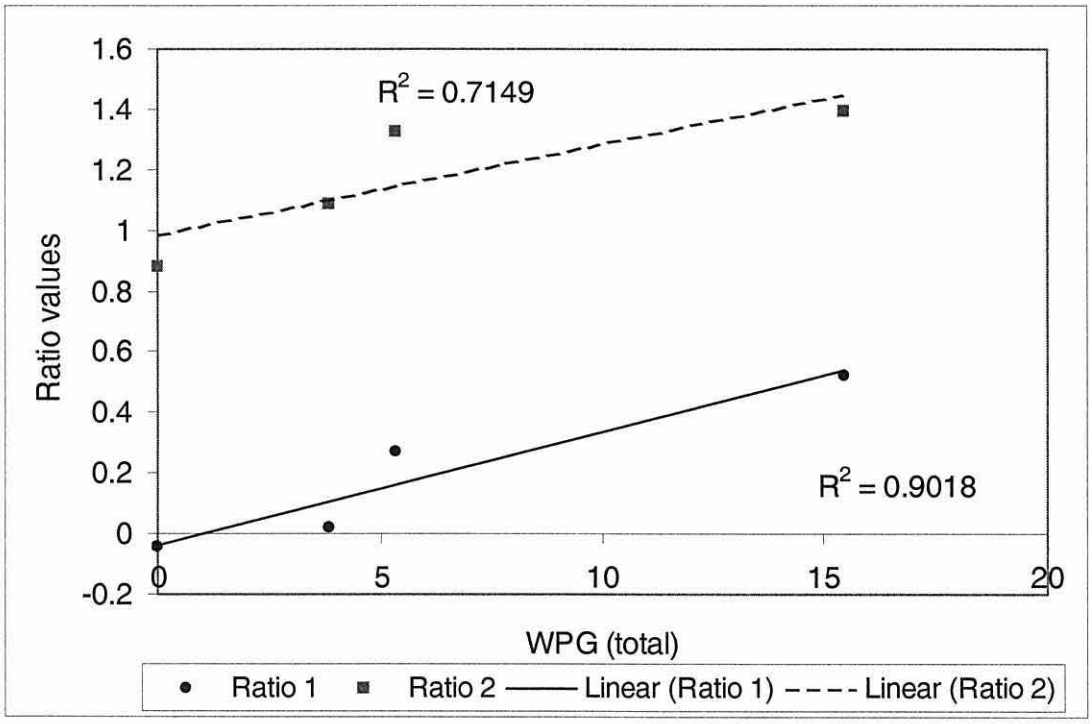

Figures 4.25 and 4.26 show the ratio values produced for the GM series of spectra against WPG, the extent of reaction measure used. It is hard to pick which ratio described WPG best, although it appears that Ratio 1 fitted best. The FTIR ratio method does not seem measure accurately at low levels of reaction.

Figure 4.27. Solid state ^{13}C NMR spectrum of acetylated glucomannan (5.85 WPGs, acetic acid-catalysed reaction)

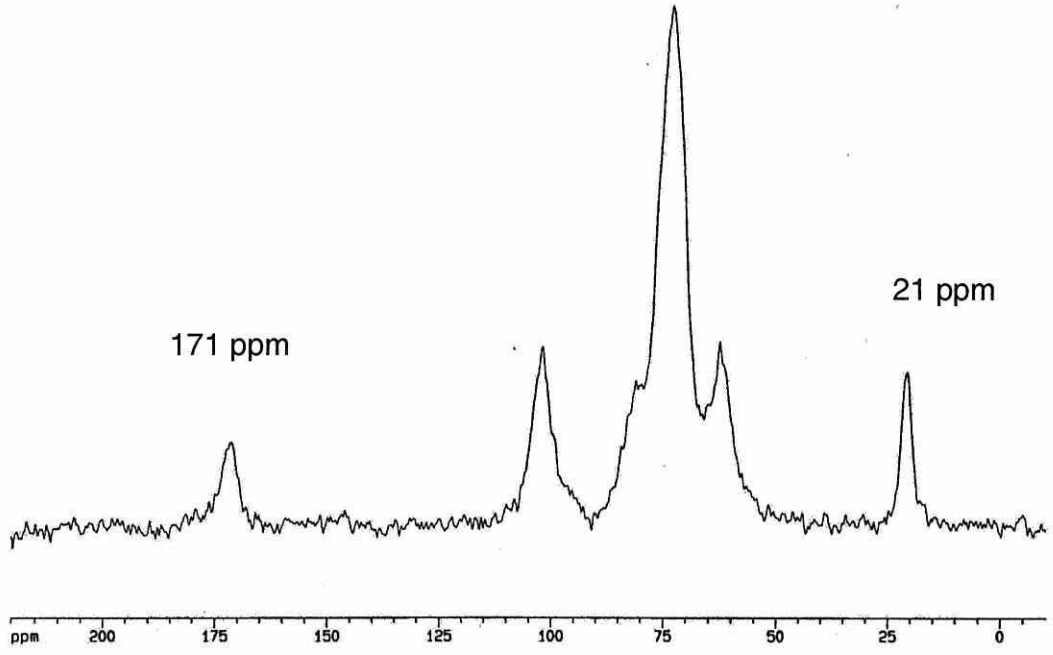

A solid state ^{13}C NMR spectrum was run of one acetylated glucomannan samples (Figure 4.27). The regions integrated were the same as for the xylan samples (previous section). When these data were compared with the WPG data, the Acet2 (171 ppm) peak area seemed to give a better relationship. However, many more samples would need to be examined in this way to validate this technique.

4.5. Discussion of wood carbohydrate reactivity

From the reaction of the holocellulose and cellulose, it was obvious that the native hemicelluloses (combined) react to a much greater extent than did the cellulose. This was in general agreement with the results from Rowell *et al.*

(1994), although it had been hoped to more fully quantify the difference in reactivity with this study. When the expected amount due from the cellulose is subtracted and the contribution from the small amount of lignin present is corrected for, the expected reaction level of the combined hemicelluloses is obtained (section 4.4).

The low level of reaction shown by cellulose was expected under these conditions. Commercially, cellulose acetate is made using a mixture of acetic anhydride, acetic acid and a mineral acid catalyst such as H_2SO_4. However, the small amount of lignin in the cellulose sample would have also contributed to the reaction level observed. When this was corrected for, the cellulose itself accounted for 80-85 % (average for each temperature) of the observed reaction level, although the range was 68-90 % for individual samples. This confirmed that the level of reaction for cellulose observed was not mainly due to "contaminants" (lignin or hemicellulose), but was reaction of cellulose itself; probably a few OH groups in the most readily accessible outer regions in the microfibrils. This result differs from that obtained in another study, where they found that cellulose did not react at all under the conditions (Rowell *et al.,* 1994).

Two hemicelluloses were isolated, xylan and glucomannan, but the initial acetylation trials showed a much lower level of reaction than expected from the holocellulose reactions. For example, reaction at 100 °C and 90 minutes achieved 2.05 WPG for xylan and 3.15 WPG for glucomannan against the expected amount for combined hemicellulose of around 7.5 WPG (not corrected for lignin contribution). Therefore, these hemicelluloses were not used in the main kinetic study, but were instead reacted with a catalyst and the reaction products were examined by FTIR. Holocellulose and cellulose were also included in these catalytic trials for comparison.

There are a number of possible explanations of the observed reactivity of the isolated hemicelluloses in contrast to that of the holocellulose and cellulose when acetylated with one of two catalysts. One of these possibilities is

swelling ability of the catalysts. However, the relative swelling ability of the two catalysts were very similar at 120 °C (Table 4.9).

Table 4.9. Volumetric swelling coefficients of wood

Reagent	120 °C (150 lb/in^2, 1 hour)	25 °C (soaking)
Water	10.0	10.0
Acetic acid	11.1	8.8
Pyridine	11.3	13.1

Note: Data are of southern pine sapwood (Rowell, 1983)

Another explanation for the observed differences in the catalyst effectiveness between the isolated hemicelluloses and the holocellulose and cellulose, is that the probable hornification of the isolated hemicelluloses not only lowered the general reactivity towards acetylation, but also changed the preference of catalysis between acetic acid and pyridine.

Cellulose microfibrils become hornified when dried from water-swollen state. The less ordered (outer) region are more highly swollen and when dried, new hydrogen bonds are formed in a "zipper-like" manner, which fuses the fibrils together (Krässig, 1985). This reduces the permeability of reagents through the fibres. However, the reactivity of the cellulose can be increased, if not restored, by various treatments (such as activation or solvent exchange).

Starch granules when dissolved or suspended in water can also hornify on drying. In fact, special care needs to be taken to avoid it; for instance, if the starch is precipitated in alcohol, and dried once water is removed (Whistler, 1945). In each case, hornified products have lower reactivity than the original samples. For the hornification of the isolated hemicelluloses, a slightly different mechanism may be involved, as there are no microfibrils surfaces to "zip" up. The isolated hemicelluloses were completely dissolved in water, and had the opportunity to fold up on itself, forming new hydrogen bonds. These bonds may have strengthened as water was removed, thus reducing its reactivity and hornifying.

The measurement of extent of reaction of an isolated hemicellulose or holocellulose sample could possibly be measured by solid state ^{13}C NMR analyses, which would allow direct measurement of the acetate formed. However, the detection limit of this technique appears to be around 2 WPG.

The holocellulose reacted significantly at longer times, indicating that at longer reaction times the native hemicelluloses do react substantially. This may mean that the lignin reacts before the hemicelluloses, once the anhydride has diffused to the local reaction sites (where the lignin and hemicelluloses are probably in close proximity). In particular, the relative dominance of the first order kinetics (activation control) or diffusion control for the holocellulose reaction appears to change over the temperature range studied, although needs to be confirmed.

4.6. Summary

The reaction of holocellulose was much lower level than the wood reaction, as expected. The initial rates at each temperature did not yield k_o values (using the exponential method) that fitted the Arrhenius equation, probably because of the high level of variability of the results. The activation energy (Ea) value obtained using k_o values from the alternative method (using the first two data points and zero) was high with high error (97 ± 25 kJ/mol). It was difficult to ascertain whether first order kinetics or diffusion controlled the holocellulose reaction, as the dominant influence appeared to change over the temperature range covered. However, the high Ea value might indicate the overall dominance of first order kinetics. This would need to be confirmed.

The reaction of cellulose was very low, as expected under these conditions. There was not a high level of temperature dependence of the reaction level obtained. The Ea value obtained for the cellulose reaction (48 ± 16 kJ/mol) under these conditions was bound to have significant error with such low reaction levels. The reaction of native hemicelluloses (found by subtraction of

the cellulose reaction from the holocellulose reaction level) was much higher of that of the cellulose, especially at longer reaction times.

The reaction of the isolated hemicelluloses (xylan and glucomannan) was found to be much lower than expected from the reaction of holocellulose and cellulose. Therefore, the hemicelluloses were examined by FTIR and further reacted with two catalysts (pyridine and acetic acid) to maximise the level of reaction. The reaction level reached by catalysis with acetic acid (17-19 WPG at 120 °C, 60 minutes) was just above the expected calculated level of the uncatalysed reaction.

It was thought that the isolated hemicelluloses had undergone some transformation during isolation, which had significantly altered their reactivity to acetylation (for example, hornification). It was therefore decided that the isolated hemicelluloses would not produce reaction or kinetic data that would be useful and so further studies on them were not pursued.

CHAPTER 5: REACTION OF THREE LIGNIN PREPARATIONS

5.1. Introduction

The structure of lignin has been extensively studied, because of to its importance in pulping processes (Gierer, 1982; Gierer and Ljunggren, 1979; Adler, 1977). However, as native lignin is a large and extremely heterogeneous compound, no definitive structure can be formulated. In addition, lignin is difficult to extract from wood and separate from wood polysaccharides, as lignin is formed in the cell wall in close association with the other two main wood components (Fengel and Wegener, 1989). In fact, each stage of lignification in the tracheid cells of radiata pine is preceded and influenced (in terms of rate and direction) by deposition of carbohydrates (Donaldson, 1991; 1994).

It has been thought that when examining uncatalysed reactions of wood hydroxyl groups that lignin is the dominant influence in the wood reaction (Rowell *et al.,* 1994). This is due to the low general reactivity of cellulose under these conditions, and the lower reactivity of the hemicelluloses. However, there have not been many studies conducted to quantify the kinetic differences between these major wood components. Therefore, the choice of lignin sample to be used for this study was crucial. It was thought to be interesting and maybe important to compare different lignin preparations to gain a greater understanding of the influence of key lignin features for these type of reactions.

There are several methods used to isolate lignin from wood. Methods that significantly change the lignin structure, such as sulphuric acid methods, were not considered to be suitable for this study, as the isolated lignin needed to be as close to wood lignin as possible. There are four types of lignin isolation methods (Fengel and Wegener, 1989):

* Lignin as a residue (Klason lignin, periodate lignin, cuoxam lignin);
* Lignin by dissolution, where there is no reaction between lignin and the solvent (MWL, CEL);

* Lignin by dissolution, where there is a reaction between lignin and the solvent (dioxane acidolysis lignin, thioglycolic acid lignin);
* Lignin derivatives by inorganic reagent (soda lignin, Kraft lignin).

Lignin isolation by dissolution, where there was no reaction between lignin and solvent was chosen as the most appropriate method type to produce the primary lignin for this study. In addition, it was thought that a comparison between very different types of lignin preparations would be interesting in this type of study, as the chemical composition can vary considerably between preparations and this may be reflected in the kinetic data produced.

5.1.1. Comparison of methods

Glasser and Barnett (1979) compared four methods of lignin isolation: milled wood lignin (MWL), cellulolytic enzyme lignin (CEL), derivatisation with thioglycolic acid, and derivatisation of hydromethylated wood with thioglycolic acid. Assessment was based on four criteria: yield, purification characteristics, reproducibility, and convenience. Of the four, MWL and CEL were the best methods. MWL was recommended as overall the best, due to its better purity and convenience, although CEL gave much higher yields.

Chang and others (1975) compared the MWL and CEL methods also, and found that both methods lowered the molecular weight and increased the α-carbonyl and phenolic content relative to native wood lignin. MWL and CEL were similar in elemental composition, and UV and IR spectra. Overall, they concluded that MWL adequately represented lignin in wood, although CEL was more representative, due to its higher yields. However, the CEL method was considered even more complex and tedious than the MWL method.

Therefore, on examination of the literature on different methods available in the category of dissolution of lignin by non-reactive solvents (and the trial of both methods), it was decided to use MWL, rather than CEL.

5.1.2. Milled Wood Lignin

Therefore, the MWL method was chosen as the most appropriate and convenient method that gave a reasonable representation of the lignin in wood (native lignin), without changing it too much during the isolation process. The method chosen was based on that of Björkman (1956), but there are a few variables in the method, such as milling set-up, extraction solvent and timing.

Ball milling is a crucial part of the MWL method. Inefficient milling can lead to very low yields (Chang *et al.,* 1975). Many factors influence milling efficiency (Björkman, 1957b): length of mill time, size of wood charge, inclusion of a non-swelling solvent for dispersion and pre-treatment with alkaline solution. Heat generation is also to be avoided if possible during milling to minimise condensation of lignin. Milling in toluene does avoid heat generation, but yields are slightly lower (Salud and Faix, 1980).

Adler (1977) noted that the molecular weight of MWL was much lower than native lignin due to the fragmentation that occurred during the ball milling step of isolation. The extraction process also increased the proportions of free phenolic and alpha-carbonyl groups. Table 5.1 shows a comparison of yields obtained using various modifications of the milled wood lignin method. There is quite a range of yields reported; from 1.6% to 9.6% (of wood). However, no two methods are exactly the same so direct comparison is difficult.

The accumulative yield of Bland and Menshun's (1967) at 100 hours (5.5%) is similar to that of Salud and Faix's (1980) at the same time (5.8%). From these data, it appears that the lignin of hardwood species is easier to extract than that of softwood species, such as radiata pine. The comparatively high yield of Chang *et al.* (1975) could have been due to the relatively small charge that was used.

Table 5.1. Comparison of MWL extraction yields, with various wood species.

Reference	Wood species	Mill type	Mill time (hours)	Extraction solvent	Final yield (%) [a]
Bland and Menshun (1967)	Eucalypt, hardwood	Dry	50	80% acetone	2.1 [b]
			100		3.4 [b]
			150		0.6 [b]
			200		3.5 [b]
					(tot=9.6%)
Chang *et al.* (1975)	Spruce, softwood	Toluene	48	96% dioxane	~4.6 [c]
		(20 g/4 l pot)			
Salud and Faix (1980)	*Shorea,* hardwood	Dry	100	80% acetone	5.8 [b,c]
		(50 g/500 ml)	200		0.9 [b,c]
			300		0.2 [b,c]
					(tot=6.9%)
Glasser and Barnett (1979)	Douglas fir, softwood	Dry	312	90% dioxane	9.2
Torr (1993)	Radiata pine, softwood	Dry	96	80% acetone	1.6
		(50 g/500 ml)			

a % purified lignin of wood
b Yield of each successive extraction
c Estimated from % Klason lignin

Bland and Menshun (1967) conducted a study on the effect of charge size (with a 5 hour mill time). They found that the smaller the charge, the higher the percentage of extracted solids, but indicated that at some point the extra effort expended would not be worth the gain in yield (Table 5.2). In addition, these workers compared the extraction efficiencies of dioxane and acetone. The method used was dry milling for 4 days with 25 g charge of wood and a 2-day extraction with the lignin solvent. The results are shown in Table 5.3.

Table 5.2. The effect of charge size on MWL yield (Bland and Menshun, 1967)

Charge size (g)	Solids (g) [1]	Yield (%) [2]
150	2.08	1.4
100	1.94	1.9
50	1.68	3.4
25	1.65	6.6

[1] Amount dissolved in 80% acetone
[2] "Yield" at this stage (of wood)

Dioxane was a slightly more efficient solvent for lignin, but tended to also solubilise significant amounts of carbohydrates as well. It is also quite toxic. Acetone was not quite as efficient a solvent for lignin, but has advantages over dioxane of being more user-friendly and more selective.

Table 5.3. Comparison of dioxane and acetone as lignin solvents (Bland and Menshun, 1967)

Solvent	Total solids (%)[1]	MWL recovered (%)[2]
Dioxane	13.6	3.5
Acetone	9.9	2.7

[1] Solids after the lignin extraction with the chosen solvent (yield of wood)
[2] After full purification (yield of wood)

The MWL method is normally carried out on a relatively small scale: 50 g (or much less) in a 500 ml capacity ball pot (Chang *et al.,* 1975; Salud and Faix, 1980; Björkman, 1956). However, a much greater quantity of purified lignin

was originally wanted (approximately 10 g MWL) for this study, so a larger scale of 300 g in 3.5 L ball pots was attempted (and failed). Therefore, the amount used in the kinetic experiments was lowered from 300 mg to 50 mg per duplicate, so that the required number of experiments with MWL could still be conducted with the time constraints present.

Detailed experimental information on the MWL isolation method used is described in Chapter 2, section 2.5.1. In summary, the method used in this study for each batch was milling about 50 g of ground wood in a 1 L pot for 4 days before extracting in 80% acetone for another 2 days. The crude MWL was then purified by dissolution in acetic acid, and precipitated into water. After freeze-drying, this product was dissolved into 2/1 dichloromethane/ ethanol, filtered and precipitated into ether before being finally dissolved into petroleum ether and film evaporated to dryness.

The MWL in this study was found to have very low carbohydrate contamination, low acid soluble lignin and was very close in C9 formulae to that in literature (see section 5.2.2.).

5.1.3. Alkali and bagasse lignin

The acetylation of an alkali lignin (from mixed softwoods) and a bagasse lignin were examined in the same way as MWL. It was considered that the chemical differences in these lignin preparations might be reflected in their acetylation behaviour. The purification method used for the alkali lignin is given in Chapter 2, section 2.5.2, and the commercial method used to isolate the bagasse lignin, which was used unpurified, is given in section 2.5.3.

The alkali lignin (AL) was obtained commercially from Aldrich. It was isolated from the kraft pulping of softwoods. The AL (as supplied) had a relatively high ash content, so it was purified by a mineral acid method. It was found that the purified AL lignin had sulphur present (1.7%, for full analysis see section 5.2.2.), but this was not expected to interfere in the overall acetylation reaction.

It was expected that such an alkali lignin would differ considerably from MWL (even if extracted from the same wood species). The AL was expected to have less β–aryl ether linkages and more condensed structures. A brief analysis of the ^{13}C NMR spectra of the fully acetylated lignins indicated that, for AL, the proportion of the primary hydroxyl (γ-OH) groups had more than halved, the number of secondary hydroxyl (α-OH) groups were reduced, and the number of phenolic OH groups had risen dramatically, compared to those in the fully acetylated MWL (Table 5.4).

Table 5.4 Relative amount of hydroxyl groups, measured as acetate in ^{13}C NMR spectra of fully acetylated lignins

Sample	Peak area [1] (%)			Total hydroxyl
	1°-OH	2°-OH	Ph-OH	(1° + 2° + Ph)
MWL	0.47 (56)	0.21 (25)	0.16 (19)	0.84
AL	0.29 (22)	0.20 (15)	0.81 (62)	1.3
BL	0.41 (38)	0.25 (23)	0.42 (39)	1.08

[1] As measured by the equivalent acetate groups per methoxyl (at 56 ppm, set to 1.0), between 168-171 ppm

Kringstad and Mörck (1983) showed, using ^{13}C NMR spectroscopy, that there had been specific changes to the lignin structure of spruce during the kraft pulping process: cleavage of the phenolic cyclic and non-cyclic benzyl-aryl ether bonds, cleavage of phenolic and non-phenolic β–aryl ether bonds, elimination of the terminal hydroxymethyl groups and cleavage of methyl-aryl ether bond, as well as condensation reactions between various entities. The longer that the kraft pulping process continued, the more β–aryl ether cleavages there were, and the more condensed structures formed. For the latter, the most common were the formation of C5 of a guaiacyl unit to various aliphatic chains, such as C5-CH=CH, C5-CH, C5-CH_2, C5-CHOH. There were also smaller increases in methyl bridges (or chains) such as C5-CH_2-C5, early in the kraft cook, and C5-CH_2-CH_2-CH_2OH, later in the kraft cook, where C5 is the fifth carbon in an aromatic ring (C3 - position of OMe in guaiacyl units). From comparing the NMR spectra (Kringstad and Mörck, 1983), the most prominent changes were the reduction of the γ-CH_2OH groups

(60.7 ppm) and the increase in the C5-aliphatic chains (116 ppm).

Other workers report a decrease in methoxyl content of lignin during alkaline/kraft pulping process (Bist and Bhandari, 1986), but this was not apparent in the work of Kringstad and Mörck (1983).

Himmel *et al.* (1990) found that the molecular weights (M_w and M_n) of alkaline-extracted (AE) lignins were lower than those of ball-milled (BM) lignin (aspen). For example, the BM lignin had M_w values of between 10000-12000, and M_n values of between 2800-3100; whereas a range of AE lignins gave comparative values of M_w = 3700-6300 and M_n = 1100-1400. This contrasted a little to the AL used in this study which had values of M_w = 14,200 and M_n = 1750 respectively (Aldrich, 2001). Glasser *et al.* (1993) reported molecular weight of a number of lignin types, including the same Aldrich product as used here ("Curan"), other kraft lignins and various bagasse lignins. They found that the molecular weights of softwood kraft lignins ranged from M_n 1700-2200 and M_w 3700-19,800 in value, giving a range of M_w/M_n or polydispersity of 2.9-9.0.

Bagasse is the stem of sugarcane after the sugar has been extracted. It is a member of the grass family. Therefore, bagasse lignin contains syringyl phenyl propane(S) units and *p*-hydroxyphenyl propane (H) units, as well as the guaiacyl phenyl propane (G) units present in the softwood alkali and milled wood lignins (Fernandez *et al.*,1990). Hardwoods also contain S units. Lignins are usually classified as G-, GS- or GSH-lignins depending on the wood or grass they are derived from. However, wood is highly variable and different parts of the wood, for example, compression wood or bark, can have different GSH ratios than the sapwood. (Fengel and Wegener, 1989). Faix (1991) reported that classification from IR spectral data gave the classification for a G-lignin of G = 85-100%, S = 0-5% and H = 0-15%, with OMe/C900 of 85-107, and for a GSH lignin of G = 35-55%, S = 5-45% and H = 20-40%, with 80-110 of OMe/C900.

The bagasse lignin (BL) used in this study had a G:S:H ratio of 1.0:0.91:0.66, and was isolated by an organosolv method without any further isolation,

treatment or purification. The BL used here was similar to a Brauns native lignin (BNL) isolated from bagasse by de Stevens and Nord (1953), which had a G:S:H ratio of 1.0 : 0.73 : 0.53. Other workers reported that the G:S:H ratio of bagasse lignin is generally about 1.0 : 1.5 : 1.1 (de Groote *et al.,* 1992). So for lignin preparations from bagasse, there is significant variation in G:S:H ratios and this seems to be dependant on extraction method to some extent. However, all these reported GSH ratios were within the range of figures given by Faix (1991).

Fernandez *et al.* (1990) reported that in addition to G, S and H units, ^{13}C NMR showed the presence in milled BL of p-coumaric acid, linked to lignin though ester bonds. Kajihara *et al.* (1993) reported the presence of p-coumaric acid from the acidolysis of milled BL of 6.5%. However, it appears that sometimes the p-coumaric acid groups can be erroneously measured as H units, which inflates their relative amount. Lapierre and Monties (1989) found that, with thioacidolysis the H units were usually less than 5% in the grasses measured, except for rice which had 8-15% H units. This observation cannot be made with analysis techniques that use oxidative methods, which cleave the C9 (C6-C3) units between the $C\alpha$ and $C\beta$, as this would degrade p-coumaric acid to the same C6-C1 compounds as the H units (Lapierre and Monties, 1989).

So it appears that the higher H ratios reported (de Stevens and Nord, 1953; de Groote *et al.*, 1992; Faix, 1991) may have been over-estimated due to the presence of p-coumaric acid. For example, the percent of H units range from 23% (de Stevens and Nord, 1953) to 30% (de Groote *et al.,* 1992), so these values may be a factor of 2-6 too high.

The bagasse (depithed and extracted) of Chen *et al.* (1998) had 22.4% Klason lignin, with 1.7% acid soluble lignin (ASL). The yield for the bagasse lignin (BL) used in this study of 12% would have meant that, based on the Chen *et al.* (1998) figures, just over half the lignin was extracted for this BL.

5.2. Characterisation of lignins

The information in this section describes, spectroscopically or chemically, the lignin samples that were used in the kinetic studies. The techniques used to examine the samples were wet chemistry techniques that included monosaccharide and lignin analysis, elemental analysis, and Fourier Transform Infrared spectroscopy (FTIR). Details of the analytical and spectroscopic techniques are given in Chapter 2.

5.2.1. Monosaccharide and lignin analyses

The results shown in Table 5.5 indicate that contamination of the lignin samples with carbohydrates was low (<1.0% in total) for the alkali lignin, moderate for the bagasse lignin (<2.0% in total) and extremely low (below detection limits of analysis) for the MWL sample.

Table 5.5. Total analysis of lignin samples (%)

Sample	Klason lignin	Acid soluble lignin	Ash	Ara	Xyl
Alkali lignin	94.3	2.58	2.27	0.36	0.36
MWL	90.8	1.4	--	BDL	BDL
Bagasse lignin	94.4	3.32	1.05	0.30	1.37

Note: All values in %. Gal, Glu and Mann were all below the detection limits (0.25%, 0.11% and 0.17% respectively). BDL = Below detection limit (0.2% for Ara and Xyl).

Total lignin contents were 96.88% (AL), and 97.72% (BL). For MWL, the total amount measured in the analysis was 92.2% which may mean that some material was lost during the analyses. The acid soluble lignin (ASL) for the MWL sample was lower than those for the AL or BL, which can probably be accounted for by the very different isolation method used and/or the type of lignin involved. Wegener and Fengel (1977) showed that MWLs from spruce have varying amounts of ASL depending on the extraction conditions, and that possibly dioxane extracted more ASL (compared to extraction with acetone as in this study), as the lowest level was 1.7% ASL.

5.2.2. Elemental analysis

The elemental analyses for the three lignin preparations are shown in Table 5.6, with samples analysed in duplicate. Both the alkali lignin samples (unpurified and purified) showed a significant level of sulphur, probably as thiol (SH) groups, as expected from the Kraft process it is derived from. Experimental details are given in Chapter 2 (section 2.7.5).

Table 5.6. Elemental analyses of lignin samples

Sample	Carbon (%)	Hydrogen (%)	OCH_3 (%)	H_2O	S (%)
Alkali lignin (as supplied)	57.66	5.61	12.09	6.62	2.23
Alkali lignin (purified)	60.33	5.43	12.03	6.43	1.72
Bagasse lignin	62.65	5.38	13.13	4.91	
MWL (purified)	60.45	5.99	13.97	6.12	

Note: Nitrogen was also analysed, but was not detected (detection limit is 0.1%).

For the calculation of C_9 formulae, these results were averaged. These data were corrected for water content and then calculated to give the formulae:

MWL (purified): $C_9 H_{7.68} O_{2.57} OMe_{0.88}$
Alkali lignin (as supplied): $C_9 H_{7.48} O_{3.14} OMe_{0.80} S_{0.14}$
Alkali lignin (purified): $C_9 H_{6.81} O_{2.71} OMe_{0.75} S_{0.10}$
Bagasse lignin: $C_9 H_{6.62} O_{2.45} OMe_{0.79}$

MWL had the highest OMe content of the three lignin preparations, which was probably due to the more mild method of isolation as well as wood source. The OMe of the AL (purified) was the lowest indicating that some demethoxylation has taken place during the kraft pulping process. Bagasse lignins contained, as discussed earlier, G, S and H units, where G contains one OMe, S contains two OMe, and H no OMe per aromatic group.

Table 5.7 gives comparison of C9 formulae of the lignin preparations in this study with ones from other workers. Faix *et al.* (1994) commented that technical lignins have shortened alkyl side chains and are partly

demethoxylated. The formulae in Table 5.7 do not correct for any polysaccharides present, so they represent a total picture rather than that just for the lignin moieties.

Table 5.7. Comparison of C9 formulae with literature values

Lignin sample	Reference	C_9 formula
Alkali lignin (purified, softwoods)	This study	$C_9 H_{6.81} O_{2.71} OMe_{0.80} S_{0.10}$
Kraft lignin, Indulin™ (mixed softwoods)	Faix *et al.*, 1994	$C_9 H_{8.38} O_{2.34} OMe_{0.81}$ (excluding OH)
MWL (*Pinus radiata*)	This study	$C_9 H_{7.68} O_{2.57} OMe_{0.88}$
MWL (pine)	Horting *et al.*, 1991	$C_9 H_{8.50} O_{2.60} OMe_{1.00}$
MWL (juvenile pine)	Sarkanen *et al.*, 1967	$C_9 H_{8.67} O_{2.78} OMe_{0.89}$
Acetosolv (*P. pinaster*)[1]	Vázquez *et al.*, 1997	$C_9 H_{9.67} O_{2.96} OMe_{0.80}$
Bagasse Lignin (OrganoSolv)	This study	$C_9 H_{6.62} O_{2.45} OMe_{0.79}$
Bagasse lignin (Acetosolv)	de Groote *et al.*, 1992	$C_9 H_{8.04} O_{2.81} OMe_{0.92} (OH)_{0.73}$ where OH was phenolic
Bagasse lignin (Acid hydrolysis)	Faix *et al.*, 1994	$C_9 H_{8.34} O_{2.48} OMe_{0.56}$ excluding OH

[1] Sample contained 0.12 % N

The MWL in this study had a lower H content, similar O content and a similar or lower OMe content to those of Horting *et al.* (1991) and Sarkanen *et al.* (1967). The comparison for BL are shown mainly for interest as the extraction methods are very different. The BL used here had a much lower H content than either shown, which may indicate more unsaturation than for the other BLs. Note also the low OMe content of the acid hydrolysis BL of Faix *et al.* (1994).

5.2.3. FTIR spectra of lignin preparations

Figures 5.1-5.3 show the FTIR spectra of MWL, AL and BL respectively. The assignments are shown in Table 5.8. Assignments were generally in agree-

ment with those of Faix (1991), Pan and Sano (1999) and Schultz and Glasser (1986). The FTIR spectra of the three lignin preparations used in this study all show large broad OH bands (3350-3460 cm^{-1}), characteristic lignin bands (1599- 1605 cm^{-1}, 1510-1514 cm^{-1}), with a variety of differences for the rest of the spectrum. In FTIR, even small differences in spectra indicate important chemical differences in the samples (Faix and Beinhoff, 1988).

The spectra most alike were the MWL and AL, both being from softwood origin. However, there were small but significant differences between the spectra of MWL and AL. In the MWL spectrum, the peak at 1219 cm^{-1} was much weaker than in the AL spectrum, where it was similar in strength to the peak at 1269 cm^{-1}. In addition, the peaks at 1140 cm^{-1} and 1032 cm^{-1} were both stronger in the MWL spectrum than they were in the AL spectrum, which may mean that there were more guaiacyl units present in MWL than in AL. In fact, the peak at 1140 cm^{-1} is typical only for G-lignins (Faix, 1991).

Figure 5.1. FTIR spectrum of milled wood lignin (MWL)

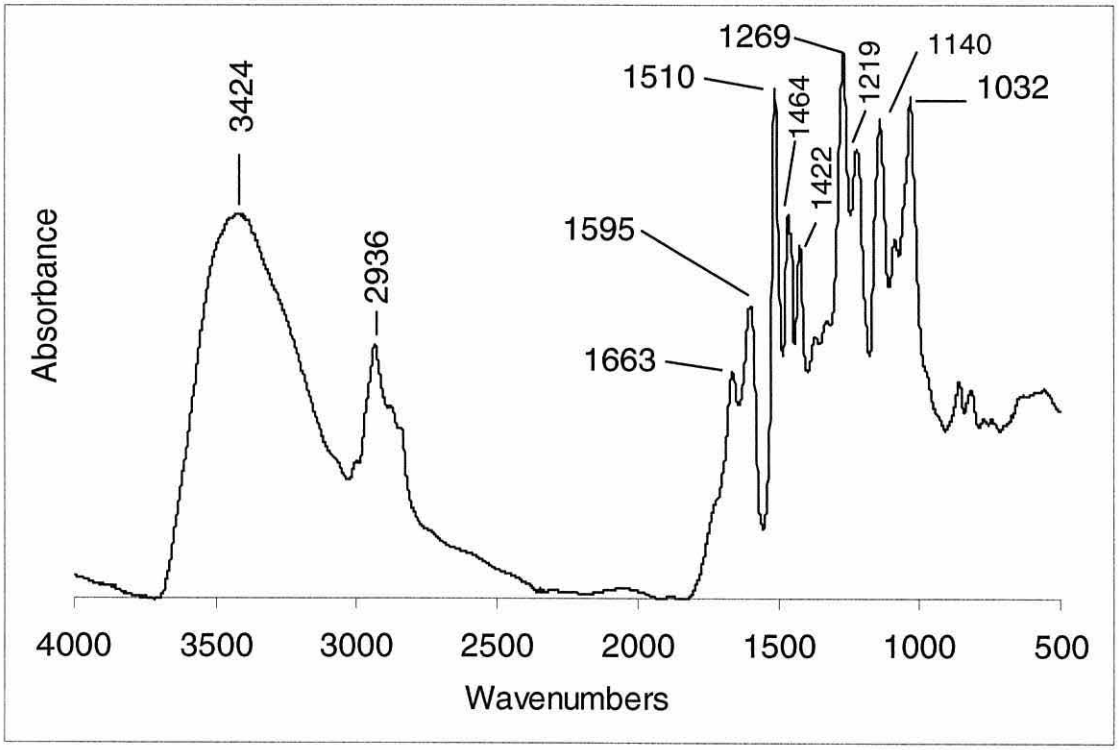

Figure 5.2. FTIR spectrum of alkali lignin, purified (AL)

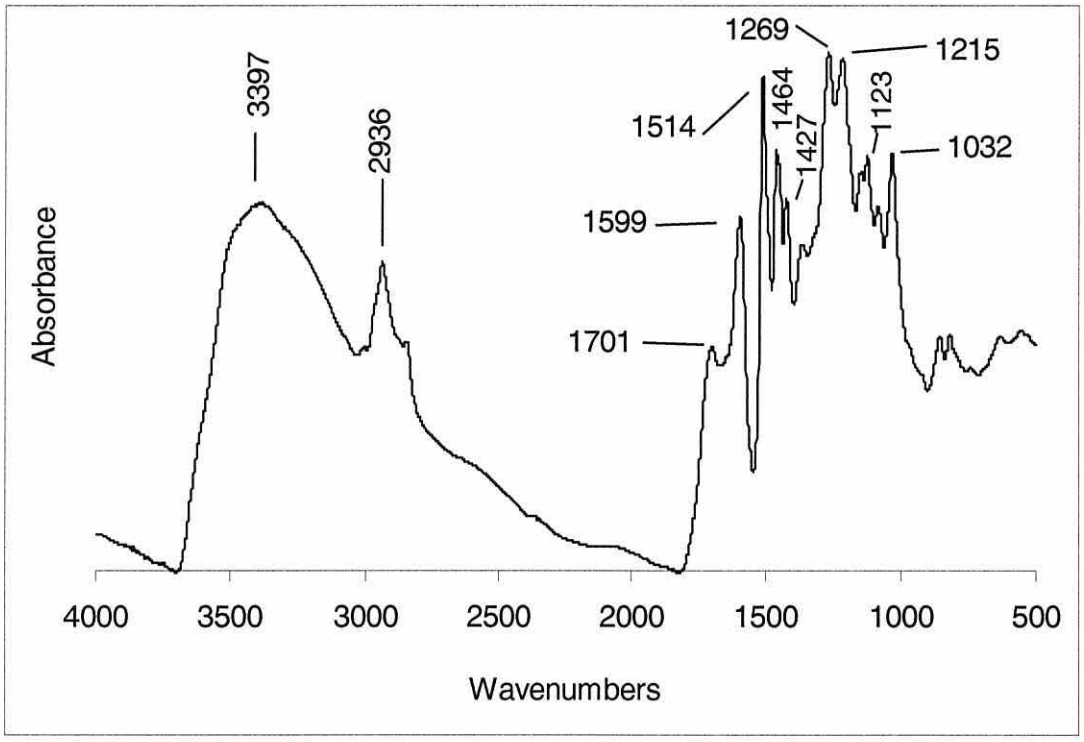

Figure 5.3. FTIR spectrum of bagasse lignin (BL)

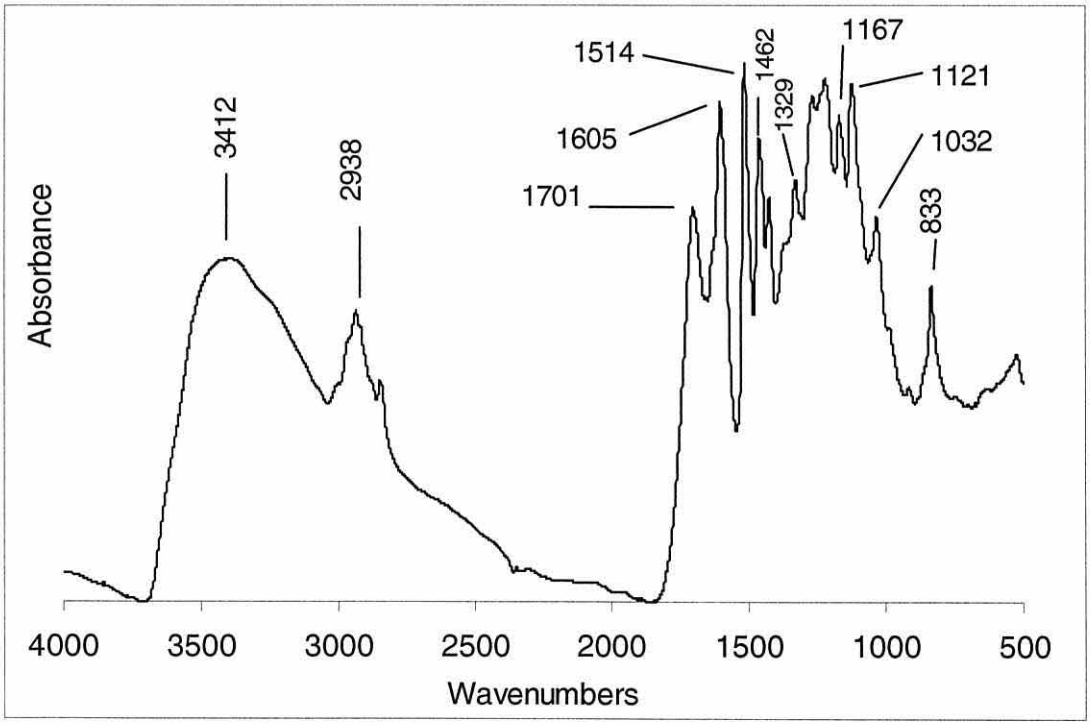

Faix (1991) notes that a few percent of S units is enough to change the absorption maximum from 1140 cm^{-1} to something below 1128 cm^{-1}, although a shift for this reason seems unlikely for the AL, due to its lower OMe content. However, the dominant bands of 1510-14 cm^{-1} and 1269 cm^{-1} were the same for both MWL and AL, which is typical for G-lignins (Faix, 1991).

The BL spectrum has a peak at 1167 cm^{-1}, typical of GSH lignins (Faix, 1991), which is absent in the MWL spectrum. There was also one well resolved peak at 833 cm^{-1} in the BL spectrum, compared to two smaller peaks in this region in the MWL spectrum.

Table 5.8. Assignments of FTIR peaks in lignin

Assignment (cm^{-1})	MWL	AL	BL
3350-3460, ν_{O-H}, bonded	3424	3397	3412
2842-3000, ν_{C-H}, CH_2/CH_3	2936	2936	2938
1740-05, $\nu_{C=O}$, unconjugated			
1715-1655, $\nu_{C=O}$, conjugated	1663	1701	1701
~1600, $\nu_{C=C}$ (aromatic)	1595	1599	1605
1510-15, $\nu_{C=C}$ (aromatic), characteristic of lignin	1510	1514	1514
1460-70, δ_{C-H}, CH_2/CH_3	1464	1464	1462
1422-30, δ_{C-H} (aromatic)	1422	1427	1425
1325-30, condensed S, G rings			1329
1266-70, G ring, $\nu_{C=O}$	1269	1269	sh
1215-30, ν_{C-C}, ν_{C-O}, $\nu_{C=O}$	1219	1215	1219
1166 $\nu_{C=O}$, typical for GSH			1167
1140, δ_{C-H} (aromatic), G units	1140	sh	
1120-28, $\nu_{C=O}$, δ_{O-H} (2^o-OH)		1123	1121
1030-35, δ_{C-H} (aromatic), δ_{O-H} (1^o-OH), $\nu_{C=O}$	1032	1032	1032
817-58, δ_{C-H} (aromatic), G or S	sm	sm	833

Key: sh shoulder present
sm small unpicked peak present

5.2.4. Nuclear magnetic resonance spectroscopy

Each lignin sample was examined by ^{13}C NMR in order to characterise the different lignin preparations and to compare them. The spectra are shown in Figures 5.4-5.6 for milled wood lignin (MWL), alkali lignin (AL) and bagasse lignin (BL) respectively. Assignments of the main peaks are shown in Table 5.9.The spectrum of the fully acetylated MWL is also shown as an example (Figure 5.7), along with the areas used for integration.

The spectrum of the MWL (Figure 5.4) was broadly similar to that of a spruce lignin (Robert, 1992). The spectrum of the AL (Figure 5.5) differed significantly as would be expected to that of the MWL, although contained peaks of a similar assignment, with differing intensities. The spectrum of the BL (from an organosolv extraction method, Figure 5.6) had some features similar to a milled bagasse lignin of Fernandez *et al.* (1990).

Figure 5.4. ^{13}C NMR spectrum of milled wood lignin

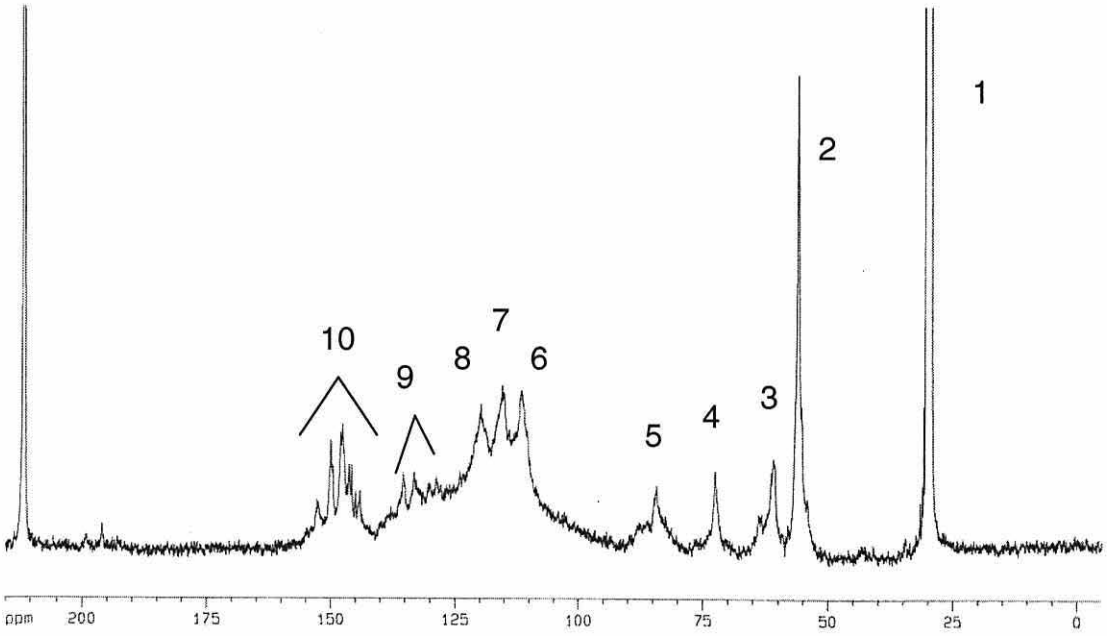

Figure 5.5. ^{13}C NMR spectrum of alkali lignin

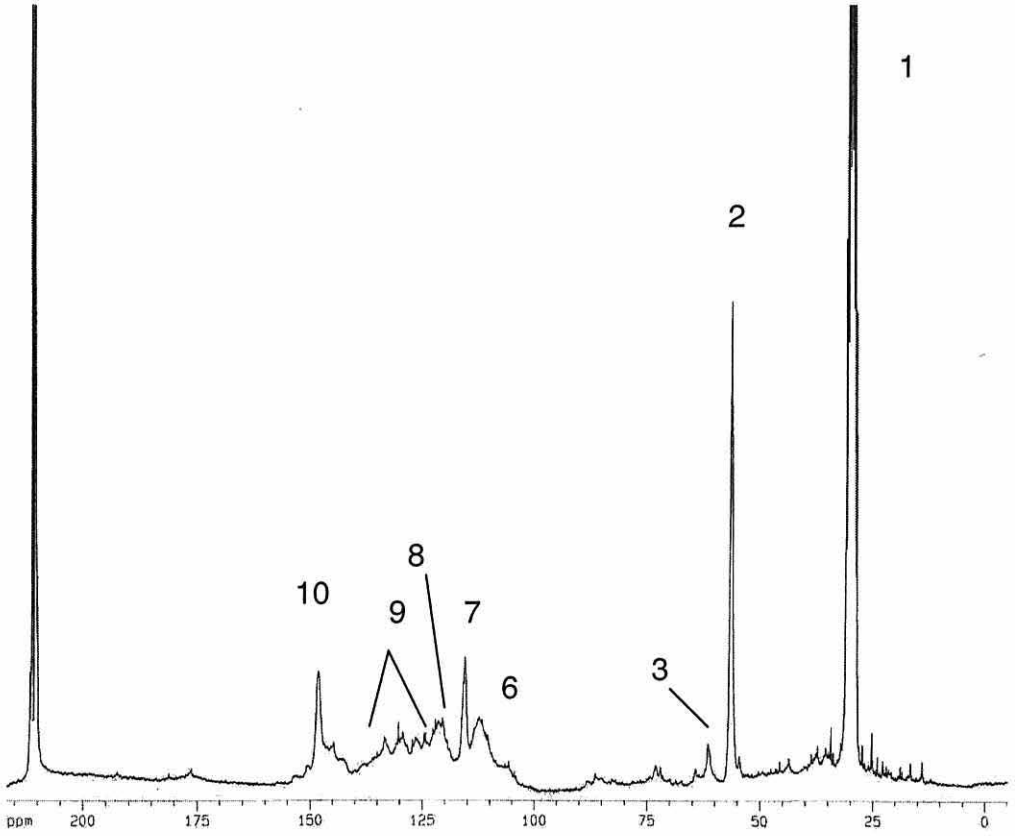

Figure 5.6. ^{13}C NMR spectrum of bagasse lignin

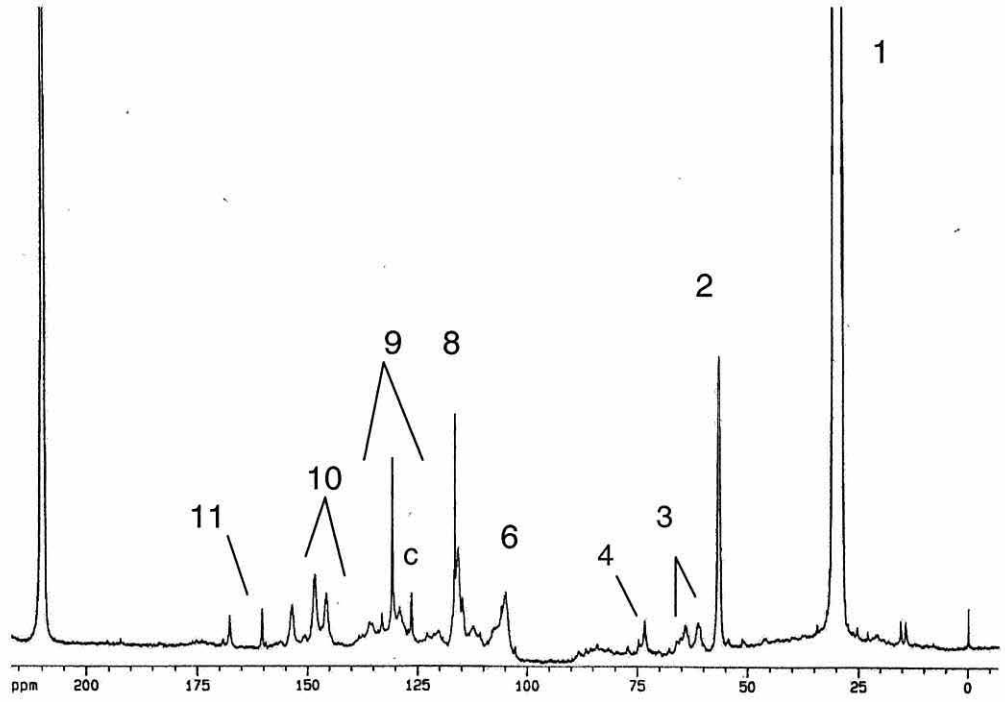

Table 5.9. Main peak assignments for the lignin ^{13}C NMR spectra

Assignment	MWL	AL	BL
1. Central acetone peak	29.8	29.8	29.8
2. Methoxyl	55.9	56.0	55.3
3. Aliphatic, Cγ	60.9, sh	61.7	59.6, 62.6
4. Aliphatic, Cα	72.6	sm	71.3[a]
5. Aliphatic, Cβ	84.2	sm	sm, br
6. Aromatic, C2	111.6	112.4	112.7
7. Aromatic, C5	115.5	115.2	
8. Aromatic, C6	119.8	117.7-127.6	122.5[b]
9. Aromatic, C1	133.2, 133.4	127.6-134.6	125-140,126.6[c]
10. Aromatic, C3, C4	144.1-152.7	shs, 147.9	141.4-155.2
11. Aromatic, C4[d]			162.3

[a] This could also be assigned to Cγ in a β-β unit (Robert, 1992)
[b] This could also be assigned to a C1 in an p-hydroxyphenyl (H) benzoate (Robert, 1992), or a C1 of a coumaric acid ester (Fernandez *et al.,* 1990)
[c] This could also be assigned to a Cβ in cinnamaldehyde (Robert, 1992)
[d] Assigned to C4 in coumaric acid ester

Figure 5.7. ^{13}C NMR spectrum of the fully acetylated milled wood lignin

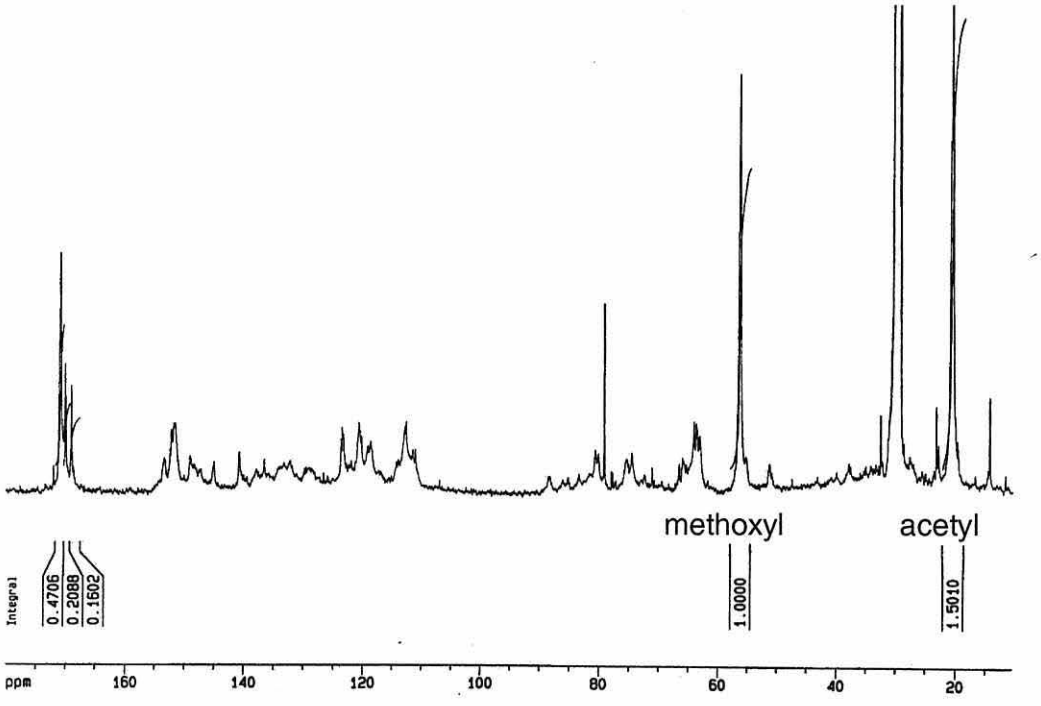

It is possible to estimate of the amount of hydroxyl in a lignin sample (MWL shown in Figure 5.7) with respect to methoxyl by making a ratio of the peak area at 21 ppm (acetyl) and 56 ppm (methoxyl). It appeared that the AL sample had the most OH groups present, significantly more than the MWL sample (Table 5.10).

Table 5.10. Total acetate levels in the fully acetylated lignin samples as estimated by ^{13}C NMR spectroscopy

Sample	Acetate per OMe[1]	OMe per C9 unit[2]	OH/C9[3]
Milled wood lignin	1.501	0.88	1.71
Alkali lignin	1.612	0.76	2.12
Bagasse lignin	1.465	0.79	1.85

[1] As measured by the ratio of acetate (21 ppm) and methoxyl (56 ppm) peak areas
[2] As measured by elemental analysis (section 5.2.2)
[3] Measured as acetate

5.3. Results

Reaction of the isolated three lignin preparations with acetic anhydride was carried out at four temperatures (80, 90, 100 and 110 °C). The reason for changing these were the increased speed of the lignin reaction compared to that of the whole wood. However, these temperatures were in the same general range to that of the wood reaction (80-120 °C). One control experiment was conducted on MWL or AL at 110 °C for 60 minutes, with acetic acid instead of acetic anhydride. This was to ascertain whether acetylation of lignin occurred with acetic acid under these conditions. NMR spectra (not shown) determined that no or very little reaction occurred.

5.3.1. Reaction profiles

Reaction profiles for milled wood lignin, alkali lignin and bagasse lignin (Figures 5.8-5.10 respectively) have been given in weight percent gain (WPG). The data were fitted using a simple exponential function in the form,

$y = a.\ (1 - b^x)$, where a was the asymptote, b was the degree of curvature, and x was the reaction time. The initial rate constant (k_o) was calculated as the derivative of the exponential equation at 10% of the asymptote for each curve, as well as the alternative initial rate method, using the first two reaction data points and zero. Degree of fit (coefficient of variance, CV%) and other raw data are given in Appendix R.

In all reaction profile plots, fitted curves are as follows:
80 °C ——— 90 °C -—-—- 100 °C - - - - - - 110 °C ———

It seems that alkali lignin (AL, Figure 5.9) reacted to a slightly greater extent than did the milled wood lignin (MWL, Figure 5.8), and a much greater extent than did the bagasse lignin (BL, Figure 5.10). The AL had the highest OH content, but the MWL had the lowest estimated OH content per C9 unit (Table 5.10).

This may indicate that the much higher phenolic content of the AL (Table 5.4) gives a faster overall reaction. Paulsson and others (1995) found that the presence of a phenolic OH in a lignin model increased the reactivity of the primary and secondary OH groups towards acetylation. It also may be that, despite the appearance from the exponential asymptote that the reaction has reached completion, the OH groups (eg α-OH) which might be slower to react, may not have fully reacted after 60 minutes at 120 °C. In fact, when the total level of reaction was measured from the fully acetylated AL, total reaction was around 36 WPG. Note that extra reactions and investigations were conducted on AL rather than MWL, solely because of the lack of MWL.

The rate of the reaction for all the lignin samples was much faster than for that of wood, as expected. Despite the variability of individual points, all the lignin samples gave meaningful reaction profiles for each temperature. For the MWL reaction at 80 °C, it appears as though there could be an initial lag phase, which may be demonstrating the effect of a lower phenolic content.

Figure 5.8. Reaction of milled wood lignin (MWL)

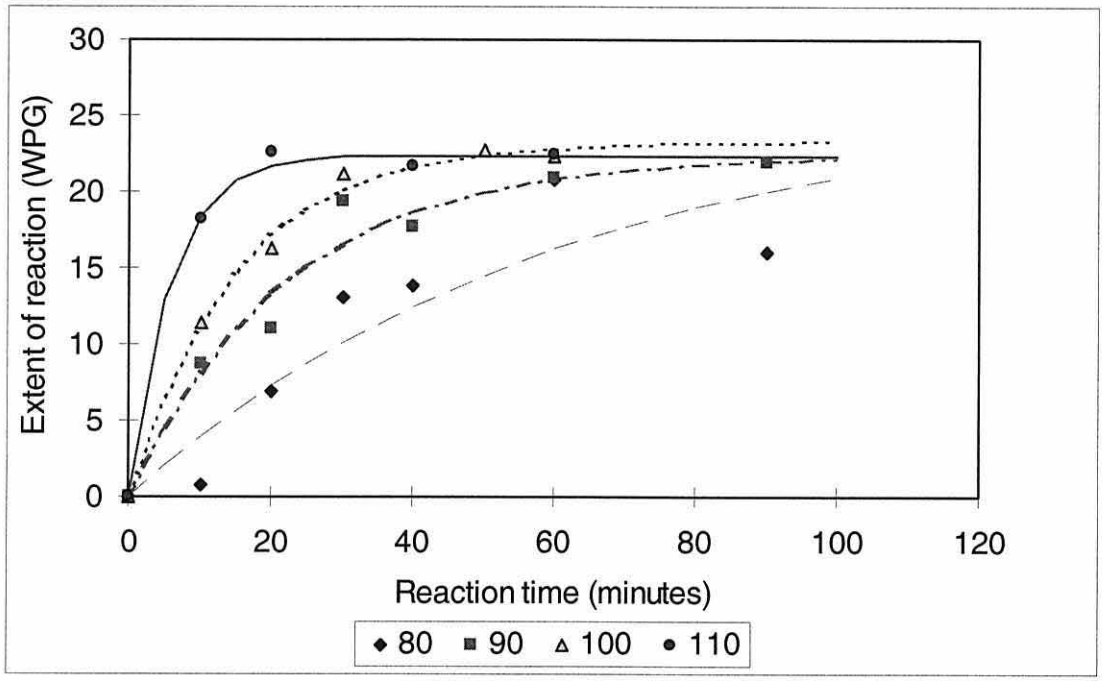

Figure 5.9. Reaction of alkali lignin (AL)

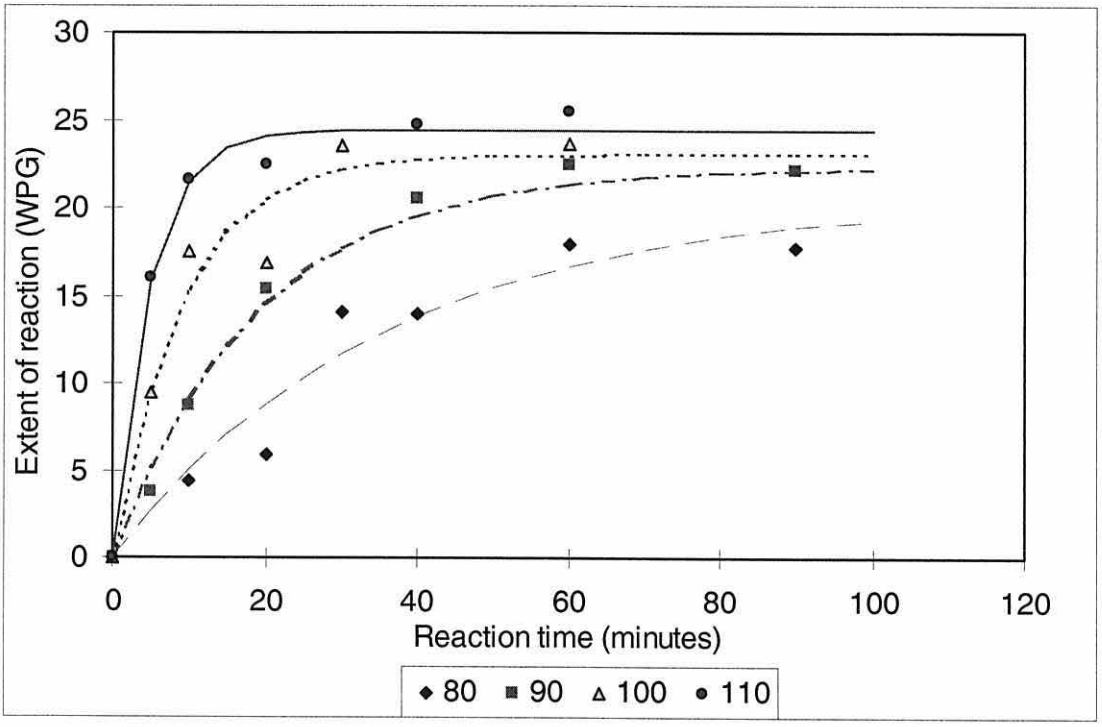

Figure 5.10. Reaction of bagasse lignin (BL)

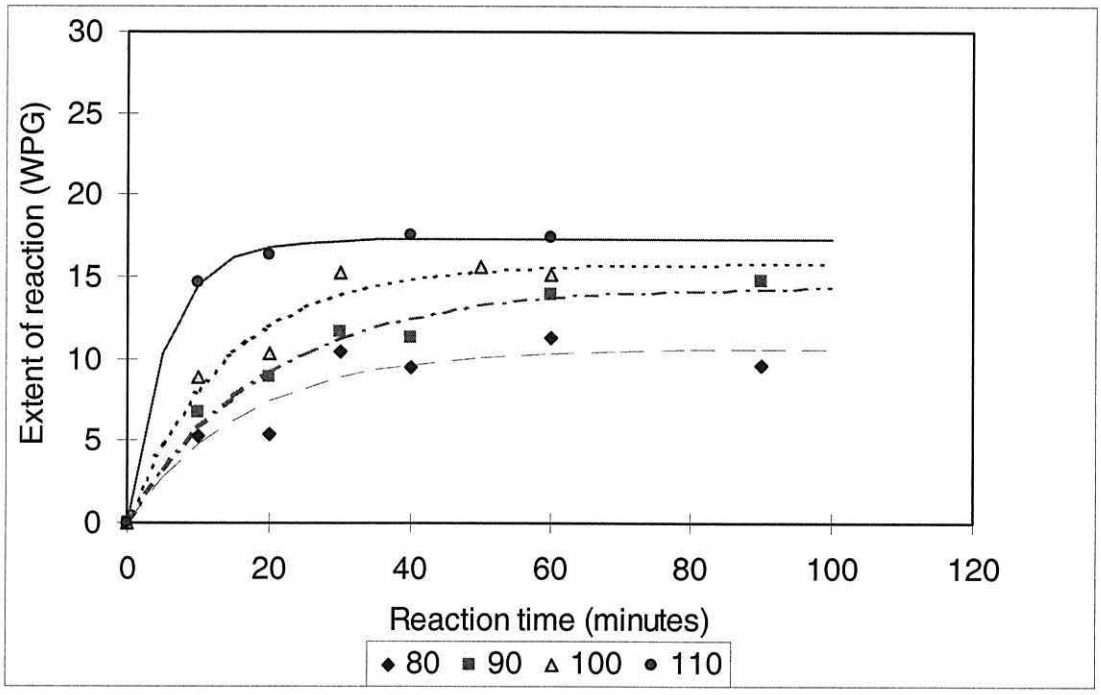

5.3.2. Kinetic data

The kinetic data were calculated using the initial rate method. The activation energy values obtained for the lignin samples are shown in Table 5.11, along with the CV% for the fitted curves that generated the k_o values used (or r^2 values for the alternate method). Raw data for the calculation of these initial rate constants are shown in Appendix S.

The Ea values were the same for AL and MWL, for the exponential methods. For these samples, the Ea values calculated using the exponential method are probably the more reliable. The problem with the k_o values derived for the alternate method (marked Z in Table 5.11) was that there were only three points for the linear regression, and some did not fit a straight line well. This could have been due the lack of reliable data at short reaction times due to the speed of the lignin reaction.

The Ea values for BL seemed to be significantly lower, although the BL data did not fit the Arrhenius equation very well (for the exponential method). Note that although BL had a lower Ea value, it also reacted to a lesser extent in the same conditions than did either MWL or AL. In addition, the k_o values (for the

all methods) were generally lower for BL than for those of either MWL or AL, with the exception of reaction at 80 °C.

Table 5.11. Kinetic data for lignin samples

Sample	Method [a]	Ea (std err) [b]	r^2	P [c]
Alkali lignin	E1	80.31 (1.82)	0.999	0.001
	E2	82.42 (1.71)	0.999	0.001
	Z	75.43 (14.23)	0.934	0.05
MWL	E	79.50 (7.71)	0.982	0.01
	Z	44.26 (1.82)	0.997	0.01
Bagasse	E	58.43 (16.61)	0.861	0.1
lignin	Z	38.63 (5.13)	0.966	0.02

[a] Method is the manner in which the k_o values were calculated. E1 or E used slope at 10% of the exponential asymptote. E2 used the same with extra reaction times for the AL sample only, and Z used the linear regression of the first two data points and zero.

[b] Activation energy (Ea) and standard error are in kJ/mol

[c] Levels of significance of Pearson's correlation coefficient on |r|, with n=4

The fact that slower initial rate of a reaction (or a lower extent of reaction) does not necessarily correspond to a higher activation energy was illustrated again with the lignin samples, where BL had a lower extent of reaction (and generally lower k_o values), but the lowest Ea value.

Activation energy is a measure of the energy barrier to reaction, or the reactivity of the hydroxyl groups themselves. Therefore, the Ea value for a reaction is not necessarily related to the absolute values of the k_o values, but rather the temperature dependence, thereof.

The Arrhenius plot (for the Ea values derived using the exponential method) for MWL is shown in Figure 5.11, as an example.

Figure 5.11. The Arrhenius plot for milled wood lignin (MWL)

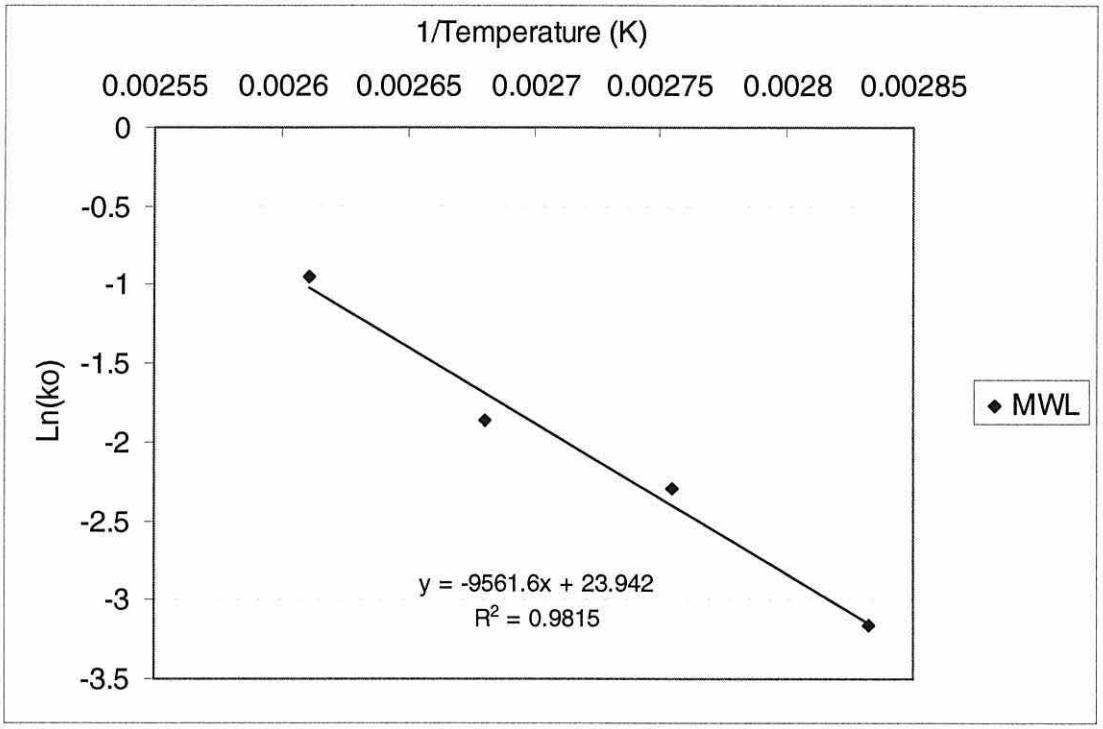

5.4. Discussion

The results of the lignin reaction and kinetic data obtained are compared with the solid wood reaction, the possibility of using isolated lignin to predict the wood reaction is discussed, and the pros and cons of using an alkali lignin versus a milled wood lignin in studying wood lignin are examined.

5.4.1. Comparison of lignin with wood reaction

A comparison between the wood and 29% of the lignin reaction are shown in Figures 5.12-5.14. The data of the two substrates (wood, MWL) seemed to lie on the same basic curve, at least initially. When the activation energy values obtained are compared, a different story is told: the Ea value for MWL is around 80 kJ/mol, whereas it is around 34 kJ/mol for solid wood (which is relatively high for a diffusion control reaction). This could be due to the fact that wood reacted while in the solid state was significantly diffusion controlled, whereas the lignin sample dissolved in the reaction solution and thus reacted as a liquid, and was not diffusion controlled but more likely activation controlled; that is, controlled by first order kinetics (Pilling, 1975).

Figure 5.12. Reaction at 80 °C: Comparison of wood with lignin

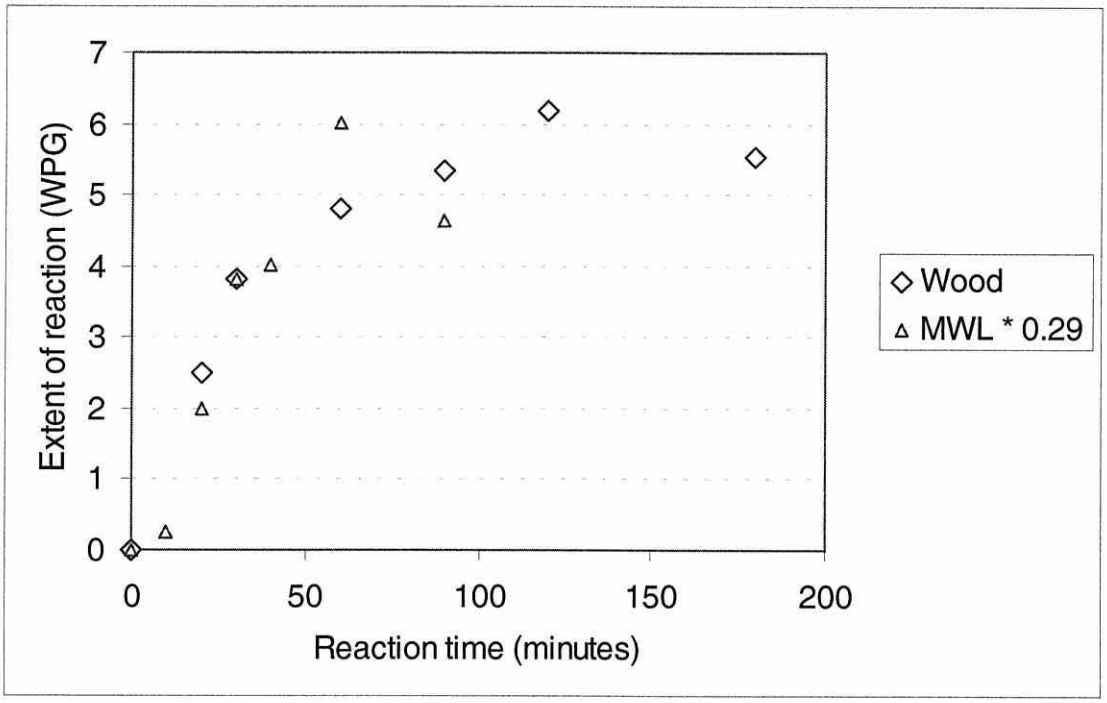

Figure 5.13. Reaction at 100 °C: Comparison of wood with lignin

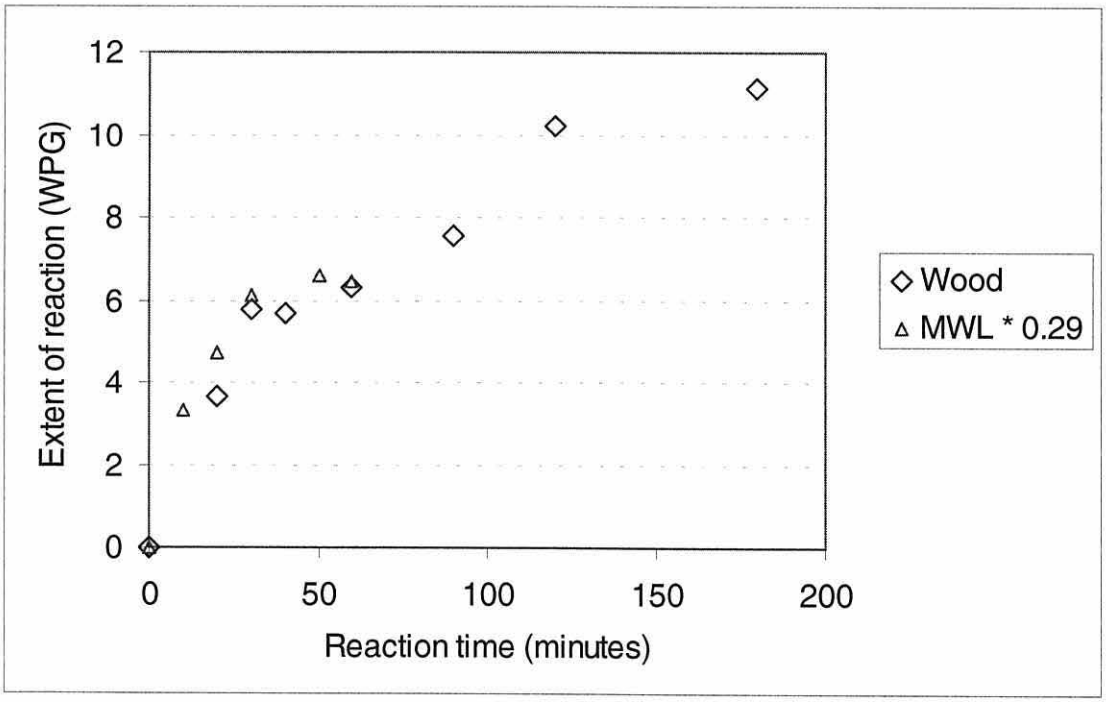

Figure 5.14. Reaction at 110 °C: Comparison of wood with lignin

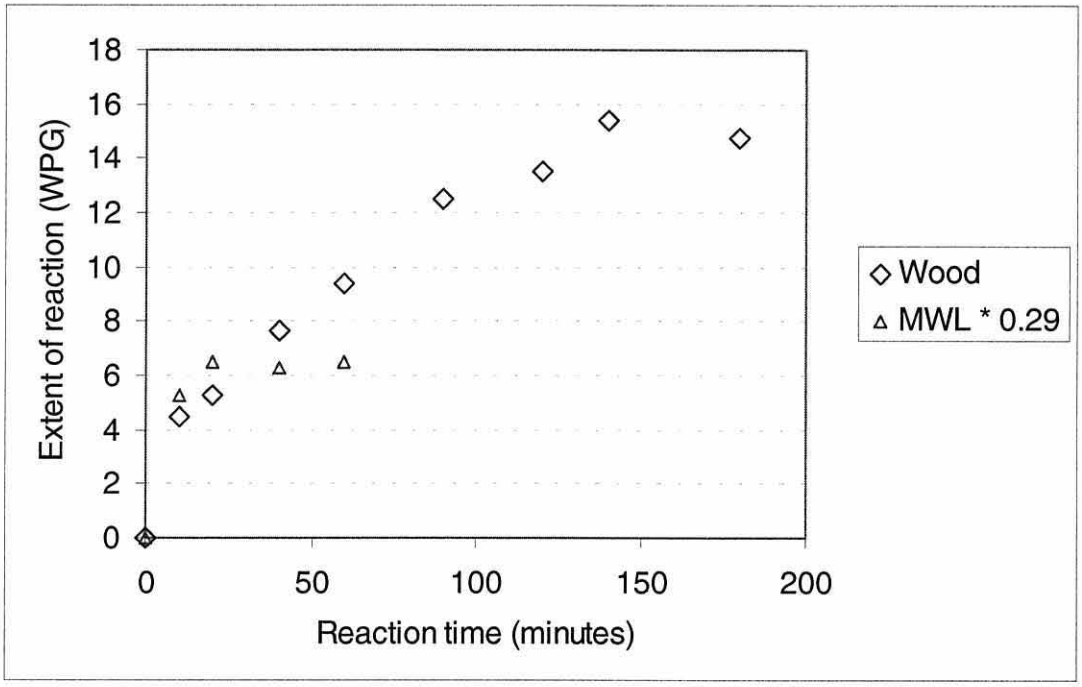

For reaction at 80 °C (Figure 5.12), one can see that 29% of the reaction of MWL was at a very similar level to that of the wood reaction, implying that the wood reaction at this temperature is dominated by the lignin reaction. For the reaction at 100 °C (Figure 5.13), the MWL reaction was also at a similar level to that of the wood reaction.

For reaction at 110 °C (Figure 5.14), acetylation of MWL was initially higher, then lower that of the wood reaction, and the lignin's reaction profile was a different shape to that of wood. This implied that initially that not all the lignin within the wood had reacted in the initial phase of the reaction, which might allow the possibility of the swelling of the wood cell wall making more lignin-OH available for reaction.

The wood structure that native lignin is part of would have a significant influence on the reactivity of the lignin *in situ*, as has been demonstrated by the diffusion control of the wood reaction. However, when the diffusion control test was applied to the lignin reaction, it showed that there was not a very good fit for MWL (for details, see Appendix T). The fit was only good for one temperature for the MWL reaction. This implies that the reaction of isolated

lignin (MWL) was activation controlled and thus dominated by first order kinetics. It is possible that the reaction is of a complex type with the different types of hydroxyl reacting in different ways and at different rate, which would complicate the overall picture kinetically.

5.4.2. Use of isolated lignin to predict wood reactions of this type

As seen by the comparison of the wood reaction to that of lignin reaction in the previous section, there were some similarities in the reaction profiles between wood and lignin. This may be somewhat surprising given the difference in substrate (solid versus dissolving powder), reaction type (homogeneous versus heterogeneous), rate-determining step (diffusion versus activation of the reaction site; that is, first order kinetics), and observed activation energy (~34 kJ/mol versus ~80 kJ/mol). The lignin reaction within the wood was suggested as the dominant reaction, particularly in the wood reaction at the lower temperature studied (eg 80 °C).

However, the isolated lignin reaction does not explain much of what happens in the wood reaction. The hemicelluloses do react to a significant extent, especially at higher temperatures and longer reaction times. In addition, the wood structure is the more influential factor in determining the reactivity of wood, rather than the reactivity of its individual components and types of OH groups. This is illustrated in the diffusion control of the wood reaction versus the probable activation control of the lignin (MWL) reaction.

So in conclusion, it is possible to obtain an indication of the general shape of the reaction profile of the wood from an isolated lignin particularly at lower temperatures, but not to predict kinetic data or type of the wood reaction.

5.4.3. Use of alkali lignin versus MWL

One of the interesting outcomes of this work was the surprising similarity of the kinetic results from AL and MWL. Although both are from softwood sources, the AL was derived from a kraft pulping process and contained sulphur (as SH). However, it would be very useful to be able to use AL for

some work instead of MWL as AL was available cheaply commercially (or readily made) and MWL is very laborious to make even in a small amount.

The fit to the diffusion equation was reasonable for the AL reaction between 80-100 °C. This reasonable fit to the diffusion equation for the AL reaction could have been due to the higher proportion of Ph-OH, which reacts faster than the 2°-OH. This might make the diffusion of the anhydride to and/or from the reaction sites relatively slow compared to the activation of the OH group. Although, the AL reaction was faster than MWL and seemed to be at least a little diffusion controlled (at the lower temperatures), the Ea values obtained were very similar to that of MWL. It might be possible to derivatise some of the extra Ph-OH in the AL sample to examine how this affected the relative control of the reaction (diffusion versus activation).

The disadvantage of the commercial AL preparation is that it would not be from the specific species of interest, in this case radiata pine. However, it would relatively easy to prepare alkali lignin from the wood species of interest. In addition, for reactions not just involving the reaction of the hydroxyl groups this similarity would probably not hold true. For example, bond cleavage such as is involved in delignification reactions. Further, it seems from the results in this study, that the AL reaction with acetic anhydride was at least partly diffusion controlled, whereas the MWL studied was largely activation controlled. This difference did not seem to influence the activation energy obtained from the initial rate constants.

5.5. Relative rates of hydroxyl reaction in lignin

The relative rate of reaction of three types of hydroxyl groups was investigated for a lignin sample (MWL). Hydroxyl groups which are in different environments do not necessarily react in the same way or at the same rate. As lignin was shown to be dominant in the wood reaction, particularly in the initial stages, it was thought that further investigation of how the lignin hydroxyl groups reacted could be informative. In addition, it was thought to be

interesting to have a comparison of the relative rate of reaction of hydroxyl in lignin to that of the lignin model compound studied (Chapter 6).

Lignin has three major types of hydroxyl group, which are denoted primary (1°), secondary (2°) and phenolic (Ph) hydroxyl. The 1°-OH in lignin is generally attached to the γ-carbon of the aliphatic side chain on an aromatic unit. The 2°-OH is generally attached to the α-carbon, although can also be attached to the β-carbon if there is an α-carbon ether (or other) linkage to another aromatic group. The Ph-OH is generally attached to para position (to the aliphatic chain or C4 of the aromatic group) of an aromatic group and adjacent to any methoxyl group.

When lignin was reacted and the extent of reaction measured, the results were for all OH groups present, so any differences in individual OH reactivities were averaged. For the comparison, the extent of reaction for all 1°-, all 2°- and all Ph-OH groups were examined separately.

5.5.1. Experimental details

A sample of MWL was fully acetylated, with pyridine and acetic anhydride, to give a 100% standard for acetylation. The partially acetylated samples from the kinetic experiment were then compared with the fully acetylated sample, using ^{13}C NMR spectroscopy.

To obtain complete acetylation, about 200 mg of lignin was stirred in a 1:1 mixture (20 ml total) of pyridine and acetic anhydride for 18 hours at 60 °C. Toluene (50 ml) was added to the mixture and evaporated to almost to dryness under reduced pressure. This was repeated two more times to remove the pyridine. The acetylated lignin was then suspended in a 1:1 ethanol (abs): water (50 ml) and evaporated to dryness under reduced pressure, three times. The solid product was dissolved in a minimum amount of chloroform (~5 ml) and precipitated with diethyl ether (~10 ml). The final acetylated product was filtered using a Buchner funnel, and dried.

The methoxyl peak (56 ppm) was used as the internal standard, and the acetate peaks (169-171 ppm) were referenced to the corresponding methoxyl peak in each spectrum. Details of the NMR instrument and variables used are given in Chapter 2 (section 2.7.2). Specifically, the peak areas analysed were:

methoxyl (reference):	54.6 - 57.9 ppm
primary acetate (1°):	170.2(.8) - 171.7 (.2) ppm
secondary (2°):	169.2(.5) - 170.2(.8) ppm
phenolic (Ph):	167.2(.5) - 169.2(.5) ppm
total acetate (TA1):	18.7 - 22.2 ppm.

The three acetate peaks (1°, 2°, Ph) were close together and the regions were integrated manually, as there were slight changes in minima between the peaks from spectrum to spectrum. The individual acetate peaks (168-171 ppm) were the chemical shifts of the acetate carbon (C) in -O-C(=O)-**C**H_3, whereas the total acetate peak (TA1) was a direct measurement of the methyl carbon (**C**) of the acetate group.

5.5.2. Results

For lignin, it was only possible to obtain relative rates of reaction of hydroxyl groups from the ^{13}C NMR spectra, as individual OH regions in the ^{1}H NMR spectra were masked by larger peaks. Four partially acetylated MWL samples which covered the range of reaction levels obtained were examined.

It was obvious from Figure 5.15 that the secondary hydroxyl (2°-OH) reacted to a much lesser extent than either the primary OH (1°-OH) or the phenolic OH (Ph-OH) at each of the temperature/reaction time combinations. There were two possible ways to measure the total acetate present: by adding the individual acetate groups together, and by measuring the CH_3 of any acetate (at 20.6 ppm). This gave rise to Total Acetate 1 (TA1, measured directly) and Total Acetate 2 (TA2, addition of the individual acetates).

The data is also shown in Table 5.12, so that clearer comparisons can be made. The raw data are given in Appendix U. The relative rates of reaction between the primary (1°), secondary (2°), and phenolic (Ph) hydroxyl groups are given over:

MWL1 (80 °C, 10 mins; 0.8 WPG):	1^{o} > Ph > 2^{o}; TA1 > TA2
MWL2 (100 °C, 10 mins; 11.5 WPG):	Ph > 1^{o} >> 2^{o}; TA1 = TA2
MWL3 (80 °C, 40 mins; 14.6 WPG)):	Ph > 1^{o} >>2^{o} ; TA1 = TA2
MWL4 (100 °C, 40 mins; 23.7 WPG):	1^{o} > Ph >> 2^{o}; TA1 < TA2

Figure 5.15. Comparison of relative rates of reaction from ^{13}C NMR of partially acetylated milled wood lignin.

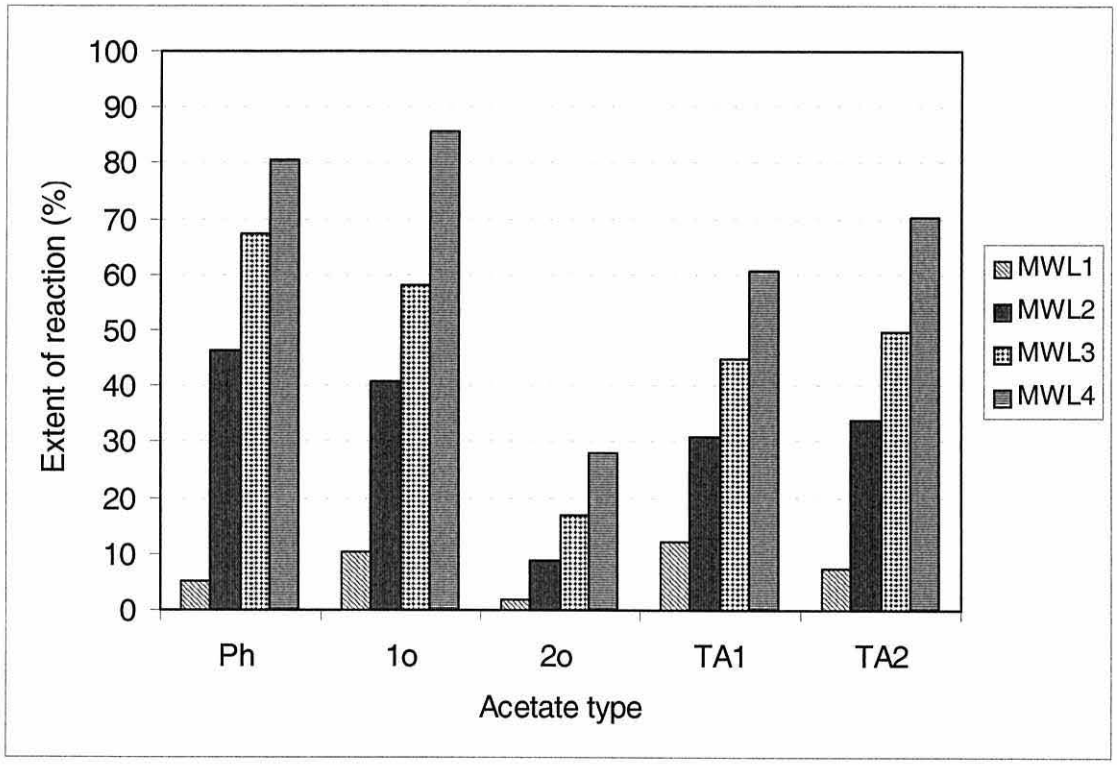

Key: Ph = Phenolic acetate,
1o = Primary acetate,
2o = Secondary acetate,
TA1 = Total acetate 1, measured directly from the acetate methyl group at 20.6 ppm
TA2 = Total acetate 2, addition of Ph + 1^{o} + 2^{o} (169-171 ppm)

It appears that at low and high levels of reaction that the primary hydroxyl reacted faster than the phenolic hydroxyl, and at intermediate levels of reaction, the phenolic hydroxyl reacted faster than the primary hydroxyl reacted. This faster reaction was implied from a higher proportion (%) of reaction for a OH group at particular reaction time/temperature combination. However, the primary and phenolic levels of reaction were within 10% units of each other, and in two cases (MWL 1 and 4) were within 5% units, which is probably within the level of error for this method. This means that to all intents

and purposes, the primary and phenolic hydroxyls reacted at approximately the same rate.

Table 5.12. Reaction of primary, secondary and phenolic hydroxyl from NMR.

Sample	Total acetate[1] (% acetylated)		Extent reaction of functional group (%)		
	TA1	TA2	1°	2°	Phenolic
MWL1 (0.83 WPG)[2]	12.2	7.24	10.4	1.72	5.18
MWL2 (11.47 WPG)[2]	31.0	33.9	40.9	8.81	46.2
MWL3 (14.57 WPG)[2]	44.9	49.6	58.1	16.9	67.4
MWL4 (23.66 WPG)[3]	60.8	70.2	85.5	27.9	80.6

[1] Two ways to measure total acetate: TA1 was the ratio of the acetate's CH_3 carbon over the methoxy peak area; TA2 was the addition of primary, secondary and phenolic acetate reaction.
[2] Samples examined were a composite of two duplicates samples for a specific reaction time an temperature, whose WPG values were averaged.
[3] Sample examined was a single sample.

Both the primary and phenolic hydroxyls reacted to a much greater extent (and therefore, faster rate) for the four samples measured than did the secondary hydroxyl. This was not unexpected due to the sterically hindered position that the secondary hydroxyl is in.

For the measurement of total acetate, TA1 and TA2 were always within 10% units of each other, and therefore, gave similar trends. Figure 5.16 shows the comparison of TA1 and TA2 with measured WPG, and indicates that either measure of total acetate showed a similar pattern when compared to the WPG level.

TA2 gave a slightly better fit to a straight line (solid line, r^2=0.9869), going through the origin than did TA1 (dotted line, r^2=0.9467). Both TA1 and TA2 seemed to over estimate reaction level at low levels of reaction, which could be due to the increased % error of measuring a small peak (or measuring a small weight difference), which can be influenced by the level of background noise.

Figure 5.16. Comparison of WPG and extent of reaction from NMR for MWL

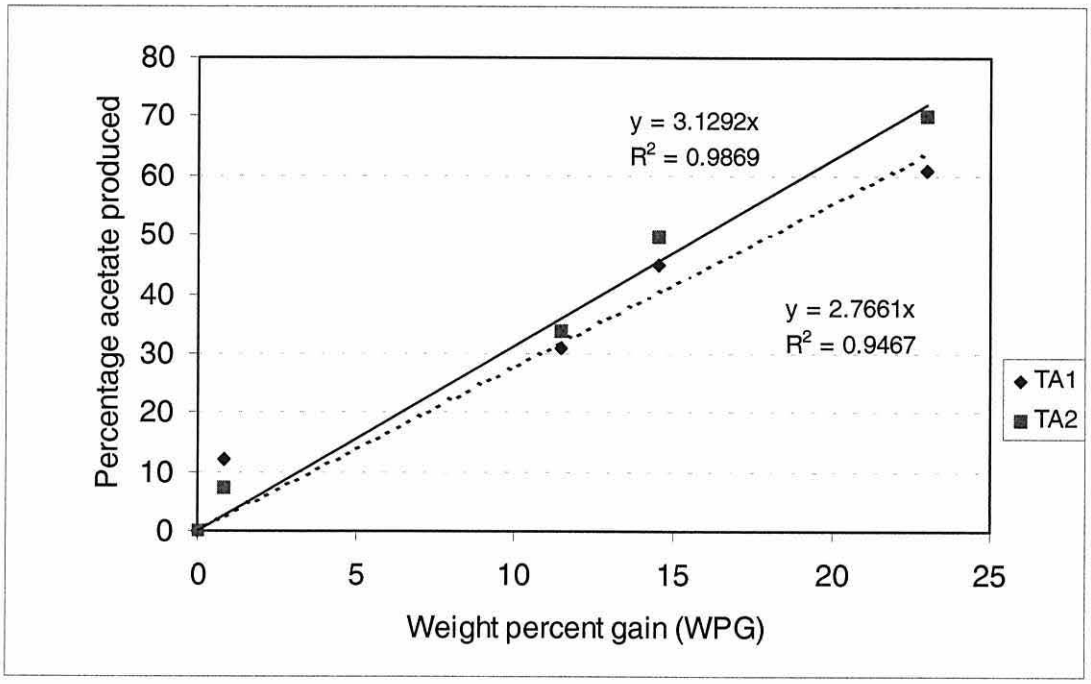

Key:
TA1 Direct measurement of acetate (18-21 ppm)
TA2 Addition of 1°, 2° and Ph acetate peaks (168-171 ppm)
_ _ _ Trend-line for TA1
_____ Trend-line for TA2

There have been no other kinetic studies on lignin acetylation that investigate the reaction over a range of temperatures and reaction times as in this study. There has been one recent study which looked at relative rates of OH reaction using three different acetylation methods. Heitner *et al.* (2001) acetylated a MWL isolated from bleached or unbleached pulp (TMP) and reacted it with acetic anhydride and pyridine at 25 °C (for 48 hours), and uncatalysed acetic anhydride at 25 °C (for 120 hours), and 100 °C (for 5 hours). They found that the pyridine–catalysed reaction and the uncatalysed reaction at 100 °C both fully derivatised all the OH groups present. However, they found that the low temperature uncatalysed reaction (at 25 °C) only fully derivatised the primary (γ-OH) hydroxyl groups, with both the phenolic and secondary OH group only partially derivatised.

In contrast, the results found here, examining four partially acetylated products reacted using the same acetylation method, found that the primary and phenolic OH groups reacted at about the same level and rate (within the experimental error of the NMR technique used), and the secondary hydroxyl reacted much slower than either the primary or phenolic hydroxyl.

5.6. Summary

It was found that the reaction profile of the commercially obtained softwood alkali lignin (AL) from a Kraft pulping process was very similar to that of the milled wood lignin (MWL) isolated from radiata pine sapwood. This was more so at the lower temperatures studied. At the higher temperatures, the AL reacted to a slightly greater extent than did the MWL. Further, the activation energy (Ea) values obtained for both AL and MWL were very similar (~80 kJ/mol, using k_o values from the exponential method).

A bagasse lignin (BL) obtained from an organosolv process reacted to a lesser extent and rate than either AL or MWL, and the E_a value for BL was also lower (~58 ± 17 kJ/mol), but had a higher level of error.

When the lignin reaction (MWL) at 29% was compared with the wood reaction, it was found that the reaction profile was similar for the reaction at 80 °C, and had a similar range of reaction level at both 100 and 110 °C. For the reaction at 110 °C, the reaction of lignin was initially greater than that of wood, then less, as the wood reaction kept increasing. From this, it was suggested that, at lower temperatures, lignin reaction probably comprises a large majority of the reaction level within wood. However, at higher temperatures, the hemicelluloses react to a greater extent and/or less accessible lignin hydroxyl groups are made more accessible by the swelling of the wood cell wall upon reaction.

It seems that while the reaction profile of the isolated lignin reaction is similar to the wood reaction at lower temperatures, it was not possible to predict

kinetic data for wood from the reaction of isolated lignins. This was probably due to the differences in the physical structure of the wood and isolated lignin preparations, as well as the contribution that hemicelluloses made to the overall wood reaction level.

The relative rates of reaction for the three main types of hydroxyl in lignin (MWL) were examined by ^{13}C NMR spectroscopy. It was found that within the errors of the method, the primary and phenolic hydroxyl reacted at about the same rate for the four partially acetylated MWL reaction products investigated. The secondary hydroxyl reacted to a lesser (usually much lesser) extent than either primary or phenolic hydroxyl. These results are compared to those obtained for the lignin model compound in Chapter 6.

CHAPTER 6: REACTION OF A LIGNIN MODEL COMPOUND

6.1. Introduction

Lignin contains three classes of derivatisable hydroxyl group: primary and secondary aliphatic OH, and phenolic OH. In order to ascertain the relative rates of each type of OH, a lignin model compound, β-O-4 model, was studied. This meant that the whole range of substrates were examined for acetylation, from solid wood blocks, to delignified ground wood (holo-cellulose), fibre, isolated wood components (lignin and carbohydrates), and finally to a lignin model compound. As time allowed for only one model to be used, it was decided to select one that had both primary and secondary hydroxyl as well as a phenolic hydroxyl.

The inclusion of a phenolic hydroxyl will potentially alter the reactivity of the other hydroxyls in the model, as the formation of a quinone methide intermediate is possible with the phenolic model but not the non-phenolic model. In addition, structural models of lignin show the majority of aromatic groups do not have a phenolic hydroxyl group present, so that between 12% (Brunow, 2001) and 32% (Adler, 1977; Glasser and Glasser, 1981; Freuden-berg and Neish, 1968 p109) of the aromatic groups have a phenolic hydroxyl. This is due to the fact that the phenolic OH undergoes reactions to form linkages with other aromatic groups during deposition in the cell wall.

A β-O-4 model was chosen as this is the most prevalent linkage in softwood lignin (Brunow, 2001; Landucci, 1995; Adler, 1977). Brunow (2001) reports that around 35% of all linkages in a typical softwood lignin are of the β-O-4 type. The next most prevalent linkage types are β-5 (10%), and 5-5-O-4 (biphenyl cyclic linkage) and β-β at around 5-6% each. Greater details of these and other lignin linkages are shown and discussed in Chapter 1 (section 1.3.2).

An interesting study was conducted on the relative acetylation rates of the hydroxyl groups in two lignin model compounds by Paulsson *et al.* (1995). They followed the phenolic and non-phenolic analogue model (*threo* form only) reaction with acetic anhydride at 100 °C using TLC and HPLC, and identified the different acetate products by ^{1}H NMR spectroscopy. It appears that for the phenolic model, the starting material (completely non-acetylated model) reacted within 10 minutes, due to the fast reaction of the phenolic hydroxyl. They found that the reaction of the phenolic model confirmed that the α-OH (2°) was more resistant than either the Ph-OH or the γ -OH (1°) towards derivitisation by acetylation (at 100 °C). From the HPLC plots of the different acetate products (mono-, di- and tri-), it appears that the presence of a phenolic OH increased the reactivity of the γ-OH (1°) and the α-OH (2°) groups towards acetylation.

This study by Paulsson *et al.* (1995) was focused on investigating the photo-stability of paper, and the work on the lignin models was conducted at one temperature, 100 °C. The work in this study (done almost in parallel) sought to extend this to a wider temperature range and obtain some kinetic information from the three different OH groups present in the phenolic model. Haque and Hill (2000) have acetylated some simple monomeric lignin models in pyridine. In general, they found that phenolic compounds (guaiacol, para-cresol, phenol) reacted faster than alcohols (benzyl alcohol). However, they did not have a range of hydroxyl groups on a side chain (for example, 1°-OH and 2°-OH) as is common in lignin.

Obtaining the relative rate of the various hydroxyl groups in a model compound is much easier than for a lignin, due to the heterogeneity and size of the latter. However, caution needs to be exercised when extrapolating results from a lignin model compound (especially when only one is studied) to lignin.

The main focus of this study is the reaction of whole wood, with isolated wood polymers being models in a sense, for wood. In the future, an extension of the

range of models might provide additional information which could give an insight of the relative reactivity of various lignin moieties.

6.2. Experimental

6.2.1. Synthetic method

The synthetic method used is given in Figure 6.1: the amounts shown represent those for one batch, as usually three or four batches were done at each step. The target compound, the β-aryl ether with propanoid side chain, a lignin model compound, is given in Figure 6.2 (Landucci *et al.,* 1981). Spectra of samples in d_6-acetone were referenced to the central acetone peak at 2.05 ppm for ^{1}H NMR and 29.8 ppm for ^{13}C NMR. Spectra of samples in $CDCl_3$ were referenced to the internal standard of TMS at 0 ppm.

Figure 6.1. Summary of the model compound synthesis

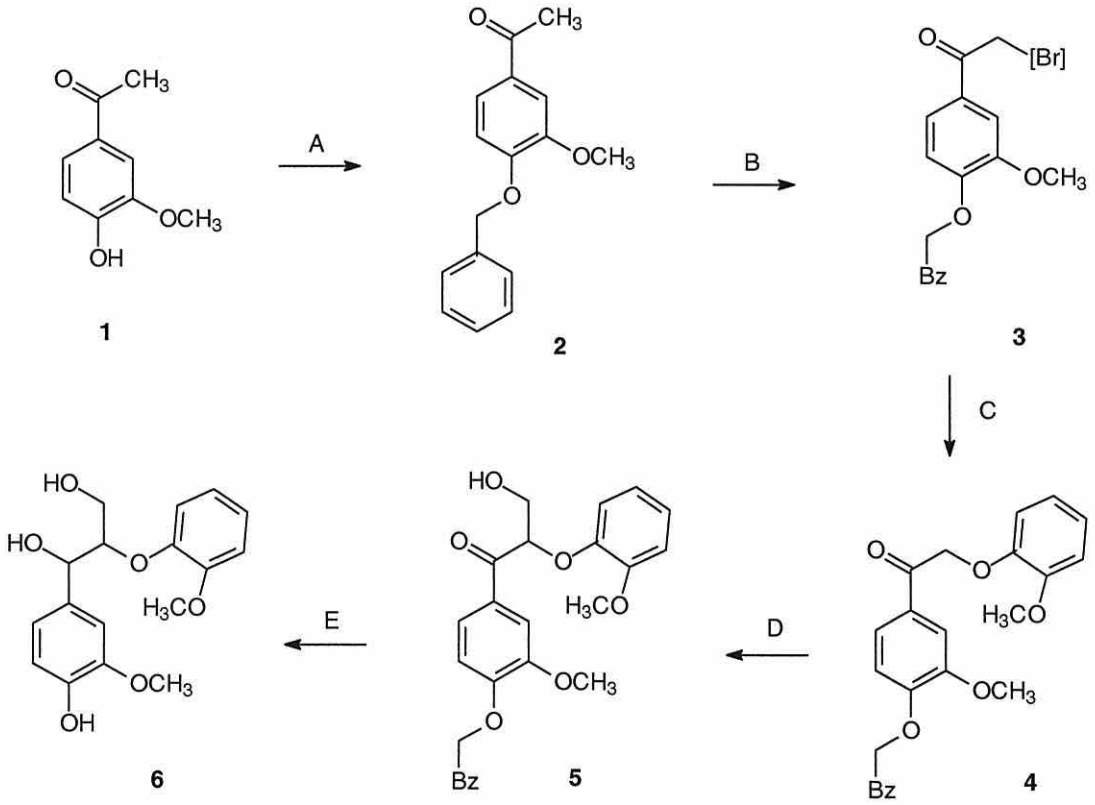

Legend: A. BzCl, K_2CO_3, KI, in acetone; refluxed O/N
B. Br_2, in EtOH
C. guaiacol, K_2CO_3, in acetone; stirred 4 h
D. K_2CO_3, HCHO, in dioxane; stirred 4 h
E.(a) $NaBH_4$ in dioxane/H_2O; stirred 3 h
E.(b) Na_2CO_3/Pd, H_2, in EtOH; stirred 3 h

Figure 6.2. Schematic of model compound

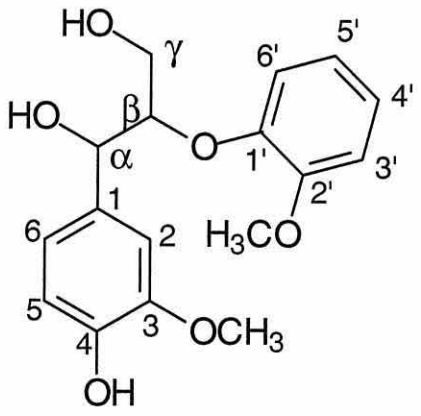

6.2.1.1. Step A: Protection of phenolic group by benzylation.

Acetovanillone **1** (17 g, 0.10 mol) was dissolved in acetone (175 ml). Then benzyl chloride (13.6 g, 0.11 mol), potassium carbonate (anhydrous, 14.8 g, 0.11 mol) and potassium iodide (1.7 g, 0.01 mol) were added (modified from Landucci *et al.,* 1981). The mixture was refluxed and stirred overnight, then cooled before being filtered through a sintered glass funnel to remove the inorganics. The acetone was removed under vacuum and the solid obtained compound **2** (24.5 g, 93% yield) was recrystallised in 95% ethanol to give fine yellow crystals. δ_H ($CDCl_3$): 2.54, s, 3H, CH_3; 3.93, s, 3H, OCH_3; 5.23, s, 2H, OCH_2Bz; 6.8-7.6, m, 8H, ArH.

6.2.1.2. Step B: Bromination of benzylated product

The benzylated product **2** from the first step (10 g, 0.039 mol) was dissolved in 95% ethanol (220 ml) in a method modified from Landucci *et al.* (1981) (Adams, 1999). A small amount of heat was used to fully dissolve the benzylated product (solution was cooled before the addition of bromine). Bromine (2.0 ml, 0.039 mol) was added drop-wise to a stirred solution as per Figure 6.3, with care taken not to generate too much heat. The separating funnel was washed through with extra ethanol, to remove all Br_2. The reaction was followed with tlc; a sample of reaction solution was added to some acetone and developed in dichloromethane with 1-2 drops of ethyl acetate (to change the polarity). After reaction was complete, the solution was cooled

(5 °C), and the pink crystals formed, were filtered, washed with cold ethanol (95%) and air-dried. The product was recrystallised in a minimum amount of hot ethanol (95%), filtered, washed and air-dried. Smaller batches were used as yield was variable (average yield 71%). δ_H (d_6-acetone): 3.94, s, 3H, OCH_3; 4.39, s, 2H, CH_2Br; 5.23 s, 2H, OCH_2Bz; 6.8-7.58, m, 8H, ArH.

Figure 6.3. Apparatus used for Step B.

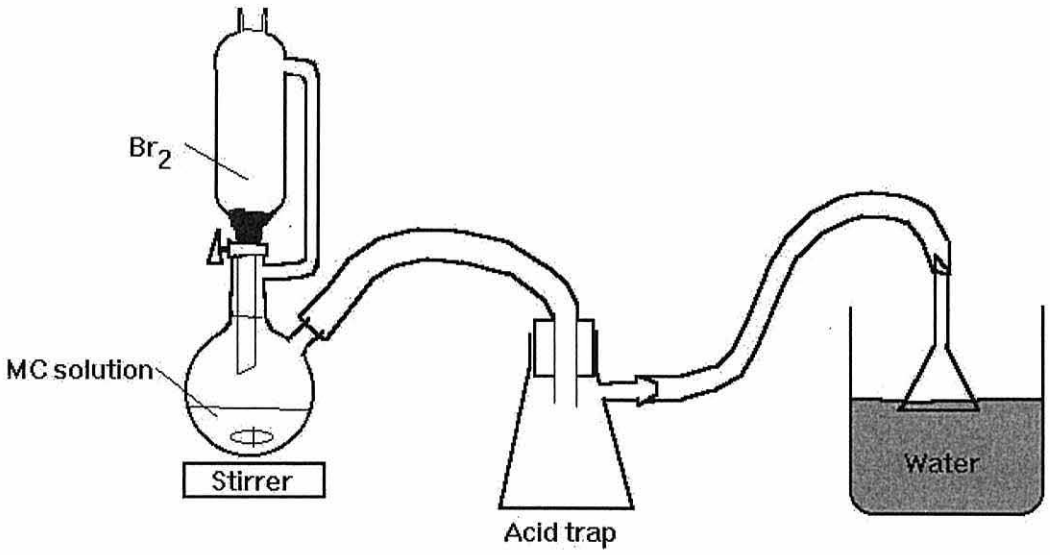

6.2.1.3. Step C: Addition of guaiacol

The brominated product **3** (3.15 g, 0.0094 mol) was dissolved in acetone (20 ml) before adding potassium carbonate (1.30 g, 0.0094 mol) and potassium iodide (0.16 g, 0.0009 mol). While stirring, guaiacol (1.035 ml) was added, according to Landucci *et al.* (1981). The mixture was refluxed and stirred for 4 hours, with a drying tube attached. The inorganic compounds were filtered off and the remaining acetone was removed under vacuum to give the product **4**. This was crystallised in 95% ethanol to give 2.98 g of product **4** (78% yield) as orange crystals. δ_H (acetone): 3.83, s, 3H, OCH_3; 3.88, s, 3H, OCH_3; 5.23, s, 2H, OCH_2Bz; 5.38, s, 2H, CH_2OAr; 6.74-7.78, m, 12H, ArH.

6.2.1.4. Step D: Addition of formaldehyde

The product **4** from Step C (2.0 g, 0.00527 mol) was dissolved in dioxane (60 ml) before the addition of potassium carbonate (6.28 g, 0.0527 mol) and formaldehyde (0.158 g, 0.0053 mol; 380 µl, 37% solution), according to the Helm modification (Helm and Ralph, 1993). The solution was stirred vigorously for 3-4 hours, and the reaction was followed by tlc. The solution was filtered through a sintered glass funnel and washed with a small amount of dioxane, before the dioxane was removed under reduced pressure. The product was a light yellow coloured oil and was dissolved in ethyl acetate, washed twice with a saturated solution of ammonium chloride in a separating funnel, and washed once with a saturated sodium chloride solution, before drying over magnesium sulphate (anhydrous). The solution was filtered and the ethyl acetate removed under reduced pressure. To crystallise, the product was dissolved in warm ethyl acetate, then petroleum ether (40-60 °C bpt fraction) was added drop-wise (to just before precipitation). Crystals (pale yellow) formed very slowly under refrigeration. The average yield was 72%, on the various batches, with a total of 6.125 g of compound **4** yielding 4.758 g of compound **5**. δ_H (acetone): 3.78, s, 3H, OCH_3; 3.86, s, 3H, OCH_3; 4.04/4.06, dd, 2H, CH_2OH; 5.22, s, 2H, OCH_2Bz; 5.53, t, 1H, CH_2OAr; 6.68-7.85, m, 12H, ArH.

6.2.1.5. Step E: De-benzylation and hydrogenation steps.

Step E was done in two parts according to Adams (1999). (a) The product **5** (200 mg, 4.96 $x10^{-4}$ mol) from step D was dissolved in a dioxane/water mix (70:30, 20 ml) and stirred, before sodium borohydride was added (0.056 g, 1.5 $x10^{-3}$ mol). The reaction was followed by tlc. When reaction was complete (3-3.5 hours), the whole solution was neutralised with ammonium chloride, then extracted into ethyl acetate using a separating funnel. The organic fraction containing the product was washed twice with ammonium chloride and once with sodium chloride (saturated solution) and dried over magnesium sulphate. The solution was filtered using a sintered glass funnel before the ethyl acetate was removed under reduced pressure.

(b) The product of part (a) (ca. 185 mg) was dissolved in ethanol (95%, ~25 ml) before sodium carbonate and palladium catalyst (on carbon) were added (a small spatula measure of each). The solution was stirred, under hydrogen (from attached balloon) for about 3 hours. The reaction was followed by tlc. Once reaction was complete, the solution was filtered through celite on a sintered glass funnel (celite was washed once with water and once with acetone before use). The celite was then washed with ethanol (95%). The ethanol was removed under reduced pressure. For some batches, there seemed to be some celite present in the final solution. Therefore, the rotovaped oil was re-dissolved into ethanol and filtered through small columns of fine glass wool to remove the celite. The filtered oil was dissolved into warm ethyl acetate, and petroleum ether (40-60 °C) was added drop-wise (as above). The crystals (off-white) were filtered off using a sintered glass funnel and air-dried in the dark. However, not all the product crystallised (as only the threo isomer crystallises fully), so the total product (both isomers) was obtained and used as an pale yellow oil. In all, 1.5319 g of compound **5** was used to generate 0.6969 g of the target model compound **6**, giving an average yield for step E of 58% as a ca 70:30 of *erythro* and *threo* isomers, obtained from ^{1}H NMR spectrum of the fully acetylated model compound. δ_H (acetone): 3.42-3.56, m, Hγ threo; 3.58-3.75, m, Hγ erythro; 3.82, 3.87, s, 3H, OCH_3; 4.15-4.24,m, Hβ, threo; 4.25-4.35, m, Hβ, erythro; 4.89, d, J=6.41 Hz, 1H, Hα, threo; 4.90, d, J=5.91 Hz, 1H, Hα, erythro; 6.73-7.23, m, 8H, ArH (~7.5, v sm, ArOH). δ_C (mostly threo due to spectrum taken of crystals): 56.13, 56.25, s, OCH_3; 61.84, s, Cγ; 73.86, s, Cα; 88.51, s, Cβ; 111.33, s, C2; 113.31, s, C3'; 115.9, s, C5; 119.97, s, C6'; 120.53, s, C6; 121.92, s, C5'; 123.41, s, C4'; 133.75, s, C1; 146.77, s, C4; 147.98, s, C3; 149.62, s, C2'; 151.74, s, C1'.

The spectra of the final product **6** is given in the Characterisation section, (section 6.3.2).

6.2.2. Reaction method

A stock solution (0.7 g in 10 ml) of the final model compound (MC) **6** was made in acetone. An aliquot of stock MC solution (1.75 ml, to give ~120 mg of

MC) was injected into pre-heated acetic anhydride solution (3.5 ml), for reaction at four temperatures, 60, 70, 80, 90 °C. The flask was gently stirred after injection of stock solution. The assumption was made that the small amount of acetone (~1.75 ml) would flash off, and thus not contribute to the total volume of reaction solution. Aliquots (0.5-0.75 ml) were taken out at six different reaction times of between 5 and 120 minutes (the final reaction time aliquot was the remainder of the solution). For the lower two temperatures (60 and 70 °C), there was enough solution remaining for a seventh reaction time of 240 minutes to be obtained.

Each aliquot of reacted MC was put into a labelled vial (teflon-lined lid) in an ice/water bath for ten minutes to cool, before chilled distilled water (1.0-1.5 ml) was added. The vial was capped and shaken vigorously at intervals to ensure full mixing and quenching of the acetic anhydride. Once the excess anhydride had quenched, the vial was removed from the ice bath and the product extracted into ethyl acetate (1 ml). The ethyl acetate layer was removed and the aqueous layer was re-extracted with ethyl acetate (0.5 ml). The ethyl acetate fractions were combined in a test-tube and washed with a saturated sodium carbonate solution until any remaining acid was neutralised, then the organic phase was washed twice with water. The MC solution was then dried by passing solution through several small magnesium sulphate columns. The ethyl acetate was removed under reduced pressure to give a straw-yellow oil - the partially acetylated model compound.

A sample of the MC **6** was fully acetylated in pyridine and acetic anhydride (as per method in Chapter 5, section 5.5.1) for reference.

There was a small level of reaction that occurred during the work up of the acetylated product before NMR analysis. On reflection, it may have been better to do the experiments in the NMR tube using d_6-acetic anhydride, to avoid this problem. This would make the examination of shorter reaction times and lower temperatures more feasible.

6.3. Characterisation of the Model Compound

The need for characterisation of the model compound was not as great as for the other substrates as by using NMR, the structure was confirmed as that intended. Therefore, the main technique used has been NMR spectroscopy. An FTIR spectrum was run of the model compound as a general comparison with other substrates used.

6.3.1. FTIR spectroscopy

A FTIR spectrum was run of the model compound, using a solution in acetone, of which a few drops were placed on a KBr disc, and left to evaporate. In this way, a film of the model compound was left on the disc (after a background spectrum of the disc had been run). This sample alone was run on a Bruker Vector 33 instrument with Windows NT OPUS software, using 4 cm^{-1} resolution and 32 scans per sample, with 64 scans per background. The spectrum of the model compound (MC) is shown in Figure 6.4, with the assignments given in Table 6.1.

Figure 6.4. FTIR spectrum of the lignin model compound

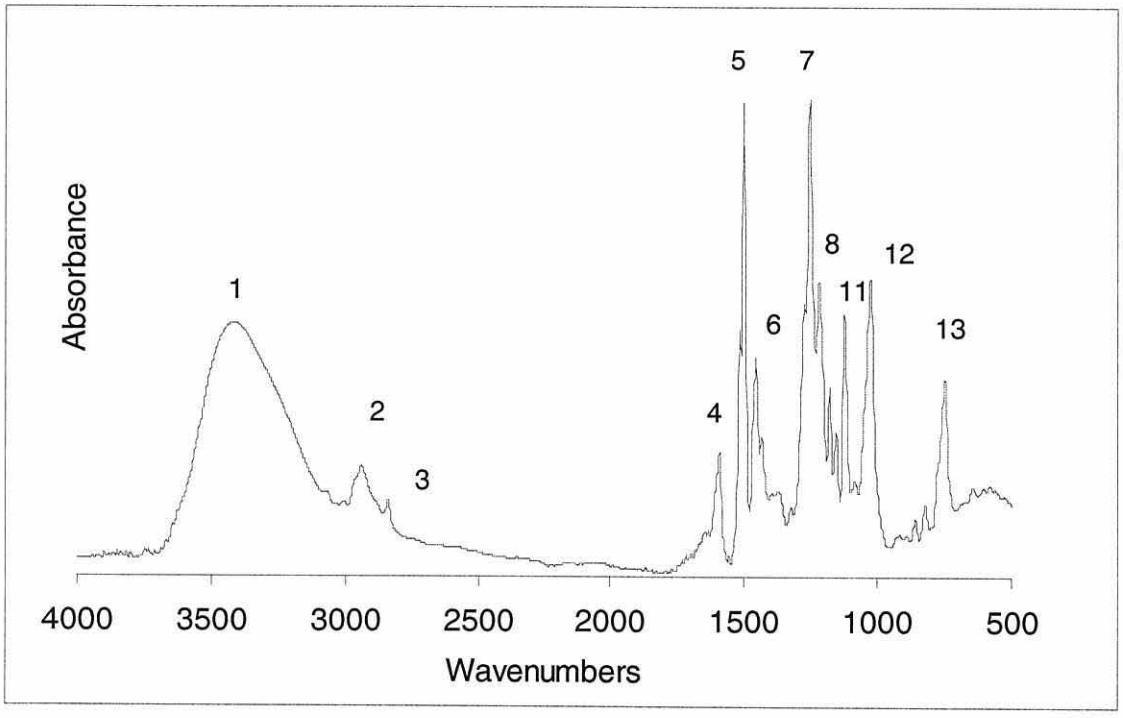

The FTIR spectrum of the model compound has more defined and sharper peaks than the MWL, as expected. A comparison of the model and MWL spectra is shown in Figure 6.5, from 2000 to 500 cm^{-1}. There were three main areas of difference between the spectra. There were no peaks in the region 1655-1715 cm^{-1}, as there are no carbonyl groups in the model. There was also a reduction in the peak to the right of peak 6 (1420 and 1435 cm^{-1} for MWL and MC respectively) and a significant rise in peak 13 (748 cm^{-1}), both assigned to aromatic C-H bend, these differences would be due to the limited number and type of aromatic groups in the model compared to lignin.

Table 6.1. Assignments of the main FTIR peaks of the lignin model compound

Peak number	Wavenumber (cm^{-1})	Assignment [a]
1	3420	ν_{O-H}, bonded
2	2939	ν_{C-H}, CH_2/CH_3
3	2839	ν_{C-H}, CH_2/CH_3
4	1593	$\nu_{C=C}$, aromatic
Sh to L of 5	1518	$\nu_{C=C}$, aromatic
5	1501	$\nu_{C=C}$, aromatic
6	1456	δ_{C-H}, CH_2/CH_3
Sh to R of 6	1435	δ_{C-H}, aromatic
7	1252	ν_{C-OMe}
8	1217	ν_{C-OH} , ν_{C-C}
9	1178	ν_{C-O}, C-OH or ν_{C-O-C}, ethers
10	1155	ν_{C-O}, C-OH or ν_{C-O-C}, ethers
11	1124	δ_{O-H} (2^{o}-OH)
12	1026	δ_{C-H} (aromatic), δ_{O-H} (1^{o}-OH)
13	748	δ_{C-H} , aromatics, out-of-plane

[a] The symbol ν means a stretch frequency and δ means a bend (scissor/wag etc) frequency, with the subscript denoting the type of bend or stretch.

There were a number of shifts in peak position and relative intensity, as would be expected when comparing a relatively simple model compound with a

complex heterogeneous polymer such as lignin. An example of this is the characteristic lignin peak at 1510 cm^{-1} in MWL, was at 1501 cm^{-1} (peak 5) for the model, with a shoulder at 1518 cm^{-1}.

Figure 6.5. Comparison of the model compound (MC) and milled wood lignin (MWL) FTIR spectra

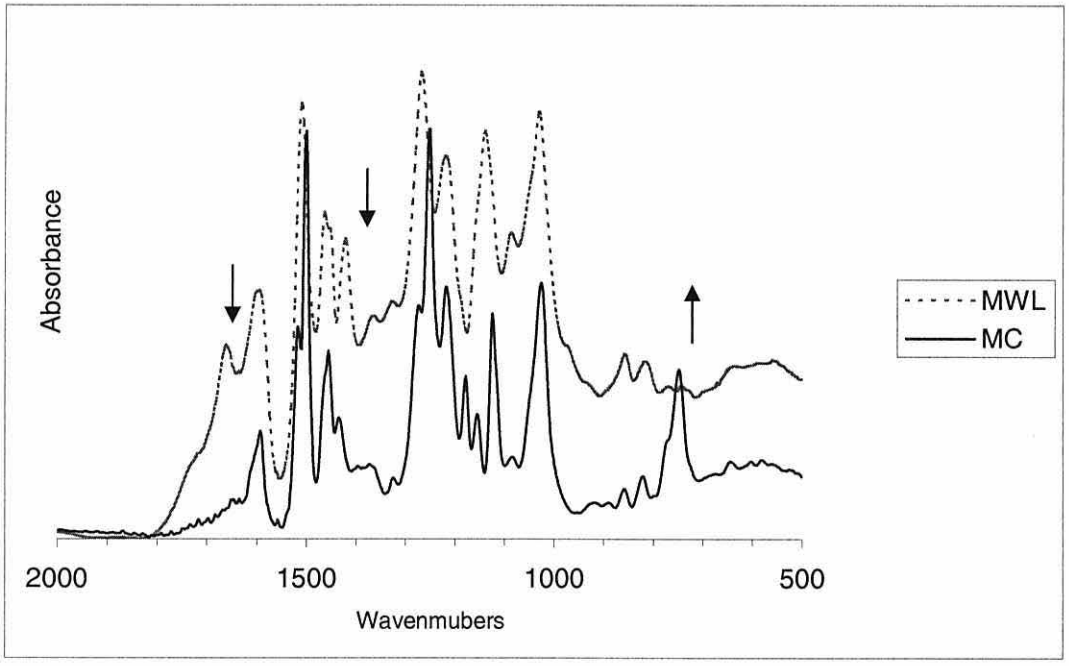

6.3.2. NMR analysis of untreated and acetylated model compound

The ^{1}H NMR spectroscopic characterisation was conducted of each of the products during the synthesis of the target model compound **6**. The details of the characteristic peaks have been given in section 6.2.1. These spectra are presented in this section, and the areas of integration used on the partially acetylated model compound products which were used in the analysis of extent of reaction and relative rates of reaction of the different OH groups.

6.3.2.1. Untreated model compound

The proton and carbon NMR spectra of the model compound (both isomers) are given in Figures 6.6 and 6.7 respectively. In Figure 6.6, Ar-H refers to the aromatic hydrogens, and e and t refer to the erythro and threo isomers respectively. The numbering of the carbons has been given previously in Figure 6.2.

Figure 6.6. Proton NMR spectrum of final model compound **6**

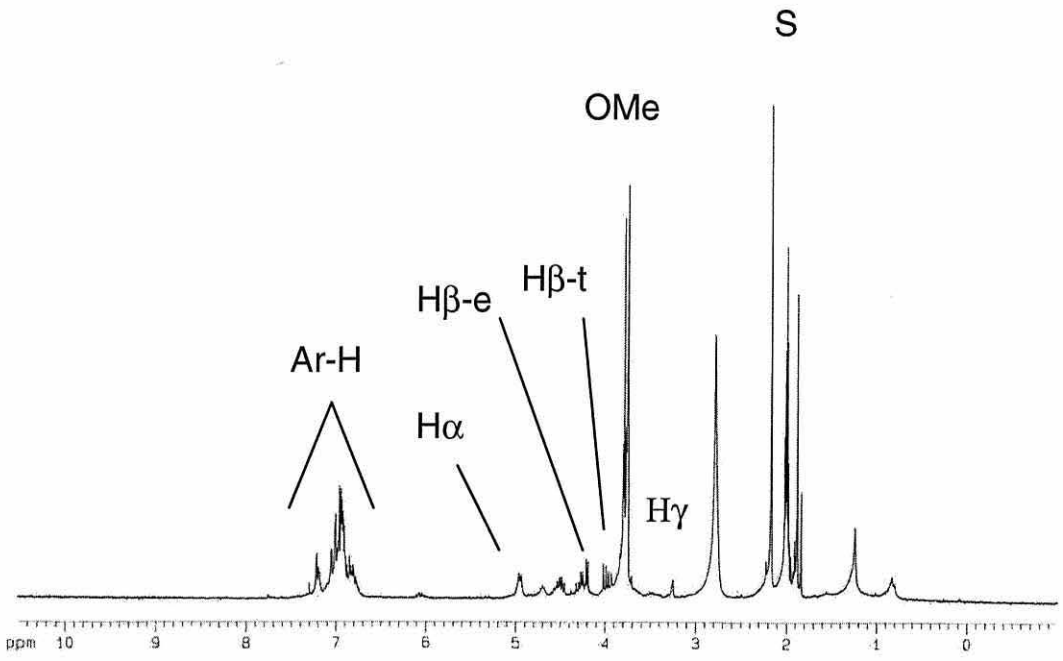

Figure 6.7. Carbon NMR spectrum of final model compound **6**

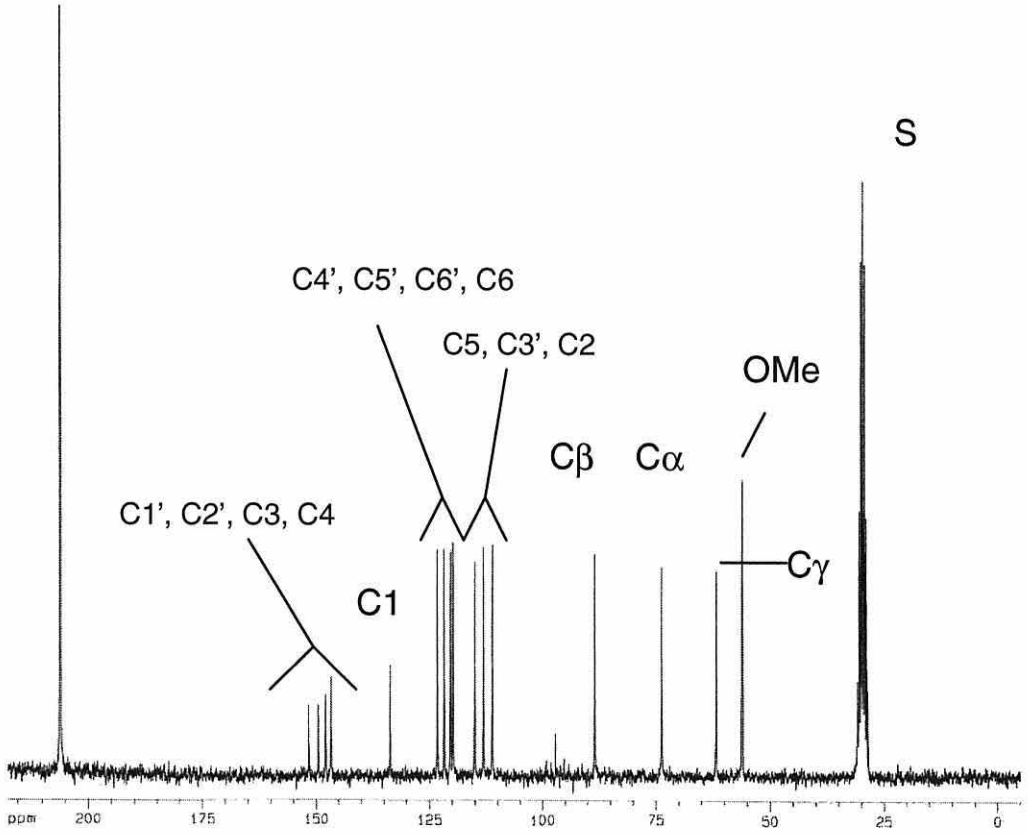

6.3.2.2. Acetylated model compound products

A sample of fully acetylated model compound was used as the 100% reaction standard. The five areas of integration are shown on the sample in Figure 6.9. The reacted product of each reaction combination was dissolved in d_6-acetone before ^{1}H-NMR spectrum was run (see Chapter 2, section 2.7.2). The spectra were processed and calibrated (to the central acetone peak at 2.05 ppm). The ^{13}C NMR spectrum of the fully acetylated model compound is also shown (Figure 6.8), with the main peaks marked with their assignments, which were used for the relative rates of reaction comparison with lignin. A few peaks in the ^{13}C NMR spectrum shifted upon acetylation. For example, untreated C4 (position of the phenolic OH) moved from 147 ppm (Figure 6.7, section 6.2.1) to the acetylated C4 at around 141 ppm, and C5 (adjacent to the phenolic OH at C4) from 116 ppm to ~119 ppm.

The peak areas of interest in the ^{1}H NMR spectra were integrated to measure the extent of reaction of the primary, secondary and phenolic hydroxyl, with the NMR region of aromatic protons used as the internal reference (peak area set to 1.0). The peak areas were compared to the values of the fully acetylated MC peak areas. Thus, a level of reaction (%) would be obtained for each of the OH groups.

The areas integrated were:

1. Primary acetate protons (1.91-2.00)
2. Phenolic acetate protons (2.18-2.38)
3. Protons attached to the carbon adjacent to the primary acetate (3.95-4.09 ppm)
4. Protons attached to the carbon adjacent to the secondary acetate (6.00-6.19 ppm) , and
5. Aromatic protons, to use as an internal reference. (6.65-7.41 ppm)

Region 3 did not give very reliable results due to the large methoxyl peak nearby, which partially overlapped. Therefore, region 1 was used in the final analysis as it gave a better estimation of the extent of reaction of the primary hydroxyl. The phenolic acetate proton peak (region 2) also had a large peak nearby, but it was a reasonable size itself, so the errors were less significant.

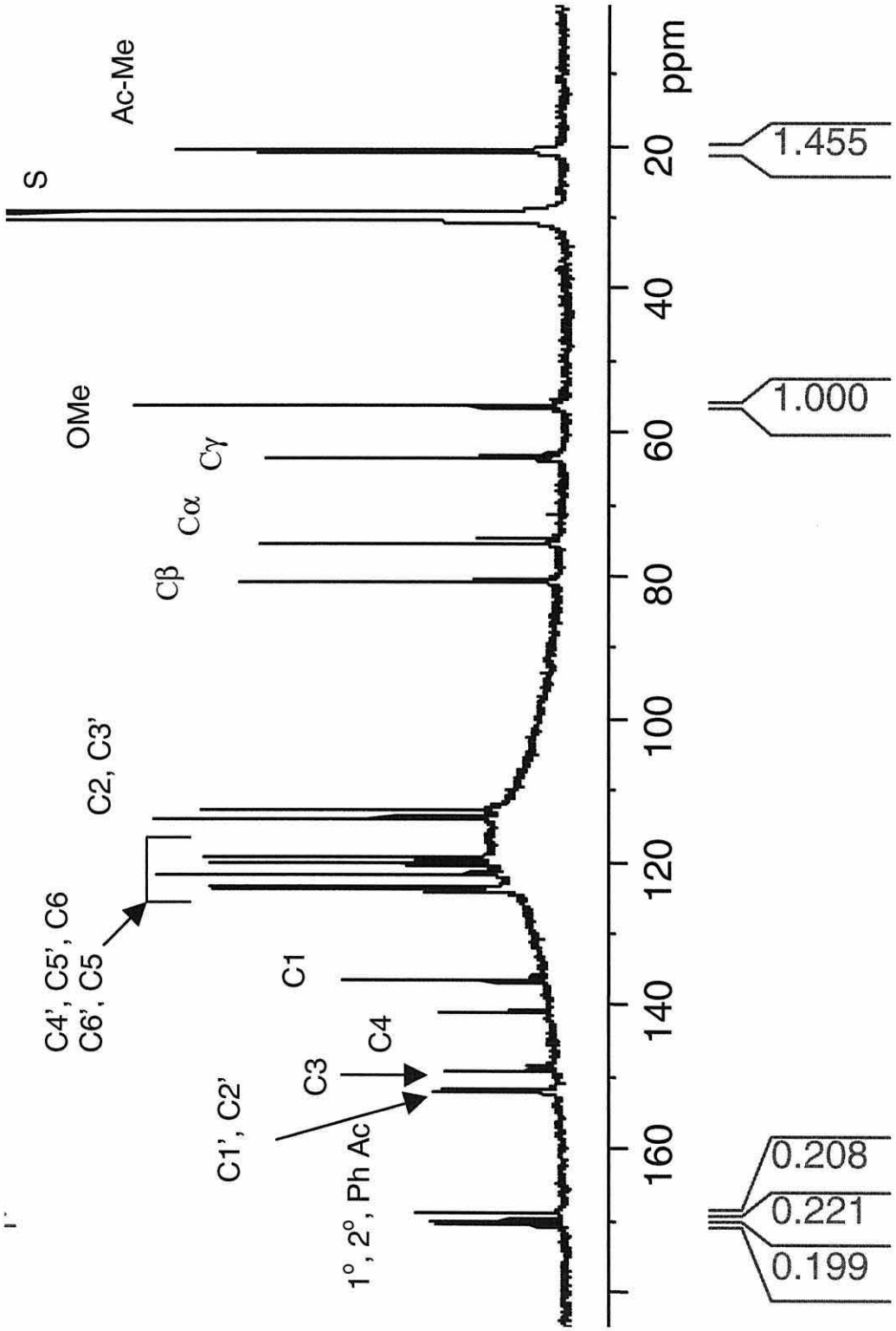

Figure 6.8. ^{13}C NMR spectrum of fully acetylated model compound

Figure 6.9. ^{1}H NMR spectrum of the fully acetylated model compound

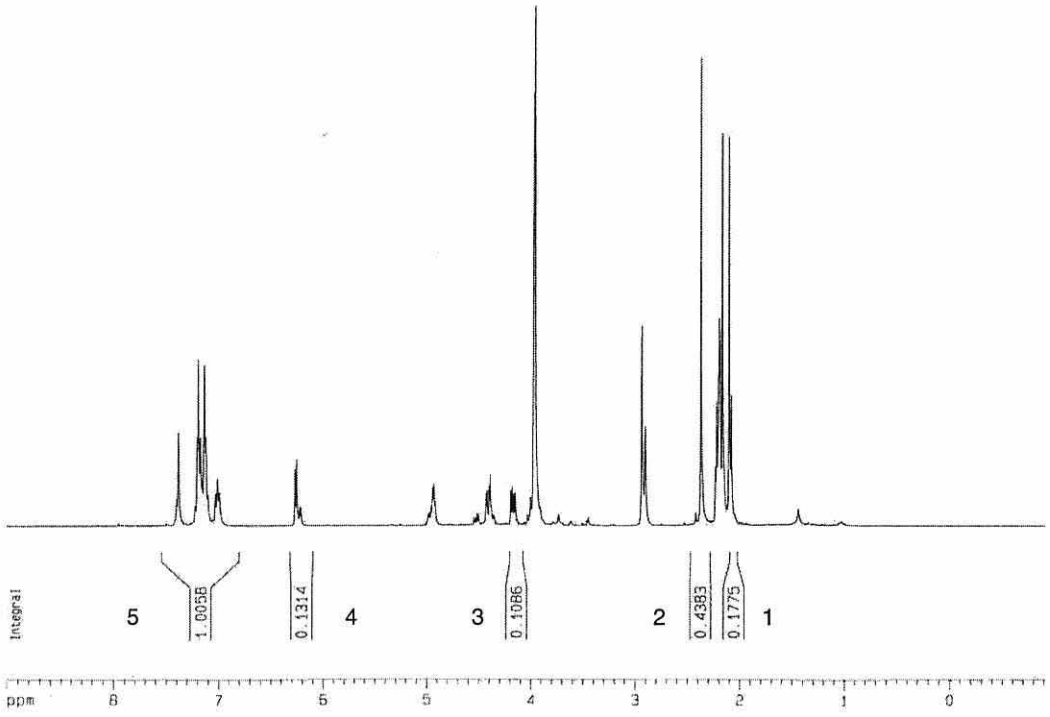

6.4. Results and discussion

The β-O-4 model compound was reacted in pure acetic anhydride at four temperatures between 60 and 90 °C. This was a lower temperature range than was used for the other substrates examined (80-120 °C), due to the speed of the homogeneous reaction of the model compound. Samples were withdrawn at 6-7 time intervals for each temperature. The extent of reaction was determined using ^{1}H NMR , as outlined in the previous section.

6.4.1. Reaction profiles

The reaction profiles are shown for each temperature, 60, 70, 80, and 90 °C, for each hydroxyl reaction studied (Figures 6.10-6.12). Unfortunately, reaction of the primary (1°) and phenolic (Ph) hydroxyl were not able to be fully analysed kinetically, because the reaction went too quickly. The reaction profiles of these two reactions are shown without curve fitting of the data (Figures 6.10 and 6.11).

Figure 6.10. Reaction profile of the phenolic hydroxyl

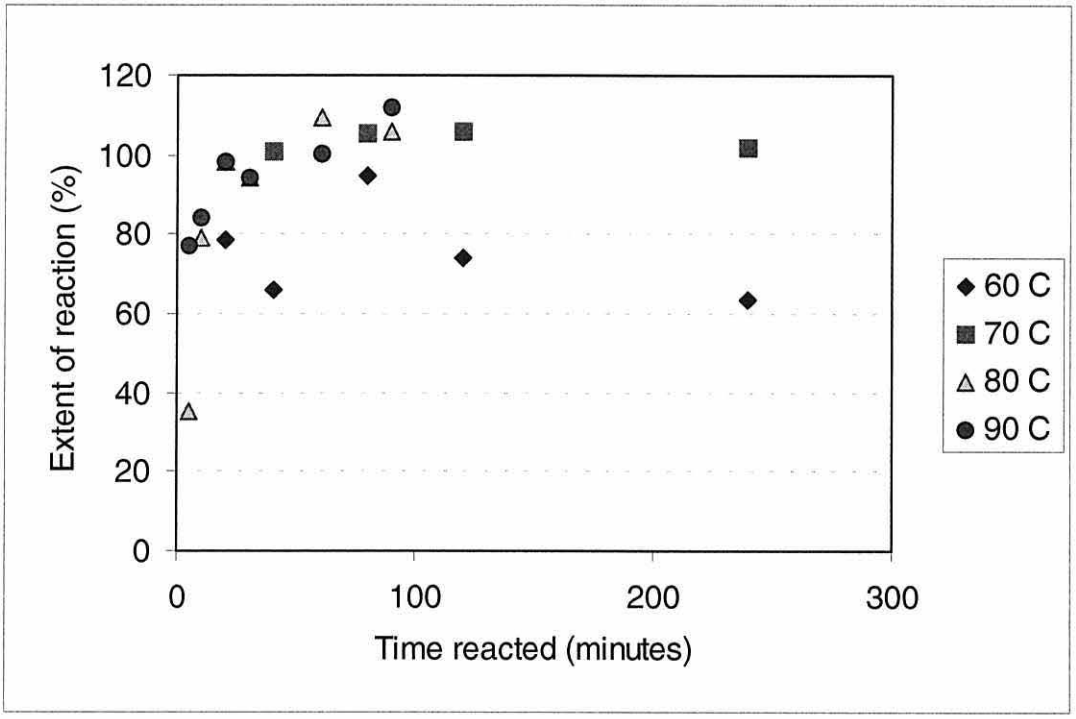

Figure 6.11. Reaction profile of the primary hydroxyl (1°-OH)

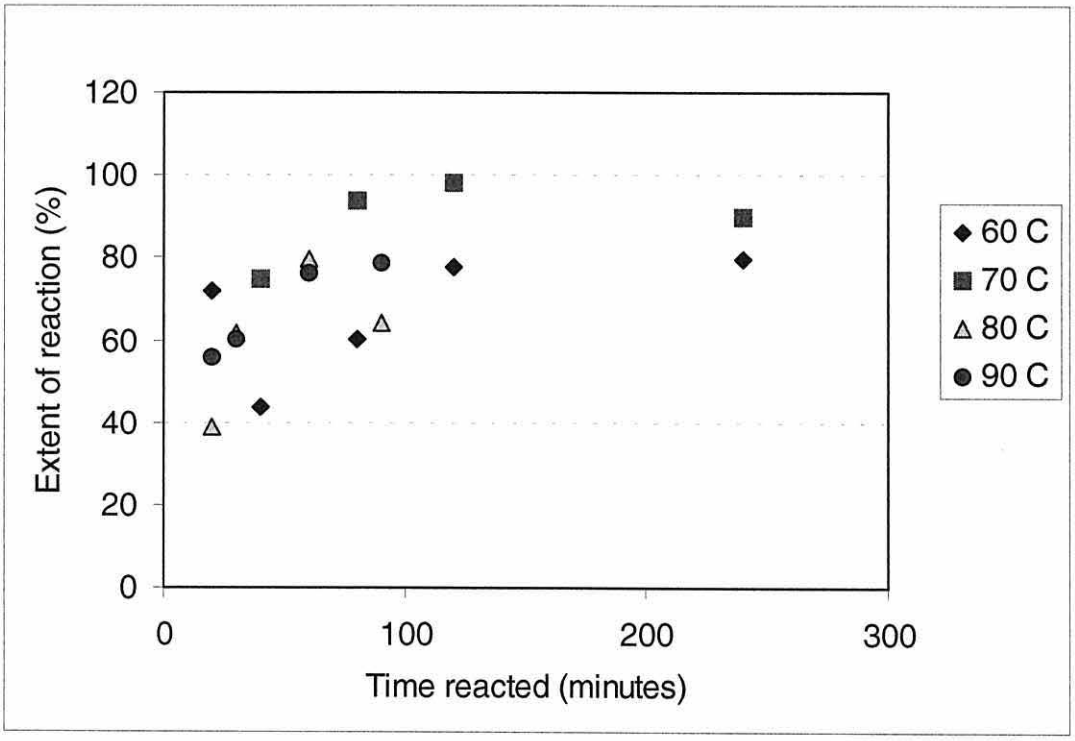

The shorter reaction times of 5 and 10 minutes were excluded from the plots for some of the data sets, due to the very high variability of the results. The full set of the raw data is shown in Appendix V. However, it is still obvious in comparing the reaction plots of the 1°-OH and Ph-OH reactions that, in general, the Ph-OH was faster than the 1°-OH reaction. So, the order of reactivity of the three OH groups towards acetylation in this model compound was: Ph-OH > 1°-OH >> 2°-OH

For the reaction of the secondary hydroxyl (Figure 6.12), the data was able to be used for calculation of kinetic data. However, at the lower temperatures (60 and 70 °C), the shorter reaction times gave seemingly random results and so were not used for the calculations.

Figure 6.12. Reaction profile of the secondary hydroxyl (with fitted curves)

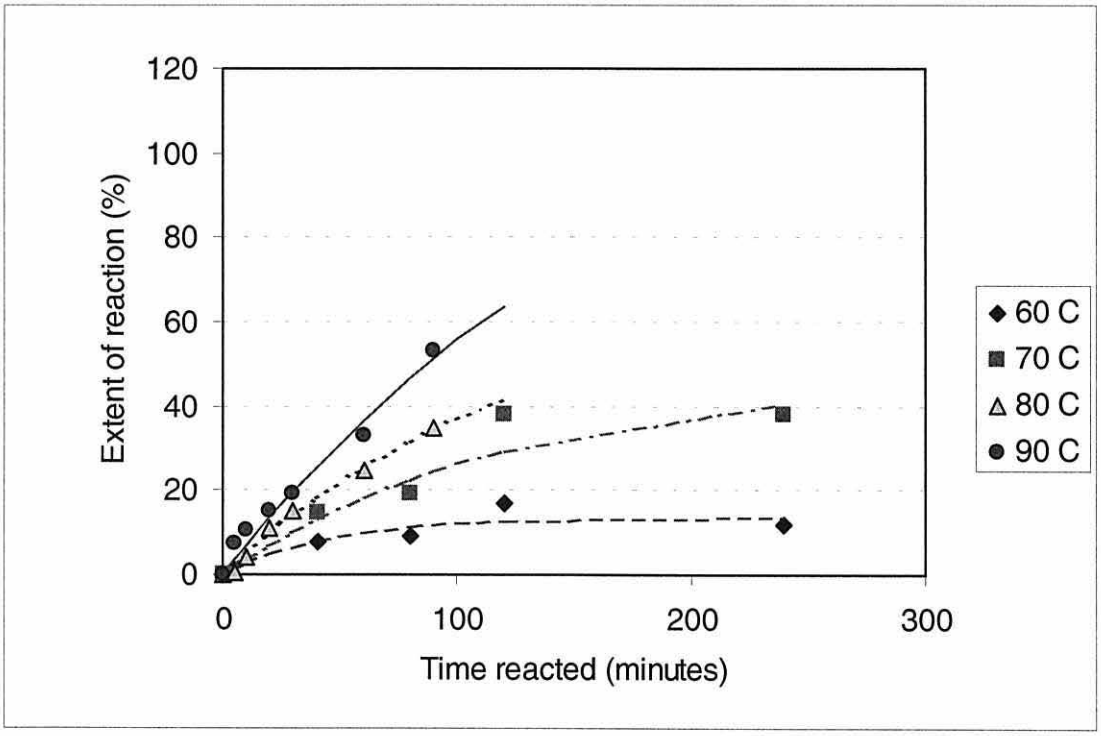

Figure 6.13 shows the reaction profile plot of the total acetate formation (or hydroxyl group reaction) based on the addition of the percentage reaction of Ph-OH, 1°-OH and 2°-OH. However, at low reaction levels especially, the data was variable, and did not allow the calculation of any kinetic data for the overall reaction.

Figure 6.13. Reaction profile of total acetate

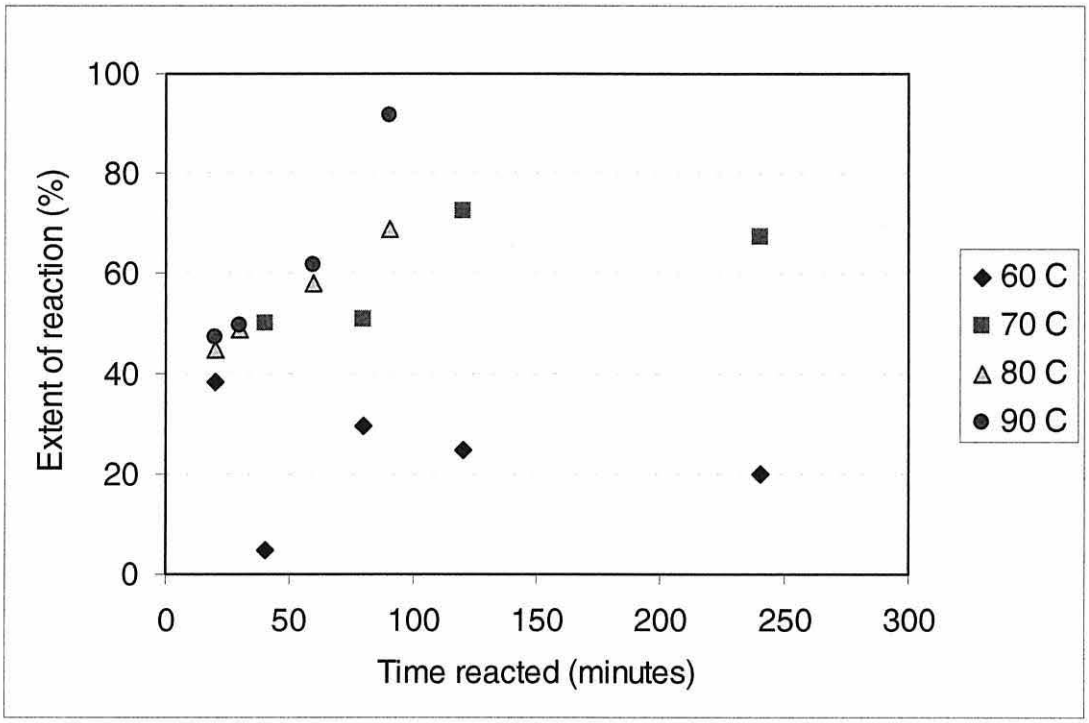

6.4.2. Kinetic data

Kinetic data were only calculated for the secondary hydroxyl reaction. A linear regression was carried out and gave rise to the Arrhenius plot shown in Figure 6.14. The activation energy (Ea) was calculated to be 29.41 ± 1.55 kJ/mol (r^2= 0.9945), with an equation of y = -3537x + 6.3984.

This activation energy (Ea) value for the 2°-OH (~30 kJ/mol) was much lower than that obtained for MWL (80 ± 8 kJ/mol), and much nearer to that obtained for wood reaction (34 kJ/mol), although the latter is probably a coincidence. However, this is the Ea values for the 2°-OH only (the slowest reacting OH group), whereas the MWL Ea value was for all the hydroxyl groups combined. In addition, the model only contains one type of each of the OH groups, whereas the MWL has a large number of groups in different nearby environments.

Figure 6.14. Arrhenius plot for the secondary hydroxyl reaction of the model

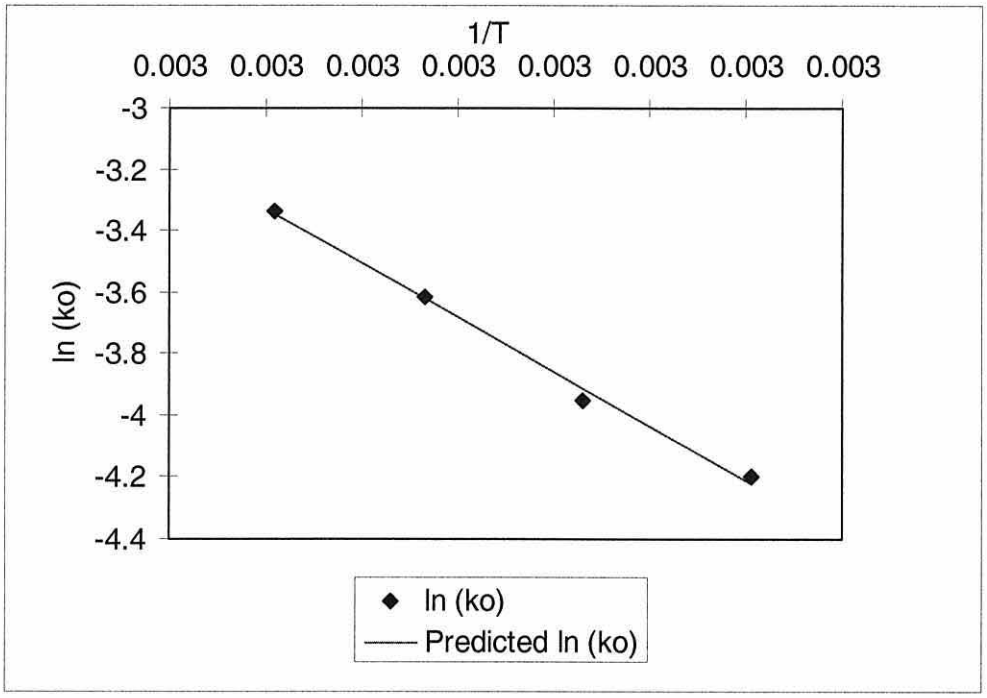

It is interesting to note that the samples that reacted faster, had higher Ea values than those who reacted slower (and to a lesser extent). This may be a reflection of the dependence of the activation of the reaction of the OH groups on the rate determining step. For example, the wood ultrastructure influences the diffusion (which is the rate-determining step) of the anhydride through the cell wall, so that the activation of the OH group is not such a factor in the speed of the reaction. In the same way, there may be steric factors involved with the slower reaction of the 2°-OH compared to the 1°-OH or the Ph-OH.

However, when the initial rate constants are calculated using a different method (the first two reaction data points and zero), the activation energy obtained is much higher (71.46 ± 5.93 kJ/mol, r^2=0.9864), and much nearer the value obtained for MWL (80 kJ/mol). This alternate Ea value is probably the more accurate one, as the exponential curves did not always fit the initial data well. The raw data for these two methods is given in Appendix W.

To the author's knowledge, this is the first time an activation energy value has been obtained for the acetylation of a specific OH group of this β-O-4 model.

6.4.3. Relative rates of reaction comparison

The relative order of reactivity obtained from the reaction plots (using ^{1}H NMR analysis) was generally: Ph-OH > 1°-OH >> 2°-OH. In order to properly compare the results with those obtained for the lignin (using ^{13}C NMR analysis), the equivalent analysis was conducted on two partially acetylated model products. Therefore, the relative rates of reaction obtained from these two methods were compared (Figures 6.15-6.16). Interestingly, the results from the ^{1}H and ^{13}C NMR analyses were not always the same in terms of order.

The lower temperature product (Figure 6.15), gave a reaction order of 1°-OH > Ph-OH >> 2°-OH from ^{1}H NMR, but Ph-OH > 1°-OH from ^{13}C NMR analysis. It may be that the analysis of the lower level reaction is at or below the detection limit for this technique. NMR analysis usually has an error of 5-10%, which would mean the differences detected between the two methods are not real. The higher temperature product (Figure 6.16) gave the same results from both methods of analyses; that is, Ph-OH > 1°-OH >> 2°-OH.

Figure 6.15. Comparison of relative rates of reaction of the model reacted at 60 °C for 40 minutes obtained by Carbon and Proton NMR spectra

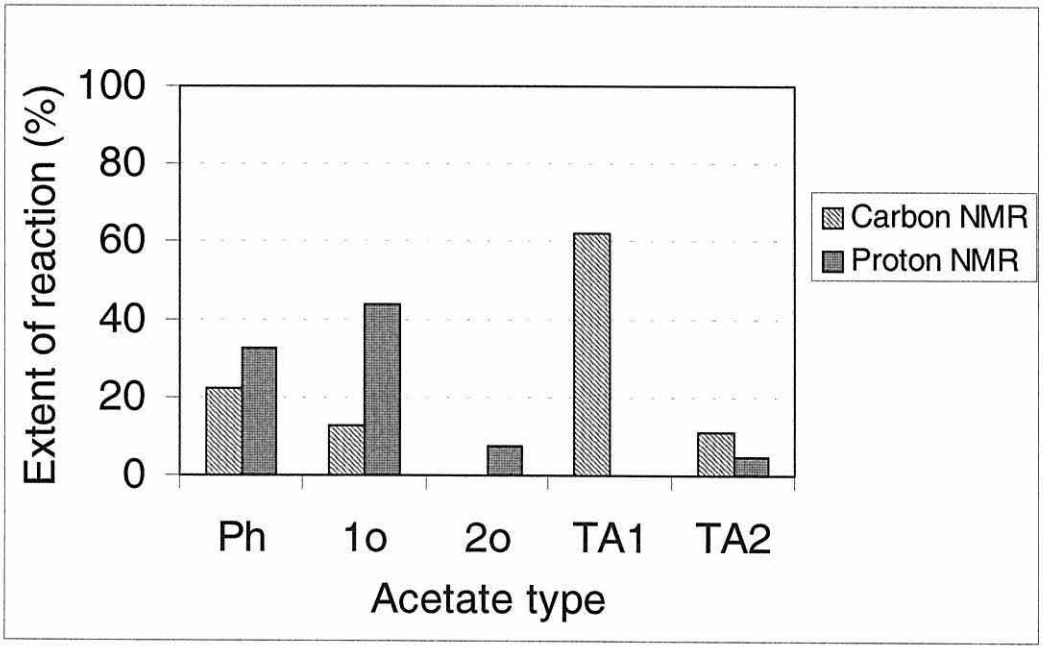

Figure 6.16. Comparison of relative rates of reaction of the model at 80 °C for 60 minutes obtained by Carbon and Proton NMR spectra

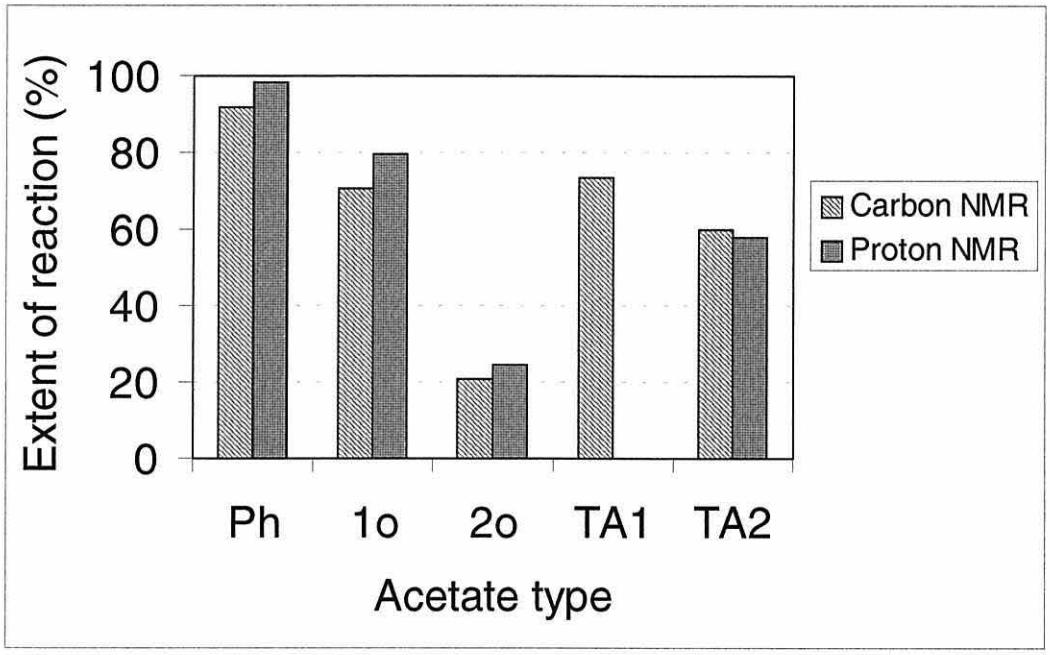

The resistance of the 2°-OH to acetylation was in agreement with results of Paulsson *et al.* (1995). In a later study (parallel to this one), Paulsson and others (1996) acetylated a range of model compounds to determine the speed and order of OH group reaction. Although they did not include the β-O-4 model with three different types of OH group (as in this study), they found the overall order of reactivity over the range of compounds studied to be: Ph-OH ≥ γ -OH (1°) >> α-OH (2°), which was in general agreement with the order found in this study. They also found that phenolic model compounds were full acetylated in a shorter time than the non-phenolic models.

The TA1 and TA2 are different because the spectra were not run under inverse-gate conditions (for quantitative spectra), but are probably generally comparable between samples. For both reaction products examined, the total acetate (TA2) obtained from both methods agreed within error.

6.4.4. Comparison to lignin data

Figure 6.17 shows the relative rates of reaction for two reaction products of the model from the Carbon NMR analysis. Figure 6.18 shows the equivalent results for the MWL samples for comparison. For both of the model reaction products analysed, the reaction order was Ph-OH > 1° >> 2°.

The results from the MWL analysis were not so clear cut, although four samples were analysed rather than just two of the MC products. At low and high levels of reaction, the 1°-OH reacted to a greater extent than the Ph-OH did, although they were no more than 5% units apart. At intermediate levels of reaction, the Ph-OH seemed to react to a greater extent than the 1°-OH, but within 10% units. However, these results are probably within the error limits of the analyses. So for MWL, the overall reaction order was: Ph-OH ≈ 1°-OH >> 2°-OH did. The results for MWL is the average for all the types of Ph-OH, 1°-OH and 2°-OH groups respectively. The model only has one specific environment for each type of OH, so a different result is not that surprising.

Figure 6.17. Relative rates of reaction for the model (Carbon NMR)

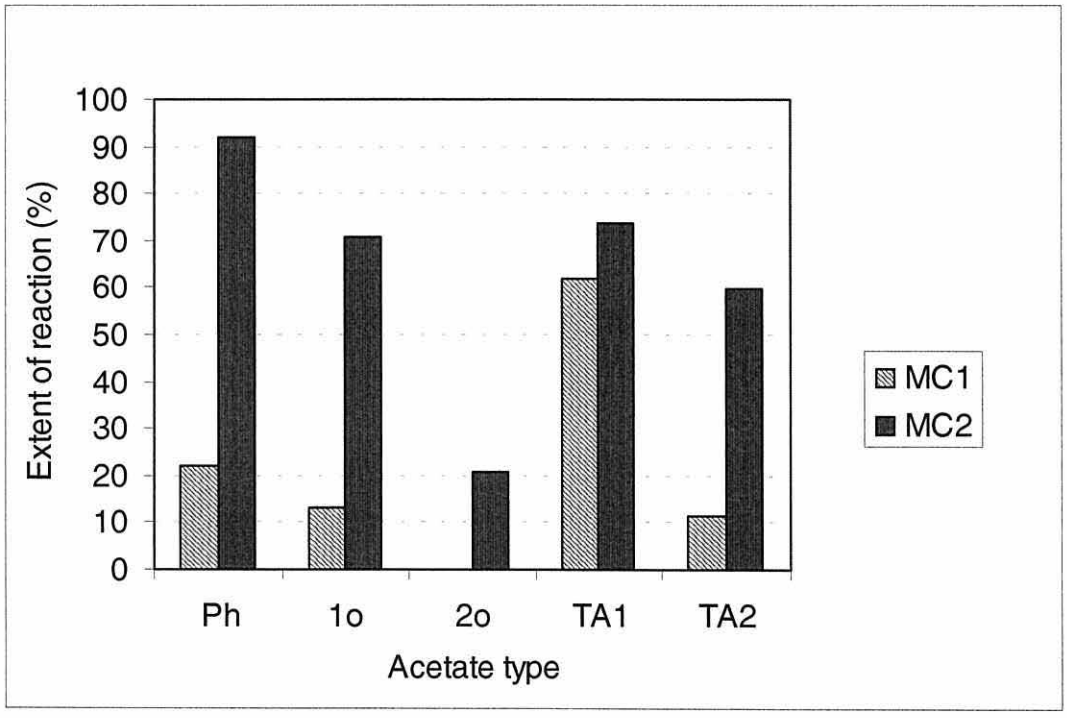

where MC1 is the partially acetylated model from reaction at 60 °C for 40 minutes, and MC2 is from the reaction at 80 °C for 60 minutes

Figure 6.18. Relative rates reaction for MWL (Carbon NMR)

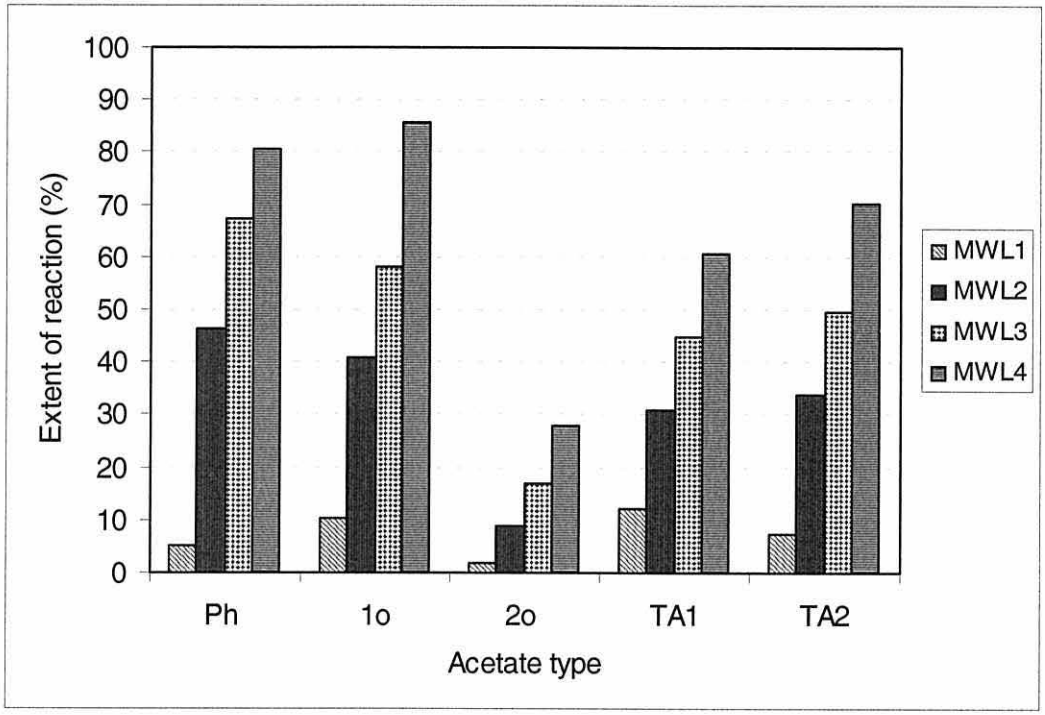

where MWL1, 2, 3, and 4 are reaction of MWL at 80 °C for 10 mins, 100 °C for 10 mins, 80 °C for 40 mins and 100 °C for 40 mins respectively

For the model, the direct measurement of total acetate (TA1) did not seem to be reliable at low levels of reaction as it greatly over-estimated the level of reaction (62.03%), compared to the additional total acetate (derived from the individual hydroxyl reaction, TA2) which was 11.35%, a much more likely figure. For MWL, the measurement of total acetate, TA1 (direct via peak at 21 ppm) and TA2 (addition of Ph + 1^{o} + 2^{o}, using peaks 168-171 ppm) generally agreed (within error) for each of the four products examined.

6.5. Summary

Acetylation of the β-O-4 model compound showed that, in general, over the temperature range studied (60-90 °C), the reaction order of the OH groups was Ph-OH > 1^{o}-OH >> 2^{o}-OH, using ^{1}H NMR spectroscopic analysis. This order was in agreement to that found by Paulsson and other (1996), who used a range of model compounds.

When the relative rate of reaction was calculated for two reaction products using ^{13}C NMR analysis, the same relative reaction order was found. For one of the two samples, the ^{1}H NMR method gave a higher level of reaction for 1^{o}-OH than for the Ph-OH, but this could have been due to the higher error of measuring a low level of reaction. In comparison, investigation of four MWL reaction products gave an overall relative order of reaction of Ph-OH $\approx$ 1^{o}-OH >> 2^{o}-OH.

Activation energy values were obtained for the first time for the 2^{o}-OH (α-OH) reaction. They were obtained by two methods of calculating the initial rate constants (k_o) and were 30 kJ/mol (using the slope at 10% of the exponential asymptote) and 71 kJ/mol (using the slope of the first two reaction data points and zero). The latter value is probably the more reliable as the initial data did not fit the exponential curve well, and was similar to that obtained for MWL (80 kJ/mol).

CHAPTER 7: SUMMARY AND CONCLUSIONS

7.1. General aims of thesis

The aim of this study was to examine the (uncatalysed) wood-acetic anhydride reaction by studying the reaction with wood substrates such as wood blocks, ground wood and MDF fibre. The acetylation of isolated wood polymers such as cellulose, hemicelluloses and lignin, were also examined. A lignin model compound was investigated in order to examine the relative rates of reaction of the different hydroxyl groups within it. The focus on the work was, however, on the reaction of wood blocks and obtaining reliable kinetic data, which may help to understand the reaction in more depth. This data may help to manipulate similar chemical modification reactions of wood to obtain desired property improvement.

7.2. Summary of reaction of wood and wood-based substrates

It was found that the reaction profiles of solid wood blocks with pure acetic anhydride fitted reasonably well (at least for the first 200 minutes) to simple exponential curves between temperatures studied of 80-120 °C. The reaction of wood blocks was found to be diffusion controlled, rather than first order with respect to wood hydroxyl concentration. The Ea value obtained by using the initial rate method was relatively high for a diffusion-controlled reaction (34 ± 9 kJ/mol), although the reaction of wood blocks was possibly activation controlled (first order) for the first part of the reaction.

MDF (HTMP) fibre was also reacted with acetic anhydride and it was found that small but significant amounts of the substrate dissolved into the reaction solution. This made accurate assessment of the true extent of reaction difficult. The MDF fibre reaction showed the same general trends as the wood block reaction. The Ea values obtained for the MDF fibre reaction were higher (38-48 kJ/mol, solid WPG), than those for the wood block reaction. The solid WPG was the measurement of the extent of reaction from the weight gain of the MDF fibre, ignoring any dissolved substrate, and the total WPG, which

was the solid WPG plus the measured amount of dissolved substances. Unfortunately, the results for the total WPG of the MDF fibre was highly variable, and calculation of kinetic data was not reliable.

Ground wood reacted to a lesser extent when compared to the reaction of wood blocks. It was also found that the ground wood reaction was diffusion controlled, at least for reaction at 100-120 °C. This indicated that the rate-determining step was diffusion through the wood cell wall: the wood cell wall is present in both the ground wood and the wood block samples. The Ea values obtained for the ground wood reaction were higher (53-62 kJ/mol) than for the wood blocks, possibly because the reaction was less diffusion-controlled. It is possible that minor differences in the experimental procedure used in the ground wood reaction (better acetone washing or no vacuum-impregnation) may account for the observed difference in the reaction levels obtained.

The reaction of the partially delignified ground wood had been devised to examine *in situ* the influence lignin had on the wood acetylation reaction. Therefore, three samples of partially delignified ground wood, which had decreasing total lignin content, were reacted and kinetic data were produced. However, reaction levels were variable and no obvious trends were found. It was thought that the increase of acid soluble lignin (ASL) in the increasingly delignified samples might have changed the overall reactivity of the samples. For example, the most delignified sample (DWD) had a lignin content of 10.69%, of which 5.74% was ASL. In addition, the removal of the lignin from the cell wall may have created more micropores, thus improving diffusion.

There seemed to be a slight negative trend in activation energy (from initial rate constants) with increasing total lignin content of the ground wood samples. When the Ea (diffusion) values were compared, the opposite trend seemed to hold for delignified samples (excluding non-delignified ground wood); that is, an increase in Ea (diffusion) with increasing total lignin content. This latter trend would support the theory that removing lignin improved diffusion.

For diffusion controlled reactions, it might be expected that a comparison of the energy of diffusion (Ea (diffusion)) would be more relevant. Thus, the Ea (diffusion) values obtained for the wood blocks (42-44 ± 10 kJ/mol) were higher than those for ground wood (34 3 kJ/mol). This would follow, as the diffusion through the ground wood sample (0.250-0.425 mm) would be less hindered than through solid wood blocks.

It was not possible to form a model of the wood reaction from that of the reaction of the isolated wood components. However, a mathematical relationship of the wood block reaction to reaction temperature and reaction time was calculated, and fitted the observed data well. With slight adjustment of two of the equation parameters, the equation was able to model most (100-120 °C) of the ground wood reaction (not delignified). The form of the equation is shown in Equation 7.1, where A, B, C_1, C_2, D_1, and D_2 are unknown parameters; WPG is the extent of reaction, T is the reaction temperature (°C) and t is the reaction time (minutes).

$$WPG = A + (A-B).\exp(-\exp(C_1 + C_2.T).t) + (D_1 + D_2.T).\sqrt{t} \quad \text{..... Equation 7.1}$$

where (for wood blocks) A = 15.62, B = 28.24, C_1 = -15.50,
C_2 = 0.09899, D_1 = -0.06565, D_2 = 0.00218

7.3. Summary of wood carbohydrate reactions

The reaction of holocellulose (delignified ground wood) was at a much lower level than the wood block reaction, as expected. The initial rates at each temperature did not yield k_o values that fitted the Arrhenius equation, probably due to the high level of variability of the results. The reaction of cellulose was very low for all the temperatures studied, as expected under these conditions. Any Ea value obtained for the cellulose reaction under these conditions would have significant error with such low reaction levels.

The reaction of native hemicelluloses (found by subtraction of the cellulose reaction from the holocellulose reaction level) was much higher of that of the cellulose, especially at longer reaction times. The reaction of the isolated hemicelluloses (xylan and glucomannan) was found to be much lower than expected for the native hemicelluloses. Therefore, the isolated hemicelluloses were examined by FTIR and further reacted with two catalysts (pyridine or acetic acid) to maximise the level of reaction. Catalysis did improve the level of reaction observed; however, the levels of acetylation reached were only a little more than expected for the uncatalysed reaction. The decrease in reactivity for the isolated hemicelluloses was probably due to hornification during drying. As neither of the catalysts increased the reaction for cellulose under these conditions, increase in the holocellulose reaction observed would be due to the native hemicelluloses present in holocellulose sample. Moreover, the more effective catalyst for holocellulose was pyridine. In contrast, the more effective catalyst for the isolated hemicelluloses was acetic acid. It was therefore decided that the isolated hemicelluloses would not produce reaction or kinetic data that would be useful and so further studies on them were not pursued.

7.4. Summary of lignin reactions

It was found that the reaction profiles of the commercially obtained softwood alkali lignin (AL) from a Kraft pulping process was very similar to that of the milled wood lignin (MWL) isolated from radiata pine sapwood. This was more so at the lower temperatures. At the higher temperatures, the AL reacted to a slightly greater extent (or rate) than did the MWL. A bagasse lignin (BL) obtained from an organosolv process reacted to a lesser extent (and rate) than either AL or MWL.

The activation energy (Ea) values obtained for both AL and MWL were very similar (~80 kJ/mol), whereas the Ea value for BL was lower (~58 ± 17 kJ/mol), but had a higher level of error.

In general, the lignin reaction (29% of the MWL reaction) was similar in shape and acetylation range obtained to that of the wood block reaction. This was less so for reaction at the higher temperatures (eg 110 °C), where the lignin reaction initially had a higher level of acetylation than the wood reaction, before levelling off as near to full reaction was obtained. However, at this point, the wood reaction kept increasing. From this, it was suggested that at lower temperatures, lignin reaction could be the dominant reaction within wood. However, it was not possible during this study to fully investigate the native hemicellulose reactivity within wood. In addition, at higher temperatures, it was thought that the hemicelluloses react to a greater extent and/or less accessible lignin hydroxyl groups are made more accessible by the swelling of the wood cell wall upon reaction.

It seems that while the reaction profile of the isolated lignin reaction is similar at lower temperatures, it was not possible to predict kinetic data for wood from the reaction of isolated lignins. This was probably due to the differences in the physical structure of the wood and isolated lignin preparations, as well as the contribution that hemicelluloses made to the overall wood reaction level.

7.5. Summary of the lignin model compound reaction

Acetylation of the β-O-4 lignin model compound showed that in general, over the temperature range studied (60-90 °C), the reaction order of the OH groups was Ph-OH > 1°-OH >> 2°-OH, using ^{1}H NMR spectroscopic analysis.

When the relative rate of reaction was calculated for two reaction products of the model using ^{13}C NMR analysis, the same relative reaction order was found. In comparison, investigation of four MWL reaction products gave an overall relative order of reaction of Ph-OH ≈ 1°-OH >> 2°-OH.

Activation energy values were obtained for the first time for the 2°-OH (α-OH) reaction. They were obtained by two methods of calculating the initial rate constants (k_o) and were 30 kJ/mol (using the slope at 10% of the exponential asymptote) and 71 kJ/mol (using the slope of the first two reaction data points and zero). The latter value is probably the more reliable as the initial data did not fit the exponential curve well, and was similar to that obtained for MWL (80 kJ/mol). This result illustrates the importance of the method for calculating initial rate constants, that the slope is a good fit of the initial data.

7.6. Conclusions

The reaction of uncatalysed acetic anhydride and solid wood blocks was confirmed to be diffusion controlled, rather than activation controlled. The diffusion is through the wood cell wall, and is also significant in influencing the rate of reaction in ground wood (0.250-0.425 mm). This has implications to how these types of wood reactions can be manipulated. Permeability and density are likely to be influential on the rate of reaction, as are swelling solvents or catalysts.

It was not possible to form a model for reaction based on the chemical composition of the wood. However, it was possible to mathematically model the wood block (and ground wood) reaction based on reaction time and temperature. This relationship may be helpful in predicting level of reaction in larger scale treatments. However, the effect of warming and cooling times would need to be determined, as well as the effect of wood dimensions on diffusion.

A relatively low apparent activation energy was obtained for radiata pinewood blocks (34 kJ/mol), which was lower than others (Hill *et al.,* 1998) have found for Corsican pine (51 kJ/mol) from initial rate constants. The equivalent value for ground wood was higher at around 53-62 kJ/mol. The reaction level was lower for the ground wood compared to the wood blocks.

The values for the activation energy of diffusion (Ea (diffusion)) supported the explanation of the rate-determining diffusion being through the cell wall. For example, the Ea (diffusion) for wood blocks was higher than for ground wood.

Examining partially delignified ground wood as a way to track the effect of a decreasing lignin content was not very successful. This may be due to the increasing acid soluble lignin content with decreasing lignin content, due to the chlorite delignification process used, or perhaps the removal of lignin created more micorpores that aided diffusion.

Examining completely delignified ground wood, holocellulose, and comparing the reaction to that of ground wood and cellulose, was a better way to examine the hemicellulose reaction than by examining isolated hemicelluloses. Solid state NMR could become a useful tool in ascertaining extent of acetylation in these and other solid samples, such as ground wood.

The reaction of a commercial alkali lignin from mixed softwoods gave surprisingly similar results to that of the milled wood lignin isolated from radiata pine. The isolated lignin reaction was not enough to explain or model the wood reaction due to the diffusion control of the latter and the reaction over longer reaction times of the hemicelluloses.

The one lignin model compound studied showed that the relative rate of reaction of the hydroxyl groups of this compound was phenolic hydroxyl reacted faster than the primary hydroxyl, which both reacted a great deal faster than the secondary hydroxyl. This was a similar result to that found for lignin (MWL), which found in four reaction products that the phenolic and the primary hydroxyl reacted at a similar rate, and were both much faster than the secondary hydroxyl.

7.7. Future work

Overall, this study demonstrated the importance of the wood ultra-structure in determining the rate of reaction of acetylation. The isolated wood components

were therefore found to be of less importance due to the diffusion control of the reaction. In particular, isolated lignin did not model the kinetics observed in solid wood.

Therefore, for future work, the focus would need to be on wood-based substrates of interest; that is, solid wood, ground wood, MDF fibre or wood pulp. Of particular interest would be the effects of block size (timber dimensions), wood density, ground wood particle size, and the influence of refining parameters for MDF fibre, as these are parameters that would potentially affect diffusion through the solid substrate. Different workers appear to obtain slightly different activation energy values for different wood species, although method differences may account for some of the range observed.

In a study of finite length, it is not possible to answer all the questions that are raised from the work. Therefore, there are a few potential areas of study that remain. These are the validation of a solid state NMR method to determine extent of reaction in acetylated samples of various kinds; further investigation of the MDF fibre and holocellulose reaction; and possible extension of the number of lignin model compounds studied.

In more detail, the validation of a solid state ^{13}C NMR spectroscopic method for determination of extent of reaction for acetylation would require a much greater number of samples which would also have extent of reaction determined by another method as well. This NMR method has great potential, as it is relatively quick, easy and non-destructive (although solid wood samples would need to be ground).

The MDF fibre reaction data obtained was highly variable, due to a significant amount of the substrate dissolving in the reaction solution. A different method of determining extent of reaction may avoid this variability. Alternatively, using a vapour phase treatment of the fibre would probably avoid the dissolution problems, although this would probably alter the kinetics from a liquid-fibre

reaction. In particular, it would be interesting to investigate how much diffusion dominates the reaction of MDF fibre.

The holocellulose reaction seemed to be diffusion controlled over the whole reaction at 120 °C, but first order kinetics seemed to be more dominant at the lower temperatures studied. The reaction of holocellulose would need to be studied in greater depth for a fuller, more definite kinetic description, taking note of the significant dissolution at longer reaction times. This is a reaction that might successfully be studied with solid state NMR spectroscopy.

An extension of the number and type of lignin model compounds may give a more accurate view of what happens in lignin within the wood. In particular, reaction information from a non-phenolic model could be useful. A change in experimental design may allow the more accurate measurement of lower temperatures and shorter reaction times; for example, the reaction of models using deuterated acetic anhydride in NMR tubes, and following extent of reaction by ^{1}H NMR spectroscopy.

Appendix A. Yields from the wood carbohydrate extractions

Sample	Batch	----- Amount (g) -----		------- Yield [c] (%) -------	
		Starting material [a]	Product	(of starting material)	(of wood [b])
Xylan	1	50	4.5	9.0	
	2	50	2.3 [d]	4.6	
	3	67	5.96	8.9	
	4	67	5.28	7.9	
	Total	234	18.04	7.7	5.6
Glucomannan	1	50	1.17	2.3	
(1st extraction)	2	50	2.10	4.2	
	3	67	3.49	5.2	
	4	67	1.93	2.9	
	Total	234	8.69	3.7	2.8
Glucomannan	1/2	100	9.85	9.9	
(2nd extraction) [e]	3/4	134	14.6	10.9	
	Total	234	24.45	10.4	7.6
Cellulose	1	50	32.5	65.0	
	2	50	29.5	59.0	
	3	67	40.97	61.1	
	4	67	42.18	63.0	
	Total	234	145.15	62.0	46.8

a Starting material was Holocellulose A (delignified wood meal)
b Calculated assuming lignin content of 27%
c Without correction for ash content
d From a batch of delignified wood meal with lower lignin content
e This second extraction of GM was found to be very high in ash, and so was not used.

Appendix B. Integrator and temperature settings for GC analysis of acetyl content

Variable	Maximum	Set	Actual
TEMP1 (°C)	400	140	140
TIME1	0.00		
INJ TEMP (°C)	400	160	160
FID TEMP (°C)	400	220	220
CHT SPD	0.2		
ZERO	10.0		
ATTN 2↑	3		
FID SGNL	+B		
SLP SENS	0.00	0.56	
AREA REJ		0	
FLOW A	0.0	0.2	
FLOW B	0.0	0.2	
STOP (time in mins)	35.00		

Appendix C. Conditions used for the carbohydrate analysis on the Dionex Ion Chromatography system.

The following conditions were used for the analysis:

Columns: CarboPac PA1 analytical column (4 x 250 mm) preceded by a CarboPac PA1 guard column (4 x 50 mm).

Eluant: A. MilliQ water B. 0.5 mol/L NaOH (carbonate-free)

Flow rate: 1 ml/min.

Sample size: 20 µl

Run time: 35 mins for separation of carbohydrates, 20 mins for column regeneration

Pump program:

Step1: for separation of carbohydrates

Time 0.00 min 100% water at 1 ml/min

Time 0.10 min open injector valve

Time 4.00 min close injector valve

Step 2: to regenerate column (remove any carbonate)

Time 35.0 min 100% water (eluant A) at 1 ml/min

Time 35.1 min 50 % A (water), 50 % B (NaOH) at 1 ml/min

Time 45.2 min 100% water (A)

Detection: Dionex pulsed amperometric detector with gold working electrode set at the following potentials: +0.2 V for 0.0 s to 0.3 s, +0.6 V for 0.3 s to 0.41 s, -0.9 V for 0.42 s to 0.72 s. Integration time 0.28-0.30 s

Post column treatment: 0.30 mol/L NaOH is added to the post column stream before the detector

Appendix D. Moisture content and reaction data from the effect of oven-drying experiment.

Sample	Air dry wt (g)	MC (%)	"OD" untreated wt (g)	Reacted OD wt (g)	WPG
W-Ma	1.0297	8.33	0.9505	1.0909	14.77
W-Mb	0.9518	8.28	0.8790	1.0057	14.41
W-Mc	1.0271	8.53	0.9464	1.0937	14.73
				Average	14.64
				s.d.	(0.20)

Appendix E. Comparison between lignin content and FTIR peak area ratio in delignified wood: Equations of fit and R^2 values.

(a) Total lignin content

(i) Linear

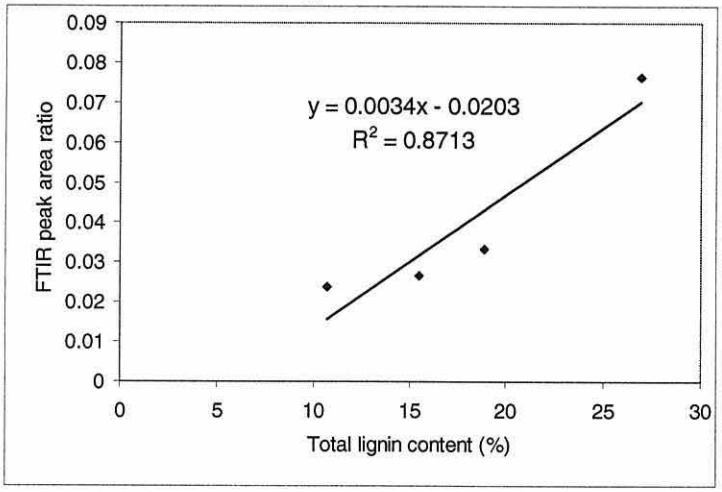

(ii) Exponential

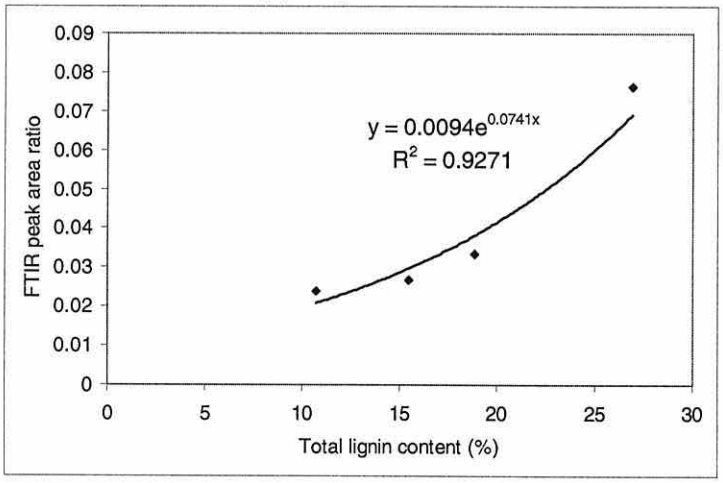

(iii) Polynomial

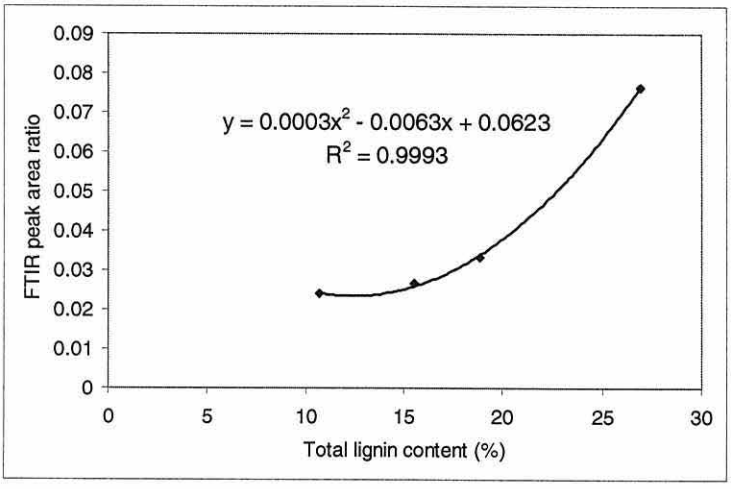

Appendix E. continued

(b) Klason lignin (KL)

(i) Linear

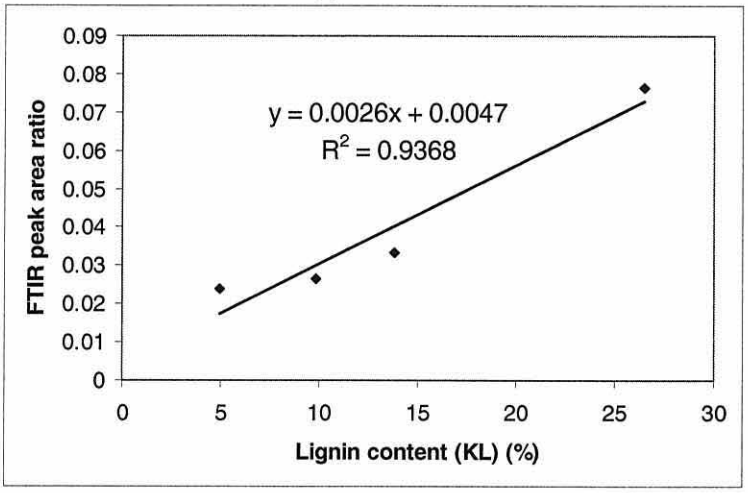

(ii) Exponential

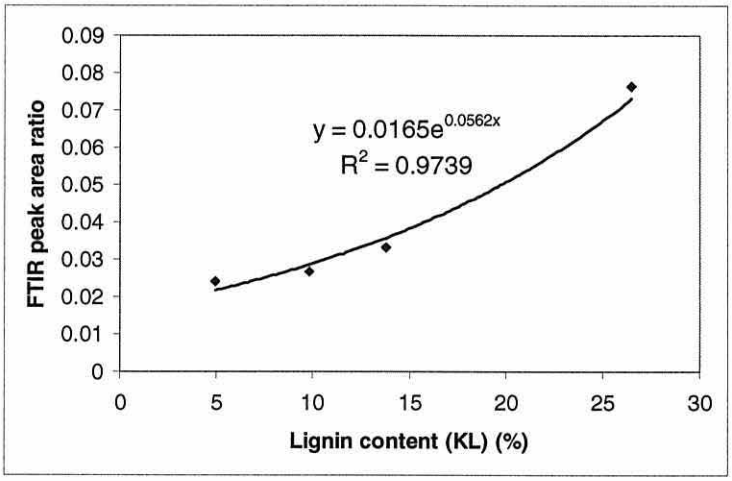

(iii) Polynomial

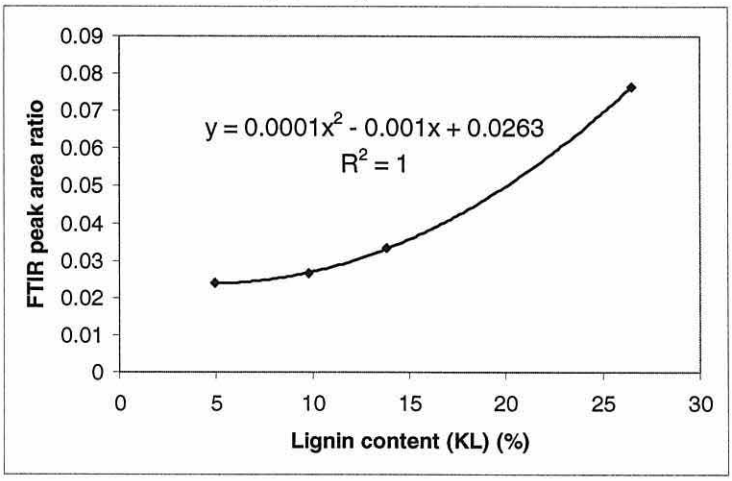

Appendix E. continued

(c) Acid soluble lignin (ASL)

(i) Linear

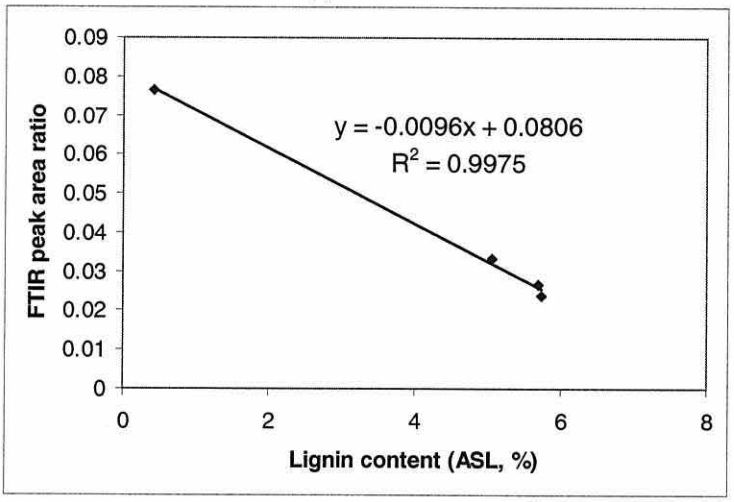

(ii) Exponential

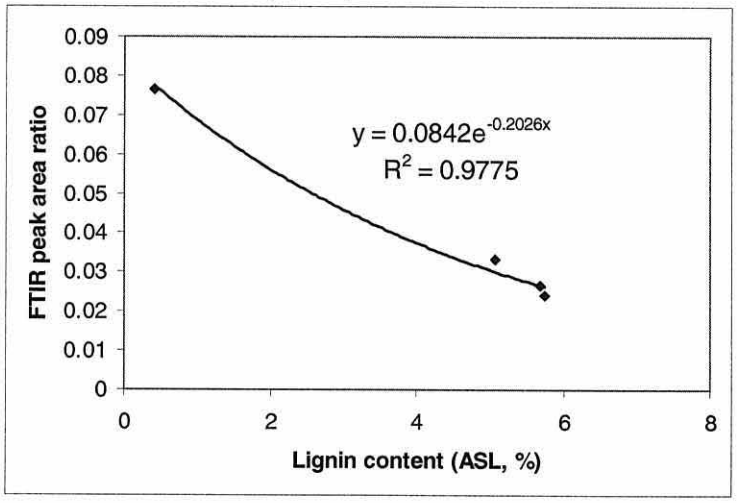

(iii) Polynomial

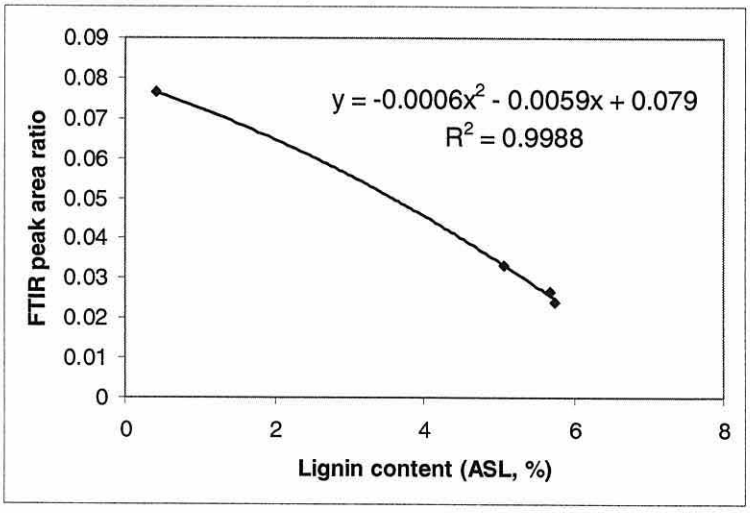

Appendix F. Raw reaction data and degree of fit of fitted curves for solid wood, fibre, holocellulose and cellulose

Data are in both WPG and mmoles reacted ($x10^4$, mol)
CV% is the co-efficient of variance (explained in Chapter 2)

(a) Solid wood blocks

Time	80 C			100 C			110 C			120 C		
reacted (mins)	Data (WPG)	Data (mol)	Curve (mol)	Data (WPG)	Data (mol)	Curve (mol)	Data (WPG)	Data (mol)	Curve (mol)	Data (WPG)	Data (mol)	Curve (mol)
0	0	0	0	0	0	0	0	0	0	0	0	0
10			3.74			5.0	4.47	10.63	6.23	7.02	14.42	13.27
20	2.51	5.98	6.47	3.67	8.740	9.078	5.25	12.49	11.41	10.09	24.00	22.22
30	3.83	9.11	8.47	5.48	14.54	12.40			15.71			28.25
40			9.92	5.69	12.956	15.12	7.65	18.65	19.29	13.64	32.47	32.31
60	4.80	11.42	11.77	6.30	15.00	19.13	9.37	22.30	24.74	14.14	33.66	36.90
90	5.34	12.7	13.06	7.59	18.06	22.79	12.50	29.74	29.93	16.43	37.56	39.55
105			13.37			23.93			31.63	15.87	37.76	40.07
120	6.19	14.73	13.56	10.2	24.31	24.77	13.53	32.20	32.91	17.20	40.94	40.36
140			13.71			25.55	15.37	36.58	34.16	17.75	42.23	40.55
180	5.53	13.16	13.83	11.11	26.42	26.43	14.73	35.05	35.61	18.53	44.1	40.68
Degree of fit - curve		80 C			100 C			110 C			120 C	
CV%		94.59			79.42			95.32			90.59	
Asymptote (a)		1.3882			2.7117			3.6944			4.0714	
Curve degree (b)		0.9691			0.9798			0.9817			0.9613	
Derivative at 10% a		0.01089			0.01382			0.01705			0.04016	

Appendix F. continued

(b) Fibre (solid WPG)

Time reacted (mins)	------ 80 C ------			------ 100 C ------			------ 110 C ------			------ 120 C ------		
	Data (WPG)	Data (mol)	Curve (mol)	Data (WPG)	Data (mol)	Curve (mol)	Data (WPG)	Data (mol)	Curve (mol)	Data (WPG)	Data (mol)	Curve (mol)
0			0			0			0			0
10			3.188			5.524			5.978	4.53	10.784	12.798
20			5.541			9.641	3.87	9.198	10.531	8.89	21.154	20.256
30			7.277	5.62	13.369	12.71			13.999			24.603
40			8.558	7.19	17.112	14.997	7.07	16.823	16.64	11.59	27.579	27.135
60	4.66	11.091	10.202	5.96	14.183	17.974	9.28	22.085	20.183	13.36	31.792	29.472
90	3.99	9.505	11.377			20.154	9.13	21.719	22.916			30.435
105			11.666			20.703			23.641	10.39	24.737	30.567
120	5.25	12.5	11.849	9.41	22.388	21.057			24.123			30.626
140			11.994			21.34			24.524	14.33	34.094	30.657
150			12.039			21.431			24.656			30.664
180	5.25	12.488	12.115			21.585			24.892			30.671
Degree of fit - curve		80 C			100 C			110 C			120 C	
CV%		20.12			57.84			93.66			84.04	
Asymptote (a)		1.2166			2.1695			2.5078			3.0673	
Curve degree (b)		0.9701			0.9710			0.9731			0.9474	
Derivative at 10% a		0.003327			0.005737			0.006146			0.01491	

Appendix F. continued

(c) Fibre (total WPG)

Time reacted	------ 80 C ------			------ 100 C ------			------ 110 C ------			------ 120 C ------		
(mins)	Data (WPG)	Data (mol)	Curve (mol)	Data (WPG)	Data (mol)	Curve (mol)	Data (WPG)	Data (mol)	Curve (mol)	Data (WPG)	Data (mol)	Curve (mol)
0			0			0			0			0
10			3.164			4.472			6.680	6.97	16.576	17.018
20			5.714			8.384	4.18	9.937	11.810	11.56	27.498	26.907
30			7.769	5.92	14.099	11.808			15.751			32.653
40			9.425	7.19	17.112	14.803	7.58	18.039	18.777	14.64	34.849	35.992
50			10.76			17.423			21.101			37.932
60	5.44	12.95	11.835	6.30	14.992	19.716	11.37	27.069	22.886	17.45	41.516	39.06
90	4.44	10.565	13.963			25.013	10.01	23.831	26.119			40.317
105			14.609			26.965			26.994	14.35	34.160	40.488
120	7.68	18.268	15.076	12.47	29.678	28.561			27.583			40.564
140			15.505			30.249			28.081	19.06	45.358	40.604
150			15.659			30.938			28.247			40.612
180	6.34	15.096	15.964			32.529			28.548			40.622
Degree of fit - curve		80 C			100 C			110 C			120 C	
CV%		26.14			78.34			84.19			86.68	
Asymptote (a)		1.6299			3.5758			2.8796			4.0624	
Curve degree (b)		0.9786			0.9867			0.9740			0.9472	
Derivative at 10% a		0.003166			0.004300			0.006840			0.01985	

Appendix F. continued

(d) Holocellulose

Time Reacted	------ 80 C ------			------ 100 C ------			------ 110 C ------			------ 120 C ------			
(mins)	Data (WPG)	Data (mol)	Curve (mol)	Data (WPG)	Data (mol)	Curve (mol)	Data (WPG)	Data (mol)	Curve (mol)	Data (WPG)	Data (mol)	Curve (mol)	Curve 2 (mol)
0		0	0		0	0		0	0		0	0	0
10			3.415			3.083			2.239	2.51	5.971	5.336	5.308
20			4.977			5.166	1.34	3.186	3.944	3.29	7.829	7.906	7.983
30	2.40	5.708	5.691	2.94	7.008	6.574			5.242			9.144	9.331
40			6.018	3.23	7.687	7.525	2.69	6.408	6.231	3.86	9.187	9.74	10.01
50			6.167			8.167			6.984	3.04	7.244	10.027	10.353
60	2.54	6.052	6.235	3.08	7.338	8.601	3.58	8.523	7.557	5.43	12.92	10.165	10.525
90	2.88	6.845	6.287			9.227	3.34	7.95	8.58	4.42	10.522	10.279	10.678
120	3.00	7.141	6.292	4.68	11.133	9.42			9.032			10.292	10.697
140			6.293			9.467			9.182			10.293	10.700
150			6.293			9.479			9.231			10.293	10.700
180	2.12	5.054	6.293			9.498			9.319				
240				3.58	8.522	9.505							

Degree of fit - curve	80 C	100 C	110 C	120 C	120 C (2)
CV%	9.445	48.25	88.74	48.59	65.26
Asymptote (a)	0.6293	0.9506	0.9389	1.0293	1.0700
Curve degree (b)	0.9248	0.9616	0.9731	0.9295	0.9338
Derivative at 10% a	0.004431	0.003354	0.002302	0.006769	0.0065995

Appendix F. continued

(e) Cellulose

Time reacted	------ 80 C ------			------ 100 C ------			------ 110 C ------			------ 120 C ------		
(mins)	Data (WPG)	Data (mol)	Curve (mol)	Data (WPG)	Data (mol)	Curve (mol)	Data (WPG)	Data (mol)	Curve (mol)	Data (WPG)	Data (mol)	Curve (mol)
0			0			0			0			0
10			1.399			1.862			2.570	1.74	4.139	4.172
20			2.427			3.058	1.48	3.519	3.795	2.03	4.835	4.664
30	1.57	3.746	3.182	1.88	4.483	3.826			4.379			4.722
40			3.738	1.70	4.052	4.319	2.12	5.052	4.657	1.53	3.648	4.728
50			4.145			4.636			4.790			4.729
60	1.65	3.937	4.445	1.62	3.843	4.839	2.36	5.623	4.853	2.38	5.670	4.729
90	1.87	4.458	4.946			5.108	1.67	3.98	4.904			4.729
120	2.25	5.345	5.145	2.74	6.527	5.179			4.910			4.729
140			5.205			5.194			4.910			4.729
150			5.224			5.197			4.910			4.729
180	2.36	5.608	5.255			5.202			4.910			4.729
240			5.273	1.90	4.528	5.204			4.910			4.729
Degree of fit - curve			80 C			100 C			110 C			120 C
CV%			64.54			17.45			39.83			10.095
Asymptote (a)			0.5276			0.5204			0.4910			0.4729
Curve degree (b)			0.9697			0.9567			0.9286			0.8075
Derivative at 10% a			0.001463			0.002074			0.003275			0.009102

Appendix G. Regression data for k_o values for the wood block reaction using both the initial methods.

T (°C)	Method [a]	k_o (x 1000)	CV % [b] or r^2	Asymptote [b] or slope (a)	Degree of curve [b] or intercept (b)
80	E	10.89	94.60	1.3882	0.9691
	Z	33.3	0.8973	0.0333	-0.1223
100	E	13.82	79.42	2.7117	0.9798
	Z	47.8	0.9946	0.0478	-0.0204
110	E	17.05	95.32	3.6944	0.9817
	Z	62.4	0.8585	0.062	0.1464
120	E	40.16	90.59	4.0715	0.9613
	Z	120	0.9866	0.12	0.0806

[a] Method is the manner in which the k_o values were calculated. E used slope at 10% of the exponential asymptote, and Z used the linear regression of the first two reaction data points and zero. Note: For the exponential method (E), the *a* and *b* values are from the equation, $y = a.(1 - b^x)$. For the zero method (Z), the *a* and *b* values are from the equation, $y = ax + b$

[b] These data related to the fit and equation of the exponential curve rather than the k_o value itself, for the E method.

Appendix H. The comparison of degree of fit for first and second order rate equations for the reaction of wood blocks.

	First order			Second order		
	k (x 1000) [a]	n [b]	r^2 (P) [c]	k (x 1000) [d]	n [b]	r^2 (P) [c]
80 °C	0.506	6	0.6543 (0.1)	30.1	6	0.6180 (0.1)
100 °C	1.0533	7	0.8472 (0.01)	101.4	7	0.9431 (0.001)
110 °C	1.6203	8	0.8933 (0.001)	164.4	8	0.8879 (0.001)
120 °C	1.864	9	0.7816 (0.01)	169.3	9	0.7276 (0.01)
			ave 0.794			ave 0.794
Ea (kJ/mol)	39.10			52.82		
Std.err.	3.43			9.08		
r^2 (P) [a]	0.9848 (0.01)			0.9442 (0.05)		

a Linear regression of a plot of ln (a_t/a_o) against reaction time, where a is the concentration of wood hydroxyl.

b Number of data pairs

c Levels of significance of Pearson's correlation coefficient on |r|.

d Linear regression of a plot of $1/a_t - 1/a_o$ against reaction time, where a is the concentration of wood hydroxyl.

Appendix I. Arrhenius plots for MDF fibre and ground wood

Arrhenius plots are obtained as follows: (a) the initial method using 10% of exponential asymptote, (b) initial rate using first two data points and zero

MDF fibre (solid WPG) (a)

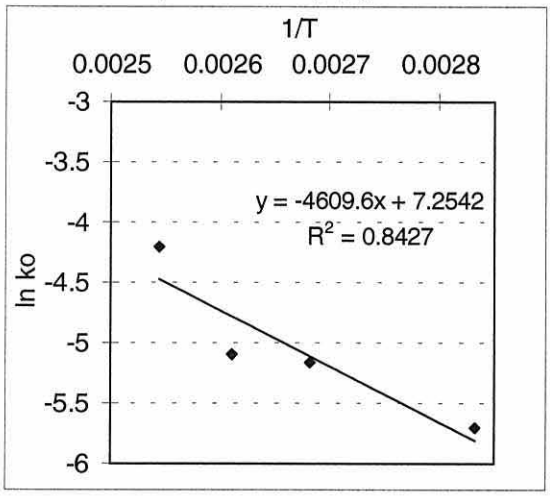

(b)

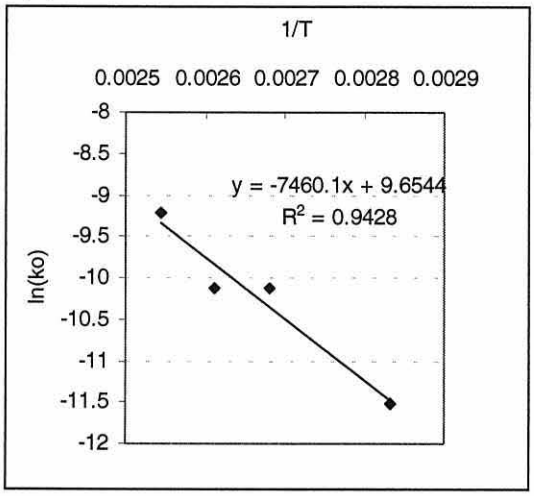

Ground wood (a)

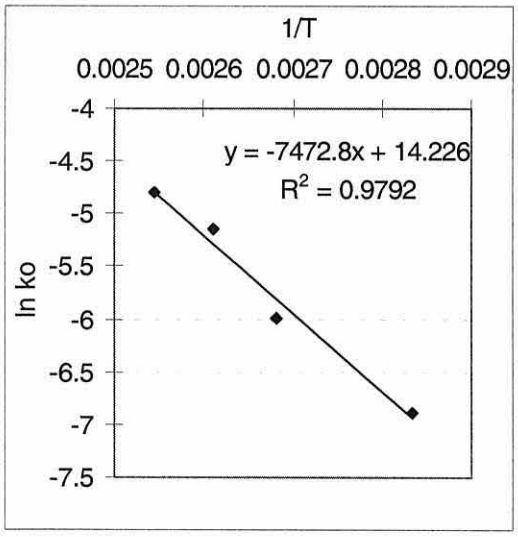

(b)

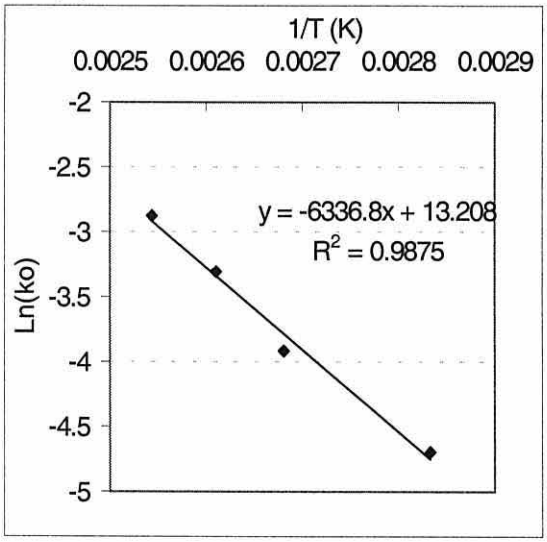

Appendix J. Comparison of the predicted wood reaction with observed wood reaction at each temperature.

These are the curves of apparent best using the lowest sum of squares. The values for PL, PH and PC were 0.2932, 0.2608, 0.4461 respectively, and the curves for the lignin, hemicellulose and cellulose were used for each temperature, rather than the data points.

Figure 1. Predicted wood reaction at 80°C

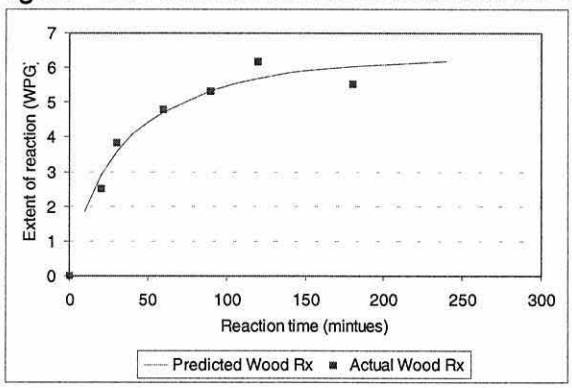

Figure 2. Predicted wood reaction at 100°C

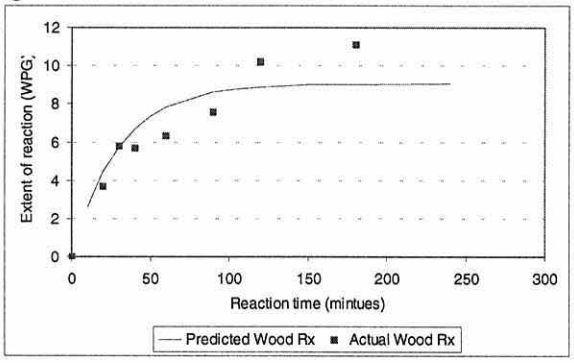

Figure 3. Predicted wood reaction at 110°C

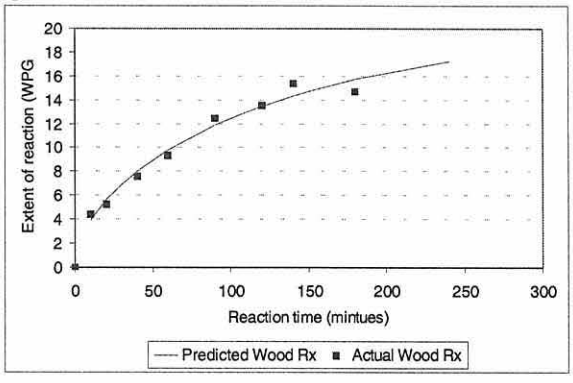

Appendix K. Degree of fit of the empirical model for the ground wood reaction.

It is obvious that a very similar curve can be obtained by using different DL, DH and DC values, as in the case of the reaction at 80°C (Figure 1). The plots are the solution for the lowest sum of squares unless stated. The data for the equation and the solutions are shown Table 1 (reproduced from Table 4.11).

Figure 1.Reaction of grd wood, 80°C

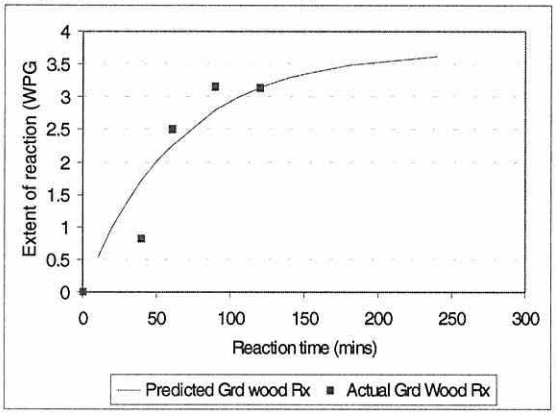

Figure 2.Reaction of grd wood, 100°C

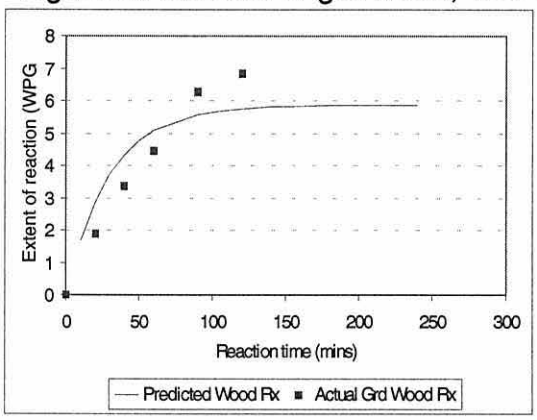

Figure 3. Reaction of ground wood at 110°C

(a) lowest sum sq.

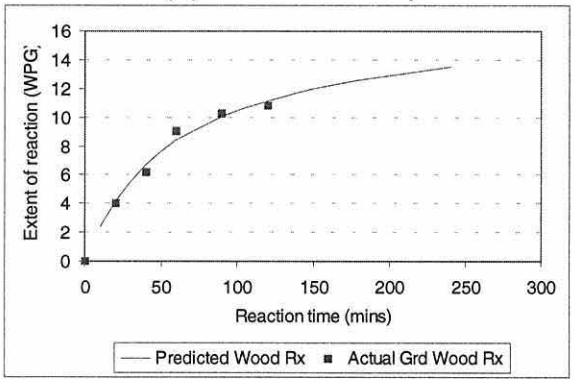

(b) sum of differences

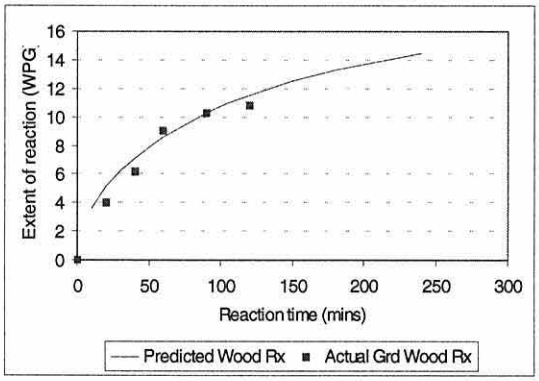

Appendix K. continued.

Table 1. Variables and degree of fit for predicted ground wood reaction equation

Temperature	DL	DH	DC	Sum sq	Sum Diff.
80°C a	0	0	3.73978	7.699	-0.2842
b	0.2	0	2.2	7.713	-0.3546
100°C a	0	2.7623	0	3.926	-0.7737
b	0.3	0.9	0.2	13.47	4.929
110 C° a	0	2.355	5.625	0.9639	0.1275
b	1	1	1	17.8	3.512
c	0.4	3	2	2.991	2.329

Appendix L. Degree of fit for the first order integral rate and diffusion equations for (a) the fibre (total) reaction, and

Reaction temperature	First order			Diffusion		
(°C)	r^2	n	P	r^2	n	P
80	0.6584	5	0.1	0.8384	5	0.05
100	0.9004	5	0.02	0.9417	5	0.01
110	0.8085	5	0.05	0.9108	5	0.02
120	0.6367	7	0.05	0.8336	7	0.01
average	0.7510			0.8811		

(b) the fibre (solid) reaction.

Reaction temperature	First order			Diffusion		
(°C)	r^2	n	P	r^2	n	P
80	0.8314	5	0.1	0.8981	5	0.02
100	0.8679	5	0.05	0.9258	5	0.01
110	0.9232	5	0.01	0.9537	5	0.01
120	0.7655	7	0.01	0.8767	7	0.01
average	0.8479			0.9136		

Note: P values are evaluated on |r| values, rather than the r^2 values listed here.

Appendix M. Reaction data and degree of fit of fitted curves for delignified ground wood samples.

Data is in mmol (ie multiplied by 1000). Curve 1 was the exponential curve, Curve 2 was the sigmoid curve

Sigmoid equation was $y=\beta^{(1/\gamma)}.(1-\exp(\alpha.t))^{(1/\gamma)}$

(a) Ground wood (26.9% total lignin content)

Time reacted	------ 80 C ------				------ 100 C ------			------ 110 C ------			------ 120 C ------		
(mins)	Data (WPG)	Data (mol)	Curve1 (mol)	Curve2 (mol)	Data (WPG)	Data (mol)	Curve1 (mol)	Data (WPG)	Data (mol)	Curve1 (mol)	Data (WPG)	Data (mol)	Curve1 (mol)
0	0	0	0	0	0	0	0	0	0	0	0	0	0
20			0.1895	0.2	1.91	0.4544	0.4493	4.02	0.9577	0.9561	5.82	1.3847	1.3664
40	0.82	0.1959	0.353	0.1955	3.36	0.7989	0.8089	6.17	1.4674	1.5962	9.51	2.2636	2.2907
60	2.50	0.5951	0.4938	0.5966	4.45	1.0587	1.0968	9.05	2.1548	2.0247	12.96	3.0832	2.9159
90	3.16	0.7511	0.6695	0.7434	630	1.4986	1.4247	10.32	2.4555	2.4172	13.42	3.1932	3.4957
120	3.15	0.7493	0.8101	0.7557	6.83	1.625	1.6595	10.82	2.5743	2.6322	16.71	3.9772	3.8183
140			0.8880	0.7565			1.7777			2.7183			3.9492

Degree of fit- curve	80 C (C1)	80 C (C2)	100 C	110 C	120 C
CV%	77.96	99.95	99.13	97.98	96.27
Asymptote (a) or α	1.3745	0.08632	2.252	2.893	4.223
Curve degree (b) or β	0.9926	0.9934	0.9889	0.9801	0.9806
Sigmoid γ		0.02377			
Slope (10% a for exp)	0.0012	0.00232	0.0025	0.0058	0.0083

Appendix M. continued

(b) Delignified ground wood sample DWB (18.9 % total lignin content)

Time reacted	------ 80 C ------				------ 100 C ------			------ 110 C ------			------ 120 C ------		
(mins)	Data (WPG)	Data (mol)	Curve1 (mol)	Curve2 (mol)	Data (WPG)	Data (mol)	Curve2 (mol)	Data (WPG)	Data (mol)	Curve1 (mol)	Data (WPG)	Data (mol)	Curve1 (mol)
0	0	0	0	0	0	0	0	0	0	0	0	0	0
20			0.1406		0.15	0.0352		1.85	0.4407	0.6736	5.08	1.2094	1.4168
40			0.1959	0.0721	1.22	0.2913	0.2373	4.91	1.1689	1.1966	10.83	2.5784	2.4229
60	0.87	0.2072	0.2177	0.2087	2.86	0.6816	0.7726	7.19	1.7122	1.6025	13.93	3.3152	3.1372
90	1.12	0.2656	0.2283	0.2336	5.82	1.3858	1.2441	9.34	2.2237	2.0478	14.82	3.5261	3.8399
120	0.86	0.2040	0.2310	0.2344	5.40	1.2843	1.3710	9.27	2.2052	2.3523	18.46	4.3928	4.2603
140				0.2345			1.3938			2.4998			4.4419

Degree of fit- curve	80 C (C1)	80 C (C2)	100 C (C2)	110 C	120 C
CV%	7.48	18.88	97.19	94.77	96.23
Asymptote (a) or α	0.2318	-0.1154	-0.0523	3.012	4.887
Curve degree (b) or β	0.9544	0.9878	1.0256	0.9874	0.9830
Sigmoid γ		0.00843	0.0001		
Slope (10% a for exp)	0.0011	0.000237	0.00185	0.0038	0.0084

Appendix M. continued

(c) Delignified ground wood sample DWC (15.5 % total lignin content)

Time reacted	------ 80 C ------			------ 100 C ------			------ 110 C ------			------ 120 C ------		
(mins)	Data (WPG)	Data (mol)	Curve1 (mol)	Data (WPG)	Data (mol)	Curve2 (mol)	Data (WPG)	Data (mol)	Curve1 (mol)	Data (WPG)	Data (mol)	Curve1 (mol)
0	0	0	0	0	0	0	0	0	0	0	0	0
20			0.1037	0.74	0.1752	0.1087	2.35	0.5589	0.7489	5.69	1.3538	1.5794
40			0.1727	1.85	0.4395	0.4627	5.56	1.3228	1.3322	12.42	2.9563	2.6657
60	0.94	0.2242	0.2185	3.37	0.8020	0.8553	7.97	1.8971	1.7864	14.69	3.4964	3.4129
90	1.04	0.2488	0.2602	5.79	1.3775	1.2846	9.95	2.3684	2.2864	15.63	3.7206	4.1199
120	1.21	0.2888	0.2827	6.18	1.4704	1.5167	10.68	2.5425	2.6301	19.88	4.7315	4.5232
140			0.2917			1.6005			2.7971			4.6904
Degree of fit- curve		80 C			100 C (C2)			110 C			120 C	
CV%		90.72			98.56			97.61			94.40	
Asymptote (a) or α		0.3095			-0.02686			3.3852			5.0587	
Curve degree (b) or β		0.9798			1.1889			0.9876			0.9815	
Sigmoid γ					0.3177							
Slope (10% a for exp)		0.00063			0.001569			0.004232			0.009467	

Appendix M. continued

(d) Delignified ground wood sample DWD (10.7 % total lignin content)

(1) Exponential curves

Time reacted	------ 80 C ------			------ 100 C ------			------ 110 C ------			------ 120 C ------		
(mins)	Data (WPG)	Data (mol)	Curve1 (mol)	Data (WPG)	Data (mol)	Curve1 (mol)	Data (WPG)	Data (mol)	Curve1 (mol)	Data (WPG)	Data (mol)	Curve1 (mol)
0	0	0	0	0	0	0	0	0	0	0	0	0
20			0.1122			0.1806	1.78	0.4238	0.6024	3.86	0.9188	1.0557
40			0.1947	1.48	0.3532	0.3495	4.16	0.9904	1.0592	8.63	2.0544	1.9148
60	0.98	0.2331	0.2553	1.84	0.4369	0.5075	6.32	1.5044	1.4056	11.67	2.7761	2.6137
90	1.50	0.3580	0.3176	3.43	0.8164	0.7256	8.34	1.9858	1.7747	12.99	3.0903	3.4258
120	1.42	0.3370	0.3569	3.74	0.8893	0.9230	7.79	1.8533	2.0184	17.53	4.1708	4.0218
140			0.3747			1.0440			2.1329			4.3282
Degree of fit- curve			80 C			100 C			110 C			120 C
CV%			71.83			93.34			98.37			99.62
Asymptote (a)			0.4241			2.7973			2.4921			5.6662
Curve degree (b)			0.9848			0.9967			0.9863			0.9897
Slope (10% a for exp)			0.00065			0.00093			0.00345			0.00584

Appendix M. continued

(d) DWD continued

(2) Sigmoid curves

Time reacted	------ 80 C ------		------ 100 C ------		------ 110 C ------		------ 120 C ------	
(mins)	Data (mol)	Curve1 (mol)	Data (mol)	Curve (mol)	Data (mol)	Curve (mol)	Data (mol)	Curve (mol)
0	0	0	0	0	0	0	0	0
20				0.1139	0.4238	0.3758	0.9188	1.0629
40		0.011	0.3532	0.3146	0.9904	1.0512	2.0544	1.9144
60	0.2331	0.2338	0.4369	0.5129	1.5044	1.5182	2.7761	2.6089
90	0.3580	0.3445	0.8164	0.7511	1.9858	1.8436	3.0903	3.4218
120	0.3370	0.3498	0.8893	0.9135	1.8533	1.9533	4.1708	4.0257
140		0.3500		0.9881		1.9807		4.3398

Degree of fit- curve	80 C	100 C	110 C	120 C
CV%	96.13	94.398	97.82	96.60
Sigm α	-0.1078	-0.0172	-0.0388	-0.00976
Sigm β	0.9960	1.0916	1.2912	5.9989
Sigm γ	0.00385	0.5273	0.3676	1.0201
Initial slope	0.0008756	0.0009139	0.00282	0.00525

Appendix N. Initial rate data for delignified ground wood series

Sample	Method [a]	k_o values (x 1000)			
		80 °C (CV%, r^2) [b]	100 °C (CV%, r^2) [b]	110 °C (CV%, r^2) [b]	120 °C (CV%, r^2) [b]
GW	E	1.020 (78.0)	2.506 (99.1)	5.804 (98.0)	8.254 (96.3)
	S	0.837 (99.9)	--	--	--
	Z	9.2 (0.859)	20.0 (0.994)	36.7 (0.970)	56.6 (0.984)
DWB	E	1.082 (7.5)	--	3.812 (94.8)	8.366 (96.2)
	S	0.237 (18.9)	1.855 (97.2)	--	--
	Z	88.8 (0.655)	619.4 (0.769)	1013.1 (0.917)	1760.7 (0.959)
DWC	E	0.632 (90.7)	--	4.232 (97.6)	9.467 (94.4)
	S	0.419 (84.8)	1.569 (98.6)	--	--
	Z	11.6 (0.850)	47.5 (0.795)	142.0 (0.951)	314.3 (0.995)
DWD	E	0.651 (71.8)	0.933 (93.3)	3.448 (98.4)	5.842 (99.6)
	S	0.876 (96.1)	0.914 (94.4)	2.820 (97.8)	5.251 (96.6)
	Z	138.7 (0.831)	367.5 (0.819)	865.3 (0.890)	1675 (0.931)

[a] Method is the manner in which the k_o values were calculated. E was the slope at 10% of the exponential asymptote, S was the initial slope of a sigmoid curve, and Z was the linear regression of the first two data points and zero.
[b] CV% is given as the fit of the data to an E or S curve (rather than the fit for the k_o itself). The r^2 values are the linear regression fit of the first two data points and zero.

Appendix O. Degree of fit for activation energy values from all types of k_o values for the delignified wood series.

Sample	Method [a]	Ea, kJ/mol (std err)	r^2 (P) [b]	Average CV% *or* r^2 [c]
GW	E	62.13 (6.40)	0.9792 (0.02)	92.84
	E/S	68.06 (5.40)	0.9815 (0.01)	98.33
	Z	52.68 (4.19)	0.9875 (0.01)	*0.9516*
DWB	E	56.02 (9.55)	0.9718 (0.02)	66.16
	E/S	102.63 (4.06)	0.9969 (0.01)	76.77
	Z	95.60 (7.57)	0.9876 (0.01)	*0.8977*
DWC	E	75.36 (5.50)	0.9948 (0.01)	94.24
	E/S	77.50 (11.56)	0.9574 (0.05)	95.32
	Z	90.43 (16.79)	0.9355 (0.05)	*0.8249*
DWD	E	65.00 (18.72)	0.8577 (0.1)	90.79
	E/S	56.17 (22.11)	0.7634 (NS)	97.13
	S	51.74 (20.31)	0.7644 (NS)	96.24
	Z	74.74 (17.06)	0.9057 (0.05)	*0.8650*

[a] Method used to calculate the k_o values where E = from 10% of exponential curves, E/S = from either sigmoid or exponential curves (whichever was the best fit), S = from sigmoid curves only, and Z = from the linear regression of the first two reaction data points and zero

[b] The r^2 values relate to the activation energy (Ea) calculations, with the Ea calculated from the best fit data. P is the probability of the result being significant from Pearson's correlation coefficient on |r|, with n=4; NS is not significant.

[c] The r^2 values here are for the linear regression of the k_o values and are shown in italics. CV% is given as the fit of the data to an E or S curve (rather than the fit for the k_o itself).

Appendix P. Degree of fit for the delignified ground wood samples' reaction data to the diffusion equation.

Sample	T (°C)	A	c	r^2	n	P
GW	80	0.3346	0.4266	0.7997	9	0.01
	100	0.7031	0.7922	0.9343	15	<0.001
	110	1.0674	0.2237	0.9617	11	<0.001
	120	1.5433	0.3178	0.9744	11	<0.001
DWB	80	0.0888	-0.0972	0.6545	7	0.05
	100	0.6194	1.4308	0.7693	10	0.001
	110	1.0131	1.259	0.917	11	<0.001
	120	1.7607	1.0025	0.9586	11	<0.001
DWC	80	0.11	-0.0287	0.9079	7	0.001
	100	0.6828	1.5818	0.8499	11	<0.001
	110	1.1185	1.2885	0.9404	11	<0.001
	120	1.8569	0.7395	0.9525	11	<0.001
DWD	80	0.1387	0.0028	0.8307	7	0.01
	100	0.3675	0.4883	0.8085	9	0.001
	110	0.8653	0.9704	0.8903	11	<0.001
	120	1.6747	1.9299	0.9306	11	<0.001

Note: these data are calculated on the extent of reaction in WPG units, on the individual data and included the origin. The diffusion equation was the extent of reaction plotted against the square root of reaction time, and the linear regression equations are given in the table and are of the form $y = ax - c$, where y is the WPG, and x is square root time.

Appendix Q. Regression data for the activation energy of diffusion values for the delignified ground wood samples

Sample	Ea (diffusion), kJ/mol (±std err)	n (P)	A (intercept)
GW	44.07 (1.41)	0.9980 (0.001)	13.90
DWB	86.61 (8.27)	0.9821 (0.01)	27.20
DWC	82.13 (7.58)	0.9833 (0.01)	25.89
DWD	71.78 (7.60)	0.9781 (0.02)	22.38

Note: these values change somewhat if zero is not used for the linear regression for the diffusion equation's *a* values. For example, for the ground wood (GW) sample, if zero is not used in the regression, an Ea (diffusion) value is 33.55 (± 2.74) kJ/mol, r^2=0.9869

Appendix R. Reaction data (WPG) and degree of fit of fitted curves for lignin.

(a) Alkali lignin (AL)

Time reacted	------ 80 C ------		------ 90 C ------		------ 100 C ------		------ 110 C ------	
(mins)	Data	Curve	Data	Curve	Data	Curve	Data	Curve
0	0	0	0	0	0	0	0	0
5		2.69	3.79	5.17	9.44	9.72	16.06	15.93
10	4.41	5.03	8.75	9.14	17.53	15.34	21.67	21.47
20	5.92	8.83	15.32	14.54	16.88	20.49	22.43	24.06
30	14.05	11.69		17.73	23.58	22.22		24.38
40	13.97	13.85	20.52	19.62		22.79	24.69	24.42
50		15.49		20.74		22.99		24.42
60	17.98	16.72	22.49	21.40	23.60	23.05	25.50	24.42
90	17.74	18.88	22.17	22.15		23.08		24.42

Degree of fit – exp curve	80 C	90 C	100 C	110 C
CV%	89.87	98.59	85.39	92.79
Asymptote (a)	20.51	22.35	23.09	24.42
Curve degree (b)	0.9723	0.9488	0.8965	0.8096
Derivative at 10% a	0.0577	0.1175	0.2523	0.5159

Appendix R. continued.

(b) Milled wood lignin (MWL)

Time reacted	------ 80 C ------		------ 90 C ------		------ 100 C ------		------ 110 C ------	
(mins)	Data	Curve	Data	Curve	Data	Curve	Data	Curve
0	0	0	0	0	0	0	0	0
10	0.83	3.92	8.68	8.12	11.47	11.32	18.17	18.45
20	6.91	7.25	11.06	13.30	16.27	17.15	22.53	21.68
30	13.14	10.07	19.34	16.60	21.12	20.14		22.25
40	13.86	12.47	17.69	18.71		21.68	21.64	22.35
50		14.51		20.05	22.73	22.47		22.37
60	20.72	16.24	20.95	20.90	22.35	22.88	22.49	22.37
90	15.97	20.02	21.92	22.02		23.25		22.37

Degree of fit - curve	80 C	90 C	100 C	110 C
CV%	89.62	90.71	97.76	89.75
Asymptote (a)	25.98	22.41	23.31	22.37
Curve degree (b)	0.9838	0.9560	0.9357	0.8401
Derivative at 10% a	0.0425	0.1008	0.1550	0.3897

Appendix R. continued.

(c) Bagasse lignin (BL)

Time reacted	------ 80 C ------		------ 90 C ------		------ 100 C ------		------ 110 C ------	
(mins)	Data	Curve	Data	Curve	Data	Curve	Data	Curve
0	0	0	0	0	0	0	0	0
10	5.28	4.75	6.75	5.74	8.86	8.07	14.63	14.46
20	5.45	7.38	8.85	9.20	10.28	12.02	16.3	16.82
30	10.47	8.84	11.58	11.28	15.24	13.96		17.21
40	9.51	9.64	11.3	12.54		14.90	17.55	17.27
50		10.09		13.29	15.64	15.37		17.28
60	11.24	10.34	13.95	13.75	15.11	15.59	17.42	17.28
90	9.58	10.59	14.76	14.28		15.78		17.28

Degree of fit - curve	80 C	90 C	100 C	110 C
CV%	74.30	93.39	86.30	93.17
Asymptote (a)	10.64	14.44	15.81	17.28
Curve degree (b)	0.9426	0.9505	0.9310	0.8343
Derivative at 10% a	0.0629	0.0732	0.1130	0.3132

Appendix S. Summary of initial rate constants of lignin reactions with different methods

Sample	Method [a]	Reaction Temperature (°C) (CV% for E or r^2 for Z)			
		80	90	100	110
Alkali lignin	E1	0.0577 (89.9)	0.1207 (98.3)	0.2371 (66.1)	0.4993 (61.3)
	E2	0.0572 (89.9)	0.1175 (98.6)	0.2523 (85.4)	0.5159 (92.8)
	Z	0.296 (*0.926*)	0.875 (*0.994*)	1.753 (*0.998*)	2.167 (*0.928*)
Milled wood lignin	E	0.0425 (89.6)	0.1008 (90.7)	0.1550 (97.8)	0.3897 (89.8)
	Z	0.346 (*0.839*)	0.553 (*0.902*)	0.814 (*0.947*)	1.127 (*0.889*)
Bagasse lignin	E	0.0629 (74.3)	0.0732 (93.4)	0.113 (86.3)	0.3132 (93.2)
	Z	0.273 (*0.773*)	0.443 (*0.916*)	0.514 (*0.851*)	0.815 (*0.826*)

[a] Method is the manner in which the k_o values were calculated. E1 or E used slope at 10% of the exponential asymptote. E2 used the same with extra reaction times for the AL sample only, and Z used the linear regression of the first two data points and zero.

[b] k_o values are given in WPG/ minute and should be used for internal comparison only.

Appendix T. Diffusion control test for the three lignin preparations.

Sample	T (°C)	r^2	n	|r|	P
AL	80	0.7958	12	0.8921	< 0.001
	90	0.8548	12	0.9246	< 0.001
	100	0.6790	19	0.8240	< 0.001
	110	0.4222	11	0.6498	0.05
	ave	0.6880			
MWL	80	0.6551	11	0.8094	0.01
	90	0.7333	10	0.8563	0.01
	100	0.8018	10	0.8954	0.001
	110	0.1825	8	0.4272	NS
	ave	0.5932			
BL	80	0.4319	11	0.6572	0.05
	90	0.9071	10	0.9524	< 0.001
	100	0.5989	10	0.7739	0.01
	110	0.4783	8	0.6916	0.1
	ave	0.6041			

Appendix U. Raw data of peak area calculations of acetates in NMR spectra from milled wood lignin reactions with acetic anhydride.

Functional group	Peak maxima (ppm)	MWL1 (0.83 WPG)	MWL2 (11.47 WPG)	MWL3 (14.57 WPG)	MWL4 (23 WPG)	MWL (fully acetylated)
1° acetate/OMe	170 / 55	0.0489	0.1923	0.2735	0.4024	0.4706
2° acetate/OMe	169 / 55	0.0036	0.0184	0.0353	0.0582	0.2088
Ph acetate/OMe	168 / 55	0.0083	0.0740	0.1079	0.1291	0.1602
Total acetate (TA1)	20 / 55	0.1828	0.4651	0.6732	0.9119	1.501
Total acetate (TA2, 1°+2°+Ph)	168-171 / 55	0.0608	0.2847	0.4167	0.5897	0.8396
% 1°		10.39	40.86	58.12	85.51	100
% 2°		1.724	8.81	16.91	27.87	100
% Ph		5.181	46.19	67.35	80.59	100
TA1		12.18	30.98	44.85	60.75	100
TA2		7.242	33.91	49.63	70.24	100

Note: The OMe peak areas were set to 1.0 for each spectrum and the other peak areas were given with respect to it. Percentages of acetates for each type (1°, 2°, phenolic) were obtained by using the ratios of acetate over OMe peak areas for the partially acetylated samples divided by the ratio for the same acetate for the fully acetylated sample.

Appendix V. Reaction data of the primary, secondary and phenolic hydroxyls of the lignin model compound.

T (°C)	Time reacted (mins)	5	4	3	2	1
FA MC	NA	1.0	0.0957	0.05378	0.3487	0.3062
Untreated	0	1.0	0.001	-0.009	-0.009	0.0024
60	5	1.0	0.0168	0.0431	0.2981	0.2343
	10	1.0	0.0218	0.05	0.3415	0.2376
	20	1.0	0.0099	0.0386	0.2858	0.0717
	40	1.0	0.0074	0.0235	*0.3021*	*0.1266*
	80	1.0	0.0088	0.0325	0.2619	0.01293
	120	1.0	0.0164	0.0417	*0.3696*	*0.1583*
	240	1.0	0.0112	0.0428	*0.1869*	*0.2565*
70	5	1.0	0.0097	0.0332	0.2837	0.1106
	10	1.0	0.0139	0.0461	0.318	0.1365
	40	1.0	0.0142	0.0403	0.3214	0.1304
	80	1.0	0.0185	0.0503	0.2875	0.1543
	120	1.0	0.0365	0.0529	0.3257	0.2627
	240	1.0	0.0365	0.0484	0.3384	0.2051
80	5	1.0	0.005	0.0021	*0.2908*	0.0898
	10	1.0	0.004	0.009	0.2252	0.079
	20	1.0	0.0107	0.0208	0.3087	0.1061
	30	1.0	0.0145	0.0333	0.3239	0.1178
	60	1.0	0.0236	0.0428	0.3437	0.1548
	90	1.0	0.0333	0.0346	0.3615	0.2071
90	5	1.0	0.007	0.0184	*0.3089*	*0.1327*
	10	1.0	0.0099	0.0127	0.3173	0.1125
	20	1.0	0.0144	0.0301	0.3094	0.1172
	30	1.0	0.0185	0.0324	0.299	0.1333
	60	1.0	0.0316	0.0411	0.3274	0.1762
	90	1.0	0.0508	0.0423	0.4503	0.2852

Regions are: 5 = ArH; 4 = 2°Ac C-H; 3 = 1°Ac C-H; 2 = PhAc H; 1 = 1° Ac H
FA MC = Fully acetylated model compound (reacted under different conditions)
Data in italics are by manual integration instead of automated integration.

Appendix W. The initial rates constants (k_o) of the secondary hydroxyl of the model compound reaction

Temperature (°C)	Method [a]	k_o values (x 1000) [b] (CV% or r^2)[c]
60	E	15.01 (45.68) [d]
	Z	113.7 (0.867)
70	E	19.17 (81.73) [e]
	Z	240.5 (0.914)
80	E	26.85 (98.95)
	Z	407.7 (0.826)
90	E	35.61 (96.93)
	Z	1024.6 (0.9474)

[a] Method is the manner in which the k_o values were calculated. E used slope at 10% of the exponential asymptote, and Z used the linear regression of the first two data points and zero.

[b] From extent of reaction calculated from ^{1}H NMR spectral analysis

[c] Degree of fit for the exponential curve of linear regression of the first two reaction data points and zero

[d] These data were calculated excluding data at 5, 10 and 20 minutes

[e] These data were calculated excluding 5 and 10 minutes data

REFERENCES

Adams, T.A. (1999) "Isolation and characterisation of *Pinus radiata* HTMP and TMP lignins" M.Sc Thesis, University of Waikato, New Zealand

Adler, E. (1977) "Lignin chemistry - Past, present and future" Wood Sci. Technol. 11(3):169-218

Aldrich (2001). Communication from Aldrich's technical science section regarding additional information about Alkali lignin, product 37,095-9, available by contacting the Customer and Technical Service section.

Ämmälahti, E., G. Brunow, M. Bardet, D. Robert and I. Kilpeläinen (1998) "Identification of side-chain structures in a poplar lignin using three-dimensional HMQA-HOHAHA NMR spectroscopy" J. Agric. Food Chem. 46:5113-5117

Andersson, M. and A-M. Tillman (1989) "Acetylation of Jute: Effects on strength, rot resistance and hydrophobicity" J. Applied Polymer Sci. 37:3437-3447

Argyropoulos, D.S. (1994) "Quantitative phosphorus-31 NMR analysis of six soluble lignins" J. Wood Chem. Technol. 14(1):65-82

Atkins, P.W. (1978) Physical Chemistry Oxford University Press, Oxford

Azuma, J-I., N. Takahashi and T. Koshijima (1981) "Isolation and characterisation of lignin-carbohydrate complexes from the milled-wood lignin faction of *Pinus densiflora* sieb. et Zucc." Carbohydrate Res. 93:91-104

Banks, W.B. and Owen, N.L. (1987) "FTIR studies of hydrophobic layers on wood" Spectrochimica Acta. 43A(12):1527-1533

Beckers, E.P.J. and H. Militz (1994) "Acetylation of solid wood. Initial trials on lab and semi industrial scale" In: Proceedings of the Second Pacific Rim Bio-Based Composites Symposium. Vancouver, Canada. 6-9 November, 1994 pp125-134

Beelik, A., R.J. Conca, J.K. Hamilton and E.V. Partlow (1967) "Selective extraction of hemicelluloses from softwood" Tappi 50(2):78-81

Bicho, P.A. (1992) "Two thermostable hemicellulases and their effects on wood pulps" PhD thesis, University of Waikato, New Zealand

Bist, V. and K.S. Bhandari (1986) "Physio-chemical properties of Brauns and soda lignins from *Eucalyptus globulus*" Holzforschung und Holzverwertung 38(3):66-69

Björkman, A.(1956) "Studies on finely divided wood Part 1. Extraction of lignin with neutral solvents" Svensk Papperstidning 59(13):477-485

Björkman, A.(1957a) "Studies on finely divided wood Part 3. Extraction of lignin-carbohydrate complexes with neutral solvents" Svensk Papperstidning 60(7):243-251

Björkman, A.(1957b) "Studies on finely divided wood Part 5. The effect of milling" Svensk Papperstidning 60(9):329-335

Bland, D.E. and M. Menshun (1967) "The liberation of lignin by pre-treatment of the wood of *Eucalyptus regnans* with alkali" Appita 21(1):17-24

Browning, B.L. (1967) Methods of Wood Chemistry Volumes 1 and 2. John Wiley, New York

Brunow, G. (2001) "Chapter 3. Methods to reveal the structure of lignin" pp89-111 In: Biopolymers Volume1: Lignin, humic substances and coal Eds. M. Hofrichter, A. Steinbüchel. Wiley-VCH, Germany

Chang, H-M., E.B. Cowling, W. Brown, E. Adler and G. Miksche (1975) "Comparative studies on cellulolytic enzyme lignin and milled wood lignin of sweetgum and spruce" Holzforschung 29(5):153-159

Chang R. (1981) Chapter 14 p438-456 In: Chemistry Random House, NY

Chen, H.-T., M. Funaoka and Y.-Z. Lai (1998) "Characteristics of bagasse lignin in situ and in alkaline delignification" Holzforschung 52: 635-639

Clermont, L.P. and F. Bender (1957) "The effect of swelling agents and catalysts on acetylation of wood" Forest Product J. (May):167-170

Côté, W.A., Jr. (1967) Wood Ultrastructure University of Washington Press, Seattle

Dawson, B. and K. Torr (1992) "Spectroscopic and colour studies on acetylated radiata pine exposed to UV and visible light" In: Proceedings of the Pacific Rim Bio-based Composites Symposium: Chemical modification of lignocellulosics, Rotorua, New Zealand, FRI Bulletin No. 176 pp 41-51

Donaldson, L.A. (1991) "Seasonal changes in lignin distribution during tracheid developments in *Pinus radiata* D. Don" Wood Sci. Technol. 25:15-24

Donaldson, L.A. (1994) "Mechanical constraints on lignin deposition during lignification" Wood Sci. Technol. 28:111-118

Dunningham, E.A., D.V. Plackett and A.P. Singh (1992) "Weathering of chemically modified wood. Natural weathering of acetylated radiata pine: Preliminary results" Holz als Roh -und Werkstoff 50(11):429-432

Ede, R.M. and G. Brunow (1992) "Application of two-dimensional homo- and heteronuclear correlation NMR spectroscopy to wood lignin structure determination" J. Org. Chem. 57(5):1477-1480

Elias, R. (1995) (personal communication dated 10/10/1995) Fax regarding what sizes a shive is for MDF fibre

Ellis, W.D. and R.M. Rowell (1984) "Reaction of isocyanates with southern pine wood to improve dimensional stability and decay resistance" Wood & Fiber Sci. 16(3):349-356

Ellis, W.D. and R.M. Rowell (1989) "Flame-retardant treatment of wood with a di-isocyanate and an oligomer phosphonate" Wood & Fiber Sci. 21(4):367-375

Evans, P.D., A.F.A. Wallis and N.L. Owen (2000) "Weathering of chemically modified wood surfaces. Natural weathering of Scots pine acetylated to different weight gains" Wood Sci. Technol. 34:151-165

Faix, O. (1991) "Classification of lignins from different botanical origins by FTIR spectroscopy" Holzforschung 45(Suppl.):21-27

Faix, O. and O. Beinhoff (1988) "FTIR spectra of milled wood lignins and lignin polymer models (DHPs) with enhanced resolution obtained by deconvolution" J. Wood Chem. Technol. 4:505-522

Faix O. and J.H. Böttcher (1992) "The influence of particle size and concentration in transmission and diffuse reflectance spectroscopy of wood" Holz als Roh-und Werkstoff 50(6):221-226

Faix, O., D.S. Argyropoulos, D. Robert and V. Neirinck (1994) "Determination of hydroxyl groups in lignins. Evaluation of ^{1}H-, ^{13}C-, ^{31}P-NMR, FTIR and wet chemistry methods" Holzforschung 48(5):387-394

Fengel, D. and G. Wegener (1989) Wood - Chemistry, Ultrastructure, Reactions W. de Gruyter, Berlin

Fernandez, N., R. Mörck, S.C. Johnsrud and K.P. Kringstad (1990) "Carbon-13 NMR study on lignin from bagasse" Holzforschung 44(1):35-38

Freudenberg, K, and A.C. Neish (1968) Constitution and biosynthesis of lignin Springer-Verlag, Berlin-Heidelberg-New York

Gierer, J. (1982) "The chemistry of delignification. A general concept. Part 1 and Part 2" Holzforschung 36(1):43-51; 36(1):55-64

Gierer, J. and S. Ljunggren (1979) "The reactions of lignin during sulphate pulping Part 17. Kinetic treatment of the formation and competing reactions of quinone methide intermediates" Svensk Papperstidning 83:503-512

Glasser, W.G. and C.A. Barnett (1979) "The structure of lignin in pulps. II. A comparative evaluation of isolation methods" Holzforschung 33(3):78-86

Glasser, W.G., V. Davé and C.E. Frazier (1993) "Molecular weight distribution of (semi-) commercial lignin derivatives" J. Wood Chem. Technol. 13(4):545-559

Glasser, W.G. and H.R. Glasser (1981) "The evaluation of lignin's chemical structure by experimental and computer simulation techniques" Paperi ja Puu 63(2):71-83

Goldstein, I.S., E.B. Jeroski, A.E. Lund, J.F. Nielson and J.W. Weaver (1961) "Acetylation of wood in lumber thickness" Forest Products J. 363-370

de Groote, R.A.M.C., A.A.S. Curvelo, P.C. Frangiosa and M.D. Zambon (1992) "Some properties of AcetoSolv sugar cane bagasse lignin" Cellulose Chem. Technol. 26:53-61

Happer, D.A.R., M. P. Hartshorn and J. Vaughan (1972) Reactions of organic functional groups p157 Whitcombe and Tombs, Christchurch, NZ

Haque, M.N and C.A.S. Hill (1998) "Chemical modification of wood flour and fibre with acetic anhydride" J. Timb. Dev. Assoc. (India) XLIV (3):25-33

Haque, M.N and C.A.S. Hill (2000) "Chemical modification of model compounds, wood flour and fibre with acetic anhydride" J. Inst. Wood Sci. 15(3):109-115

Harrington, J. (1996) Softwood structure poster. Artwork by M. Harrington. Copyright University of Canterbury.

Haw, J.F., G.E. Maciel and H.A. Schroeder (1984) "Carbon-13 nuclear resonance spectrometric study of wood and wood pulping with cross-polarization and magic-angle spinning" Anal. Chem. 56:1323-1329

Harwood, V.D. (1972) "Studies on the cell wall polysaccharides of *Pinus radiata* I. Isolation and structure of a xylan" Svensk Papperstid. 75(6):207-212

Harwood, V.D. (1973) "Studies on the cell wall polysaccharides of *Pinus radiata* II. Structure of a glucomannan" Svensk Papperstid. 76(10):377-379

Heitner, C., R. St. John Manley, B. Ahvazi and J. Wang (2001) "The effect of acetylation on the photodegradation of milled wood lignin" J. Pulp Paper Sci. 27(10):325-329

Helm, R.F and J. Ralph (1993) "Lignin-hydroxycinnamyl model compounds related to forage cell wall structure. 2. Ester-linked structures" J. Agri. Food Chem. 41:570-576

Hill, C.A.S. and D. Jones (1996) "The dimensional stabilisation of Corsican pine sapwood by reaction with carboxylic acid anhydrides. The effect of chain length" Holzforschung 50(5):457-462

Hill, C.A.S., D. Jones, G. Strickland and N.S. Cetin (1998) "Kinetic and mechanistic aspects of the acetylation of wood with acetic anhydride" Holzforschung 52(6):623-629

Hill, C. A. S. and S. Mallon (1998) "The chemical modification of Scots pine with succinic anhydride or octenyl anhydride. I. Dimensional stability" Holzforschung 52(4):427-433

Hill, C.A.S. and J.G. Hillier (1999) "Studies of the reaction of carboxylic acid anhydrides with wood. Experimental determination and modelling of kinetic profiles" Phys. Chem. Chem. Phys. 1:1569-1576

Hill, C.A.S., N.S. Cetin, and N. Ozmen (2000) "Potential catalysts for the acetylation of wood" Holzforschung 54(3):269-272

Hill, C.A.S. and A.N. Papadopoulos (2002) "The pyridine-catalysed acylation of pine sapwood and phenolic model compounds with carboxylic acid anhydrides. Determination of activation energies and entropy of activation" Holzforschung 56(2):150-156

Himmel, M.E., K. Tatsumoto and K. Grohmann (1990) "Molecular weight distribution of aspen lignins from conventional gel permeation chromatography, universal calibration and sedimentation equilibrium" J. Chromatography 498:93-104

Hon, D.N-S. (1995) "Stabilization of wood color: Is acetylation blocking effective?" Wood & Fiber Sci. 27(4):360-367

Hortling, B., K. Poppius and J. Sundquist (1991) "Formic acid/peroxyformic acid pulping IV. Lignins isolated from spent liquor of 3-stage peroxyformic acid pulping" Holzforschung 45(2):109-120

Imamura, Y. and K. Nishimoto (1987) "Some aspects on resistance of acetylated wood against biodeterioration" Wood Research 74:33-44

Ingold, C.K. (1969) Structure and mechanism in organic chemistry pp1144-1163 Second edition. G. Bell & Sons, London

Kajihara, J-I., T. Hattori, H. Shirono and M. Shimada (1993) "Characterization of antiviral water-soluble lignin from bagasse degraded by *Lentinus edodes*" Holzforschung 47(6):479-485

Kerr, A.J. and D.A.I. Goring (1976) "Kraft pulping of pressure-refined fibres. Reactivity of exposed middle lamella lignin" Svensk papperstid. 79(1):20-23

Kiguchi M. (1992) "Photo-deterioration of chemically modified wood surfaces - Preliminary study with ESCA" In: Proceedings of the Pacific Rim Bio-based Composites Symposium: Chemical modification of lignocellulosics, Rotorua New Zealand, FRI Bulletin No. 176 pp77-86

Kilpeläinen, I. J. Sipilä, G. Brunow, K. Lundquist and R.M. Ede (1994) "Application of two-dimensional NMR spectroscopy to wood lignin structure determination and identification of some minor structural units of hard- and softwood lignins" J. Agric. Food Chem. 42:2790-2794

Krässig, D.H. (1985) Chapter 1. Structure of cellulose and its relation to properties of cellulose fibers" pp 3-26 In: Cellulose and its derivatives: Chemistry, biochemistry and applications, Eds. J.F. Kennedy, G.O. Phillips, D.J. Wedlock, P.A. Williams. Ellis Horwood Ltd. England

Kringstad, K.P. and R. Mörck (1983) "^{13}C-NMR spectra of Kraft lignins" Holzforschung 37(5):237-244

Kumar, S. (1994) "Chemical modification of wood" Wood and Fiber Sci. 26(2):270-280

Landucci, L.L., S.A. Geddes and T.K. Kirk (1981) "Synthesis of ^{14}C labelled 3-methoxy-4-hydroxy-α-(2-methoxy-phenoxy)-β-hydroxypropiophenone, a lignin model compound" Holzforschung 35(2):67-70

Landucci L.L. (1995) "Reaction of ρ-hyroxycinnamyl alcohols with transition metal salts. 1. Oligolignols and polylignols (DHPs) from coniferyl alcohol" J. Wood Chem. Technol. 15(3):349-368

Landucci, L.L., S.A. Ralph and K.E. Hammel (1998) "^{13}C NMR characterization of guaiacyl, guaiacyl/syringyl and syringyl dehydrogenation polymers" Holzforschung 52(2):160-170

Lapierre, C. and B. Monties (1989) "Structural information gained from the thioacidolysis of grass lignins and their relation with alkali solubility" In: Tappi Proceedings: International Symposium on Wood & Pulping Chem. NC State University, Raleigh NC. May 22-25 1989 pp 615-621

Leopold, B. (1961) "Chemical composition and physical properties of wood fibers" Tappi 44(3):230-240

Liitiä, T. S.L. Maunu and B. Hortling (2000a) "Solid state NMR studies of residual lignin and its association with carbohydrates" J. Pulp Paper Sci. 26(9):323-330

Liitiä, T. S.L. Maunu and B. Hortling (2000b) "Solid state NMR studies on cellulose crystallinity in fines and bulk fibres separated from refined kraft pulp" Holzforschung 54(6):618-624

Maekawa, E., T. Ichizawa and T. Koshijima (1989) "An evaluation of the acid-soluble lignin determination in analyses of lignin by the sulfuric acid method" J. Wood Chem. Technol. 9(4):549-567

Mallari Jr, V.C., K. Fukuda, N. Morohoshi and T. Haraguchi (1989) "Biodegradation of particleboard I. Decay resistance of chemically-modified wood and qualities of particleboard" Mokuzai Gakkaishi 35(9):832-838

Mallari Jr, V.C., K. Fukuda, N. Morohoshi and T. Haraguchi (1990) "Biodegradation of particleboard II. Decay resistance of chemically-modified particleboard" Mokuzai Gakkaishi 36(2):139-146

Matsuda, H. (1987) "Preparation and utilization of esterified woods bearing carboxyl groups" Wood Sci. Technol. 21:75-88

Matsuda, H., M. Ueda and K. Murakami (1988a) "Oligoesterified woods based on anhydride and epoxide I. Preparation and dimensional stability of oligo-esterified woods by step-wise addition reactions" Mokuzai Gakkaishi 34(2):140-148

Matsuda, H., M. Ueda and K. Murakami (1988b) "Oligoesterified woods based on anhydride and epoxide II. Preparation and dimensional stability of oligoesterified woods by heating wood immersed in anhydride-epoxide solution" Mokuzai Gakkaishi 34(7):597-603

Matsuda, H., K. Murakami and M. Ueda (1988c) "Oligoesterified woods based on anhydride and epoxide III. Preparation and dimensional stability of oligoesterified woods by heating wood impregnated with anhydride-epoxide solution" Mokuzai Gakkaishi 34(10):844-850

Matsuda, H. (1996) "Chapter 6. Chemical modification of solid wood" pp159-183 In: Chemical modification of lignocellulosic materials Ed. D.N-S Hon, Marcel Dekker NY

McDonald, A.G. A.B. Clare and A.R Meder (1999) "Chemical characterisation of the neutral water-soluble components from radiata pine high temperature TMP fibre" pp 641-647 In: 53rd Appita Annual Conference. Volume 2

McKenzie, A.W. and H.G. Higgins (1955a) "The reactivity of cellulose. I. The effect of beating and other physical treatments on rate of acetylation" Holzforschung 9(5): 150-153

McKenzie, A.W. and H.G. Higgins (1955b) " The reactivity of cellulose. II. Kinetics of heterogeneous acetylation of Eucalypt α-cellulose in the presence of pyridine" Holzforschung 9(6):179-184

Miyamoto, T., Y. Sato, T. Shibata, H. Inagaki and M. Tanahashi (1984) "^{13}C nuclear magnetic resonance studies of cellulose acetate" J. Polymer Sci. 22:2363-2370

Moore, W.J. (1957) Physical Chemistry p529 3rd Ed. Longmans Green

Murakami, K. and H. Matsuda (1990) "Oligoesterified woods based on anhydride and epoxide VIII. Resistances of oligoesterified woods against weathering and biodeterioration" Mokuzai Gakkaishi 36(7):538-544

Nevell, T.P. and S.H. Zeronian (1962) "The action of ethylamine on cellulose. Part 1. The acetylation of ethylamine-treated cellulose" Polymer 3:187-194

Newman, R.H. and J.A. Hemmingson (1990) "Determination of the degree of cellulose crystallinity in wood by carbon-13 nuclear magnetic resonance spectroscopy" Holzforschung 44(5):351-355

Newman, R.H. (1994) "Crystalline forms of cellulose in softwoods and hardwoods" J. Wood Chem. Technol. 14(3):451-466

Newman, R.H. (1999) "Estimation of relative proportions of cellulose I_α and I_β in wood by carbon -13 NMR spectroscopy" Holzforschung 53(4):335-340

NZ FOA (1995) "Forestry - facts and figures booklet" New Zealand Forest Owners Association Inc.

Ohkoshi M. and A. Kato (1993) "Determination of substituent distribution of DSMO-soluble portion of acetylated wood meal by ^{13}C NMR spectroscopy" Mokuzai Gakkashi 39(7):849-854

Ohkoshi M., A. Kato and N. Hayashi (1997) "^{13}C NMR analysis of acetyl groups in acetylated wood I. Acetyl groups in cellulose and hemicellulose" Mokuzai Gakkashi 43(4):327-336

Ohkoshi M. and A. Kato (1997) "^{13}C NMR analysis of acetyl groups in acetylated wood II. Acetyl groups in lignin" Mokuzai Gakkashi 43(4):364-369

Pan, X-J. and Y. Sano (1999) "Atmospheric acetic acid pulping of rice straw IV: Physio-chemical characterization of acetic acid lignins from rice straw and woods. Part 1. Physical characteristics" Holzforschung 53(5):511-518

Pandey, K.K. and K.S. Theagarajan (1997) "Analysis of wood surfaces and ground wood by diffuse reflectance (DRIFT) and photoacoustic (PAS) Fourier transform infrared spectroscopic techniques" Holz als Roh-und Werkstoff 55(6):383-390

Pannitier, M.J. and P. Souchay (1967) "Chapter 11. Heterogeneous kinetics limited by diffusion" pp410-414 In: Chemical kinetics Elsevier, Amsterdam

Paulsson, M. , R. Simonson and U. Westermark (1995) "Photostabilization of paper made from high-yield pulps by acetylation" In: the Proceedings of the 8th International Symposium on Wood and Pulping Chemistry, 6-9 June 1995, Helsinki, Finland VIII pp61-66

Paulsson, M., S. Li, K. Lundquist, R. Simonson, and U. Westermark (1996) "Chemical modification of lignin-rich paper. Part 3. Acetylation of lignin model compounds representative of β-O-4 structures of the β-guaiacyl ether type" Nord. Pulp Paper Res. J. 11(2):109-114

Pettersen, R.C. and V.H. Schwandt (1991) "Wood sugar analysis by anion chromatography" J. Wood Chem. Technol. 11(4):495-501

Pilling, M.J. (1975) Reaction kinetics Oxford University Press, London

Plackett, D.V., E.A. Dunningham and A.P. Singh (1992) "Weathering of chemically modified wood. Accelerated weathering of acetylated radiata pine" Holz als Roh -und Werkstoff 50(4):135-140

Popper, R and M. Bariska (1975) "Acetylation of wood (3) Swelling and shrinking behavior" Holz Roh-werkstoff 33(11):415-419

Qian, P., A. Islam, K.V. Sarkanan and J.L. McCarthy (1992) "Certain characteristics of the dissolved alkali lignins of four angiosperm plant species" Holzforschung 46(4):321-324

Ramsden, M.J. and F.S.R. Blake (1997) "A kinetic study of the acetylation of cellulose, hemicellulose and lignin components in wood" Wood Sci. Technol. 31(1):45-50

Robert, D. (1992) "5.4. Carbon-13 nuclear magnetic resonance spectrometry" pp250-273. In: Methods in lignin chemistry Eds. S.Y. Lin and C.W. Dence, Springer-Verlag, Berlin, Heidelberg

Rowell R.M. (1980) "Distribution of reacted chemicals in southern pine modified with methyl isocyanate" Wood Sci. 13(2):102-110

Rowell, R.M., W.C. Feist and W.D. Ellis (1981) "Weathering of chemically modified southern pine" Wood Sci. 13(4): 202-208

Rowell, R.M. (1983) "Chemical modification of wood" Forest Products Abstracts Review Article:363-382

Rowell, R.M., R.H.S. Wang and J.A. Hyatt (1986) "Flakeboards made from aspen and southern pine wood flakes reacted with gaseous ketene" J. Wood Chem. Technol. 6(3):449-471

Rowell, R.M., J.A. Youngquist, J.S. Rowell, and J.A. Hyatt (1991) "Dimensional stability of aspen fiberboard made from acetylation fiber" Wood & Fiber Sci. 23(4):558-566

Rowell R.M., R. Simonson, S. Hess, D.V . Plackett, D.R Cronshaw and E.A. Dunningham (1994) "Acetyl distribution in acetylated whole wood and reactivity of isolated wood cell-wall components to acetic anhydride" Wood & Fiber Sci. 26(1):11-18

Rowell, R.M. (1996) "Chapter 12. Physical and mechanical properties of chemically modified wood" pp 295-310 In: Chemical modification of lignocellulosic materials Ed. D.N-S Hon , Marcel Dekker NY

Salud, E.C. and O. Faix (1980) "The isolation and characterisation of lignins of *Shorea* species" Holzforschung 34(4):113-121

Sarkanen, K.V., Hou-Min Chang and G.G. Allan (1967) "Species variation in lignins. II. Conifer lignins" Tappi 50(12):583-587

Schöning, A. G. and G. Johansson (1965) "Absorptiometric determination of acid-soluble lignin in semi-chemical bisulfite pulps and in some woods and plants" Svensk Papperstidn. 68(18):607-613

Schultz, T.P. and W.G. Glasser (1986) "Quantitative structural analysis of lignin by diffuse reflectance FTIR spectroscopy" Holzforschung 40(Suppl.):37-44

Sen, M.K. and M. Ramaswamy (1957) "6 - Kinetics of fibrous acetylation of cotton and jute" J. Text. Inst. Trans. 48:T75-T80

Siau, J.F. (1984) Transport processes in wood Springer-Verlag, Berlin, NY

Sjöström, E. (1981) Wood Chemistry. Fundamentals and Applications Academic Press, London

Spurlin, H.M. (1938) Trans. Electrochem. Soc. 73:95

Stamm, A.J. and R.H. Baechler (1960) "Decay resistance and dimensional stability of five modified woods" Forest Products J. January :22-26

de Stevens, G. and F.F. Nord (1953) "Investigations on lignin and lignification XI. Structural studies on bagasse native lignin " J. Am. Chem. Soc. 75:305-309

Swan, B (1965) "Isolation of acid-soluble lignin from the Klason lignin determination" Svensk Papperstid. 68(22):791-795

Takahashi, M., Y. Imamura and M. Tanahashi (1989) "Effect of acetylation on decay resistance of wood against brown-rot, white-rot and soft-rot fungi" IRG/WP/3540:1-16

TAPPI (1996) "Acid-insoluble lignin in wood and pulp" T222 om-88 In: TAPPI Test methods

TAPPI (1991) "Acid-soluble lignin in wood and pulp" UM 250 pp47-48 In: TAPPI Useful methods

Thumm, A. and W. Grigsby (2001) "Determination of resin distribution and coverage in MDF by fibre staining" A Composite Panels Research Group confidential commercial report, August 2001

Timell, T.E. (1967) "Recent progress in the chemistry of wood hemicelluloses" Wood Sci. Technol. 1(1):45-70

Tolvaj L. and O. Faix (1995) "Artificial ageing of wood monitored by DRIFT spectroscopy and CIE L*a*b* color measurements. 1. Effect of UV light" Holzforschung 49(5):397-404

Torr, K. (1994) "The role of acetylation in inhibiting photoyellowing and photodegradation of *Pinus radiata* wood and lignin" MSc thesis, University of Waikato

Turner, E.E. and M.M. Harris (1952) Organic chemistry p100. Longmans, London

Uprichard, J.M. (1965) "The alpha-cellulose content of wood by the chlorite procedure" Appita 19(2):36-39

Uprichard, J.M. (1991) "Chapter 4. Chemistry of wood and bark" pp4.1-4.42 In: Properties and uses of New Zealand Radiata Pine. Volume 1 - Wood Properties Eds. Kininmonth, J.A. and L.J. Whitehouse, NZ Min. Forestry, Forest Research Institute, Rotorua, New Zealand

van Hazendonk, J.M, E.J.M. Reinerrink, P. de Waard, J.E.G van Dam (1996) "Structural analysis of acetylated hemicellulose polysaccharides from fibre flax (*Linum visitatissimum* L.)" Carbohydrate Res. 291:141-154

Varma, A.J. (1996) per. comms, a series of faxes

Vázquez, G., G. Antorrena, J. González and S. Freire (1997) "FTIR, ^{1}H and ^{13}C NMR characterization of Acetosolv-solubilized pine and eucalyptus lignins" Holzforschung 51(2):158-166

Vick, C.B., A. Krzysik and J.E. Wood Jr. (1991) "Acetylated, isocyanate-bonded flakeboards after accelerated ageing. Dimensional stability and mechanical properties" Holz als Roh- und Werkstoff 49:221-228

Wakeling, R.N., D.V. Plackett and D.R. Cronshaw (1991) "The susceptibility of acetylated *Pinus radiata* to mould and stain fungi" In: Proceedings of the International Symposium on Chemical Modification of Wood, May 1991, Kyoto, Japan. pp 142-147

Walas, S.M. (1959) Reaction kinetics for chemical engineers McGraw-Hill Book Company Inc. International Student Edition

Walker, J.C.F. (1993). Primary wood processing. Principles and practice Chapman & Hall, London , UK

Wegener, G. and D. Fengel (1977) "Studies on milled wood lignins from spruce. Part 1. Composition and molecular properties" Wood Sci. Technol. 11:133-145

West, H. and W.B. Banks (1986) " Topochemistry of the wood-isocyanate reaction. An analysis of reaction profiles" J. Wood Chem. Technol. 6(3):411-425

West, H. (1988) "Kinetics and mechanism of wood-isocyanate reactions" PhD thesis, University of Wales Bangor

Whistler, R.L. (1945) "Chapter: Preparation and properties of starch esters" pp279-307 In: Advances in carbohydrate chemistry Vol. 1. Academic Press

Whistler, R.L. and C-C. Chen (1991) "Chapter 7. Hemicelluloses" pp287-319 In: Wood structure and composition Eds. M. Lewin and I.S. Goldstein. Marcel Dekker, NY

Wood, C.W., A.K. Holliday and R.J.S Beer (1968) Organic chemistry. An introductory test p 126 Third Edition Butterworths, London

Wu, T.K. (1980) "Carbon-13 and proton nuclear magnetic resonance studies of cellulose nitrates" Macromolecules 13:74-79

Yano, H., M. Norimoto and T. Yamada (1986) "Changes in acoustic properties of Sitka spruce due to acetylation" Mokuzai Gakkaishi 32(12):990-995

Yasuda, S. and N. Murase (1995) "Chemical structures of sulfuric acid lignin. Part XII. Reaction of lignin models with carbohydrates in 72% H_2SO_4" Holzforschung 49(5):418-422

Yusuf, S., Y. Imamura, M. Takahashi and K. Minato (1995) "Weathering properties of chemically modified wood with some cross-linking agents and its decay resistance after weathering" Mokuzai Gakkaishi 41(8):785-793

Zanuttini M, M. Citroni and M.J. Matínez (1998) "Application of diffuse reflectance infrared Fourier transform spectroscopy to the quantitative determination of acetyl groups in wood" Holzforschung 52(3):263-267